The role of the aryl hydrocarbon receptor (AHR) in immune regulation in the human intestine

Submitted in partial fulfilment of the requirements of the

Degree of Doctor of Philosophy

By

Paul Harrow

Centre for Immunobiology, Blizard Institute

Barts and The London School of Medicine and Dentistry

Queen Mary, University of London

United Kingdom

July 2020

Statement of originality

I, Paul Harrow, confirm that the research included within this thesis is my own work, or that where it has been carried out in collaboration with or supported by others, that this is duly acknowledged below and my contribution indicated. Previously published material is also acknowledged below.

I attest that I have exercised reasonable care to ensure that the work is original, and does not to the best of my knowledge break any UK law, infringe any third party's copyright or other Intellectual Property Right, or contain any confidential material.

I accept that the College has the right to use plagiarism detection software to check the electronic version of the thesis.

I confirm that this thesis has not been previously submitted for the award of a degree by this or any other university.

Signature:

Date: 18th July 2020

Abstract

Environmental factors play a major role in the development of inflammatory bowel disease (IBD). However, current understanding about how environmental factors influence disease is limited and there is a major unmet need for advice to allow patients and at-risk individuals to modify their risk of disease.

The aryl hydrocarbon receptor (AHR) is a ligand activated transcription factor and functions as an environmental sensor. Diverse murine studies have shown activating this receptor has immunoregulatory consequences and is beneficial in models of IBD. However, few studies have examined this pathway in the human intestine. It has been proposed that low AHR activity may play a role in IBD aetiopathology and AHR stimulation is beneficial.

In this study a quantitative measure of AHR activation, *CYP1A1* gene expression, is optimised and validated. This assay is used show that the AHR pathway is not less active in IBD than health. Unexpectedly the AHR pathway is more active and sensitive to stimulation in non-haematopoietic cells than intestinal immune cells and this difference is greater in Crohn's disease than health. I demonstrate an important consequence of this difference could be an increased ability of intestinal stromal cells to degrade AHR ligands.

The impact of AHR activation on intestinal immune cells is not known. This is of particular importance now medication targeting AHR has entered clinical trials. In this study, single cell sequencing is used to precisely characterise the immune cells expressing AHR. AHR expression is seen in a minority of cells (6.4%) and the majority of these cells are lymphocytes, although AHR expression is seen in antigen presenting cells and other cell types. I determine the impact of AHR stimulation in intestinal immune cells using RNASeq. This work newly identifies a number of genes associated with IBD as regulated by AHR. In addition, novels of effects of AHR signalling including pH sensing, cytoskeletal and microtubule arrangement and Rap 1 Signalling are reveal and provide many avenues for future research.

Acknowledgements

During this project I received first class mentorship from two leaders in this field James Lindsay and Andrew Stagg. Andrew patiently welcomed another clinician into his lab and provided considered and constructive advice throughout the project. His depth of knowledge in the field inspired me and he fostered my love of science.

James inspired me to pursue a career in IBD and has always set an example for me to follow in his approach to science and clinical care. He not only welcomed me into the lab but also the clinic and trials unit and there could be no better apprenticeship for a career in IBD than he provided over the last 5 years.

I must thank all members of the lab who helped me during my time in the Blizard and I wanted to thank you all for your advice and friendship. I must particularly thank Neil McCarthy who has become a great friend. I will miss your acerbic wit, veracity and many engaging conversations. Inva, Neil, Eve and Martha all welcomed me into the lab as a novice and I thank you for the time and patience you showed while sharing your expertise with me.

There are too many colleagues and friends in the Blizard to highlight but I must thank Mel, Gary, John, Hal, Will and Jean-Marie for your support. I also extend my thanks to the collaborators, patients and clinical staff, without whom this work would not have been possible.

Finally, I must thank my wife for her patience and (mostly) unfailing support particularly while writing-up this thesis with a clinical job. I look forward to spending more time together in the coming months.

Contents

Abbreviations

AHR – aryl hydrocarbon receptor

AHRE - aryl hydrocarbon response element

AHRR – aryl hydrocarbon receptor repressor

AMPK – adenoside monophosphate-activated protein kinase

ANOVA – analysis of variance

ARNT - aryl hydrocarbon receptor nuclear translocator

ATP – adenosine triphosphate

BATF – Basic leucine zipper transcription factor, ATF-like

BCG – Bacillie Calmette- Guerin (TB vaccine)

BMDC – bone marrow-derived dendritic cell

CD – Crohn's disease

CD- – cluster of differentiation

cDC – conventional DC

cDNA – complementary DNA

CNS – central nervous system

Ct – cycle threshold

CYP1A1 – cytochrome p450 enzyme family 1, subfamily A, polypeptide 1

DAPI – 4',6-diamidino-2-phenylindole

DC – dendritic cell

DIM - 3,3'-diindolylmethane

DMSO - dimethyl sulfoxide

DNA – deoxyribonucleic acid

DRE – dioxin response element (also called XRE)

DSS – dextran sodium sulfate

EAE – experimental autoimmune encephalopathy

EC50 – half maximal effective concentration

EpCAM – epithelial cell adhesion molecule

FACS – fluorescence activated cell sorting

FCS - fetal calf serum

FDR – false discovery rate

FICZ - 6-formylindolo[3,2-b]carbazole

FITC - fluorescein isothiocyanate

FSC – forward scatter

GM-CSF – granulocyte-macrophage colony-stimulating factor

GO – gene ontology

GPR – G protein-coupled receptor

GWAS – genome wide association study

HIF – hypoxia inducible factor

HIV – human immunodeficiency virus

HLA – human leucocyte antigen

IBD – Inflammatory bowel disease

I3A - indole-3-aldehyde

IC50 – half maximal inhibitory concentration

IDO - indoleamine 2 3-dioxygenase

IEC – intestinal epithelial cell

IL – Interleukin

IEL – intra-epithelial lymphocytes

ILC – innate lymphoid cells

INFγ – interferon gamma

IQR – interquartile range

LC-MS – liquid chromatography – mass spectrometry

LPMC – lamina propria mononuclear cell

LPS – lipopolysaccharide

MACS – Magnetic-activated cell sorting

MFI – mean fluorescence intensity

miRNA – micro RNA

mRNA – messenger RNA

moDC – monocyte-derived dendritic cell

mTORC – mammalian target of rapamycin complex

NIR – near infra-red

NSAID – non-steroidal anti-inflammatory drug

OR – odds ratio

PBMC – peripheral blood mononuclear cell

PCA - principal component analysis

PCR – polymerase chain reaction

PPAR – peroxisome proliferator-activated receptor

RIN – RNA integrity number

RNA – ribonucleic acid

RORγt – RAR-related orphan receptor gamma (thymic isoform)

rRNA – ribosomal RNA

RT-qPCR – reverse transcriptase quantitative polymerase chain reaction

SCFA – short chain fatty acid

SD – standard deviation

SFB – segmented filamentous bacteria

SNP – single nucleotide polymorphism

SSC – side scatter

TB – Tuberculosis

TCR – T-cell receptor

TGFβ - Transforming growth factor beta

Th – T-helper

TLR – Toll-like receptor

TNF – Tumour necrosis factor

Tr1 – Type 1 regulatory cells

tSNE - t-distributed stochastic neighbour embedding

UC – Ulcerative colitis

UCB – unconjugated bilirubin

UV – ultra violet

XRE – xenobiotic response element (also called DRE)

Chapter 1 – Introduction

The gastrointestinal epithelium forms the largest barrier surface separating the human body from its external environment. It is a unique interface that enables absorption of dietary nutrients and maintenance of immunological tolerance to food and other harmless antigens whilst providing a robust defence against pathogens and supporting co-existence with symbiotic commensal bacteria (Belkaid and Harrison 2017). This complex relationship between host and environment has evolved over time. Dysfunction of the barrier surface underlies a breadth of gastrointestinal diseases including infection, inflammatory bowel disease and cancer.

1.1 Introduction to Inflammatory bowel disease (IBD)

Crohn's disease (CD) and ulcerative colitis (UC) are the two major types of IBD. Both diseases cause chronic inflammation of the gastrointestinal tract. CD can affect the entire gastrointestinal tract while in UC inflammation is restricted to the colon. Characteristically CD causes transmural inflammation and consequently leads to complications such as fistulae and strictures. Ulcerative colitis causes a confluent inflammation extending proximally from the rectum. Although inflammation is superficial in UC, it can cause toxic megacolon and, despite advances in treatment, more than 10% patients still require a colectomy within 15 years of diagnosis (Parragi et al. 2018). In reality there is considerable overlap in the clinical presentation and appearance of CD and UC. The vast majority of the common medical therapies, which all modify the immune system, are licenced to treat both conditions. In addition, there is considerable overlap in the genetic risk factors for these conditions suggesting in reality there is a continuum of inflammatory bowel disorders (Cleynen et al. 2016).

The incidence of IBD worldwide increased rapidly in developed countries in the 20th century (Molodecky et al. 2012) reaching a prevalence above 0.8% in northern European areas like Lothian, Scotland (Jones et al. 2019). Prevalence continues to increase rapidly in developing countries today (Ng et al. 2017). The cause of this relatively rapid increase is not known but is commonly thought to

be due to a combination of environmental factors in the context of host genetic risk factors and intestinal dysbiosis.

1.2 Aetiopathology of IBD

1.2.1 Characteristic pathology in IBD

Both Crohn's and ulcerative colitis are characterised by chronic intestinal inflammation. Immune cells are enriched in inflamed tissues from patients with IBD. Sustained intestinal inflammation is thought to require the presence of commensal enteric bacteria and is characterised by activated CD4+ T-lymphocytes, which are abundant in inflamed tissue. A prominent hypothesis in the field is that in IBD there is a loss of immunologic tolerance to normal commensal intestinal bacteria. The key immunological findings are summarised below.

Many early studies focused on the dysregulation of the adaptive immune response. Established inflammation is characterised by the presence of lymphoid infiltrates and plasmacytosis (Surawicz et al. 1994). CD was considered to be caused by a Th1 response while UC was attributed to a Th2 response (Strong et al. 1998). However, in reality the adaptive immune response observed is more complex and the importance of the innate immune system has also been recognised more recently. Increased numbers of macrophages are detected in macroscopically normal mucosa in patients with CD (Yao et al. 1996). In health, tolerogenic intestinal macrophages (defined by a lack of CD11c, CCR2 and CX3CR1 expression) are derived from circulating monocytes. These cells prevent damaging inflammatory responses to commensal bacteria by promoting the expansion of regulatory T-cells (Tregs) via the production of IL-10 (Bernardo et al. 2018).

In IBD there is an accumulation of pro-inflammatory monocyte-like cells (which express CD11c, CCR2, CX3CR1) and show impaired maturation and impaired clearance of intracellular bacteria which leads

to persistent immune activation (Bain et al. 2013; Marks et al. 2006; Ogino et al. 2013). These cells secrete IL-23 and TNFα (Kamada and Núñez 2013) and induce Th17 cells, which are characterised by IL-17 and IL-17A expression and play a key role in immunity at barrier sites like the skin and gut (Weaver et al. 2013). IL-17 expression in the intestinal mucosa is significantly elevated in both CD and UC (Fujino et al. 2003).

However, unexpectedly while blockade of IL-17A was beneficial in psoriasis, this actually led to worsening of Crohn's disease. This may be explained in part by redundant inflammatory pathways, increased Th1 polarisation is seen in the absence of IL-17A (O'Connor Jr et al. 2009). However, another important theory is that IL-17 also promotes effects which protect the barrier, highlighting the challenges of modifying the immune system. For example, blockade of IL-17 leads to impaired production of fibroblast growth factor, increased intestinal permeability (S. H. Lee 2015) and impaired production of antimicrobial peptides such as Defb1, Reg3g, and S100a8 (Maxwell et al. 2015).

More recently different subsets of lymphocytes have been recognised with innate behaviours. Innate lymphoid cells (ILC) resemble adaptive lymphocytes but lack antigen-specific receptors. Group 3 ILC are a heterogenous group which can produce IL-22 or IL-17 while Group 1 ILC produce IFN-γ (Rankin et al. 2013). The number and subtype of ILC is also altered in IBD; the frequency of IFN-γ producing ILC1 is increased in Crohn's disease while the NKp44+ ILC3, which characteristically produce IL-22 (Hoorweg et al. 2012), is reduced (Bernink et al. 2013). Other studies have found an increase in IL-17 producing ILC3 in Crohn's disease which was not seen in UC.

Gamma delta cells constitute up to 40% of intraepithelial lymphocytes in the mucosa (Andreu-Ballester et al. 2012). Human intestinal mucosal tissues are dominated by host stress-responsive Vδ1+ T-cells and microbe-responsive Vδ2+ T-cells (McCarthy et al. 2013). Studies in the intestinal mucosa have shown conflicting results. A number of studies have shown reduced numbers of Vδ1+ T-cells cells (H. B. Lee et al. 1997) while other studies found Vδ1+ T-cells were significantly expanded in IBD (Catalan-Serra et al. 2017). Recently a greater appreciation of the complexity of γδ T cells subsets has

developed. A distinct subtype of Vδ1+ T cells that express CD8αβ+ are decreased in Crohn's disease (Kadivar et al. 2016).

In addition to immune cells, stromal cells and intestinal epithelial cells (IEC) play an important role in IBD pathology. Stromal cells comprise fibroblasts and myofibroblasts which have key roles maintaining the extracellular matrix and epithelial renewal respectively (Barnhoorn et al. 2020). Different stromal cells behaviours are seen in IBD. Inflammatory fibroblasts show expression of podoplanin, oncostatin M receptor and membrane bound TNF (Smillie et al. 2019). They produce IL-6, IL-13, and IL-1β promoting recruitment of monocytes and T cells (Kinchen et al. 2018).

Genetic studies (more detail below) have identified a number of susceptibility loci which implicate abnormal intestinal epithelial cell function in the pathogenesis of IBD. The chloride and bicarbonate channel bestrophin2 (BEST2) is through to play an important role in normal mucus formation. BEST2 expression is down-regulated in UC (Ito et al. 2013). Mutations in NOD2, an intracellular receptor for bacterial lipopolysaccharide (LPS), are seen in Crohn's disease lead to impaired α-defensin production (Wehkamp et al. 2004).

Variants in the autophagy protein ATG16L1 are associated with increased risk of Crohn's disease and lead to impaired autophagy in IECs in response to bacterial infection or metabolic stress (Murthy et al. 2014). Our understanding of the role of non-haematopoietic cells in the pathogenesis of IBD is less developed than our knowledge about immune cells.

1.2.2 Genetic risk factors for IBD

Much of our understanding about the pathogenesis of IBD comes from genetic studies. It has long been known that there is an increased prevalence of IBD in the relatives of patients with IBD. The first twin studies showed twin-twin concordance for IBD was ~18% in UC and ~50% Crohn's disease

(Halfvarson et al. 2003; Tysk et al. 1988). The first specific gene associated with Crohn's disease, NOD2 was identified in 2001 (Hugot et al. 2001). Subsequent, increasingly massive genome-wide association studies have identified more than 240 risk loci for IBD (Jostins et al. 2012; de Lange et al. 2017; J. Z. Liu et al. 2015). Studies across different ethnic groups have also identified differential risk associations; for example, NOD2 is a major risk factor in European populations while TNFSF15 is more important in East Asian populations (J. Z. Liu et al. 2015). The genes identified can be classified using different approaches (summarised in Table 1.1 adapted from Graham and Xavier 2020). However, the function of every gene, and more importantly, impact of most variants associated with IBD is not known. In part this is due to the complexity and diversity of interactions between host immune cells, intestinal microbiome and the environment. Regulation of gene expression depends on the cell type and tissue context.

Functional Grouping	**Implicated Genes from GWAS**
Innate immunity and bacterial sensing	NOD2, CARD9, MEFV, TNFAIP3
Adaptive immunity	HLA, PRDM1, BACH2, IL2RA
Cytokine signalling	IL6ST, IL12B, TYK2, RORC, IL17RA, GPR65
Epithelial barrier integrity and repair	C1ORF106, RNF186, RSPO3
Fibrosis	OSMR, SMAD3, TAB2
Cellular stress response	ATG161L, TMEM258, SDF2L
Inflammasome	MEFV, NLRP7, NLRC4

Table 1.1: IBD risk genes influence a complex network of overlapping and interconnected pathways. Key functional groupings (gene ontology) are shown here with the implicated genes (adapted from (Graham and Xavier 2020))

These genetic studies have undoubtedly advanced our understanding of IBD pathogenesis. However, despite inclusion of 60,000 subjects in the latest IBD genome-wide association studies (GWAS) (de Lange et al. 2017) the total disease heritability explained by known genetic variants is below 20%. This missing heritability will not be found by simply enlarging the study size. However, it may be in part explained by genetic interactions (Zuk et al. 2012), common variants which have an effect size too small to be detected or interactions not detected by current GWAS study designs (Golan, Lander, and

Rosset 2014). Most importantly, these studies also do not consider the interaction between gene variants and microbial or environmental factors.

1.2.3 Microbiota dysbiosis in IBD

It has long been known that the composition of the intestinal microbiota is altered in IBD (Mangin et al. 2004). The evidence for the role of bacteria in the pathogenesis of disease is strongest for Crohn's disease. In CD antimicrobial therapies are known to have a modest clinical benefit particularly after surgical resection (Rutgeerts et al. 1995). Studies using have shown reduced bacterial diversity and altered composition of faecal bacteria and mucosal bacteria in IBD (Gophna et al. 2006). Early studies used a limited number of fluorescent in situ hybridization probes and found reduced *Clostridia sp*. in both UC and CD (Sokol et al. 2006). Studies using a 16S rRNA sequencing demonstrated reductions in *bifidobacteria* and *lactobacilli* in UC (Mylonaki et al. 2005). Other studies showed decreased abundance of Firmicutes particularly *Faecalibacterium prausnitzii* in patients with Crohn's disease; this correlated with higher rates of disease recurrence after surgery (Sokol et al. 2008).

The clinical impact of this understanding has, so far, been limited. Modification of the intestinal bacteria by probiotics has been shown to have modest benefit in ulcerative colitis. Three randomised controlled trials have compared *Escherichia coli Nissle* to mesalazine to maintain remission in UC and found the probiotic treatment to be not inferior to the standard first line treatment mesalazine (Harbord et al. 2016). VSL#3®, a mixture of four species of *lactobacilli*, three species of *bifidobacteria* and *Streptococcus thermophilus* has shown clear benefit in the unique situation of pouchitis, an inflamed surgically formed pouch (C. Hedin, Whelan, and Lindsay 2007).

Faecal microbiota transplant, the transfer of stool from one or multiple donors has also been shown to have a modest but statistically significant benefit in the treatment of UC (Moayyedi et al. 2015;

Paramsothy et al. 2017). The cost, tolerability and practicalities of preparing, storing and delivering the donor faeces compared to the pharmacological standard of care has limited adoption of this intervention.

A number of challenges remain. There is large inter-individual variation in the composition of intestinal bacteria in both health and IBD (Willing et al. 2009). It is also unclear which alterations in the intestinal bacteria precede or are caused by intestinal inflammation. An altered gut microbiome is seen in the stool of infants born to mothers with IBD (Torres et al. 2020) and unaffected siblings of patients with Crohn's disease also show dysbiosis (C. R. Hedin et al. 2014) but it has not been proven whether these changes predict the development of IBD in the future.

Another challenge has been understanding how numerous specific bacteria interact with each other or the host to modify IBD. Diverse bacteria can produce specific metabolites which alter the host immune function. Metabolomics is the study of metabolite profiles using techniques like liquid chromatography–mass spectrometry (LC–MS). This has allowed the functional impact of altered microbiota to be examined, independently to the particular bacterial species generating the metabolite. Many classes of metabolite are altered in IBD including an overabundance of primary bile acids and sphingolipids and depletion of triacylglycerols and haem metabolites (Franzosa et al. 2019). Tryptophan metabolism is also significantly influenced by the gut bacteria. Microbial enzymes convert tryptophan from the diet into tryptamine and indoles which can directly influence the host (Zelante et al. 2013). Importantly, levels of a range of indoles derived from tryptophan are reduced in the serum of patients with Crohn's disease (Yunjia Lai et al. 2019).

Better understanding of the signalling pathways these metabolites active is crucial to understanding host-microbiome interactions. Undoubtedly gut bacterial metabolism is also influenced by diet and other environmental factors. Defining and measuring these environmental variables and understanding how they integrate with the known host genomic factors and microbiota to cause inflammation remains an enormous challenge in the field.

1.2.4 Environmental risk factors for IBD

There is compelling evidence to suggest environmental factors play an important role in the aetiopathology of common gastrointestinal diseases such as IBD (Kaplan and Ng 2017) and colorectal cancer (Lichtenstein et al., 2000). Genetic factors alone cannot be responsible for the aetiology of IBD. As discussed above, despite vast genome wide association studies, identified genetic factors only explain a minority of observed heritability (Jostins et al. 2012). Monozygotic twin-twin concordance is also incomplete; estimates suggest no more than 50% for Crohn's disease and 20% for UC (Gordon et al. 2015). The lack of complete penetrance must be accounted for by additional factors in disease aetiology. Genetics alone also cannot account for the rapid rise of IBD prevalence in the 20th century in the developed world and the ongoing increase in developing countries (Ng et al. 2017). Environmental factors must play a major role in the pathogenesis of disease.

Several approaches have been used to try to determine specific environmental risk factors which influence the development of IBD. In contrast, there is far less evidence demonstrating environmental factors influence the course of established disease.

A wide variety of environmental factors have been implicated in the development of conditions like IBD (Kaplan and Ng 2017). The most important reported factors identified are summarised in Table 1.2. The first environmental factor described was smoking. Smokers are twice as likely to develop Crohn's disease as non-smokers, while smokers are less likely to develop UC (Parkes, Whelan, and Lindsay 2014). The mechanism of this effect is not understood. Trials of nicotine replacement in UC suggest this is not a key mechanism (Nikfar et al. 2010). Smoking is also associated with adverse clinical outcomes in patients diagnosed with CD including an increased risk of surgery, while smokers with UC have less extensive disease and fewer flares compared to non-smokers (Parkes, Whelan, and Lindsay 2014).

Several studies report a protective effect from breastfeeding and both CD and UC (Molodecky and Kaplan 2010; Ng et al. 2015). Breastfeeding plays an important role in the establishment of the gut microbiome and is important for acquiring oral tolerance to microflora and food antigens (van den Elsen et al. 2019).

Non-steroidal anti-inflammatory drugs (NSAIDs) cause damage to the intestinal mucosa and increase intestinal permeability. A number of retrospective and prospective studies have found NSAID intake increased the risk of both CD and UC (Ananthakrishnan et al. 2012; Tanner and Raghunath 1988). Intake of NSAIDs is also associated with an increased risk of flare in patients with established IBD (Long et al. 2016; Takeuchi et al. 2006).

	Crohn's disease	**Ulcerative colitis**
Reduce risk of developing disease	Breastfeeding Tea (Ng et al. 2015) Regular exercise H. Pylori infection (Luther et al. 2010) Fruit and vegetable fibre (Ananthakrishnan et al. 2013)	Breastfeeding Coffee/Tea (Ng et al. 2015) H. Pylori (Luther et al. 2010) Appendicectomy (Molodecky and Kaplan 2010) Pertussis vaccine (Ng et al. 2015)
Increase risk of developing disease	Smoking (Parkes 2014) BCG vaccine (Ng et al. 2015) Migrating to region of high prevalence (Williams 2008) NSAID use	Stopping smoking NSAID use Migrating to region of high prevalence Polyunsaturated omega-6 fatty acids (de Silva et al. 2010)

Table 1.2 Environmental risk factors for IBD. The most important reported environmental risk factors which influence the development of Crohn's disease and ulcerative colitis are shown in this table.

Diet is one of largest sources of environmental variation affecting the gastrointestinal tract. The interactions between diet, host and microbiota are complex and unravelling these relationships is challenging. Researchers and patients both agree a better understanding of the role diet plays intestinal diseases like IBD is a top priority (James Lind Alliance 2015).

Retrospective studies in Europe and Asia suggest a "*Western*" diet high in saturated fat and refined sugars is associated with an increased risk of IBD (Amre,Devendra; D'Souza, Savio; Morgan 2007),

(Hou, Abraham, and El-serag 2011). However, the mechanism of this effect is not clear and these studies are limited by recall bias. More recent large, high quality prospective epidemiological studies have identified associations between specific diets and GI disease. The Nurse Cohort Study recorded dietary information in 170,000 subjects over 26 years using a validated, semi-quantitative, food frequency questionnaire every 4 years. 607 new cases of IBD were identified during the study period. Using a Cox proportional hazards model adjusting for potential confounders, the study found a 41% risk reduction in CD in individuals with the highest intake of dietary fibre (95% CI 0.39 – 0.90) (Ananthakrishnan et al. 2013).

The benefits of dietary fibre are not confined to IBD. Another large study, The European Prospective Investigation into Cancer and Nutrition (EPIC) has followed over 500,000 individuals using dietary questionnaires starting in 1992. By 2003 there were 1065 cases of colorectal cancer in the cohort. Dietary fibre intake was inversely related to the incidence of colorectal cancer (CRC), with an adjusted relative risk of 0.58 (95% CI 0.41–0.85) (Bingham et al. 2003).

To date the impact of these findings on advice for patients has been limited. No specific diet has been proven to prevent IBD or maintain remission in the long term although a recent prospective study using a highly restricted diet has shown a benefit in paediatric Crohn's disease (Levine et al. 2019).

A large case control study in the Asia-Pacific region examined the impact of 87 different environmental variables using a case-control study design. A protective effect of prolonged breastfeeding was also seen in this cohort and number of interesting observations including a protective effect from tea drinking and an increased risk of Crohn's disease with BCG vaccination, which has been reported by other groups in other populations (Baron et al. 2005; Ng et al. 2015). However, the most striking finding from this study is that the majority of the candidate environmental risk factors, which had been identified by an international panel of experts (IOIBD), had no impact on the risk of developing IBD after adjusting for age, sex, income and multiple testing (Ng et al. 2015).

Defining the key environmental risk factors for IBD has proved challenging. The most recent high-quality prospective studies have only identified a small number of specific environmental factors which influence the risk of incident disease. Most studies did not examine the effect of environmental factors on the natural history of disease. Studies have also found contrasting results in different populations. For example, antibiotic exposure in childhood is associated with the development of IBD in Western countries (Theochari et al. 2018) while the opposite effect is seen in Asian populations, where antibiotic exposure is protective (Ng et al. 2015).

1.3 The Exposome

One of the greatest challenges in understanding which environmental factors impact IBD is the enormous diversity of environmental exposures, the potential for interactions between these different environmental variables and with host genetic variants, in addition to unanswered questions about whether the timing of exposure in life or even *in-utero* is important.

The full gamut of factors can be described by the proposed term "exposome" which encompasses the cumulative environmental exposures of a lifetime and immediately draws attention to the challenge of recording and analysing this vast data set and infinite number of possible combined exposures (Wild 2005).

The challenge is enormous. Certain environmental exposures may only be relevant with specific host genetics. For example, exposure to smoking and the risk of inflammation depends on specific host factors. ATG16L1 forms part of an autophagy complex. The single nucleotide polymorphism (SNP) T300A of ATG161L1 is associated with Crohn's. This SNP has been shown to confer Paneth cell defects (including apoptosis, metabolic dysregulation, and downregulation of the PPARγ) specifically when triggered by tobacco smoke (T. Liu et al. 2018).

Others effects may depend on the length of time of exposure or exposure in a critical window, for example *in-utero* (Gomez de Agüero et al. 2016) or breastfeeding (Xu et al., 2018). Adding another layer of complexity is the gut microbiome. The presence of billions of metabolically active organisms in the gut lumen means it can be difficult to determine whether the impact of a particular factor is due to a direct effect on the host or an indirect effect through alterations in the gut microbiome (Spor, Koren, and Ley 2011). As a result of these challenges there have been few practical *lifestyle* recommendations for individuals with or at risk of IBD.

1.4 Environmental sensing mechanisms at the intestinal barrier

A different approach to attempting to measure the myriad environmental variables is to consider the pathway by which these variables impact on the host cell. Unlike environmental variables, the molecular sensors and signalling pathways that link the environment to the function of immune cells are finite and increasingly well understood (Figure 1.1).

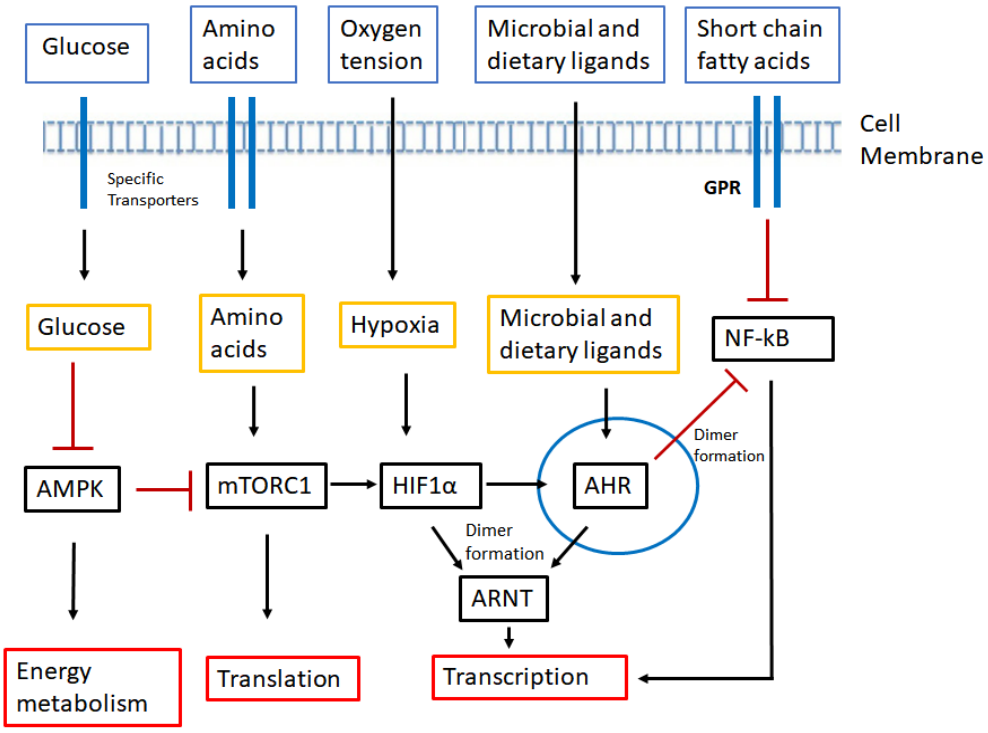

Figure 1.1: Key metabolic and environmental sensors and mechanisms that modulate immune cell function. Multiple environmental variables (in blue boxes) are detected and integrated by the interaction of transcription factors (in black boxes) which includes AHR leading to global changes in cell function (shown in red boxes). Abbreviations: Adenosine monophosphate-activated protein kinase (AMPK), hypoxia inducible factor 1α (HIF1α), mammalian target of rapamycin complex 1 (mTORC1), AHR nuclear translocator (ARNT), G-protein coupled receptor (GPR) Adapted from Ramsay and Cantrell 2015.(Ramsay and Cantrell 2015)

These environmental sensors are evolutionary conserved in structure and function (Hahn et al. 2017; Soulard, Cohen, and Hall 2009; van Uden et al. 2011). Metabolic sensors such as mammalian target of rapamycin complex 1 (mTORc1) and adenosine monophosphate-activated protein kinase (AMPK) allow the energy requirements of immune activation to be linked to nutrient availability and uptake.

Amino acid availability is sensed by mTORC1 via interactions with GTPases on the lysosomal surface. mTORC1 then stimulates translation of HIF1α, activation of (peroxisome proliferator-activated receptors) PPARs and expression of MYC leading to reprogramming from oxidative phosphorylation towards glycolysis driving proliferation of immune cells (Weichhart, Hengstschläger, and Linke 2015).

Conversely, AMPK senses falling cellular glucose states directly, and indirectly via changes in adenine nucleotides, through complex interactions with ATPase which also take place at the lysosomal surface. These pathways are closely linked. AMPK antagonises mTORC1 through phosphorylation inhibiting proliferation (Lin and Hardie 2018).

A limited number of unique transcription factors are direct environmental sensors. For example, HIF-1α functions as a direct oxygen sensor. In normoxia HIF-1α is hydroxylated, ubiquitinated and targeted for degradation. In hypoxic conditions HIF-1α is stable and can bind DNA leading to transcription.

PPARs are also directly activated by binding fatty acids including arachidonic acid, eicosanoids and other polyunsaturated fatty acids such as palmitoleic acid. PPARs heterodimerize with the retinoid X receptor leading to transcription (Berger and Moller 2002).

AHR responds to specific dietary and bacterial components as well as synthetic toxicants. There is increasing evidence that the AHR pathway, reviewed in detail here, is a critical component in the maintenance of barrier function and immune homeostasis in the intestine.

1.5 AHR signalling pathway

AHR is a ligand activated transcription factor located in the cytoplasm. Its biological importance was first recognised when it was discovered that AHR mediates the chemical toxicity, including carcinogenicity, of environmental pollutants like dioxins and specific polycyclic aromatic hydrocarbons (Poland, Glover, and Kende 1976). More recently, an additional key role in the immune system has been identified through murine studies that have shown AHR signalling plays a critical role in the maintenance and function of cells, including intra-epithelial lymphocytes and innate lymphoid cells in the intestinal mucosa (Kiss et al. 2011; Y. Li et al. 2011).

1.5.1 Classical AHR signalling

The canonical AHR signalling pathway has been characterised in detail (Denison and Nagy 2003). On ligand binding, cytoplasmic AHR translocates to the nucleus where it binds Aryl hydrocarbon receptor nuclear translocator (ARNT) and regulates gene expression by binding to xenobiotic response elements (XRE, also referred to as DRE and AHRE) in the promoter region of target genes (Figure 1.2).

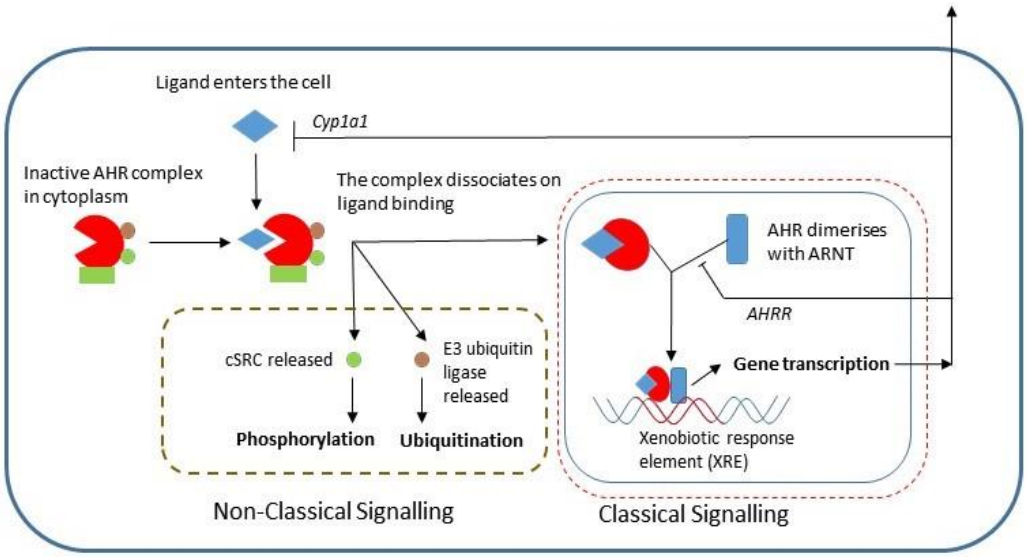

Figure 1.2 Summary of AHR molecular interactions. Cytochrome p450 family 1 member A1 (Cyp1a1), Aryl hydrocarbon receptor nuclear translocator (ARNT), proto-oncogene cellular SRC (cSRC). Classically, on ligand binding AHR translocates to the nucleus, dimerises with ARNT and promotes transcription via specific response elements (XRE). Non-classical signalling is mediated by the actions of enzymes released from the AHR complex on ligand binding including a protein kinase and ubiquitin ligase.

Classically, AHR serves a detoxifying role through upregulation of genes encoding cytochrome p450 enzymes (*CYP1A1* and *CYP1B1)*, which metabolise a wide range of organic compounds, toxins, drugs and polycyclic chemical pollutants (Denison and Nagy 2003).

CYP1A1 is part of the cytochrome p450 enzyme superfamily. CYP1A1 catalyses a key step in the metabolism of aromatic hydrocarbons, the oxidation into epoxides. Metabolites formed by the metabolism of these synthetic toxicants are carcinogenic (Beresford 1993). In fact, CYP1A1 metabolism of a variety of xenobiotic chemicals into carcinogens is implicated in the formation of a range of human cancers (Go, Hwang, and Choi 2015).

CYP1A1 also metabolises endogenous ligands such as polyunsaturated fatty acids into functionally active metabolites. CYP1A1 has monooxygenase activity in that it metabolizes arachidonic acid to 19-hydroxyeicosatetraenoic acid (19-HETE). 19-HETE is an inhibitor of 20-HETE, another active signalling molecule (Wiest et al. 2016). CYP1A1 also plays a role in omega-3-fatty acid metabolism particularly

the formation of epoxides which play a role in nitric-oxide dependent blood pressure regulation (Agbor et al. 2014) and inflammatory responses (Wang et al. 2008).

Studies in a human breast cancer cell line and mouse hepatoma cell lines showed that *CYP1A1* has the largest increase in expression, following ligand exposure, of all AHR regulated genes in these tissues, but expression of a variety of genes including those associated with fatty acid and carbohydrate metabolism (PLA2G4A, H6PD) apoptosis (I, *FAM32A*), vesicle trafficking (*ALS2CL*), drug and xenobiotic metabolism (*CYP1A1, ALDH3A1*) and tryptophan metabolism was observed in response to AHR signalling (Lo and Matthews 2012; Nault et al. 2013). AHR bound regions were also reported in genes associated with ERK/MAPK signalling (Yang et al. 2018).

It has been proposed that the expression of important immunological genes including *foxp3*, *IL10*, *IDO1* (indoleamine 2,3-dioxygenase) and *IL22* are subject to regulation by AHR. XRE are reported upstream of these genes. However, expression of *IL10* and *IDO1* has been shown to require other co-activators (Apetoh et al. 2010) while expression of *foxp3* also requires additional epigenetic regulation, via miRNA and methylation (Singh et al. 2011).

In reality like many genes, there are likely to be different AHR dependent gene expression is likely to vary between different cell types depending on the tissue context (Lo and Matthews 2012).

1.5.2 Non-classical AHR signalling: Protein-protein interactions

AHR can also signal through non-genomic mechanisms. Ligand bound AHR can activate an E3 ubiquitin ligase complex, cullin 4B (Figure 1.2) (Ohtake, Fujii-Kuriyama, and Kato 2009). This complex can ubiquitinate a variety of targets promoting their degradation. One such target is the oestrogen receptor (ERα) and this mechanism appears to mediate the anti-oestrogen effects of AHR ligands (Ohtake, Fujii-Kuriyama, and Kato 2009). In addition, inactive AHR is located in the cytoplasm as part of a protein complex with severe chaperone proteins which includes the tyrosine kinase c-SRC.

Dissociation of the complex on ligand binding releases c-SRC which phosphorylates target proteins modifying function independently of any effect on transcription (Figure 1.2) (Bessede et al. 2014).

1.5.3 Feedback regulation of AHR at multiple levels

Regulatory control of this pathway is complex and has been described at a number of levels, reflecting the importance of tight regulation of AHR controlled genes. In the nucleus of cells, the aryl hydrocarbon receptor repressor (AHRR) inhibits AHR activity by competing with ARNT for binding to AHR (Brandstätter et al. 2016) and by binding to XRE which promotes the recruitment of histone deacetylases (HDACs) inhibiting AHR promoted transcription (Oshima 2007). Transcription of AHRR itself is controlled by the AHR itself, one example of the many negative feedback mechanisms regulating AHR (Figure 1.2).

The importance of regulation by *AHRR* varies between AHR expressing cell types. AHRR is widely expressed in murine tissues. However in some tissues, for example, murine brain and cardiac tissue, AHRR expression is constitutive and not regulated by AHR (Bernshausen et al. 2006).

A study in human breast cancer cells showed the binding of AHRR does not perfectly correlate with AHR binding supporting the hypothesis that it is a context-dependent and selective repressor of AHR (Yang et al. 2018). In the intestine *AHRR* expression can be induced by environmental ligands in an AHR-dependent manner. *AHRR* expression is largely restricted to immune cells at the skin and intestinal barrier and is absent from intestinal epithelial cells (Brandstätter et al. 2016). At the intestinal barrier AHRR signalling contributes to the maintenance of colonic intraepithelial lymphocytes and prevents excessive production of IL-1β and differentiation of Th17/Tc17 cells (Brandstätter et al. 2016).

Many ligands for AHR are modified by the very cytochrome p450 enzymes they induce leading to their degradation, thereby limiting their activity. This mechanism of feedback control of AHR signalling by p450 enzymes can also occur via neighbouring cells. For example, intestinal epithelial cells can reduce AHR signalling in underlying immune cells by depleting the availability of AHR ligands (Schiering et al. 2017).

Variation in the susceptibility of ligands to degradation may contribute to the different biological effects reported in some studies (Mitchell and Elferink 2009). Certain synthetic ligands, including dioxins, resist degradation and prolonged activation of the pathway is one proposed mechanism of toxicity (Denison and Nagy 2003; Inouye, Shinkyo, Takita, Ohta, and Toshiyuki 2002). Moreover, inhibitors of cyp450 activity, such as omeprazole may be erroneously identified as AHR ligands because they inhibit degradation of a natural ligands and therefore potentiate AHR signalling indirectly (Wincent et al. 2012).

In addition to feedback inhibition by p450 enzymes, microRNA (*miR-203*) induced by AHR activation binds the 3' region of *AHR* mRNA suppressing transcription and translation (D. Li et al. 2014). Other epigenetic and post-transcriptional regulatory mechanisms have also been reported including methylation of the promotor regions of *AHR* (Reynolds et al. 2015) and *AHRR* (Zhao et al. 2013). Ligand-independent AHR activity via constitutive nucleocytoplasmic shuttling has also been proposed (Pollenz and Dougherty 2005). However, it is difficult to confidently generate ligand free environments. For example, AHR ligands can be generated from tryptophan in culture media exposure to standard laboratory light (Öberg et al. 2005).

1.5.4 AHR interactions with other signalling pathways

AHR interacts with a wide range of other signalling pathways that control immune cell function (Figure 1.3).

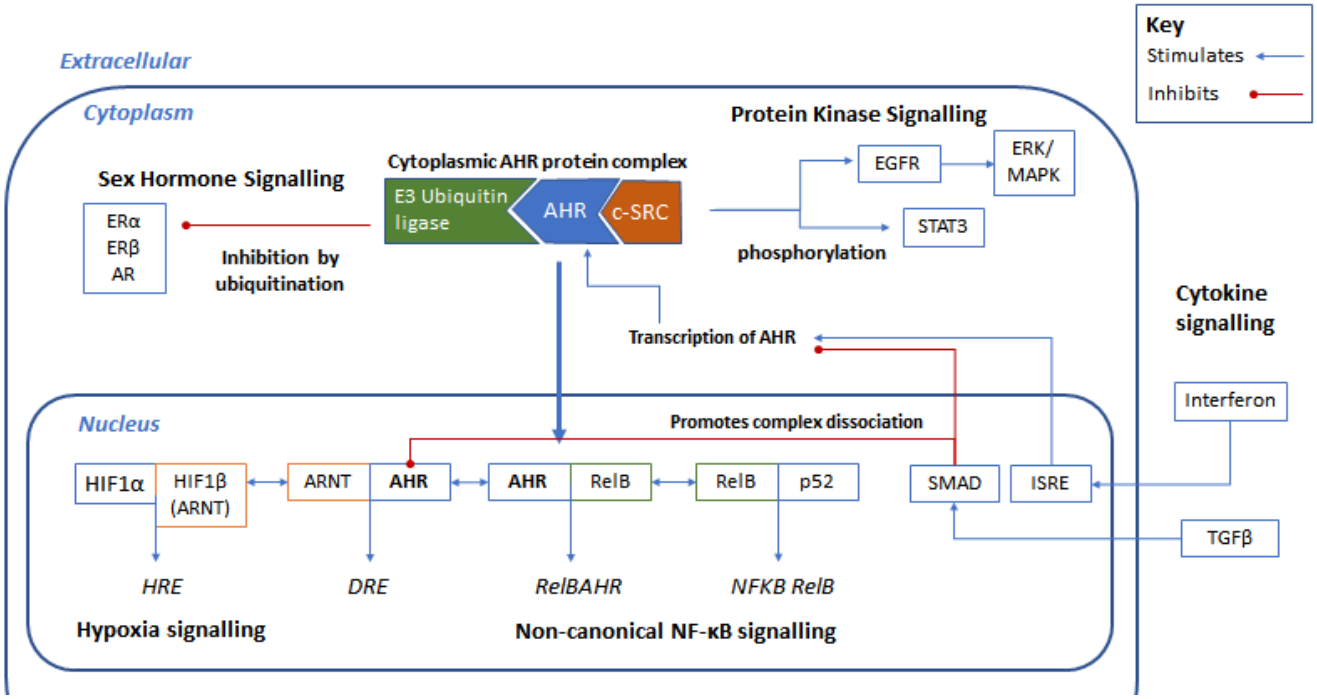

Figure 1.3 AHR interactions with other signalling pathways. Chaperone proteins in the cytoplasmic AHR protein complex are functional enzymes released on ligand binding. SRC kinase has been shown to phosphorylate STAT3, EGFR and ERK. E3 ubiquitin ligase promotes the degradation of sex hormone receptors (ERα, ERβ, AR) inhibiting these signalling pathways. In the nucleus AHR classically partners ARNT. ARNT is a shared heterodimer subunit with HIF1α (it is also called HIF1β), a key hypoxia signalling molecule. AHR can bind also bind RelB in the nucleus directly altering gene expression and indirectly inhibiting non-canonical NF-κB signalling. Extracellular cytokines also regulate AHR expression and activity. Interferon and TGFβ specific response elements have been identified upstream of AHR. TGFβ inhibits the expression of AHR and promotes AHR-ARNT complex dissociation. Interferon increases AHR expression.

In the nucleus, AHR and its heterodimer ARNT can bind other partners. For example, ARNT also binds HIF1β and AHR can bind RelB. The NF-κB/Rel complex controls transcription of many important genes mediating inflammation such as TNFα. Human and murine dendritic cell maturation is critically regulated by the NF-κB signalling pathway (Hernandez et al. 2007; van de Laar et al. 2010; Rescigno et al. 1998). AHR and RelB form a heterodimer which is capable of inducing transcription. RelBAHR

response elements are described in the promotor regions of *IL8*, *BAFF*, *IRF3* and *CCL1* (Vogel et al. 2007; Vogel and Matsumura 2009). In addition, binding RelB competitively restrict its availability and may inhibit non-canonical NF-KB signalling (Vogel et al. 2007).

Other direct and indirect interactions with immune signalling pathways are proposed. Interferon-sensitive response elements are reported in both the *AHR* and *IDO* promoter region (Dai 1990; Rothhammer et al. 2016). Type I interferons lead to increased AHR expression in astrocyte, a CNS stromal-like cell (Rothhammer et al. 2016).

In the intestine TGF-β is a key regulatory signal promoting intestinal healing. Importantly, there is evidence to suggest TGF-β dependent AHR activity is impaired in Crohn's disease (Monteleone, Marafini, et al. 2016). TGF-β has been shown to inhibit AHR signalling by promoting the dissociation of AHR and ARNT through the binding of SMAD3 (Nakano et al. 2020). Similarly, putative SMAD binding elements have been identified in the *AHR* promoter region potentially mediating inhibitory TGF-β signals (Wolff et al. 2001). Conversely loss of AHR signalling in fibroblast cell culture and mice is associated with higher TGF-β expression providing evidence of bidirectional negative feedback (Sarić et al. 2020).

It is important note both TGF-β and AHR are important for the differentiation of regulatory T-cells and Th17 cells. It maybe these signals are required at different stages of T-cell differentiation.

As previously highlighted, one route for AHR signalling is through protein-protein interactions. A ubiquitin ligase released from the AHR complex on ligand binding promotes the degradation of steroid hormone receptors particularly the oestrogen receptor (ERα) and androgen receptor (AR) inhibiting this pathway (Matthews 2013). SRC kinase, also liberated from the protein complex, has been proposed to phosphorylate a wide range of targets including STAT3, EGFR and other proteins in the ERK/MAPK pathway (Xie 2015).

The relative importance of these interactions in different tissues and contexts is not clear. Many of the interactions reported have not been studied in human cells or in the gut. Better understanding of the relationships between AHR and other immune signalling pathways and the key tissue specific effects in the intestine is important when considering the translational impact of this pathway.

1.6 AHR ligands

The first described ligands of AHR were environmental pollutants like dioxin and other toxic aromatic hydrocarbons but it is unlikely that AHR evolved to interact with these modern chemicals. More recently natural, biologically relevant candidate ligands have emerged. The most important candidates are derived from tryptophan. These compounds share aromatic hydrocarbon structures such as phenyl or indole groups.

The unequivocal identification of AHR ligands has been challenging because some molecules enhance AHR signalling without directly engaging the receptor by inhibiting negative feedback mechanisms. In addition, species differences in ligand activity are reported. For example, the agonist indoxyl sulfate exhibits 500-fold greater potency on human AHR than mouse AHR while tetrachlorodibenzodioxin (TCDD) is less potent in humans (Schroeder et al. 2010). Stemregenin1 is an AHR antagonist in humans but not mice (Boitano et al. 2010). This difference appears to be related to small structural variations in AHR between species (Fraccalvieri et al. 2013). It has also been suggested that specific AHR ligands may bind to different sites on the AHR altering the resulting conformational change and subsequent impact on gene expression (Bessede et al. 2014; Gargaro et al. 2016). Acknowledging these challenges, the strongest candidate ligands are described below.

1.6.1 Dietary ligands

The greatest source of human exposure to AHR ligands is likely to be our diet (Denison and Nagy 2003). Plants commonly contain compounds that act as AHR ligands or can be converted into ligands in the body. Cruciferous vegetables (Brassicae) contain glucobrassicin, an aromatic glucosinolate derived from tryptophan. When plant cells are damaged by chopping or chewing, they release the enzyme myrosinase which hydrolyses glucosinolates forming indole-3-carbinol (I3C). In the acidic conditions of the stomach I3C molecules combine through condensation to form potent AHR ligands like indolo-3,2-carbazole (ICZ) and 3,3-diindolylmethane (DIM) (Denison and Nagy 2003).

Although the total intake of cruciferous vegetables varies between populations, they appear to be a component of diets on all continents around the globe (IARC Handbook of Cancer Prevention Volume 9 2004).

Natural flavonoids, found ubiquitously in fruit and vegetables are also proposed as AHR ligands (Denison and Nagy 2003). A wide variety of food and herbal extracts including tea, ginseng and ginko biloba, as well extracts from corn have demonstrated AHR activation (Jeuken et al. 2003). These natural dietary ligands are susceptible to degradation by cytochrome p450 enzymes like CYP1A1 (Denison and Nagy 2003). Importantly animal models demonstrate these dietary ligands are necessary and sufficient for the maintenance and survival of specialised gut immune cells (Kiss et al. 2011; Li et al. 2011) as discussed in detail below.

1.6.2 Synthetic ligands

Cigarette smoke, diesel exhaust and other urban pollutants contain potent AHR ligands such as polycyclic aromatic hydrocarbons, polychlorinated biphenyls, and halogenated aromatic hydrocarbons (Lewis 1998). Many of these molecules bind AHR with high affinity and lead to prolonged stimulation. Some of these molecules are not susceptible to breakdown by detoxifying enzymes like CYP1A1; for example the half-life of TCDD in humans is many years (Inouye, Shinkyo,

Takita, Ohta, and Sakaki 2002; Kerger et al. 2006). This leads to vastly different kinetics of activation which is one proposed mechanism to explain differences in gene expression and effects on cell cycle observed with different ligands (Mitchell and Elferink 2009).

All AHR ligands are hydrophobic and soluble in solvents such as DMSO or ethanol. Synthetic ligands are particularly hydrophobic while indole-derived ligands such as FICZ and flavonoids have a degree of polarity (Giani Tagliabue et al. 2019). AHR ligands have been identified in extracts of paper, rubber and everyday plastics. This has particular relevance when considering analysis of the AHR pathway in the laboratory where it may be impossible to completely eliminate AHR ligands. *In-vitro* studies may in fact be a comparison of low or high AHR ligand availability.

1.6.3 Commensal microbiota derived ligands

Mammals lack the enzymatic machinery to generate potent tryptophan-derived AHR ligands. However, a wide variety of intestinal commensal bacterial species including *Lactobacilli and Clostridia* strains express the enzyme tryptophanase which allows them to synthesise potent ligands in the indole family, including indole-3-aldehyde (I3A) and tryptamine, from tryptophan (Lamas et al. 2016; Takamura et al. 2011; L. S. Zhang and Davies 2016). Some bacteria also generate other classes of AHR ligands, for example phenazine pigments (Moura-Alves et al. 2014).

In mice a wide variety of bacterial derived ligands are generated at meaningful concentrations (Jin et al. 2014). These ligands have been shown to modify immune responses and barrier function with symbiotic benefits. For example, in tryptophan-rich dietary conditions *Lactobacilli reuteri* in the murine intestine synthesise I3A from tryptophan. This leads to IL-22 production and ILC3 expansion and functionally, colonization resistance to *Candida Sp* through production of antimicrobial proteins (Zelante et al. 2013).

In murine models, the effects of these ligands are not confined to the intestine. They have a systemic impact at distant sites, for instance improving survival in models of encephalitis (Rothhammer et al.

2016; Zelante et al. 2013). Vertical transfer of bacterial ligands, which can cross the placental barrier, has also been shown to support the development of the innate immune system in the growing fetus (Gomez de Agüero et al. 2016).

1.6.4 Endogenous ligands

The importance of endogenous AHR ligands is not well understood. In the skin 6-formylindolo (3,2-b)carbazole (FICZ), a potent AHR agonist, can be generated by the direct action of UV light on tryptophan (Fritsche et al. 2007). Similar tryptophan-derived ligands can also develop in light exposed tissue culture media which may be incorrectly inferred as endogenous activity in *in vitro* experiments (Öberg et al. 2005).

The best described endogenous ligand is kynurenine, a relatively weak tryptophan derivative synthesised by mammalian cells. Processing through via the kynurenine pathway accounts for more than 90% of tryptophan metabolism (Murray and Perdew 2017). Levels of kynurenine and its metabolites increase in sepsis and IBD due to increased metabolism of tryptophan by indoleamine 2,3-dioxygenase (IDO) (Darcy et al. 2011; Nikolaus et al. 2017). However, it is not clear whether the ligands are present at sufficient levels to impact AHR signalling. The IC50 value for L-kynurenine to competitively displace TCDD is 36.2µM which is more than 10 times the concentration observed in plasma (Bessede et al. 2014; Darcy et al. 2011).

Bile pigments derived from haem degradation also have AHR activity (Denison and Nagy 2003). Patients with Gilbert's syndrome have high serum levels of unconjugated bilirubin (UCB). Gilbert's is associated with a significantly lower risk of Crohn's disease (de Vries et al. 2012). In murine models, UCB ameliorates colitis by promoting immunosuppressive responses in Th17 cells via an AHR dependent mechanism, specifically the upregulation of foxp3 and CD39 expression which depletes extracellular adenosine triphosphate (Longhi et al. 2017).

Although a variety of dietary, bacterial and endogenous ligands have AHR activity *in vitro*. The relative importance of different ligands *in vivo* is not known. When considering AHR ligands, cellular context is important. It is also likely different pharmacokinetic properties, for example half-life of activation, have different effects in the presence of different tissue specific co-activators and repressors (Brandstätter et al. 2016).

1.7 The role of AHR in immune cells

AHR is expressed by a number of different immune cells. Numerous studies have shown that AHR signalling plays important roles in the immune system in health and disease. It is recognised that AHR plays a key regulatory role in a wide variety of immune cell types (Gutiérrez-Vázquez and Quintana 2018; Rothhammer and Quintana 2019; Stockinger et al. 2014). Here, the key effects of AHR signalling in immune cells are summarised, with focus on the relevance to the intestinal immune system.

1.7.1 T-Cells

T-cells play a crucial role in intestinal disease (T. T. MacDonald 1990). AHR has important effects regulating both the differentiation and function of T-cell subsets (Carbo et al. 2014; Korn 2010).

Following activation, naïve CD4 T cells differentiate into distinct effector or inhibitory subsets depending on the cytokine and metabolic environment present at the time of antigen recognition (Dang et al. 2011). In mice, naïve T-cells lack AHR but expression is acquired during differentiation of certain sub-sets (Th17, Th22, Treg). Thus, AHR activity is important in development of Th17, Th22 which produce IL-22 as well as the regulatory populations Treg and Tr1 cells (Figure 1.4). This is discussed in more detail below.

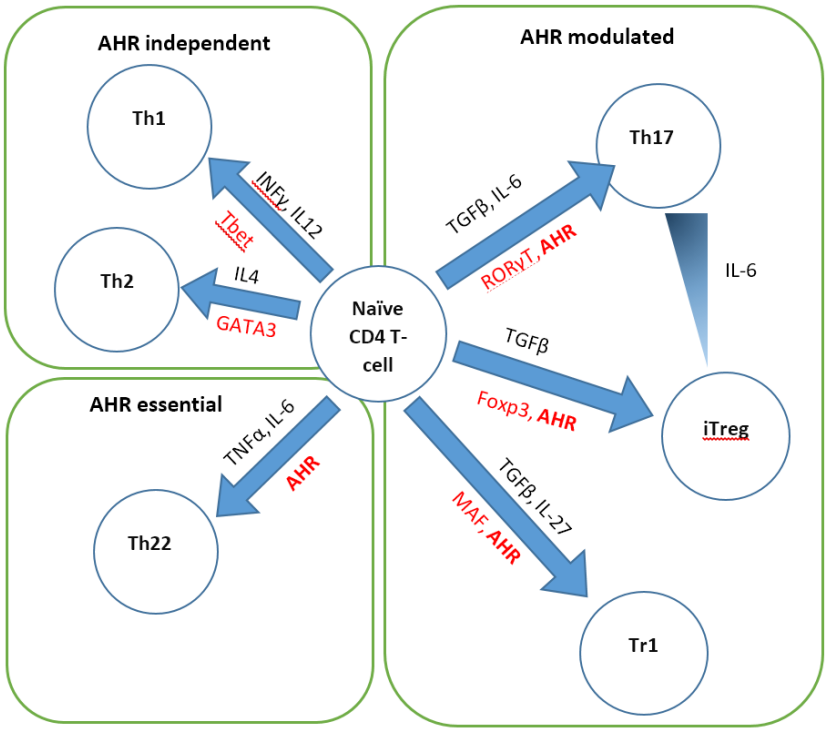

Figure 1.4: Key factors in the differentiation of murine T-cell lineages. Naïve CD4 T cells differentiate into distinct Th-cell lineages differentiate under the control of specific cytokines (Black) and transcription factors (red). Adapted from Korn 2010 and Carbo 2014.

1.7.1.1 T-helper cells

T helper cells express CD4 and have a major role in adaptive immune responses. Historically T cells were divided into Th1 or Th2 cells, defined by the cytokines they produce and the transcription factors that drive their differentiation. It is now recognised that the human CD4 compartment contains a many different T-cell subsets with which produce different characteristic cytokines (Geginat et al. 2014).

1.7.1.2 Th17 cells

Th17 cells are a characterised by the production of IL-17 regulated by *RORγt* expression (Mangan et al. 2006; Park et al. 2005). In mice, differentiation of Th17 cells requires the presence of IL-6 and TGF-β and is enhanced by IL-23. Murine and human Th17 cells express high levels of *AHR* (Veldhoen et al.

2008). Elevated levels of Th17 cells and the Th17-related cytokines IL-17, IL-21 and IL-22 are observed in both UC and Crohn's disease (Jiang et al. 2014). Inhibition of AHR or genetic deletion leads to reduced expression of IL-22 by Th17 cells (Hayes et al. 2014; Veldhoen et al. 2008). AHR binding sites have been identified in the *Il22* promotor region (Qiu et al. 2012). However, expression of *IL17* does not appear to be directly controlled by AHR. Instead, miRNA 132/212, whose expression is directly controlled by AHR, increases *IL17* expression (Nakahama et al. 2013). Addition of AHR ligands (FICZ or β-naphthoflavone) to naïve T-cells in Th17 polarising conditions increases expression of *Il17* and *Il22* whereas $Ahr^{-/-}$ mice completely lack *Il22* but not *Il17* (Veldhoen et al. 2008). Thus IL-22 but not IL-17 production in Th17 cells is dependent on AHR.

Th22 cells, a distinct subset of T-cells which produce IL-22 but not IL-17, have been described in humans and mice (Trifari et al. 2009; Zheng et al. 2007). These cells are defined by expression of *IL22* and AHR is essential for the development of this population (Carbo et al. 2014), (Heller et al. 2012). IL-22 is a member of the IL-10 family and acts on epithelial cells and other non-immune populations to promote the integrity of the epithelial barrier. IL-22 acts primarily on non-immune cells, for example leading to increased production of mucin by goblet cells and production of innate antimicrobial peptides like Reg3γ, as well as β-defensins and calprotectin by intestinal epithelial cells (IEC) and Paneth cells (Dudakov et al. 2015). It drives proliferation of intestinal stem cells facilitating repair after injury (Lindemans, Calafiore, Mertelsmann, Margaret, et al. 2015). Th22 cells play an important role in barrier repair in mouse models and have been shown to be depleted in ulcerative colitis (Basu et al. 2013; Leung et al. 2014).

1.7.1.3 Th1 and Th2 cells

Th1 cells are characterized by high production of IFN-γ and are play a critical role in the clearance of intracellular pathogens. IFN-γ and IL-12 drive the differentiation of Th1 cells while IL-4 is crucial for the differentiation of Th2 cells. Th2 cells are a key component of the host defence against extracellular

pathogens (Korn et al. 2009). Expression of *AHR* is reportedly much lower in Th1 and Th2 lineage cells. Although this difference is less marked in humans than mice (Veldhoen et al. 2008).

1.7.1.4 Regulatory T-cells

Inducible regulatory T cells generated from naïve CD4+ cells play a critical role in limiting immune reactivity to the commensal microbiota. The development of foxp3+ Treg cells is closely, but reciprocally, related to Th17 cells (Quintana et al. 2008). *AHR* is expressed by foxp3+ Treg cells and is one of the defining transcription factors of this subset (Hill et al. 2007). XRE have been identified in the promoter region of *foxp3* in mice (Quintana et al. 2008).

However, there are conflicting reports about the impact of AHR ligands on the development of foxp3+ Treg. For example, TCDD slightly increased the number of foxp3^{+} Treg generated from naïve T-cells, while FICZ did not have this effect (Quintana et al. 2008). Other groups found neither FICZ, nor deletion of AHR affected foxp3+ Treg numbers, although this does not preclude an impact on function after differentiation. These differences maybe depend on cellular context, for example differences in the amount of TGFβ, IL-2 or TCR co-stimulation. Differences between ligands may also explain divergent results in different models of inflammatory disease. TCDD and ITE are reported to ameliorate experimental allergic encephalitis (EAE, a model of multiple sclerosis) while FICZ worsens it. Ligand variable effects are also reported in human naïve T-cell differentiation. For example, in a murine study of naïve T-cell differentiation (using anti-CD3 & anti-CD28 antibodies, TCDD led to an increase in Treg and reduction in Th17 cells while FICZ led to opposite findings, increased Th17 and reduced Treg differentiation (Quintana et al. 2008). In a separate study differentiation of T-cells in the presence of TGFβ and IL-6 the addition of FICZ or β-naphthoflavone had no impact on Treg differentiation but increased the differentiation of Th17 cells. The differences in ligand pharmacokinetic properties that explain this are not clear and were already considered above. It also been proposed that differential

activation of classical (DRE mediated) AHR signalling and non-classic signalling (via protein kinases or ubiquitination) may also contribute to variable effects between ligands (Mohinta et al. 2015).

Type 1 regulatory (Tr1) cells are another type of inducible regulatory cell which lack foxp3 but also effect regulatory responses via IL-10. *IL10* transcription by Tr1 cells depends on transactivation by both the transcription factors c-maf and AHR. Blockade of AHR by miRNA reduces but does not completely inhibit IL-10 production or Tr1 differentiation suggesting a synergistic but not essential role for AHR (Apetoh et al. 2010).

One of the challenges when examining the impact of AHR on different T-cell subsets is that T-cells exhibit mixed polarity and subset plasticity (Geginat et al. 2014). For example, co-expression of Th17 and Treg signature genes has been reported in the same cells (Beriou et al. 2009). Th17 cells have also been shown to lose expression of IL-17 and start expressing *LAG3* and *IL-10* (markers of Tr1 cells (Geginat et al. 2014). AHR activation enhances this Th17 – Tr1 trans-differentiation, in the presence of TGF-β (Gagliani et al. 2015). Studies have shown murine Tregs can trans-differentiate into Th17 subsets. Importantly human intestinal Tregs and Th17 cells can acquire different phenotypes in IBD including Th22 (Gagliani et al. 2015; Komatsu et al. 2014; Ueno et al. 2015).

1.7.2 Intestinal epithelial lymphocytes (IEL) and innate lymphoid cells (ILC)

Other specialised lymphoid lineage cells rare or absent in the circulation are enriched at the intestinal barrier. The intestinal epithelium contains large numbers of IELs that promote barrier function. Most IELs express a TCR and can be divided based on expression of either αβ TCR which are most abundant or γδ TCR, which comprise approximately 15% of IELs (Nielsen, Witherden, and Havran 2017). Most IELs either enter the epithelium after antigen encounter in the periphery or immediately after

development (Olivares-Villagómez and Van Kaer 2018). These cells provide the first line of defence against pathogens. Studies in AHR-/- mice have shown a profound deficiency in the proportion and numbers of TCRγδ and TCR αβ+CD8αα+ IELs in the small intestine soon after birth and again the effects seems to due to an absolute requirement for AHR signalling for the survival of these cell populations beyond weaning age (Y. Li et al. 2011). A dependence on AHR signalling is not confined to populations in the intestine. Epidermal dendritic epidermal T-cells (DETC), which express invariant Vγ5Vδ1 T-cell receptors reside in the murine epidermis and detect injury, and CD69+ skin resident memory T cells, both require AHR for their maintenance (Kadow et al. 2011; Zaid et al. 2014). Neither study reported the effects on conventional αβ T-cells.

Innate lymphoid cells (ILC) are a family of innate immune cells that lack the recombination activating gene (RAG) meaning they do not express antigen specific receptors (Vivier et al. 2018). There are several distinct ILC populations with distinct patterns of cytokine production that closely mirror the cytokine production profiles of T helper cell subsets (Spits et al. 2013).

Group 3 ILCs (ILC3) are defined by the production of the cytokines IL-17 and/or IL-22. They share defining transcription factors like RORγt with Th17 (Rankin et al. 2013). IL-22 producing ILC3 constitute the majority of ILCs in the healthy intestine. In the murine intestine, ILC are the dominant source of IL-22 early in the inflammatory response, but CD4 T cells produce IL-22 in response to IL-6 as this increases later in inflammation (Gury-BenAri et al. 2016; Trifari et al. 2009).

Like the specific IEL previously describe, the maintenance of ILC3 in the intestinal mucosa critically depends on the AHR. In AHR-/- mice there is no defect in the proliferation and tissue accumulation of these cells. However, the persistence of the cells in the mucosa is impaired suggesting a tonic AHR signal may be required to maintain this population. Again this difference was only observed beyond weaning age (Qiu et al. 2012). A number of potential mechanisms for this have been described

including the inhibition of apoptosis (Qiu et al. 2012) and prevention of the conversion of ILC3 to ILC1 (J. Li, Doty, and Glover 2016).

Loss of ILC3 was associated with reduced expression of several antimicrobial peptides including Reg3γ and S100A9, a subunit of calprotectin, and Muc2 mucin (Kiss et al. 2011; Metidji et al. 2018).

Group 1 ILCs, which includes NK cells, express AHR and respond to AHR ligands. AHR is required for the maintenance of liver-resident natural killer cells (L. H. Zhang et al. 2016). The impact of AHR signalling in ILC1 in the intestine is not well described.

Group 2 ILCs play an important role in the immune response to helminths and show some homology with Th2 cells. AHR signalling has been shown to reduce the number of ILC2 and inhibit expression of the key cytokines IL-5 and IL-13 (S. Li et al. 2018).

1.7.3 Dendritic cells

Dendritic cells (DC) residing in the intestinal mucosa form a close network, optimally positioned to sense the local environment and regulate intestinal responses. Dendritic cell function depends on their activation state and localisation. Mirroring T-cells, the effect of AHR ligands on DC function is complex and depends on context. Numerous studies have shown AHR signalling can influence both DC development and function.

AHR signalling favours the differentiation of monocytes to DC-like cells rather than macrophages (Goudot et al. 2017) and can influence their maturation status as determined by expression of MHC molecules (Bankoti 2010; Vogel et al. 2013). Studies in murine bone marrow derived DC (BMDC) show a range of AHR ligands increase DC maturation (expression of MHC II) and co-stimulatory capacity (CD86). AHR ligands can promote the regulatory activity of human and murine DC by inducing expression of the enzymes IDO1 & 2 (indoleamine 2,3-dioxygenase) (Vogel 2008; Vogel et al. 2013). IDO enzymes catabolise tryptophan to kynurenine. Depletion of tryptophan by this process can

indirectly inhibit activation of effector T cells (Fallarino et al. 2006; Nguyen et al. 2010) while kynurenine can promote regulatory T cell development (Nguyen et al. 2010).

Studies in murine DC have shown AHR induces *IDO* transcription via XRE (canonical signalling) and c-SRC-mediated phosphorylation (Bessede et al. 2014; Vogel 2008). Importantly, the degradation product IDO generates (kyunerenine), is itself an AHR ligand, thus forming another positive feedback loop. AHR signalling also induces a tryptophan-selective amino acid transporter in mouse DC and human colonic epithelial cells providing another positive feedback mechanism by which tryptophan can be depleted (Bhutia, Babu, and Ganapathy 2015). Tonic depletion of tryptophan via these feedback mechanisms may help limit immune reactivity to the intestinal microbiota.

1.8 The role of AHR on non-immune cells in the intestine

1.8.1 Epithelial cells

Intestinal epithelial cells (IECs) provide a barrier that separates the host from the commensal bacteria and food in the lumen of the gut. The majority of cells lining the intestine are absorptive enterocytes. However, a variety of specialised IECs perform functions crucial in the maintenance of the intestinal barrier and physiological immune function. Specialised secretory IECs called goblet cells, secrete mucins and antimicrobial peptides. Microfold cells (M-cells) mediate transport of luminal antigens and bacteria across the epithelial barrier to antigen presenting cells. Like haematopoietic immune cells, epithelial cells express pattern-recognition receptors like TLRs and NOD-like receptors which recognise luminal microbiota leading to cytokine production (Peterson and Artis 2014).

Signals from the intestinal microbiota are essential for the maintenance of the intestinal barrier. It has long been known that IECs derive the majority of their energy from short chain fatty acids (SCFAs) generated by intestinal bacteria (Roediger 1980). More recently, using a human intestinal epithelial cell line containing a reporter, it has been shown that SCFAs such as butyrate are also ligands for AHR

(Marinelli et al. 2019). However, the functional impact and relative importance of this signalling, compared to classical signalling through cell surface G-protein coupled receptors, is not known.

Global or epithelial cell specific deletion of AHR leads to increased inflammation and development of colorectal cancer (derived from epithelial cells) in murine models (Ikuta et al. 2013; Metidji et al. 2018). AHR signalling promotes crypt stem cell differentiation through inhibition of Wnt signalling (Metidji et al. 2018). However, it appears excess of AHR signalling is also harmful. Mice exposed to TCDD developed wide intercellular spaces in villi leading to malabsorption (Ishida et al. 2005).

The effects of AHR may vary between specialised IECs. For example, in mice, genetic deletion of AHR led to the loss of goblet cells via impaired differentiation but this effect is not seen in enterocytes generally. A murine studied showed the AHR ligand promotes goblet cell maturation and mucus production via up-regulation of Muc2. It is not known if other secretory cells are affected (Yin et al. 2019).

The impact of AHR on cytokine and anti-microbial peptide production is also not clear. It can be difficult to determine whether the effect on a particular cell type of manipulating AHR, is due to altered activity within that particular type of cell, or secondary to altered activity within another cell in the same model.

For example, ILC3, known to be highly dependent on AHR, drive the expression of antimicrobial peptides such as calprotectin and RegIIIγ in epithelial cells (Zelante et al. 2013). However, a more recent study has shown tissue specific deletion of AHR in CD11c-expressing cells (antigen presenting cells) leads to significantly impaired goblet cell differentiation and mucin expression (Chng et al. 2016). Thus, the dominant effect of AHR on epithelial cells may be indirect via the impact on immune cells.

These indirect effects of AHR are also seen in the other direction. CYP enzymes are a family of enzymes that oxidise a wide variety of compounds and are important in drug, toxin and steroid metabolism. As

discussed above, the expression of genes in the CYP1 family are highly regulated by AHR and metabolise many AHR ligands forming a natural negative feedback loop. In another tissue-specific murine model *Cyp1a1* was constitutively over expressed in IECs. This led to depletion of ILC3 and Th17 cells mimicking the AHR-/- phenotype. This phenotype could be reverse by increasing intake of AHR ligands in the diet (Schiering et al. 2017). This study suggests IEC may serve an important role in regulating AHR ligand availability.

1.8.2 Intestinal stromal cells

A variety of stromal cells are found in the intestinal lamina propria forming the supportive structure or connective tissue. These include myofibroblasts, fibroblasts, endothelial cells and other uncommon cells. Compared with the intestinal immune system, our knowledge about the origin, composition and role of different stromal populations in homeostasis and disease is sparse (Owens 2015; Owens and Simmons 2012).

Stromal cell activation occurs during inflammation. This can trigger behaviours analogous to haematopoetic immune cells, for example cytokine and chemokine production and thus indirect activation of innate immune cells. Importantly, activation of stromal cells leads to upregulation of cellular adhesion molecules and collagen production and subsequent fibrosis which is a key pathogenic process in Crohn's disease (Owens and Simmons 2012).

The first studies of AHR knockout mice identified bile duct and liver fibrosis (Fernandez-Salguero et al. 1995). Subsequent studies in mice and humans showed AHR is expressed in fibroblasts. However, the genes regulated by AHR are different to those observed in immune or hepatoma cells. Murine embryonic fibroblasts or human mammary fibroblasts showed very little expression of *CYP1A1* and its expression did not change with addition of TCDD. (Beedanagari, Taylor, and Hankinson 2010; Eltom, Larsen, and Jefcoate 1998). However, *CYP1B1* expression did seem to be AHR regulated in these

tissues. Individual genes regulated by AHR vary between tissues but no transcriptomic studies of this have been published in fibroblasts.

Other groups have examined the impact of AHR on cultured human intestinal fibroblasts. Incubation with AHR ligand inhibited TGFβ induced collagen production (Monteleone, Zorzi, Marafini, Di Fusco, Dinallo, Caruso, Izzo, Franz, et al. 2016). The impact on other fibroblast genes and function is not known. A point of caution is highlighted in another study which shows the selection of adherent cells and repeated passaging leads to higher AHR expression and exaggerated responses to AHR ligands (Eltom, Larsen, and Jefcoate 1998). Cultured fibroblasts, offer the practical advantage of convenience, but do not encompass the variety of stromal cells found *in-vivo* in the intestine, which include subepithelial myofibroblast and other specialised cells (Strong et al. 1998). They also do not allow modelling of the interactions between immune cells and stromal cells. It is important to acknowledge these limitations when drawing conclusions about the role of AHR from examination of these cells alone.

1.9 The AHR-microbiota axis

The gut microbiota plays a fundamental role in the development and normal function of the host immune system. Over millennia an interlinked host-microbiota axis has developed in which the host and bacteria communicate and influence each other. This process depends on the interaction of many different immune cells and a variety of signalling pathways.

From birth innate immune cells are able to recognise microbe-associated molecular patterns via toll-like receptors (TLRs) and other pattern recognition receptors. Exposure to TLR ligands from the microbiota early in life programs tolerance in adult life through mechanisms such as histone acetylation (Alenghat et al. 2013). Treg cells play a key role in the tolerance of commensal bacteria through suppression of inflammation and regulation of IgA responses. These effects have been shown to increase bacterial diversity (Kawamoto et al. 2014).

Many bacterial metabolites directly influence immune cell function in the gut. SCFA, which are produced from dietary fibre by gut bacteria, activate G protein-coupled receptors in by epithelial and immune cells. These SCFA have been shown to suppress the response of intestinal macrophages to commensal colonic bacteria (Chang et al. 2014).

Bile acids secreted into the intestine are metabolised by bacterial 7α-dehydroxylase expressed by *Clostridium* and *Eubacterium* into secondary bile acids such as deoxycholic acid and lithocholic acid. These bacterial metabolites act on G-protein bile acid receptor 1 (GPBAR1) and Farnesoid-X-Receptor (FXR) in macrophages to promote tolerogenic M2 macrophages (Biagioli et al. 2017).

Complex interactions between the host and intestinal microbiota are mediated through AHR. The composition of the intestinal flora is influenced by AHR driven responses and generation of AHR ligands by bacteria modulates inflammation in a variety of murine models with symbiotic outcomes.

In the healthy gut, the microbiota is largely comprised of anaerobes. The dominant phyla are bacteroidetes and firmicutes (including *Clostridia* and *lactobacillales*). An altered gut microbiome is observed in *Ahr-/-* mice and mice fed a diet deficient in AHR ligands (Y. Li et al. 2011; Qiu et al. 2013). There are significant increases in segmental filamentous bacteria (SFB), *Bacteroides* and *Verrucomicrobia*. These microbial changes are also associated with an increased inflammatory tone including expanded Th17 and CD14+ populations, reduced *IL22* expression and increased expression of acute phase proteins (for example; SAA1) (Murray et al. 2016). Microbial transfer from *Ahr*-/- to heterozygous *Ahr+/-* mice leads to increased inflammation in recipient mice. A divergence in microbiota is exaggerated when Ahr null and heterozygous mice are separated after co-housing. Metabolomic analysis shows significant decreases in short chain fatty acids (SCFA) with in the luminal content of *Ahr*-/- mice (Murray et al. 2016). Conversely, AHR ligands reduce ratio of firmicute to bacteroides and reduce SFB and Clostridia species (Korecka et al. 2016). Certain subsets of Bacteroides and Clostridia are known to induce Tregs (Kamada and Núñez 2013).

AHR ligands also alter the metabolic activity of the microbiome. Mice fed tetrachlorodibenzofuran (TCDF) a potent synthetic AHR ligand developed a reduced Firmicutes/Bacteroidetes ratio and significantly elevated the levels of the short SCFAs propionate and n-butyrate determined by H-NMR based metabolomics of faeces and caecal contents (L. Zhang et al. 2015). Supplemental SCFA particularly sodium butyrate have been shown to ameliorate colitis in mouse models (Guangxin Chen et al. 2018). However, the evidence of benefit on IBD is less clear with small or statistically insignificant benefits despite decades of clinical studies and efforts to optimise the delivery of butyrate to the colon (Facchin et al. 2020; Vernia et al. 2000).

AHR signalling alters the composition of the microbiota through different mechanisms. In mice, *lactobacilli* have been shown to have the ability to metabolise tryptophan generating the AHR ligand I3A which promotes increased IL-22 production via an expansion of Group 3 ILC. In turn, this IL-22 response promotes survival of some microbial communities, like the *lactobacilli*, but also suppresses the fungus *Candida albicans* (Zelante et al. 2013).

The enzyme fucosyltransferase 2 catalyses fucosylation of intestinal epithelial cells. In a murine antibiotic model, *Fut2* expression by IEC in response to AHR-regulated IL-22 and LTα, derived from ILC3, was reduced by exposure to a cocktail of antibiotics showing the importance of bacterial ligands (Goto et al. 2014). Epithelial fucosylation allows colonization by commensal bacteria including *Bacteroides species* which can metabolise fucosylated protein as a source of energy (Goto et al. 2014; Pacheco et al. 2012). Impaired fucosylation was associated with higher bacterial load and worse outcomes with the enteropathogenic bacterium *S. typhimurium*.

Thus, host AHR can modify the microbiota and the microbiota can modify host immune responses.

Recent work provides further insight into this complex relationship. Mice deficient in *CARD9*, an adaptor molecule that integrates signals from diverse fungal pattern recognition receptors and the bacterial-sensing NOD2 pathway, develop a dysbiosis that results in a reduced capacity to generate AHR ligands (Lamas et al. 2016). This reduction in AHR ligands results in reduced IL-22 and worse

outcomes in the DSS colitis model. Transfer of this abnormal microbiota alone to wild-type mice recreates the phenotype or the genetic knockout whereas transfer of wild-type microbiota, *Lactobacilli* strains known to synthesise AHR ligands, or addition of FICZ restores IL-22 responses and protects against colitis (Lamas et al. 2016). Thus, dysbiosis of any cause, in this example host deficiencies in microbial sensing pathways, not directly related to AHR, can impair synthesis of AHR ligands by the intestinal microbiota leading to impaired AHR activation and inflammatory consequences.

AHR does not have uniformly beneficial effects on the gut microbiome. IL-22 induces the expression of antimicrobial proteins such as lipocalin-2 and calprotectin which sequester iron and zinc and can suppress the growth of the commensal flora (for example, *Enterobacter*). Other pathogenic bacteria (for example*, Salmonella typhimurium*) are able to overcome these effects through alternative siderophores and zinc transporters (Behnsen et al. 2014).

In addition, there may be pathogenic organisms that have evolved to commandeer this process for parasitic gain. For example, *Malezzia* yeast, a skin commensal and opportunistic pathogen, can also generate AHR ligands which inhibit immune responses against the yeast but influence the development of skin infections, dermatitis and basal cell carcinomas (Gaitanis et al. 2012). Similar interactions could be important in the intestine.

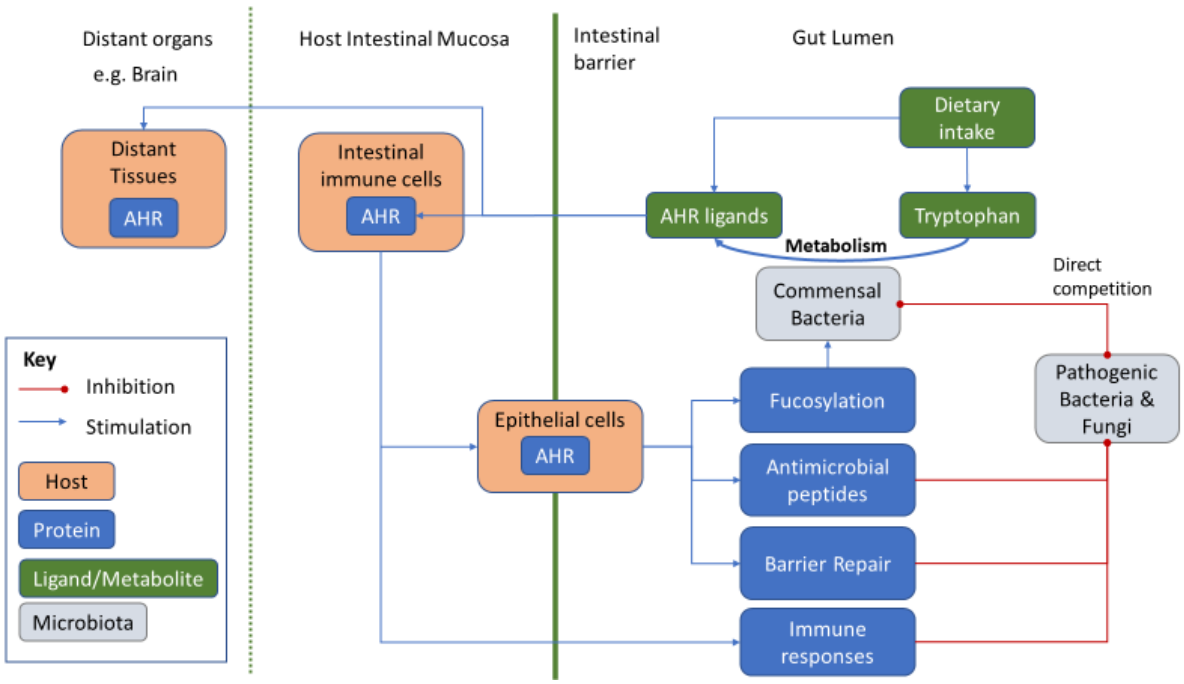

Figure 1.5: AHR mediates a symbiotic relationship between host and commensal bacteria to maintain the intestinal barrier and suppress pathogens. Commensal intestinal bacteria can synthesis potent AHR ligands from tryptophan which have been demonstrated to alter host intestinal mucosal immune responses. These include promoting the expression of *IL22* which drives the expression of antimicrobial peptides, crypt proliferation and fucosylation in epithelial cell function which supports the commensal flora in a symbiotic manner and supports immunosuppression and repair responses to pathogenic bacteria and fungi

To summarise, intestinal bacteria are a key source of AHR ligands. However, the relationship between host, and commensal or pathogenic bacteria is complex and interdependent. There are a number of examples where bacteria-derived AHR ligands influence the host to suppresses competitor pathogens or provide nutritional support for commensal bacteria which appear clearly symbiotic.

1.10 The impact of AHR signalling in murine models of gastrointestinal disease

1.10.1 Murine models of colitis

The important effects of AHR signalling on intestinal immune and non-immune cells described above highlight a crucial role in regulatory responses and maintaining the integrity of the intestinal barrier.

Whole organism mouse models of gastrointestinal disease have proved invaluable in understanding the relevance of these effects *in-vivo*.

Ahr knockout mice show reduced accumulation of lymphocytes in the periphery including the intestine, altered intestinal mucous secretion and development of spontaneous mild colitis (Fernandez-Salguero et al. 1995; Gonzalez and Fernandez-salguero 1998). This pathology appears dependent on pathogens in the housing environment and is not observed in microbe-free environments (Schmidt et al. 1996).

In diverse mouse models of colitis, stimulating AHR improves outcomes, whilst reducing AHR activity is harmful (summarised in Table 1.3). Immunological analyses in these models indicate that mechanisms for this anti-inflammatory effect are broadly consistent with *in-vitro* experiments. A number of groups have demonstrated reduction in Th17 responses and reciprocal increased *foxp3* expression and Treg numbers in the lamina propria (Huang et al. 2013; Singh et al. 2011). Reduced AHR signalling results in increased colonic TNFα, IL-1β, INFγ and IL-6. Increasing AHR signalling leads to a reduction in these cytokines with increased IL-22.

Many models generate a low AHR state through global genetic deletion however it is worth highlighting a key study which restricted AHR activity through the use of a diet low in AHR ligands (Y. Li et al. 2011). In this study 3% DSS was administered to mice for 6 days. A full recovery in weight was seen in control mice while in mice fed a low AHR diet weight loss was accelerated and did not recover after withdrawal of DSS. Crucially supplementation with the AHR ligand indole-3-carbinol actually led to less severe colitis and weight loss than control animals (Y. Li et al. 2011).

AHR manipulation		Model of colitis	Systemic Impact	Immune Effects
Low AHR activity				
Ahr-/-		DSS	**↑weight loss** **↑colitis**	↑TNFα ↑IL-1β ↑IL-6 (Furumatsu et al. 2011)
		Tcell-transfer-induced colitis	**↑weight loss** **↑colitis**	↑INFγ ↑IL-17
Low AHR ligand diet		DSS	**↑weight loss** **↑colitis**	↓IEL ↑INFγ (Y. Li et al. 2011)
Low AHR ligand production by bacteria		DSS	**↑weight loss** **↑colitis**	↓IL-22 (Lamas et al. 2016)
High AHR activity				
AHR Ligand:	TCDD	DSS	**↓weight loss** **↓colitis**	↑PGE2 ↓TNFα (Takamura et al. 2010)
		Trinitrobenzene sulphonic acid		↑Treg ↓IL-6, IL-12 ↔IL-10, IL-17 (Benson and Shepherd 2011)
	Sulforaphane	DSS	**↓weight loss** **↓colitis**	↓IL-6, IL-1β ↓TNFα, ↓INFγ (Wagner et al. 2013)
	DIM	Oxazolone	**↓weight loss** **↓colitis**	↓Th17 ↑Treg ↓ERα ↓GATA3 ↓IL-4, IL-5, IL-10, IL-17 (Huang et al. 2013)
	FICZ	DSS	**↓weight loss** **↓colitis**	↑IL-22, ↓TNFα, ↓INFγ (Monteleone et al. 2011) ↓IL-7 (Ji et al. 2015)
		T-cell transfer colitis		

Table 1.3: Outcomes from mouse models of colitis with different AHR manipulation. In diverse mouse models of colitis inhibiting AHR by deletion or dietary restriction leads to worse outcomes while increasing AHR activity with a variety of AHR ligands is beneficial.

1.10.2 Murine models of gastrointestinal infection

AHR-dependent pathways are also important in control of gastrointestinal infections in mice. *Citrobacter rodentium* is a prototypal Gram-negative bacterial pathogen of mice which causes an

infectious colitis. Control of *C. rodentium* infection is dependent on IL-23 and IL-22 (Satoh-Takayama et al. 2009). RORγt^{+} ILCs in *Ahr*-/- mice are unable to produce IL-22 in response to IL-23. This is associated with reduced survival from this infection (Qiu et al. 2012).

Listeria monocytogenes replicates in the gastrointestinal tract, causing Listeriosis, a major source of foodborne illness in humans. Following infection with *L. monocytogenes*, *Ahr*-/- mice had higher bacterial titres of *Listeria* with delayed clearance of the pathogen (Kimura et al. 2009).

Prior supplementation with I3C protects mice from *Clostridium difficile* associated pathology. Mice fed a standard diet showed severe weight loss with 50% mortality by day 3. Mice fed a diet deficient in AHR ligands also showed a more severe onset of disease while mice fed a diet supplemented with I3C were protected (Julliard et al. 2017). AHR activation with TCDD suppresses lymphocyte numbers and antibody production in response to *Leishmania major* infection although perhaps counterintuitively, treatment with TCDD was also associated with a reduced parasite burden (Bowers et al. 2006). *Toxoplasma gondii* is a protozoan carried by millions of people worldwide. *Ahr*-/- mice showed reduced survival with more liver damage than wild-type mice following infection with *T. gondii* (Sanchez et al. 2010).

An important limitation of these studies is that the composition of the resting microbiota, is not considered. This makes it difficult to determine if the impact of AHR deletion or altered diet is also caused by altered intestinal bacteria (dysbiosis) or changes in the host immune response alone.

Low AHR activity (Ahr$^{-/-}$ or low AHR ligand diets)	**Activated AHR (Supplemental AHR ligands)**
↑ Mortality from *Clostridium difficile*	↓ Mortality from *Clostridium difficile*
↑*Listeria monocytogenes* titres but variable pathology	↑ Leishmania burden but reduced pathology
↑ Mortality from *T. gondii*	
↑ Mortality from *Citrobacter rodentium*	

Table 1.4: Summary of impact of AHR in models of infection AHR influences the outcome in these different infections in mice.

1.10.3 Murine models of colon cancer

There has been considerable interest in the role of AHR in cancer biology. Many of the effects of AHR signalling described could theoretically influence the initiation, progression and metastasis of cancer.

Immune checkpoint signals are recognised as an important mechanism of tumour escape from immune surveillance. Inhibition of these pathways through monoclonal antibody are established therapies for many cancers including colorectal cancer (Altmann 2018). The immunoregulatory consequences of AHR activation could impair immune-surveillance and anti-tumour cytotoxic actions.

Increased production of pro-angiogenic factors and altered extracellular matrix by fibroblasts and endothelial cells could influence growth and metastasis. AHR also directly influences transcription of genes involved in apoptosis and the cell cycle (Sartor et al. 2009).

However, there is conflicting data from experimental models and epidemiological evidence regarding the carcinogenic effects of AHR activation. For example, in rodents, long-term TCDD treatment leads to the development of extra-intestinal tumours (liver, thyroid, skin and lung). These observations led to the assumption TCDD is also a human carcinogen. However, a critical review of epidemiologic studies of occupational and community exposure to dioxins found no increased relative risk of cancer overall (Cole et al. 2003).

The impact of AHR deletion has been examined in Ahr-/- mice. In some studies, *Ahr*-/- mice exposed to normal laboratory intestinal flora spontaneously develop caecal tumours and intestinal inflammation, although this effect is only observed after 12 weeks of age (Kawajiri et al. 2009). This may explain why other studies have not reported this observation; many others only examined mice under this age (Y. Li et al. 2011; Zelante et al. 2013). It is also not clear if the development of cancer is

secondary to specific alterations in microbiota, intestinal inflammation seen in these mice or a loss of tumour suppressive effect from an inhibition of anti-cancer immune responses.

β-catenin is a subunit of the cadherin protein complex and acts as an intracellular signal transducer in the Wnt signaling pathway (B. T. MacDonald, Tamai, and He 2009). β-catenin is also proto-oncogene; mutations and overexpression of β-catenin are associated with many cancers (B. T. MacDonald, Tamai, and He 2009). *Ahr*-/- mice do show higher levels of intestinal β-catenin and its downstream target c-myc, while AHR ligands, acting via the non-classical signalling pathway, enhance E3 ubiquitin ligase activity leading to degradation of β-catenin (Kawajiri et al. 2009). Germ free *Ahr*-/- mice do not spontaneously develop intestinal cancer suggesting interaction with microbiota and associated intestinal inflammation are essential for tumour development (Ikuta et al. 2013).

The combination of AHR modulation with models of colorectal cancer has proved more informative. AHR deletion increases tumour burden in a colorectal cancer model (APC Min/+) (Kawajiri et al. 2009). ASC, a murine homolog of *PYCARD*, mediates apoptosis via the activation of caspase. ASC−/− mice rarely develop spontaneous intestinal tumours. *Ahr*-/- ASC-/- knockout mice show reduced intestinal inflammation and reduced spontaneous tumour development, compared to *Ahr*-/- mice, suggesting that the inflammatory state in Ahr-/- mice contributes to tumorigenesis (Ikuta et al. 2013).

The addition of the carcinogen azoxymethane to the DSS colitis model leads to the development of colitis-associated colorectal tumours after 16 weeks (Díaz-Díaz et al. 2016). Tumour burden is increased in Ahr-/- mice but the induction of tumours can be reduce by 92% by the co-administration of an AHR ligand (I3C) showing the degree of AHR activation has an impact on tumour development (Díaz-Díaz et al. 2016).

Taken together these data from a variety of mouse models show that loss of *Ahr* increases tumorigenesis but it remains unclear if this is due to direct effects on colonic epithelial cells or to indirect effects on the microbiota or immune response. Tissue specific genetic deletion of AHR

combined with host genetic and microbiome analyses may lead to a better understanding of this process.

1.10.4 Murine models summary

In summary, murine models have shown diet and intestinal bacteria are a key sources of AHR ligands. Outcomes in a variety of models of intestinal infection, inflammation or cancer are worse when key bacteria, ligand precursors (e.g. tryptophan) or enzymes are absent resulting in a loss AHR signalling. The relationship between host, apparently commensal or pathogenic bacteria and fungi is complex and interdependent. There are a number of examples where bacteria-derived AHR ligands influence the host to suppresses competitor pathogens or provide nutritional support for commensal bacteria which appear clearly symbiotic.

A number of unanswered questions remain. What is the relative importance or redundancy of bacteria-derived and dietary ligands? Most murine models have used global AHR deletion or manipulation. In which cells is AHR activity most important and how does its function differ in different cells in the intestinal mucosa? Finally, how important are these findings to human health. Are there individuals with low ligand exposure and importantly, would augmenting AHR improve intestinal health or outcomes in human intestinal inflammatory bowel disease or infection? A summary of the evidence for the impact of AHR in human intestinal inflammation with a particular focus on IBD follows.

1.11 AHR in the human intestine

1.11.1 AHR gene polymorphisms and IBD risk

Large genome-wide association studies have identified more than 240 risk loci for IBD (de Lange et al. 2017). Importantly, these loci map to genes which include AHR. The AHR SNP rs1077773 is associated

with a reduced risk of UC (J. Z. Liu et al. 2015). In vertebrates, including humans, AHR expression is highly conserved. A search of a large human genome database identified only a single case where a mutation predicted loss of function (www.genesandhealth.org/research/scientific-data-downloads). Separate studies found no association between *CYP1A1* gene polymorphisms and Crohn's disease (de Jong et al. 2003) while *IDO1* polymorphisms are associated with a more severe clinical course (A. Lee et al. 2014). Intriguingly, AHR polymorphisms are also independently associated with differences in lifestyle such as smoking behaviour and caffeine intake perhaps through variations in toxin clearance and consequent tolerability (D. Chen et al. 2009; Sulem et al. 2011). This highlights the difficulty in untangling genetic and environmental variables.

1.11.2 AHR provides a mechanism for environmental risk factors to influence IBD

A wide variety of environmental variables that can influence cells exert their effects through a more limited number of molecular environmental sensors. Examining the downstream effects of these environmental variables may provide an opportunity to determine the effects of environmental variables, agnostic to the precise ligand or other environmental exposure.

The aryl hydrocarbon receptor is one example of a direct environmental sensors. There are a number of plausible mechanisms to allow the environmental variables known to impact IBD, to exert their influence via AHR.

1.11.2.1 Dietary ligands

There are number of possible mechanisms to explain the impact of diet in CD, particularly the impact of fruit and vegetable fibre. Direct host receptor-nutrient interactions maybe important. Specific vegetables such as Brassicae contain high levels of AHR ligands which can directly act on the intestinal mucosa as described above (Denison and Nagy 2003). Responses to and even the intake of Brassica

species appears to depend on the host genetics. For example; glucosinolates and isothiocyanates, which form potent AHR ligands, are metabolised by the host enzyme glutathione S-transferase Mu 1 (GSTM1) (Denison and Nagy 2003; B.-L. Wang et al. 2019). An important polymorphism in the GSTM1 gene, (rs 366631) which leads to partial deletion and complete loss of enzyme activity, is more common in IBD (OR 1.76) particularly CD (3.3) (Moini et al. 2017). It is plausible this SNP alters Brassica derived AHR ligand availability. Variation in taste receptors such as T2R38 are known to alter the perceived bitterness of brassicae such as broccoli and may influence intake (Lipchock et al. 2013) although no association with disease has been demonstrated to date.

There are a number of other important nutrient-host receptors on the intestine, including those that mediate interactions of SCFA with G-protein couple receptors and hypoxia-inducible factor and dietary amino acids particular tryptophan (Sugihara, Morhardt, and Kamada 2019) which depend on the interactions between host, dietary intake and the actions of intestinal bacteria.

1.11.2.2 Smoking

Smoking is the best described environmental risk factors for IBD. There is high quality evidence that tobacco smoking increases the risk and severity of Crohn's disease whilst reducing the risk of UC. This effect is not explained by nicotine (Parkes, Whelan, and Lindsay 2014). Cigarette smoke contains AHR ligands which modify *IL22* expression (Xue et al. 2016), Th17 cell activity (Talbot et al. 2018) and PD-L1 expression on epithelial cells (G.-Z. Wang et al. 2019). Therefore, it is possible AHR signalling is one of the mechanisms mediating the impact of smoking on IBD. The evidence for an impaired innate immune response in Crohn's disease and an exaggerated macrophage response to bacterial products in UC (Marks et al. 2006) provides a model for how the immunosuppressive effect of AHR could have inverse clinical effects.

1.11.2.3 Pregnancy and breastfeeding

Studies in mice have shown the maternal microbiota influences the development of the intestinal immune system in pups (Gomez de Agüero et al. 2016). Breastfeeding influences the development of the intestinal microbiome via a variety of mechanisms (Ho et al. 2018).

Particularly relevant to this study, is an observation in mice that maternal antibodies carrying ^{13}C-labelled AHR ligands, derived from maternal intestinal bacteria, are able to cross the placenta and able to promote the expansion of ILC3 in the developing pups intestine (Gomez de Agüero et al. 2016). Carbon-13 radiolabelling was also used to show AHR ligands were also transferred to the neonate in maternal breastmilk (Gomez de Agüero et al. 2016).

These examples highlight the range of mechanisms by which AHR could play an important role in mediating the effects of major environmental risk factors for IBD.

1.11.3 Altered AHR expression in IBD but conflicting results

Few studies have examined AHR in the human intestine and they report contrasting results. One group found a reduction in relative expression of *AHR* mRNA in homogenised colonic biopsies, and reduced AHR protein levels in unselected lamina propria mononuclear cells (LPMCs) in patients with Crohn's disease compared with healthy controls. *AHR* expression was also lower in inflamed tissue compared to uninvolved tissue in Crohn's disease. No difference was seen in UC (E. Mann 2013; Monteleone et al. 2011). Another group reported *AHR* expression was also reduced in isolated human intestinal dendritic cells in UC patients (E. Mann et al. 2013). This difference highlights the importance of defining the cell type and context when examining AHR.

In contrast to the evidence for a reduction in AHR in IBD, another group published findings showing AHR protein was higher in Crohn's disease than healthy controls using immunohistochemistry to examine whole biopsies (Arsenescu et al. 2011). However, there are limitations to both studies. The greatest difference in *AHR* expression was seen between inflamed and uninflamed tissue, rather than

health and disease, meaning observed differences may reflect a non-specific feature of inflammation. Importantly, measuring the amount of *AHR* alone is less informative than determining pathway activation and its consequences. Both studies considered aspects of this in isolation. *CYP1A1* mRNA levels in the colonic mucosa are low in health (Bulus et al. 2019). A 20-fold increase in *CYP1A1* expression was seen in homogenised, unstimulated whole biopsies in Crohn's disease compared with tissue from healthy controls by the group reporting elevated AHR but no functional or immunological outcomes were examined and the relative expression in different cells was not considered (Arsenescu et al. 2011).

Previous studies have also examined *IL22* expression in response to FICZ in intestinal immune cells. Lamina propria mononuclear cells were isolated from intestinal biopsies of patients with Crohn's disease. Cells were incubated with FICZ or control for 1 hour then T-cells were stimulated with anti-CD3/anti-CD28 antibodies for 24 hours. Expression of *IL22* increased in a dose dependent fashion confirming that the pathway is active in Crohn's disease. However, the responses in healthy controls were not shown so it is not possible to compare the response between health and disease (Monteleone et al. 2011). In addition, the mechanism of stimulation is potent, but specific to T-cells which may mask effects in innate lymphoid cells which also produce IL-22.

Without a clear measure of AHR activation it is difficult to interpret these results. Does incubation with 100nM FICZ increase AHR activity equally in health and IBD or are there inherent differences in AHR responsiveness? Can you augment AHR activity in IBD or is the pathway insensitive to stimulation?

The phenotype of AHR+ cells in IBD was also not considered in these experiments which used whole biopsies or density gradients to separate digested biopsies; an enrichment rather than purification step which also leads to unequal loss of some key populations of cells including macrophages and dendritic cells (Harusato, Geem, and Denning 2016). Better measures of AHR activation are necessary, measured in parallel with functional outcomes to determine what are the AHR-dependent

immunological outcomes in clearly defined mucosal populations. These measures must also be considered with reference to *ex-vivo* measures of AHR activity particularly when considering the translational relevance.

1.11.4 Altered AHR ligand availability in IBD

Other studies have examined whether AHR ligand exposure is different in IBD. Faecal samples from healthy controls induced greater activation of AHR in reporter cell lines, than samples from patients with IBD in remission (both UC and CD). Specifically, in IBD the levels of faecal tryptophan and indole-3-acetic acid (I3A) were reduced while the level of kynurenine was increased (Lamas et al. 2016). It is likely this is due to reduced bacterial metabolism of tryptophan into indoles like I3A in IBD while host metabolism into kynurenine is increased (although this ligand is less effective at activating AHR and, reducing inflammation). It would be interesting to examine the microbiome in these patients to determine what species are responsible for this difference.

An alternative explanation for different AHR ligand exposure in IBD was proposed by another group. Increased expression of Kyn-pathway enzymes, higher kynurenine and lower serum tryptophan levels was observed in patients with active IBD (CD more than UC). This was associated with higher *IL22* expression (Nikolaus et al. 2017). This suggests there is also increased metabolism of tryptophan to AHR ligands by the host not only by the microbiome in IBD.

It is difficult to determine whether elevated host metabolism of AHR ligands is a physiological response to inflammation at the intestinal barrier, or a pathogenic cause of disease. Examining these metabolites in other causes of intestinal inflammation such as infection may help untangle this.

1.11.5 Role of AHR in medical therapy for IBD

The cytochrome p450 enzymes classically associated with AHR signalling (CYP1A1, CYP1A2 and CYP1B1) are important in the metabolism of a wide variety of compounds including antibiotics (quinolones and macrolides), caffeine and retinoic acid. However, these enzymes do not metabolise commonly prescribed immunosuppressive agents used in IBD (Flockhart DA. Drug Interactions: Cytochrome P450 Drug Interaction Table. Indiana University School of Medicine (2007). https://drug-interactions.medicine.iu.edu Accessed 2020).

Instead, recent studies suggest AHR signalling may be relevant to the mechanism of action for a number of medications used to treat IBD although determining a direct effect is difficult due to cross-talk with other immune pathways.

Treatment of wild-type mice with mesalamine, a commonly used treatment for IBD, results in an increase in *Cyp1a1* expression and Treg accumulation (Oh-oka et al. 2017). However, an AHR reporter mouse suggests this may be an indirect effect; AHR activation after exposure to mesalamine was only seen after 3 days, while TGF-β increased *Cyp1a1* expression immediately after mesalamine. Antibody inhibition of TGF-β alone was sufficient to suppress the effects of mesalamine on *Cyp1a1* expression suggesting this may not be an AHR specific effect. Signalling via AHR and TGF-β has also been shown to be mutually inhibitory via negative feedback loops (see above) which also makes these observations difficult to interpret. It would be valuable to examine this further comparing the impact of mesalamine to classical AHR ligands and antagonists with robust measurement of AHR activation *in-vitro* or *ex-vivo* human tissue.

A number of investigatory products still in clinical trials are proposed to act via AHR. The most relevant of these is indigo naturalis, derived from a Chinese herbal medicine known as Qing-Dai. It contains the active ingredients indigo and indirubin which are indole-derived AHR agonists (Sugimoto, Naganuma, and Kanai 2016) and which had previously shown benefit in small case series (Suzuki et al. 2013). The efficacy of this agent in treating ulcerative colitis was recently demonstrated in a multi-centre

randomised controlled trial. The efficacy of indigo naturalis at 3 different doses was compared to placebo in 86 patients with active ulcerative colitis (Naganuma et al. 2018). The clinical response and remission rates were significantly better than placebo with mucosal healing 48-60% in the treated groups compared to 14% with placebo, albeit in a relatively treatment naïve population (which is associated with a higher response rate to many treatment for IBD (Gisbert and Chaparro 2019)).

This treatment was not without side effects, including an increase in liver enzymes in a significant minority of patients (Naganuma et al. 2018). A subsequent survey of open-label use of this medication in 877 individuals also revealed a more serious complication: pulmonary hypertension, which was observed in 1.3% users (Naganuma et al. 2019). A subsequent study in rats has suggested this may be due to the interaction of AHR and vascular endothelial growth factor-2 on pulmonary vessel remodelling (Takahiro et al. 2019). Other groups have also reported AHR directly induces VEGF expression in human hepatoblastoma cells if cells are cultured in a hypoglycaemic environment (Terashima et al. 2013). Another 1.1% of users experienced symptomatic intestinal intussusception with 40% requiring surgical resection (Naganuma et al. 2019). The mechanism of this effect is not clear. It would be interesting to know what the histology of these resection showed given the effects of AHR on crypt proliferation.

Another important limitation of this study is that the activation of the AHR receptor was not confirmed or quantified in this study. CYP enzyme expression, or any other surrogate or activation was not measured. It is important to demonstrate this ligand activates the AHR pathway in human intestinal cells. It would also be interesting to know if the clinical or endoscopic response or development of side effects correlated with the degree of AHR activation.

Another previously proposed treatment for CD and UC (Mongersen®) also appeared to act via TGF-β and AHR. It has been proposed that in Crohn's disease, elevated Smad7 inhibits TGF-β signalling and indirectly affects *AHR* expression. Addition of Mongersen, anti-sense Smad7, restored normal TGF-β

sensitivity and increased *AHR* expression in phase 2 studies. However, it is not clear if the anti-inflammatory effect observed was due to changes in AHR expression or other effects of TGF-β. Interestingly, while Mongersen increased *IL22* expression in response to FICZ, addition of FICZ alone also significantly increased *IL22* expression suggesting TGF-β signalling is not absolutely required and targeting AHR directly is an alternative therapeutic option. (Monteleone, Marafini, et al. 2016). Unfortunately, in phase 3 clinical trial this agent proved no more effective than placebo at treating CD (Sands et al. 2019). It is also important to note that, a number of other *in-vitro* studies have found evidence of mutual inhibition of AHR and TGF-β signalling.

There are a number of agents in clinical use or trial to treat chronic inflammatory disorders in other organ systems such as laquinimod for multiple sclerosis (Kaye et al. 2016) or coal tar and tapinarof (Benvitimod) for psoriasis which have been shown in murine knockout and *in-vitro* models to exert their effects AHR (van den Bogaard et al. 2013; Smith et al. 2017). A phase 2 study of laquinimod in CD suggested some benefit but there was no clear dose-benefit relationship and the drug does not appear to have been taken into phase 3 study (D'Haens et al. 2015). Lastly, the impact of a high- versus low-tryptophan diet on AHR activation in small and large intestinal biopsies is being examined healthy participants but has yet to report (clinicaltrials.gov identifier NCT03059862).

1.12 Summary

The aryl hydrocarbon receptor is a ligand activated transcription factor that allows defined environmental signals from our diet, intestinal bacteria and synthetic chemicals to influence the gene expression and therefore behaviour of host cells.

A breadth of evidence supports a role for impaired AHR-dependent immune responses in IBD. There are observed differences in intestinal AHR ligand availability and metabolism. There are differences in the number and function of AHR+ cells. Importantly, a variety of therapies in development for IBD and

similar chronic inflammatory conditions also exert benefit via AHR signalling. However, many questions remain unanswered AHR. Expression of AHR in diverse cells and tissues, with differing effects, means that predicting the effects of global AHR modulation difficult. A number of concerning side effects have been observed in clinical trials of agents which systemically activate AHR with worrying parallels to the toxicity observed with dioxins (TCDD). It may be necessary to develop medications which are not systemically absorbed or use drug-delivery mechanisms to target specific cell types.

There are number of important developments necessary for the development of safe effective therapies to modulate AHR in the intestine. A better understanding of the specific cell types which respond to AHR is needed, particularly the pathways regulated by AHR in different cell types. It is also essential to understand if there are differences in AHR activation in health and IBD and whether there are any inherent defects in AHR pathway activation and thus whether pharmacological, bacterial or dietary manipulation of AHR is likely to be successful.

1.13 Hypothesis and study aims

Previous work has demonstrated the immunoregulatory potential of the AHR in the intestine. This has attractive translational potential to human health particular in the management of IBD but important unanswered questions remain which raise concerns about the potential futility or side effects of AHR activation in the human intestine.

In this study I test the hypothesis that the AHR pathway is less activated or less responsive to AHR ligands in the intestinal mucosa in Crohn's disease compared to health.

I also test the hypothesis that only specific sub-types of immune cells and non-haematopoietic cells in the intestinal mucosa possess a functional AHR pathway and use transcriptomic approaches to comprehensively determine the impact of AHR signalling.

1.14 Specific aims:

- Develop a methodology for quantitative measurement and manipulation of AHR activity
- Determine if the AHR pathway is less active or responsive in defined cell populations from the intestinal mucosa in Crohn's disease compared to healthy controls
- Determine which in which cells in the intestinal mucosa is the AHR pathway functional
- Determine the consequences of AHR activation in intestinal immune cells

Chapter 2 - Materials and Methods

2.1 Materials

2.1.1 Chemicals and reagents

- Ficoll-Paque Plus

A sterile, ready-to-use density media containing Ficoll PM400, sodium diatrizoate and disodium calcium EDTA. The density has been optimized for the isolation of human mononuclear cells from peripheral blood.
VWR UK, 17-1440-03

- DMSO

Dimethyl sulfoxide is an organosulfur compound $(CH_3)_2SO$. It is a colourless solvent that dissolves both polar and nonpolar compounds and is miscible in a wide range of organic solvents and water.
Sigma, D8418

- Sodium azide

Sodium azide (NaN3) is a highly toxic salt. It is added to FACS buffer to preventing capping, shedding, and internalization of the antibody-antigen complex after the antibodies bind to the receptor.
Sigma, S2002-25G

- L-Glutamine

L-Glutamine is an essential amino acid required by virtually all mammalian cells grown in culture. It is added to cell culture media and serves as a major energy source for cells in culture.
Sigma, G7513

- CH223191

CH223191 is a potent and specific aryl hydrocarbon receptor antagonist (1-Methyl-N-[2-methyl-4-[2-(2-methylphenyl)diazenyl]phen yl-1H-pyrazole-5-carboxamide, 2-Methyl-2H-pyrazole-3-carboxylic acid (2-methyl-4-o-tolylazo-phenyl)-amide).
Sigma C8124

-FICZ

6-Formylindolo[3,2-b]carbazole is a tryptophan-derived high affinity AHR agonist
Sigma SML1489

-DTT

Dithiothreitol is a reducing agent. It is functions as a mucolytic by reducing the disulfide bonds of mucus glycoprotein allowing the mucus layer to be removed during intestinal tissue processing.
ThermoFisher R0861

-EDTA

Ethylenediaminetetraacetic acid is a chelating agent that scavenges metal ions particularly calcium. This is effect is used to facilitate the dissociation of epithelial cells from the mucosa. It is also added to FACS buffer to prevent clumping of cells.
Invitrogen AM9261

-Penicillin-Streptomycin

Penicillin is a beta lactam antibiotic and Streptomycin is an aminoglycoside antibiotic. These are added to cell culture medium to suppress bacterial growth.
Sigma P0781

-Gentamicin
Gentamicin is an aminoglycoside antibiotic used to suppress intestinal bacterial growth when culturing intestinal tissues
Gibco Fisher Scientific 15710049

- DNase I
Deoxyribonuclease I is an enzyme used to digest liberated DNA during collagenase digestion. This prevents clumping of cells.
Roche 11284932001

-Collagenase D
Collagenase is an enzyme which degrades collagen, a key extra-cellular matrix protein, thus allows dissociation of intestinal tissues

– Fetal calf serum (FCS)
Fetal calf serum (FCS) (also called fetal bovine serum; FBS) is the liquid fraction of clotted blood from fetal calves, depleted of cells, fibrin and clotting factors, but containing a large number of nutritional and macromolecular factors essential for the maintenance and growth of cultured cells. This is used to supplement culture medium and in FACS buffer to inhibit non-specific antibody binding.
ThermoFisher 12676011

– BSA powder
Bovine Serum Albumin (BSA) Low Endotoxin Powder
ThermoFisher 12877172

- Trypan blue solution (0.4%)
Used to count cells and determine viability. Live cells are not coloured.
ThermoFisher 15250061

- Zombie NIF fixability viability dye
An amine-reactive fluorescent dye that is non-permeant to live cells but enters dead cells
Biolegend 423105

-Leucoperm
Leucoperm is a proprietary reagent to allow staining of intracellular proteins. It comprises Leucoperm A which is a formaldehyde based fixation medium and Leucoperm B a permeabilization medium.
Bio Rad BUF09B

-Trypsin - TrypLE Express
Trypsin is an enzyme used to cleave the proteins holding cultured cells to the dish in-vitro. This allows cells to be removed from tissue culture plates.
Invitrogen, #12605-010

-OCT compound
Optimal cutting temperature compound is used as an embedding medium for frozen tissue specimens.
Tissue-Tek 4583

-Triton X-100

A detergent used to permeabilise tissue specimens for immunofluoresence by removing cellular membrane lipids which allows antibodies to bind nuclear and cytoplasmic antigens.
ThermoFisher 85111

- VectaShield HardSet
Mounting media which contains the DNA stain DAPI.
Vector Labs H-1200

-Diindolylmethane (DIM)
3,3'-Diindolylmethane is derived from indole-3-carbinol, a phytochemical naturally found in Brassicaceae vegetables.
Sigma D9568-5G

2.1.2 Culture media and buffers

- RPMI-1640 Medium (Dutch modification)

  Roswell Park Memorial Institute (RPMI) 1640 medium is a base medium containing a bicarbonate buffer. It contains glutathione and high concentrations of vitamins but no proteins, lipids or growth factors. The Dutch modification includes the addition of HEPES.

- Complete cell culture medium:

  RPMI-1640 Medium (Dutch modification) with the addition of 10% FCS, 100µg/ml penicillin, 100µg/ml streptomycin and 20mM L-glutamine. 25µg/ml of gentamicin was added for the culture of intestinal cells

- Fibroblast culture medium

  Eagle's Minimum essential medium with the addition of 10% fetal calf serum and 100ug/ml penicillin, 100µg/ml streptomycin, and 20mM L-glutamine

- HBSS

  Hank's balanced salt solution) is a salt-based buffer medium containing bicarbonate ions, only used as a buffer system for experiments in atmospheric CO_2 (Sigma).

- PBS (phosphate buffered saline)

A water-based salt solution containing NaCl 137mmol/l, KCl 2.7 mmol/l, Na_2HPO_4 10mmol/l and KH_2PO_4 1.8 mmol/l

- FACS buffer

  PBS with the addition of 2% FCS, 1mM EDTA and 0.2% (w/v) sodium azide. Sodium azide was omitted from the FACS buffer used for cell sorting live cells and the buffer was sterile filtered using a syringe filter with 0.2µm pore (VWR)

- Minimacs buffer

  PBS with the addition of 0.5 % (w/v) BSA and 2mM EDTA. The buffer was sterile filtered before use.

- 10 X Single cell sorting buffer

  PBS with the addition of 0.04% (w/v) BSA. The buffer was sterile filtered before use.

- PFA 1 - 4%

  4g Paraformalydehyde powder was added to 100ml 1X PBS. pH was adjusted to pH 7.4, using NaOH or HCl as needed. The 4% solution was diluted with PBS as needed.

2.1.3 PCR Primers

QuantiTect Primer Assays for use with SYBR Green dye were purchased from Qiagen and are shown below in Table 2.1.

Gene	**Assay name**	**Catalogue Number**
RPL30	Hs_RPL30_1_SG	QT00056651
CYP1A1	Hs_CYP1A1_1_SG	QT00012341
CYP1A2	Hs_CYP1A2_1_SG	QT00000917
CYP1B1	Hs_CYP1B1_1_SG	QT00209496
AHR	Hs_AHR_2_SG	QT02422938
AHRR	Hs_ AHRR_1_SG	QT00249900
CD68	Hs_CD68_1_SG	QT00037184
CD1A1	Hs_CD1A_1_SG	QT00000840
CXCL10	Hs_CXCL10_1_SG	QT01003065
IL1B	Hs_IL1B_1_SG	QT00021385
IL22	Hs_IL22_1_SG	QT00034853

HLA-DPA1	Hs_HLA-DPA1_1_SG	QT00049840
GPR35	Hs_GPR35_2_SG	QT02403128

Table 2.1 Primers used for RT-qPCR All primers were sourced from Qiagen®

2.1.4 Antibodies

The antibodies used for flow cytometry including flow sorting are shown below in Table 2.2. The antibodies used for IHC are shown later in this chapter.

Target	Fluorochrome	Clone	Host / Isotype	Supplier
AHR	PE	FF3399	Mouse IgG2b	eBioscience
CD11c	Brilliant Violet 510	3.9	Mouse IgG1	BioLegend
CD19	APC	UIB19	Mouse IgG1	BioLegend
CD31	APC	WM59	Mouse IgG1	BioLegend
CD45	Pacific Blue	HI30	Mouse IgG1	BioLegend
CD123 (IL3R)	PerCP or Cy5.5	6H6	Mouse IgG1	BioLegend
CD303 (BDCA2)	FITC	201A	Mouse IgG2a	BioLegend
CD326 (EpCAM)	PerCP or Cy5.5	9C4	Mouse IgG2b	BioLegend
HLA-DR	APC or PE Cy7	L243	Mouse IgG2a	BioLegend
TCR γ/δ	APC	B1	Mouse IgG1	BD
Lineage Cocktail (CD3, CD14, CD16, CD19, CD20, CD56)	FITC or APC	UCHT1, HCD14, 3G8, HIB19, 2H7, HCD56	Mouse IgG1, Mouse IgG2b	BioLegend

Table 2.2 Antibodies used for flow cytometry

2.1.5 Cytokines

- GM-CSF

Granulocyte-macrophage colony-stimulating factor signals via STAT5 to promote the differentiation of monocytes into macrophages or dendritic cells. It was used for the differentiation of CD14+ monocytes with the addition of IL-4. The cytokine was reconstituted with sterile water and stored in aliquots at a concentration of 100µg/ml at -80˚C

(Peprotech -AF-300-03-20)

- IL-4

Interleukin 4 is a cytokine with many biological roles. It inhibits classical activation of macrophages into M1 cells. It was used with GM-CSF to differentiate monocytes into dendritic cells. The cytokine was reconstituted with sterile water and stored in aliquots at a concentration of 100µg/ml at -80˚C (Peprotech 200-04)

2.1.6 Kits and other materials

- Anti-Mouse Ig, κ/Negative Control Compensation Particles Set
  Used for single colour compensation controls for flow cytometry
  BD 552843

- RT-qPCR kits (all from Qiagen)
  - RNeasy Micro Kit 74004– used for RNA purification
  - RNeasy Mini Kit 74104 – used for RNA clean-up including on-column genomic DNA digestion prior to RNA sequencing
  - QuantiTect Reverse Transcription Kit 205313 –used for cDNA synthesis
  - QuantiFast SYBR Green PCR Kit 204056 – for qPCR

- MiniMACS™ separation kits (all from Miltenyi Biotech)
  - MS columns 130-042-201
  - CD45 Microbeads, human 130-045-801
  - CD14 MicroBeads, human 130-050-201

- Foxp3 / Transcription Factor Staining Buffer Set
  eBioscience 00-5523-00

- Shandon™ EZ Single Cytofunnel™
  Thermo Scientific A78710003

2.2 Methods

2.2.1 Patient recruitment and sample collection

2.2.1.1 Study Ethics

Patient and healthy donor recruitment was completed according to the standard outlined in Good Clinical Practice (GCP) (www.nihr.ac.uk/health-and-care-professionals/learning-and-support/good-clinical-practice.htm). The study received ethical approval (16/LO/0800; 15/LO/2127). All participants provided written consent.

2.2.1.2 Patient characteristics

Healthy volunteers were all staff from the Blizard Institute, QMUL invited to provide blood samples only. Intestinal tissue samples were collected from IBD patients and control patients who were invited to participate prior to planned clinical procedures at the Royal London Hospital. Only participants between the age of 18 and 70 were included in this study. The demographics of each donor was recorded prospectively and is described in detail for each experiment in the Appendix. Patients and healthy volunteers were recruited from October 2015 – May 2019.

Patients with IBD were only included if they had a confirmed diagnosis of Crohn's disease or ulcerative colitis (not IBD-U or other causes of intestinal inflammation). Control patients were only included if the colon was macroscopically normal, less than 4 adenomatous polyps all below 1cm were permitted. Patients with major comorbidities including any immunological disease or immunomodulatory drugs or chronic infections (TB, HIV, hepatitis) were excluded.

Intestinal tissue was also included from fresh surgical resection specimens from patients with IBD and from macroscopically normal intestine in individuals with colon cancer, considered healthy controls in this study.

2.2.1.3 Blood

Peripheral blood was collected by venepuncture into 10ml sodium heparin Vacutainer tubes (BD VS368480).

2.2.1.4 Intestinal tissue

Eight intestinal biopsies were collected at the time of colonoscopy and placed into either RPMI 1640 (Dutch modification) culture medium on ice for live cell extraction or RLT Lysis Buffer® for RNA extraction.

Surgical resection specimens were transferred to the laboratory in culture medium. The intestinal mucosa was dissected from the deeper layers of the intestinal wall using a scalpel. The mucosa was then either cut into pieces of a similar size to intestinal biopsies (~2mm^3) and processed using the same techniques or cut in to 1cm squares and fixed for microscopy as described below.

2.2.2 Purifying primary cell populations

2.2.2.1 Isolating peripheral blood mononuclear cells using density gradient separation

Blood samples were mixed with base medium (RPMI 1640 Dutch Modification) in a 2:1 ratio. This mix was gently layered over 15ml Ficoll-Paque Plus (GE Healthcare) in a 50ml falcon tube using a Pasteur pipette. The tubes were centrifuged at 650g for 20 minutes with the brake set on the lowest setting to prevent disruption of the layers during deceleration. Mononuclear cells at the interface of the plasma and Ficoll were carefully aspirated using a Pasteur pipette. The cells were diluted with 5ml RPMI1640 Dutch Modification in 15ml Falcon tubes and centrifuged at 650g for 10 minutes. The supernatant was discarded, and the pellets were resuspended in complete medium and pooled into a 5ml FACS tube (BD).

2.2.2.2 Isolating intestinal mucosal cells

Collagenase digestion was used to derive a single cell suspension from intestinal biopsies (Bell et al. 2001). Intestinal biopsies were first washed in 1mM DTT (Sigma-Aldrich) in HBSS (Hank's Buffered Salt solution) for 20 minutes at room temperature in a T25 tissue culture flask to remove adherent mucus and faeces. This solution was aspirated using a Pasteur pipette and the biopsies were washed by adding 10ml of HBSS to the flask and shaking then aspirating the HBSS. The biopsies were then incubated in 25ml 1mM EDTA (Sigma-Aldrich) in HBSS on a heater-shaker at 37°C which continually agitated the flask. EDTA dissociates the epithelial cell layer. After 30 minutes the EDTA solution was aspirated, the biopsies washed with 10ml HBSS and another 25ml 1mM EDTA in HBSS was added and the flask was incubated as before for another 30 minutes. The biopsies were washed with HBSS and transferred to a new flask containing 15ml pre-warmed Dutch RPMI 1640 medium (Sigma-Aldrich) containing 1mg/ml Collagenase D (Roche), 2% FCS and 20µg/ml DNAse I (Roche). This flask was placed on a heater-shaker for 37°C with continual mechanical agitation for 2 hours. The resulting cell suspension was passed through a 70µm cell strainer and washed with complete medium. The EDTA washing step was omitted prior to FACS sorting cells to characterise AHR in epithelial cells (4.4.10).

2.2.2.3 Cell counting

To count cells 50µl cell suspension was mixed with 50µl 0.4% Trypan Blue solution (Thermo Fisher) and 150µl RPMI. This was applied to a Brightline haemocytometer (Neubauer improved). All cells within a 4 x 4 grid were counted. An average count from at least 3 grids was taken. The cell concentration was calculated using this formula:

Number of cells per 4 x 4 grid x 5x 10^4 = cells / ml

2.2.2.4 Isolating CD14+ PBMC or CD45+ intestinal mucosal cells by magnetic-activated cell sorting (MACS)

CD14+ monocytes and CD45+ intestinal mucosal cells were purified by positive selection using this magnetic separation method. A cell suspension of PBMC or intestinal mucosal cells was obtained using the methods described above. Cells were centrifuged at 400g for 5 minutes, supernatant was discarded and the cells were re-suspended in 2ml ice cold MACS buffer. This was repeated twice. The cell pellet was then carefully re-suspended in 100µl MACS buffer and labelled with 20µl anti-CD14 microbeads per 10^7 total PBMC or 10µl anti-CD45 microbeads for intestinal mucosal cells (Miltenyi Biotec) and incubated for 10 minutes at 4°C. The cells were washed with 2ml MACS buffer and centrifuged at 400g for 5 minutes. The supernatant was discarded and the cells suspended in 500µl MACS buffer. An MS column was placed in a miniMACS separator magnet (Miltenyi Biotec) and primed with 500µl MACS buffer. The cell suspension was added to the column and allowed to run through completely before 3 washes with 500µl MACS buffer. The negative cells flow through the column and were collected where necessary. The positive cells are retained in the column by the magnetic field. To collect positive cells, the column was removed from the magnet, 500µl MACS buffer was added and the cells were eluted by manually depressing the plunger. Collected cells were centrifuged at 400g and washed back into complete medium (www.methods.info/Methods/Cell_biology/CD14microbeads.pdf). The purity of MACS separation was determined using FACS and is described in the Appendix 1 and Chapter 4.

2.2.2.5 Isolation of PBMC populations or intestinal mucosal cells by fluorescence activated cell sorting (FACS)

Cell suspensions of PBMC or intestinal mucosal cells collected using collagenase digestion were washed into sterile PBS. Intestinal mucosal cells (not PBMC) were then resuspended in the viability dye Zombie NIR™ (Biolegend) diluted in PBS 1:100 and left for 20 minutes at room temperature. Cells

were then washed with the addition of 2ml sterile-filtered sodium azide-free FACS buffer followed by centrifugation at 400g for 5 minutes. This was repeated once. Cells were resuspended in 100µl azide-free FACS buffer. Cells were incubated with monoclonal antibodies against the required cell surface targets on ice for 20 minutes. Various cell populations were then sorted using the BD Biosciences FACSAria II flowcytometer within a Class II biosafety cabinet with the assistance of Gary Warnes, Blizard Institute, QMUL. The population and gating strategy used to identify different populations are described in the relevant chapter. Cells were collected into sterile polyethylene round bottomed test tubes (VWR) containing 1ml complete cell culture medium.

Previously killed PBMC were used to discriminate between live and dead cells. To generate these a tube of PMBC was incubated in a water bath at 55°C for 10 minutes. The tube was cooled and combined with live cells to generate a sample with viable and dead cells.

There was clear separation between positive and negative staining for the surface markers used for PBMC (CD19, γδ-TCR, HLA-DR) (Figure 2.1) and intestinal mucosal cells (CD45, EpCAM, CD31) (Figure 2.2) so isotype controls were not routinely used.

A

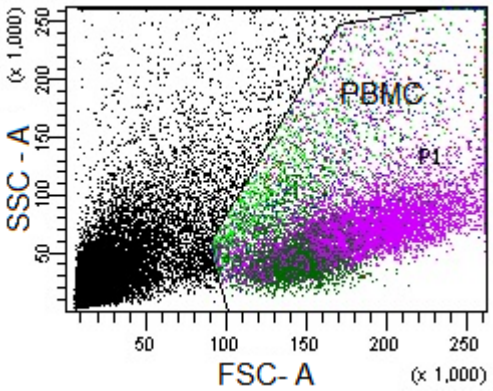

B

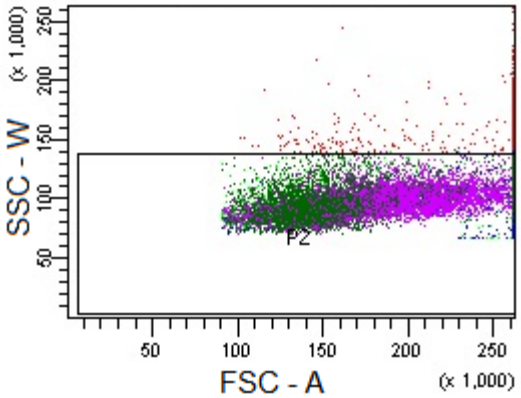

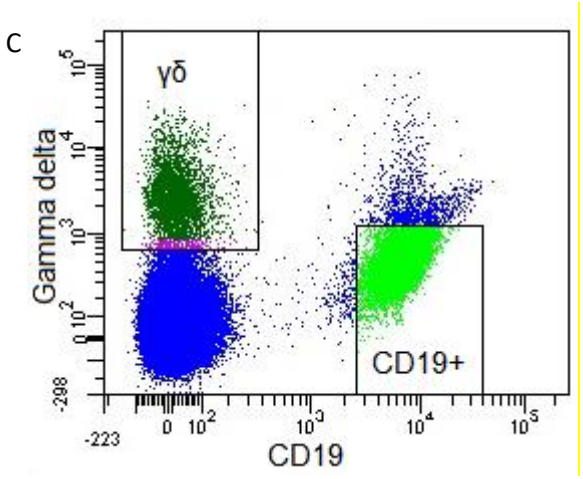

Figure 2.1 FACS sorting peripheral blood mononuclear cells
Cell sorting was performed using the Aria III cell sorter with the assistance of Gary Warnes, QMUL. PBMC from healthy donors were isolated and labelled. A) PBMC were identified based on FSC and SSC properties. B) Doublet discrimination was performed C) Distinct immune cell populations were identified by surface staining, for example; γδ cells and B-cells

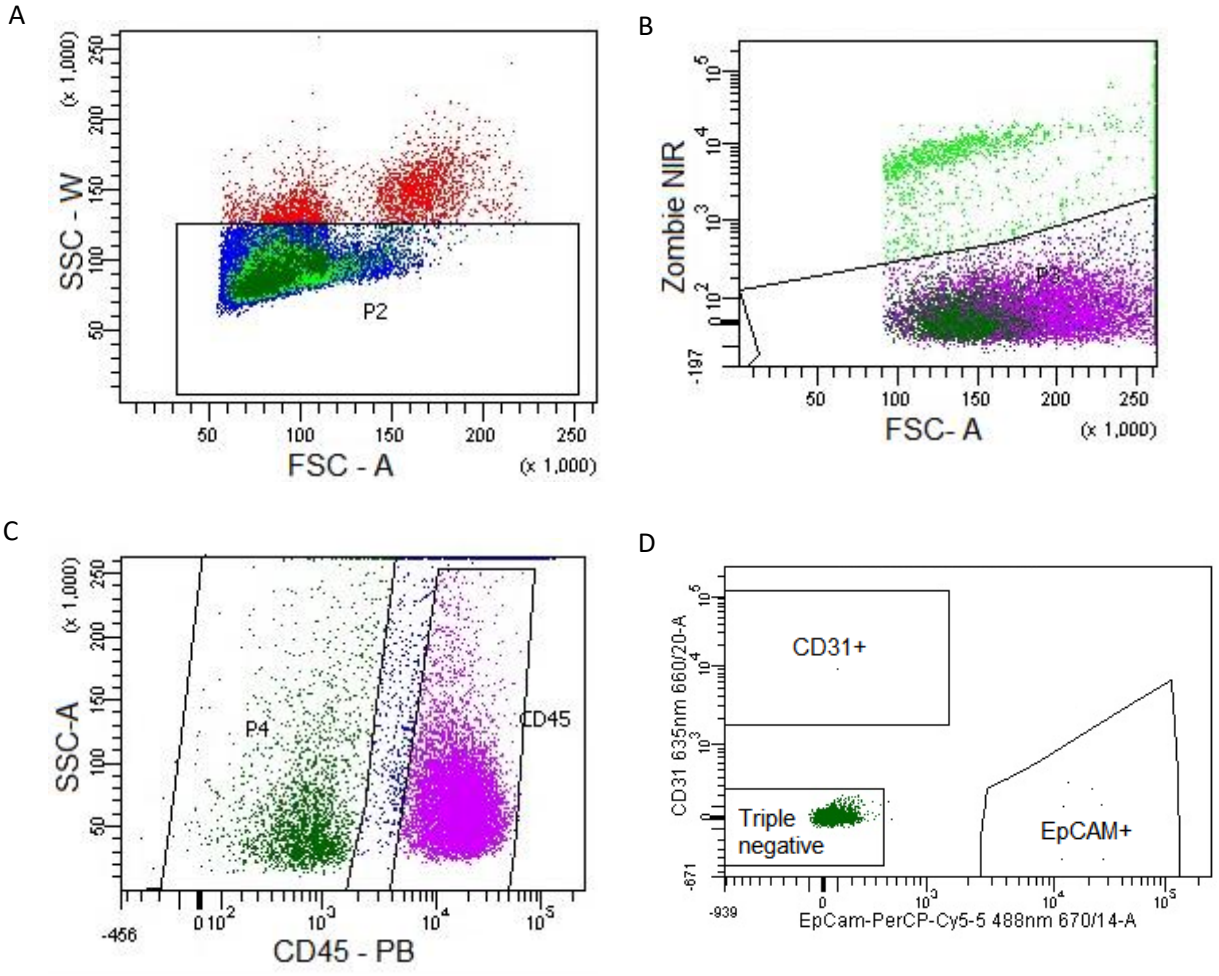

Figure 2.2 FACS sorting intestinal mucosal cells

Intestinal mucosal cells were also sorted using the Aria III cell sorter with the assistance of Gary Warnes. Intestinal biopsies from patients were washed and then digested using collagenase. A 70µm cell strainer was used to generate a single cell suspension which was labelled for surface targets.
A) Mucosal cells were identified based on FSC and SSC properties. Doublet discrimination was performed (not shown) B) Live cells were identified using Zombie NIR® viability dye. C) Intestinal immune cells were first identified using CD45 D) Epithelial and CD31 (Endothelial) cells were isolated using surface staining in the CD45- fraction. A triple negative (stromal) fraction was collected.

2.2.3 Cell culture and stimulation

2.2.3.1 Differentiation of monocyte-derived dendritic cells (moDC)

CD14+ monocytes were purified from PBMC as described above. These cells were then cultured in Complete cell culture medium in the presence of GM-CSF (Granulocyte-macrophage colony stimulating factor) 100ng/ml (1000IU/ml) and IL-4 100ng/ml (500IU/ml) for 7 days (5 x10^5 per well). After 3 days 500µl medium was refreshed adding a further 100ng/ml GM-CSF and IL-4. Dendritic cells were harvested and counted on day 7 (Sallusto and Lanzavecchia 1994).

2.2.3.2 moDC stimulation

After counting 100,000 moDC were transferred to wells on flat bottomed 96 well plates (VWR) and incubated in Complete medium with the addition of 0.16% DMSO, FICZ (0.5 – 500nM) with or without CH223191 (10µM or 100µM) for 4 hours at 37°C.

CH223191 solubility in aqueous solutions is poor. A stock solution of CH223191 in DMSO (molar mass 333g/mol) was prepared at 60mM (20mg CH223191 was dissolved in 1ml sterile DMSO) which is the maximum reported concentration on the manufacturer's literature (Sigma Aldrich). The peak inhibitory effect is seen at 100µM (Zhao et al. 2010) therefore a final concentration of 0.16% DMSO was added to these conditions. This DMSO concentration was also used in the control wells but additional DMSO was not added to the other wells to ensure well volumes were matched.

A previous study examining gene expression in human embryonic palates showed a 10-fold increase in CYP1A1 mRNA expression after 4 hour of culture (Abbott et al. 1999) supporting the selection of this time point to observe gene expression in moDC incubated with AHR agonists or antagonists. Importantly, expression of the reference gene *RPL30* was not affected by 4 hours incubation with concentrations of FICZ from 0-500nM with or without CH223191 100µM (Figure 2.3A and 2.3B).

A long time period of incubation (24 hours) did lead to a larger increase in *CYP1A1* expression but was associated with reference gene instability (Figure 2.3C) which was not observed at 4 hours.

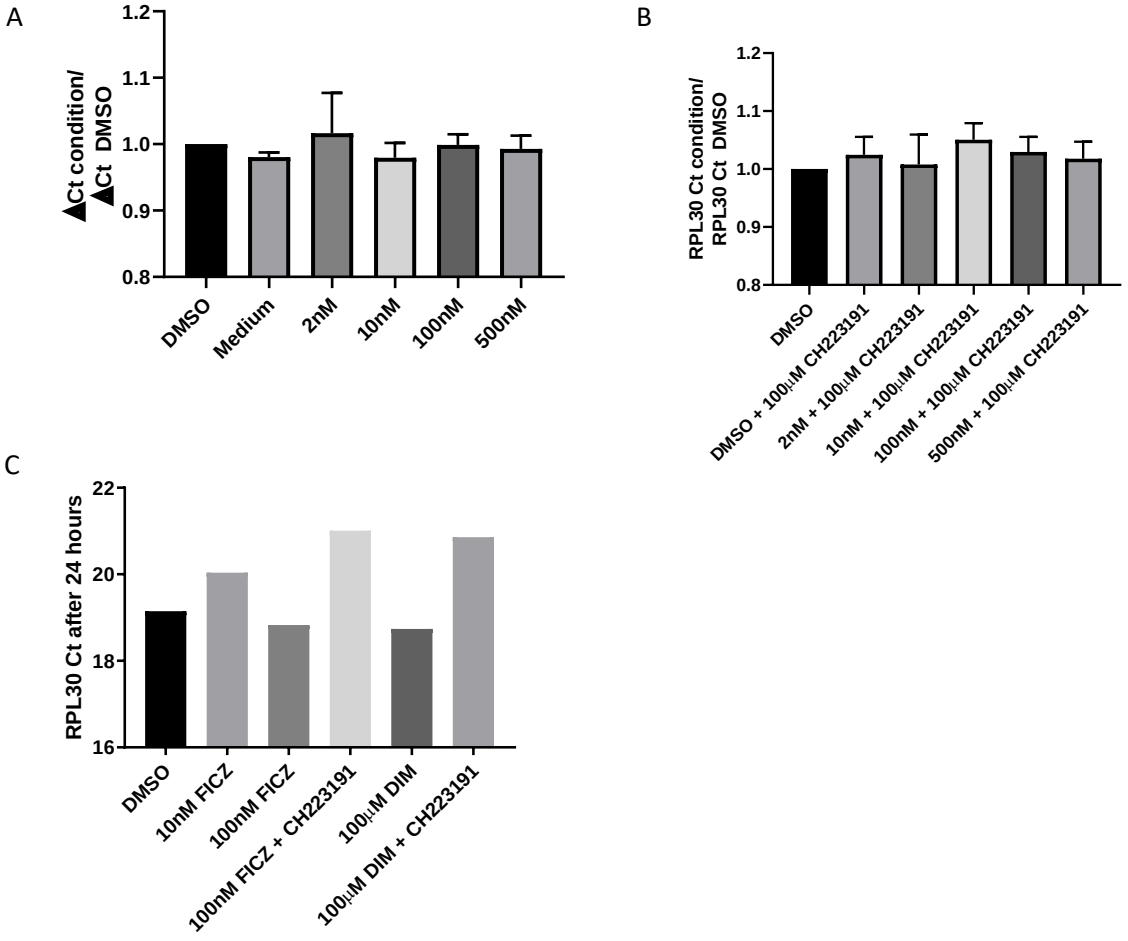

Figure 2.3 A) *RPL30* expression in moDC incubated with different concentrations of FICZ compared to expression with DMSO control. B) *RPL30* expression in moDC incubated with different concentrations of FICZ and CH233191 compared to expression with DMSO control. C) Reference gene (RPL30) expression in moDC after 24 hours incubation (n=1),

2.2.3.3 Isolated Intestinal cell stimulation

Intestinal immune (CD45+) cells isolated by MACS were manually counted and transferred to flat bottomed 96 well plates (VWR) with ~100,000 cells per well. Cells were incubated in Complete medium with the addition of 0.16% DMSO, FICZ (10nM-100nM) with or without CH223191 (100µM) for 4 hours at 37°C.

Intestinal immune (CD45+), epithelial cells (EpCAM+) and stromal cells (CD45- EpCAM- CD31-) isolated by FACS sorting were also transferred and divided wells but were not manually re-counted due to the small number of cells recovered; cell concentration was estimated using events counted on the cell sorter. Very few CD31 cells were recovered so the entire sample was transferred into a single well. Cells were incubated in Complete medium with the addition of 0.16% DMSO, FICZ (100nM) with or without CH223191 (100Mµ) for 4 hours at 37°C.

2.2.4 Quantitative Reverse transcription PCR

RNA extraction, cDNA synthesis and quantitative PCR were performed using Qiagen kits and validated primers according to the manufacturer's instructions as summarised below.

2.2.4.1 RNA preservation and extraction

Cells of all tissue types were resuspended in their culture medium and transferred into 1.5ml Eppendorf tubes. The wells were washed with a further 200µl sterile PBS. After centrifugation (400g for 5 minutes) the supernatant was carefully removed. The cell pellet was re-suspended in 350µl Qiagen buffer RLT, a proprietary lysis buffer containing high concentration of guanidine isothiocycanate. The sample was vortexed for 1 minute to lyse the cells. The lysate was then stored at -80°C until further processing.

Whole biopsies for RNA extraction were collected in endoscopy into 1.5ml Eppendorf tubes containing 350µl ice-cold buffer RLT (10µl ß-Mercaptoethanol per 1 ml Buffer RLT). ß-Mercaptoethanol was added to inhibit the action of RNAses released during tissue homogenisation (RNeasy Micro Handbook). The biopsies were homogenised using a probe sonicator (2 bursts of up to 30 seconds). The Eppendorf was then vortexed for 1 minute. The lysate was stored at -80°C

Spin columns were used for the extraction of the RNA. Spin columns use the principle of solid phase extraction to purify RNA. Nucleic acids are suspended in a solution containing ethanol or isopropanol. The nucleic acids bind to silica in the columns and waste passes through the column and can be removed (Ali et al. 2017). Samples were defrosted and 350µl of 70% ethanol was added to the lysate. Samples were then vortexed for 1 minute and transferred to Qiagen spin columns placed in 2ml collection tubes. The columns were centrifuged for at 8000g for 15 seconds and the flow-through was discarded. 700µl of the wash Buffer RW1 was added and the centrifugation step was repeated (8000g for 15 seconds) and the flow-through was discarded and the spin column transferred to a fresh 2ml collection. 500µl of RPE buffer was added and the spin columns were centrifuged again (8000g for 15 seconds) and the flow-through was discarded (ethanol was added to the stock RPE buffer before use the first time). 500µl of 80% ethanol was added and the spin columns were centrifuges at 8000g for 2 minutes. The flow-through and collection tube were discarded and the spin columns were placed in new 2ml collection tubes. Columns were then centrifuged with open lids at full speed (12000g) for 5 minutes to allow any residual ethanol to evaporate. Ethanol is one of many described inhibitors of the downstream PCR reaction (Schrader et al. 2012). To elute the RNA the spin column was transferred to a 1.5ml collection tube. 15µl RNAse-free water was added directly to the centre of the spin column membrane. The sample was then centrifuged for at full speed for 1 minute. The 13µl RNA flow-through was collected and transferred to 0.2 ml, flat capped tubes and stored on ice to prevent degradation.

2.2.4.2 RNA quantification and purity assessment

RNA quantity and purity were measured using the NanoDrop 2000 (Thermo Scientific) spectrophotometer or Bioanalyzer.

The NanoDrop 2000 (Thermo Scientific) is a spectrophotometer that uses UV and visible light to determine the amount of RNA or DNA. Nucleic acids absorb light in the UV wavelength with a maximum at 260nm. After calibrating the machine with RNA/DNA-free water 1µl RNA was added to the Nanodrop. The concentration of RNA recovered (ng/µl) and 260/280 and 260/230 ratios were recorded. The absorption of light at 230nm, 260nm and 280nm is related to the purity of isolated RNA. Contaminants such as genomic DNA, proteins, kit buffers, particularly guanidine salts in column-based kits, can reduce the ratio below the desired standard >1.8.

The Bioanalyzer is a chip-based capillary electrophoresis machine. RNA fragments of different size move through a gel at different speeds. A standard RNA ladder is used to determine the size of fragments in a sample. RNA Integrity Number (RIN) is derived from a proprietary software algorithm developed by Agilent® which is designed to describe RNA strand integrity while avoiding the variation of user-dependent interpretation of results. It considers the 18S and 28S ribosomal peak height as well as the different regions in the electropherogram (Figure 2.4).

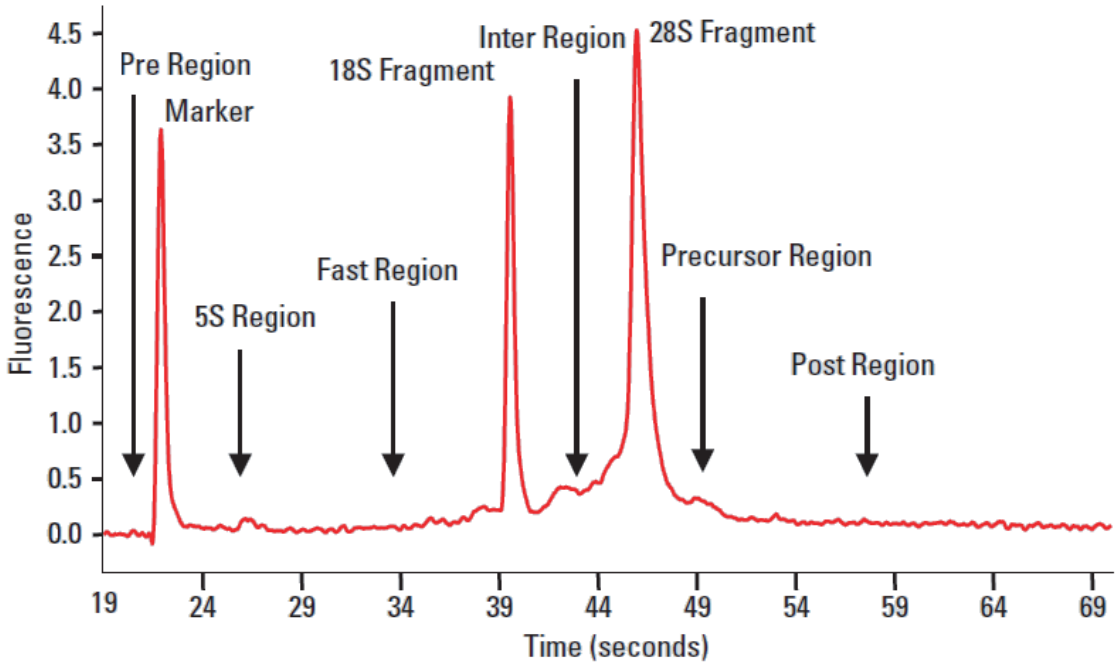

Figure 2.4. Idealised electropherogram showing the different regions used to derived RIN value (https://www.agilent.com/ Bioanalyzer manual)

A lower RIN value suggests higher strand fragmentation. Fragmentation makes alignment of the sequenced reads to a reference genome more difficult, but also increases the chance of failing to sequence strands altogether. Protein-coding mRNAs contain a poly (A) tail. This poly (A) tail is used in standard RNA-Seq protocols to enrich mRNA from total cellular RNA, the greatest proportion of which is non-coding rRNA. Cleavage of this tail will prevent enrichment and subsequent sequencing (Hrdlickova 2017 Interdisc Rev RNA).

2.2.4.3 Reverse transcription

Reverse transcription, to generate cDNA from purified RNA, was performed using the QuantiTect Reverse Transcription Kit. RNA was kept on ice to reduce degradation. First genomic DNA was enzymatically depleted. 2µl gDNA Wipeout buffer was added to the sample in 0.2 ml tubes. This was incubated for 2 min at 42°C, then immediately placed on ice. The reverse-transcription master mix was prepared on ice. 1µl reverse transcriptase, 1µl primer mix (containing the deoxyribose nucleoside

triphosphate bases) and 4µl RT buffer was added to each RNA sample and mixed. The sample was incubated for 15 minutes at 42°C to generate cDNA. Finally, the mix was incubated for 3 minutes at 95°C to inactivate the reverse transcriptase.

2.2.4.4 Quantitative real-time PCR

SYBR family dyes intercalate between base pairs or the minor-groove in double stranded DNA and fluoresce in response to light allow quantification of the amount of DNA present in samples.

In each well of a 96 well PCR plate 12.5µl QuantiTect SYBR Green mix was added to 2.5µl QuantiTect primer assay for the genes of interest and 8µl water. 2µl cDNA from the relevant sample was added to each well. The plate was covered in an adhesive PCR Plate Seal and briefly covered. The PCR reaction was performed using a 7500 Fast Real Time PCR system (Applied Biosystem) or StepOnePlus real time PCR machine (ThermoFisher).

Each plate design included triplicates of all conditions and at least 1 well without sample cDNA (non-template control) for each gene of interest. The reference gene used was *RPL30*. This gene encodes a ribosomal protein sub-unit with stable expression across a wide range of human tissues and following different treatments (de Jonge et al. 2007).

The QuantiTect SYBR Green mix contains at hot start DNA Polymerase. The plate was first incubated for 5 minutes at 95°C to activate this enzyme. A denaturation step of 10 seconds at 95°C was followed by a 30 second annealing and extension incubation at 60°C. This cycle was repeated 40 times. The cycle threshold (Ct) was automatically calculated by the qPCR machine. A melt curve was performed at the end of each experiment to ensure a homogenous amplification product (Ririe, Rasmussen, and Wittwer 1997). These settings are summarised in Table 2.3.

Table 2.3: RT-qPCR temperature settings and times

Step	Time	Temperature	Ramp rate
Activation step	5 minutes	95°C	Maximum
Two-step cycling for 40 cycles			
Denaturation	10 seconds	95°C	Maximum
Annealing & extension	30 seconds	60°C	Maximum
Melt curve			
Melt curve	30 seconds	0.5°C increments (60 – 95°C)	

2.2.4.5 qPCR analysis

The difference in expression between reference and target gene was expressed as delta Ct (ΔCt).

Thus, the difference in expression of the target gene between two conditions is expressed as delta delta Ct (Livak and Schmittgen 2001). This method assumes perfect PCR efficiency, that is a doubling in copies after each PCR cycle and equal efficiency between reference and target genes. This relationship was examined in the reference gene *RPL30* (de Jonge 2007) and a key gene for this project (*CYP1A1*). There was a linear relationship between input cDNA and cycle number and the relative expression of CYP1A1 (delta Ct value) remained constant across a wide range (Figure 2.5).

Relative expression of genes was also normalised to expression in control cells using the $2^{-\Delta\Delta Ct}$ method (MW Pfaffl, 2001).

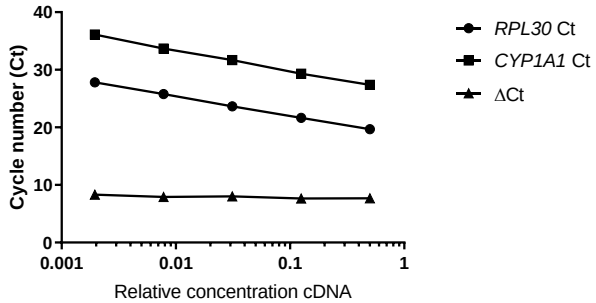

Figure 2.5 A dilutional series to determine the linearity of the SYBR green qPCR reaction. cDNA from FICZ stimulated monocyte-derived dendritic cells from a single donor was serially diluted from 1:2 to

1:512 with sterile water. There was a linear relationship between the concentration of cDNA added and the measured expression of both CYP1A1 and RPL30 to the limit of this experiment. The delta Ct value (CYP1A1 – RPL30) used to determine relative expression was unchanged between dilutions at 7.93 ± 0.27 (standard deviation).

2.2.5 Immunohistochemistry

2.2.5.1 Fixation of tissue and sectioning of tissue

Intestinal mucosa from surgical resections was cut into 1cm^2 squares and was fixed in 4% PFA for 4 hours at 4°C. Sucrose was used to cryoprotect the tissue for freezing (Griffiths G. et al. 1984). The samples were washed with PBS and transferred to 30% sucrose solution and left overnight. Next tissue was transferred to a solution comprising equal parts Optimum Cutting Temperature (OCT) compound (Tissue-Tek®) and 30% sucrose solution for 24 hours. Samples were transferred into 15 x 15 x 15 mm tissue moulds (Tissue-Tek) filled with OCT and frozen in a beaker of isopentane placed in a Dewar of liquid nitrogen. Samples were stored at -80°C until sectioning. A cryostat microtome was used to cut the frozen tissue into sections 7µm thick which were mounted onto SuperFrost® Plus microscopy slides (VWR).

2.2.5.2 Immunofluorescence

The fixed frozen sections were stained using a primary-secondary antibody methodology. A hydrophobic margin was drawn around the tissue on each slide using an ImmEdge Hydrophobic Barrier PAP Pen (Vector Labs). The samples were rehydrated with PBS and then a universal protein block (Dako®) was applied to each slide for 1 hour to reduce non-specific binding of antibodies. The protein block was poured off and the slide blotted on tissue paper. The primary antibody was diluted in PBS containing 0.2% Triton X-100. The concentration used was determined using a dilutional series for each antibody. 200µl diluted primary antibody was applied to each side to ensure the tissue was completely covered and then the slides were incubated overnight at 4°C. The following day the slides were washed 3 times in PBS in a foil covered slide rack for 5 minutes on an agitator at 100rpm. The

slides were blotted dry with tissue paper and the species-specific secondary antibody was applied after diluting the stock 1:400 with PBS. The secondary antibody was left to incubate for 1 hour at room temperature in the dark. The slides were washed again in PBS and dried. A small drop of VectaShield HardSet mounting media, which contains the DNA stain DAPI, was applied to each slide and a coverslip was applied and left to dry. For each experiment a *non-primary control* was included for each fluorochrome where only the secondary antibody was added to the slide to control for non-specific primary antibody binding. Slides were stored in the dark at 4°C and images captured within 24 hours. The antibodies used are shown in Table 2.4.

Table 2.4 – Primary and secondary antibodies used for Immunofluorescence

Primary antibody	Antibody clone	Manufacturer and catalogue number	Dilution used	Species of origin
Anti-human AHR	Monoclonal FF3399	Ebioscience 14-9854-82	1:200	Mouse
Anti-human CD45	Monoclonal EP322Y	Abcam ab40763	1:100	Goat

Secondary antibody	Fluorochrome	Manufacturer and catalogue number	Dilution used
Goat anti-mouse	Alexa Fluor 488	ThermoFisher A-11001	1:400
Goat anti-rabbit	Alexa Fluor 546	ThermoFisher A27034	1:400

2.2.5.3 Cytospin

To apply cell suspensions to slides for microscopy, a cell suspension was prepared at 1 x 10^6/ml. This concentration allowed enough space for cells to form a monolayer without overlap or too much space between cells. A polylysine coated slide (Thermos Scientific) were placed inside each EZ Cytofunnel™ (ThermoFisher). 50µl cell suspension (5 x10^4 cells) were placed in the funnel mouth. The Cytofunnels were spun on the Cytospin 4 Cytocentrifuge (ThermoFisher) for 5 minutes at 1000 rpm. After the spin an ImmEdge hydrophobic barrier pen was used to draw around the droplet of cells on the slide. A drop

of 4% PFA was added to the slide using a Pasteur pipette and left for 20 minutes at room temperature to fix the cells. This was removed by blotting the slide on absorbent paper. The slide was not washed using the slide rack to prevent loss of cells. Instead a drop of sterile PBS was added to wash the slide before blotting again. Primary and secondary antibodies were then applied using the technique described above before mounting with VectaShield and a cover slip.

2.2.5.4 Image capture

Images were acquired using an LSM 710 confocal or Leica DM5000 epi-fluorescent microscope. Laser power and contrast were adjusted to ensure each channel was not oversaturated. Laser power was only used up to 5 to prevent photobleaching. Gain was adjusted and kept below 800. The pin hole was set to 1 AU but increased if the image could not be acquired within the laser power and gain limits specified. All images were acquired with a resolution of at least 1024 x 1024 and colour depth of 12 with an acquisition speed below 6. All images were captured within 24 hours of staining to minimise degradation of fluorescence. Image files were exported to Fiji (http://fiji.sc/) for image analysis. Composite and single colour high resolution images generated were exported as high quality JPG files for this document.

2.2.6 Flow cytometry

2.2.6.1 Staining cell surface targets

Isolated PBMC, moDC or intestinal cells were transferred into 5ml FACS tubes (VWR) and washed by centrifugation (400g for 5 minutes) after the addition of 1ml cold FACS buffer. The supernatant was discarded. Monoclonal antibodies against extra-cellular targets were added to the residual volume (100µl) and cells were manually resuspended and incubated on ice for 20 minutes in the dark. The

cells were then washed twice in cold FACS buffer. If no intracellular targets were required, the cells were fixed in 300µl 1% PFA (paraformaldehyde) prior to acquisition on the same day.

2.2.6.2 Intracellular staining for AHR

AHR is an intra-cellular protein which resides in the nucleus or cytoplasm depending on ligand binding status (Denison and Nagy 2003). To ensure antibodies have access to intra-cellular targets like AHR, cells require permeabilization before staining. Three different commercially available methods of permeabilization for intra-cellular labelling are described below and were compared.

2.2.6.2.1 Leucoperm (Bio-rad)

After extracellular targets were labelled the cells were fixed in 100µl Leucoperm A solution (Bio-Rad) for 20 minutes. The cells were washed by adding 2ml FACS buffer and centrifuged at 400g for 5 minutes. The supernatant was discarded and 100µl Leucoperm B solution (Bio-Rad) was added with the required monoclonal antibodies (5µl/antibody). The sample was agitated and incubated in the dark at room temperature for 30 minutes. The cells were washed again twice with 2ml FACS buffer and centrifuged at 400g for 5 minutes. The cells were fixed in 300µl 1% PFA.

2.2.6.2.2 Foxp3 / Transcription Factor Staining Buffer Set (Ebioscience)

After extracellular labelling cells were centrifuged at 400g for 5 minutes and supernatant was discarded. 1ml of Foxp3 Fix/Perm (Ebioscience) working solution was added. The cells were agitated and incubated for 45 minutes at 4°C in the dark. 2ml 1X Perm buffer (Ebioscience) was added and cells were centrifuged at 400g for 5 minutes. The cells were re-suspended in 100µl 1X Perm Buffer with 2µl FCS and the required monoclonal antibodies (5µl/antibody). The sample was agitated and incubated for 30 minutes at room temperature. The cells were washed twice using 2ml 1X Perm buffer, centrifuging at 400g for 5 minutes and discarding the supernatant before cells were re-suspended in FACS buffer.

2.2.6.2.3 Methanol

After extracellular labelling the cells were centrifuged at 400g for 5 minutes. The supernatant was discarded. Cells were fixed in 2% PFA for 15 minutes in a 37°C water bath. The cells were centrifuged at 400g for 5 minutes, the supernatant discarded and 2ml PBS added before centrifuging again at 400g for 5 minutes. Cells were re-suspended in 1ml 70% ice-cold methanol and incubated for 30 minutes on ice. The sample was centrifuged at 400g for 5 minutes, supernatant discarded and washed with 2ml FACS buffer. This was repeated. The cells were re-suspended in 100µl FACS buffer with the required monoclonal antibodies (5µl/antibody) and incubated at room temperature for 45 minutes. The cells were centrifuged at 400g for 5 minutes, supernatant discarded and washed with 2ml FACS buffer again before re-suspending in 300µl FACS buffer.

To compare these three techniques moDC were generated from CD14+ monocytes as described in this chapter. Cells were permeabilised using the different methods and stained with PE conjugated anti-AHR or an isotype control. Positive gates were defined strictly using the isotype control (0.25%) (Figure 2.6A). The percentage of positive cells using each method was compared and is shown below (Table 2.5). MoDC from the same donor are a usually considered a homogenous population (Guilliams and van de Laar 2015). Therefore, an assumption was made that if AHR was expressed, it should be detected in all cells. In addition, from a practical perspective the approach that yielded the brightest staining above control would be more sensitive in complex multicolour experiments.

The eBioscience foxp3 transcription factor kit identified the greatest percentage of cells as positive (87.4%) (Figure 2.6B). Staining brightness was also compared using the mean fluorescence intensity of the whole sample. The ratio of mean fluorescence intensity (MFI), comparing isotype control and AHR stained moDC, was also highest using the foxp3 transcription factor staining buffer set (Table 2.5).

The observed difference may reflect different nuclear permeabilization efficiencies or differing impacts on the epitope which could alter antibody binding.

A Isotype Control **B** Anti-AHR

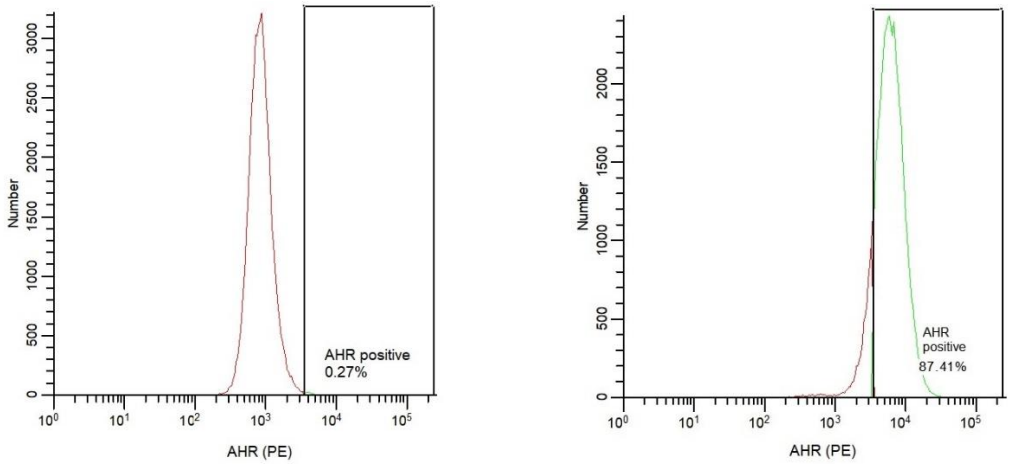

Figure 2.6: Single colour flow cytometry plot comparing AHR staining (PE) of moDC with isotype control in cells permeablised using Ebioscience® Foxp3 transcription factor kit. A Staining with isotype control is shown. **B** Using this gate 87.4% cells were detected as positive. There was a positive shift in the entire population without increase in standard deviation

Table 2.5: Single colour flow cytometry staining of moDC for AHR (PE) compared to isotype control using different permeabilisation methodology

Permeabilisation Method	Isotype gate (%)	AHR+ (%)	MFI (mean fluorescence intensity) isotype control	MFI (mean fluorescence intensity) AHR	MFI Ratio
Leucoperm (BioRad)	0.27	29.96	2077	4541	2.19
Foxp3 / TF Factor Staining Buffer Set (Ebioscience)	0.27	87.41	868	5919	6.82
70% Methanol	0.26	40.10	1728	7525	4.35

2.2.6.3 Sample acquisition and analysis

2.2.6.3.1 Compensation controls

In multicolour experiments single fluorochrome compensations controls are required because of the physical overlap of the emission spectra of many commonly used fluorochromes. This effect can be overcome through compensation. Single colour compensation controls were generated using

compensation beads (CompBeads BD). These contain positive beads which have been coupled to an antibody specific to the kappa light chain of Ig from mice and negative beads which do not bind Ig. This creates a clear positive and a negative population when incubated with each individual antibody-conjugated fluorochrome used in a given experiment. Flow-cytometry analysis software (FlowJo) can determine the signal from a given fluorochrome and measure the overlap and correct for the contribution of signal from other overlapping fluorochromes. Where no species-specific compensation beads were available PBMC stained with a single fluorochrome were used as a compensation control.

2.2.6.3.2 Acquisition using flow cytometer

Labelled cells were acquired using the Canto II or LSR II (BD Bioscience). At least 25,000 events were acquired for each sample and up to 3,000,000 events were acquired when examining rare populations such as circulating dendritic cells. Single colour compensation controls were generated by labelling BD™ CompBeads to create a positive and negative population for each fluorochrome. Data were exported as FCS files and analysed using WinList (Verity) and FlowJo (BD). Compensation was applied using the single colour fluorochrome controls prior to data analysis. Where reported a matched isotype control antibody was used to determine positive staining in the population of interest. For some populations the positive and negative populations were consistently distinct and isotype controls were not used. Staining was compared by recording the percentage of positive cells and the mean fluorescence intensity.

2.2.7 Intestinal Fibroblast culture

CCD18co (ATCC® CRL-1459™) were purchased from the American Type Culture Collection (ATTC).

This is a semi-immortal cell line of healthy human intestinal derived from an anonymous paediatric patient. This cell line has been used as a model of *in-vivo* human intestinal fibroblasts for more than 20 years (Duckworth et al. 2013; Jeffers et al. 2002). Cells were cultured in fibroblast growth medium and cultured according to the manufacturers' protocol at 37°C under a humidified atmosphere containing 5% CO_2, and 21% O_2. Cells were split using TrypLE Express (Invitrogen, #12605-010) to resuspend the cells when 70-80% confluent in the flask. Cells were passaged 3 times after defrosting before use in experiments.

2.2.7.1 Intestinal fibroblast stimulation and RNA extraction

For stimulation CCD18co cells were counted using Trypan Blue as described and seeded into a tissue-culture treated 96-well plate (5000 cells per well). The plate was incubated overnight with 100µl fibroblast culture medium to allow cells to adhere. The wells were washed with PBS to removed dead or non-adherent cells before stimulation. Adherence was confirmed using a light microscope. Cells were incubated in fibroblast medium with the addition of 0.16% DMSO, FICZ (10nM-100nM) with or without CH223191 (100µM) for 4 hours at 37°C. After stimulation the supernatant was aspirated and discarded. RNA was harvested by lysing the fibroblasts *in-situ* using RLT Lysis Buffer (5 minutes). The lysate was then stored at -80°C until further processing.

2.2.7.2 Generating fibroblast-conditioned media and moDC stimulation

To examine the ability of intestinal fibroblasts to metabolise AHR ligands and thus the potential to regulate the availability of AHR ligands to intestinal immune cells, CCD18Co cells were incubated with the AHR ligand FICZ. Specifically, CCD18Co cells in T-25 were cultured until at 70%-80% confluent (approximately 2 million fibroblasts). The flask was washed twice with sterile PBS. 3ml freshly prepared fibroblast culture medium with or without 100nM FICZ was added.

This concentration was selected to ensure a robust response. As shown in this study, only a small change in gene expression was seen in intestinal cells exposed to 10nM. It is likely AHR ligand exposure in the intestinal lumen is high but it is not known if this represents a physiological stimulus.

The flask was incubated for 24 hours at 37°C. The culture medium was aspirated into a 15mL Falcon™ conical centrifuge tube and centrifuged at 400g for 5 minutes to sediment any cells or debris. The culture medium was aspirated and stored at -20°C. For stimulation moDC were first washed in fibroblast culture medium and manually counted using Trypan Blue as described. 100,000 moDC were added to a 1.5ml Eppendorf tube for each condition. The Eppendorf tubes were centrifuged at 400g for 5 minutes and the supernatant was carefully aspirated to leave the cell pellet. moDC were culture for 4 hours in either fresh fibroblast media containing 0.005% DMSO or 100nM FICZ or defrosted fibroblast exposed media containing 100nM or with the addition of a further 100nM fresh FICZ.

Unlike CH223191 which was not used in this experiment, FICZ is highly soluble in DMSO and the control concentration of DMSO was matched and therefore significantly lower. After stimulation the cells were harvested and lysed for RNA as described previously.

2.2.8 RNA sequencing

RNASeq was used to determine the gene expression regulated by AHR in intestinal immune cells. Intestinal immune cells were isolated using the enzymatic digestion and MACS sorting method described in previously. Cells were incubated in Complete medium containing 0.16% DMSO, FICZ 100nM or CH223191 100µM for 4 hours. RNA was harvest and purified, as described previously, using the Qiagen RNeasy Micro kit.

2.2.8.1 Determining RNA quality and quantity

RNA quantity was determined using a NanoDrop 2000 (Thermo Scientific) spectrophotometer. Only samples with RNA quantity >50ng in all three conditions were included in the study. This is the minimum required by the Illumina NGS protocol.

RNA quality was examined using the Agilent bioanalyzer and performed by the Genome Centre, QMUL. The Bioanalyzer is a chip-based capillary electrophoresis machine used to determine RNA strand length. RIN values are a measure of strand length and integrity (discussed in more detail in Chapter 6). RIN values above 8.0 are ideal but values >6.0 are acceptable (Pereira 2017 Applications of RNA-Seq and Omic Strategies).

2.2.8.2 RNA Clean-up protocol

The RIN values recovered from the first 6 samples collected for RNASeq showed low RIN values. The electrophoretic pattern suggested genomic DNA (gDNA) contamination was the cause of this. To remove gDNA and any other contaminants samples were re-processed using the RNA clean-up protocol provided by Qiagen (RNeasy Mini Handbook 2012).

Before starting the protocol it was necessary to prepare a DNase mix. DNase I was reconstituted with 550µl RNase free water. DNase mix was generated by adding 10µl DNase I to 70µl buffer RDD. The volume of the RNA samples generated using the RNease micro kit were adjusted to 100µl by the addition of RNase free water. 350µl Buffer RLT was added and mixed well. Then 250µl 100% ethanol was added and mixed well by pipetting. The samples were transferred to the mini spin columns and centrifuged for 15 seconds at 8000g. The flow through was discarded. 350µl RW1 wash was added and the sample was centrifuged for 15 seconds at 8000g. The flow through was discarded. 80µl of the pre-prepared DNAse mix was added to each sample and left at room temperature for 15 minutes to digest genomic DNA. Another 350µl RW1 was added to wash the sample and the sample was centrifuged for 15 seconds at 8000g. The flow through was discarded. 500µl RPE was added and the

sample was centrifuged for 15 seconds at 8000g and the flow through was discarded. Another 500µl RPE was added and the sample was centrifuged for 2 minutes at 8000g and the flow through was discarded. The spin column was transferred to a new 2ml collection tube and spun at full speed (12000g) for 1 minute to dry. Finally, the column was transferred to a 1.5ml collection tube. 30µl RNase free water was added directly to centre of the spin column membrane and the sample was centrifuged at 8000g for 1 minute to elute the RNA. The samples were then stored at -80°C.

2.2.8.3 Sequencing

mRNA-focused sequencing libraries were generated using Illumina RNA library prep kits by the Genome Centre, QMUL. Sequencing was performed using the Illumina NextSeq 500 with a target of 10 million reads per sample.

2.2.8.4 RNASeq exploratory data analysis and quality control

Following RNA sequencing reads were pseudo-aligned using kallisto (Bray et al., 2016) on the high-performance computing cluster at QMUL using the reference genome GRCh38.p10, Ensembl version 91. The subsequent analysis was conducted in R v.3.5.3 by David Watson, post-doctoral scientist in Professor Michael Barnes' translational bioinformatics laboratory, QMUL. The full code is included for reference in Appendix 2.

Transcript-level reads were aggregated to gene-level using the tximport package giving counts per gene. Normalisation to correct for differences in raw counts due to the side of different transcripts was performed using dds from the DESeq2 pipeline (Love et al., 2014).

Dimensionality reduction techniques were then used to check for outliers and perform unsupervised clustering. Gene dispersion (a measure of variation) varies depending on the level of expression of a

given gene. The plot_dispersion tool was used to identify gene expression outliers whose read counts significantly deviated from expectation (Figure 2.7).

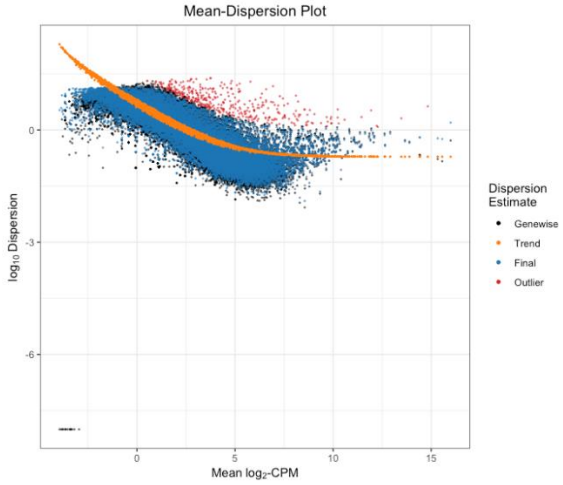

Figure 2.7 Mean dispersion plot. "gene-wise" dispersion estimates are first calculated with the data from each gene. Then a smooth curve is generated to provide an accurate estimate for the expected dispersion value for genes of a given expression. Gene expression outliers whose read counts significantly deviated from expectation (shown in red) are removed during subsequent differential expression testing.

A density plot using plot_density (Figure 2.8A) and sample similarity matrix using plot_similarity (Figure 2.8B) were used to inspect for outliers.

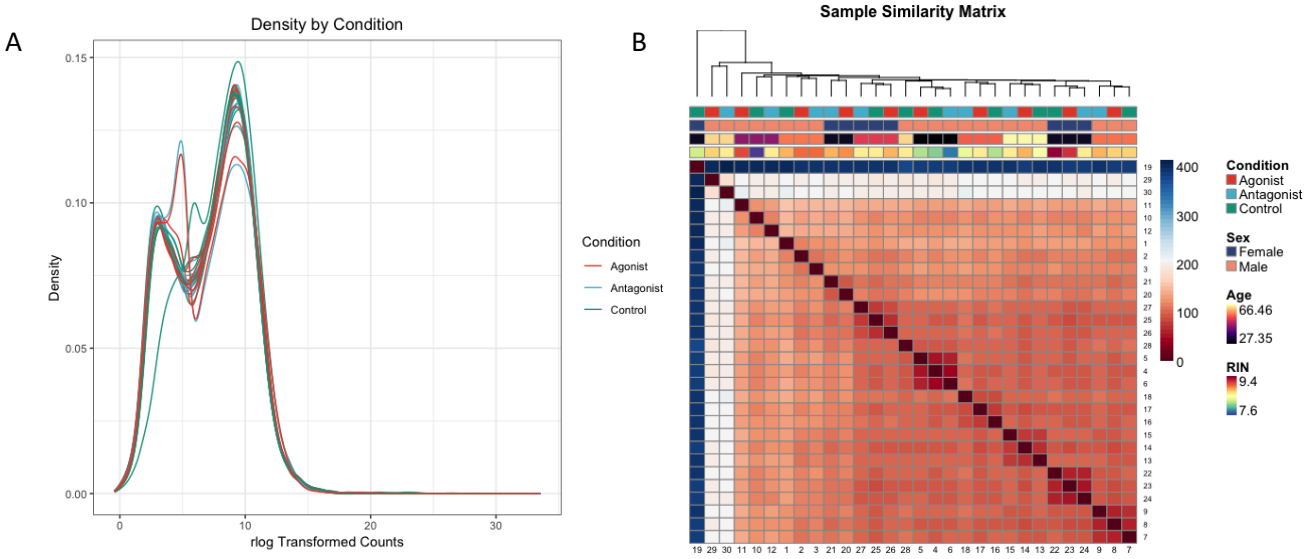

Figure 2.8A Expression density plot. Expression densities for each sample were plotted for each sample. Non-overlapping curves suggested some of the samples were outliers. **B) Sample similarity matrix.** Pairwise Euclidean distance (distance between two points in multidimensional space) was calculated to build a hierarchical clustering dendrogram. Three outliers are identified in the top left corner.

A principal component analysis was performed using plot_pca. PCA is a type of linear transformation on a multidimensional data set that combines a certain number of variables into a new projection or component. Each component sums up a certain percentage of the total variation in the dataset. The first component explained the most amount of variance in the sample but multiple components can be generated. In this example two principal components were examined. These showed three samples were extreme outliers (Figure 2.9A). In fact, these three samples explain more than 50% of the differences observed in the entire dataset. Identical results were seen with both a Salmon (Patro et al 2017) and Kallisto aligned data suggesting the problem was not related to pseudo-alignment rather biological or sequencing sample quality. These three outlier samples were removed from the subsequent analysis otherwise it would have significantly impaired the ability to perform differential expression analysis. After removing three outlying samples the PCA showed that samples were clustered by patient which is expected (Figure 2.9B).

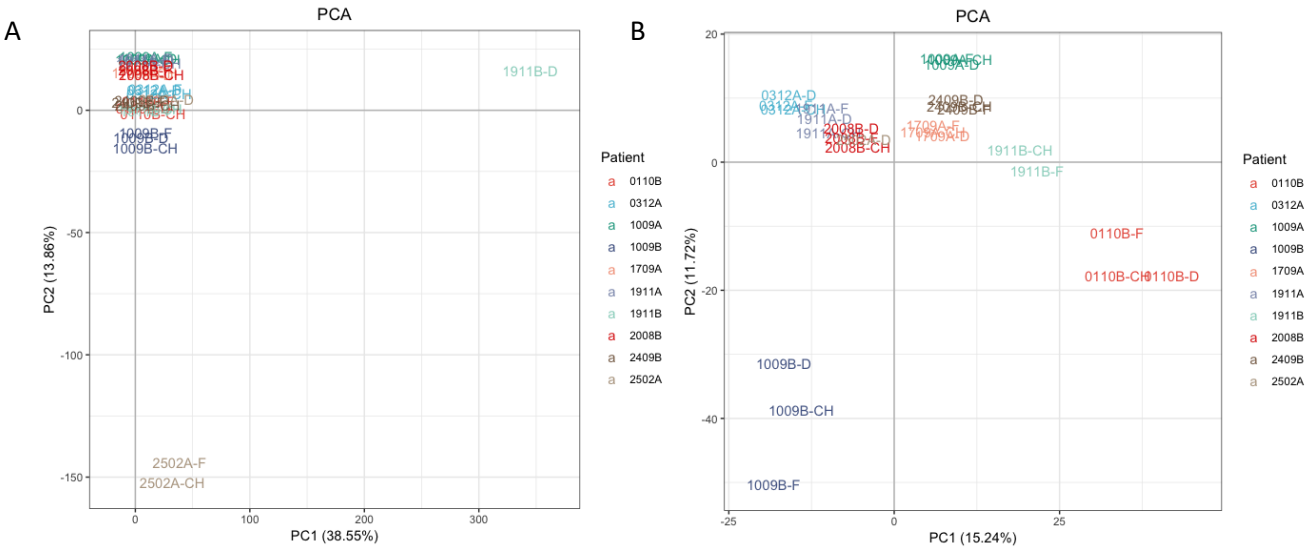

Figure 2.9 A) Primary PCA plot of gene expression data to identify outliers. Extreme outliers were identified using a PCA. These samples were removed from subsequent analysis because the presence of extreme outliers limits the power to detect differentially expressed genes between samples. **B)**

Repeat PCA plot of the same data after removal of 3 outlier samples. Samples appear to cluster by patient.

To support these observations these data were also analysed using a second dimensionality reduction technique plot_tsne. t-distributed stochastic neighbour embedding (t-SNE) is a machine learning algorithm that uses probability modelling to group similar data points (ref). The t-SNE plot showed a similar pattern to the PCA but with a more uniform spread of data (see Appendix 3).

2.2.8.5 Differential gene expression analysis

David Watson wrote custom R code that used the results and lfcShrink functions within DESeq2 to test for differential expression between agonist and control and then antagonist and control with internal gene filtering (removes low expressed genes) and p-value adjustment for multiple comparisons (Ignatiadis et al., 2016) with a target FDR of 5% (q).

The top 1000 differentially expressed genes, irrespective of adjusted p-value were visualised in a mean difference plot plot_md, volcano plot plot_volcano and heat map plot_heatmap which are shown and discussed in Chapter 6.

2.2.8.6 Exploring the function of differentially expressed genes

A systematic search was performed using publicly available databases with the differential expressed genes using GeneCards® (https://www.genecards.org/) and the Entrez Gene database (https://www.ncbi.nlm.nih.gov/gene/). Up to 3 reported gene functions were included in the summary tables with a restricted focus on functions reported in haematopoietic immune cells given the input tissue (Chapter 6).

Gene ontology was examined using DAVID functional annotation (https://david.ncifcrf.gov). Gene lists were uploaded in text format, the identifier “Official_Gene_Symbol” was selected. The species “Homo

sapiens" was selected. Genes were grouped using GO terms and Kegg pathway analysis. The number of genes in each group were recorded.

A second methodology was used to perform gene otology and functional analysis. Metascape combined multiple different resources to group genes and using a tool called Cytoscape can generate visual networks of related genes (https://metascape.org/gp/index.html#/main/step1). Gene ID lists were uploaded in text format. The species "H. sapiens" was selected.

Pathway & Process Enrichment was performed with the following standard settings: Min Overlap 3

3, P Value Cutoff 0.01 and Min Enrichment 1.5.

2.2.9 Single cell sequencing

A single patient was recruited for single cell sequencing. Eight colonic biopsies were collected from the right colon of a healthy male donor who underwent a normal colonoscopy. Biopsies were digested using the collagenase method described above and left in a T-25 tissue culture flask in 3ml freshly prepared Complete medium overnight (12 hours). On the subsequent day intestinal cells were washed into sterile PBS and transferred into a 5ml FACS tube. The samples were centrifuged at 400g for 5 minutes and the supernatant discarded. The cells were resuspended in 100µl Zombie NIR™ fixability dye (BioLegend) diluted 1:200 with PBS. Cells were incubated in the dark at room temperature for 20 minutes. 2ml sterile azide-free FACS buffer was added and the samples were centrifuged at 400g for 5 minutes. The supernatant was discarded and the cells were resuspended in 100µl sterile *Azide-free* FACS buffer. 5µl Pacific Blue™ anti-human CD45 (BioLegend) was added to each sample followed by incubation for 20 minutes on ice. Single colour compensation controls were prepared using BD™ CompBeads labelled with Pacific Blue™ and APC Cy7. Live intestinal $CD45^+$ cells were sorted using the FACS Aria flow cytometer (Becton Dickinson), with the assistance of Gary Warnes, Flow Cytometry

Core Facility, Blizard Institute. The cell sorter is located within a Class II sterile hood and cells were collected into sterile FACS tubes containing 1ml Complete medium.

After cell sorting, 150,000 CD45+ cells were stimulated for 4 hours as described previously. Cells were then harvest and transferred into the Chromium recommended buffer, cold sterile PBS containing 0.04% BSA with a target concentration 500-1000 cells/µl for optimal cell capture and labelling. A target of 1000 cells with a read depth of 50,000 read pairs per cell was selected but this was exceeded due to an underestimation of the performance of the machines. This commonly occurs due to inaccuracies in cell counting, higher than expected cell viability or low cell aggregation.

Gene expression analysis was performed using Loupe Cell Browser®. The top 10 genes characterising the algorithmically generated clusters and manually gated populates (using Boolean logic) were recorded. Publicly available databases were used as described previously to assign functions identified genes.

2.2.10 Statistics

Statistical analyses were performed using Prism 8 (GraphPad Software, USA).

The normal distribution of the continuous variables was assessed using the D'Agostino-Pearson test for normality. t-tests were used to compare two groups of normally distributed data (paired and unpaired), with Welch's correction for unequal standard deviations (SD) for unpaired data. Mann-Whitney tests were used to compare two groups of unpaired data that were non-normally distributed. Paired Wilcoxon signed-rank tests were used to compare two groups of non-normally distributed paired data.

Datasets containing more than two groups of unpaired and normally distributed data were compared using a one-way ANOVA with a Tukey test to correct for multiple comparisons. More than two groups

of data that were unpaired and not normally distributed were compared using a Kruskal-Wallis test. Mean and SD are displayed for normally distributed data sets, while median and interquartile range (IQR) are displayed for non-normally distributed data sets. Correlation between gene expression and other variables was assess by univariate logistic regression.

The EC50 was determined using the dose-response models in GraphPad Prism.

P-values were regarded as statistically significant when $p < 0.05$. All p values were reported as 2 sided.

Gene expression data were analysed by David Watson using R version 3.5.3. The methodology is summarised in this chapter and the full code is included in Appendix 2.

Chapter 3 - Using monocyte-derived dendritic cells as an *in-vitro* model to interrogate the aryl hydrocarbon receptor pathway

3.1 Chapter Summary

This chapter describes the development of an *in-vitro* model to validate methodology to examine the AHR pathway. Monocyte-derived dendritic cells (moDC), a relevant and accessible cultured human immune cell, are used to detect AHR and AHR-dependent gene expression.

AHR protein is measured using flow-cytometry and microscopy and a functional AHR pathway is proven by the direct visualisation of nuclear translocation of AHR with agonist and observed gene expression. AHR-specific agonists (FICZ and DIM) are used to validate multiple AHR-dependent genes in the cytochrome p450 family and highlight important differences with existing murine and cell line datasets. Further supporting the specificity of this effect, a small molecule antagonist (CH223191) is shown to reverse the effects of AHR ligands. The factors contributing variation in the response to AHR ligands is explored in moDC derived from heathy individuals. Finally, AHR gene and protein expression is examined in selected circulating immune cells.

These data inform the examination of AHR pathway in intestinal cells in future chapters.

3.2 Introduction

3.2.1 Background

In diverse murine models of colitis, including DSS, trinitrobenzene sulphonic acid and oxazolone induced colitis and T-cell transfer colitis, augmentation of AHR activity reduces inflammation and weight loss whereas inhibiting AHR signalling is harmful (Furumutsu 2011, Li 2011, Takamura 2010, Huang 2013, Benson 2011). This leads to the important translational question as to whether augmenting AHR activity would be useful therapy in IBD? There are significant cost and ethical barriers to interventional studies in humans without *ex vivo* confirmation of benefit. To help determine the value and inform the design of such a study it is important to determine a number of properties about AHR signalling in the human intestine. Specifically, is the AHR pathway active in the human intestine

in health and is activity reduced in IBD? It is also important to understand if the pathway can be activated beyond the existing state and what concentration of agonist is required to achieve this in a selective manner.

Our primary goal is to answer these questions in human intestinal tissue. However, relatively few immune cells can be recovered from a standard intestinal biopsy taken at the time of a colonoscopy and the recovered cell populations are heterogenous. This makes intestinal tissue a poor choice for initial assay development.

3.2.2 Selecting the monocyte-derived dendritic cell to examine the AHR pathway

To optimise methodology to examine AHR pathway in the human intestine it was necessary to use a more readily available, abundant but relevant cell type. Dendritic cells in the human intestine accumulate at sites of inflammation in IBD (Bell SJ 2001) and have long been recognised to play an important role in the coordination of T-cell responses (Stagg 2003). Particularly relevant to AHR, these cells are in contact with and can directly sample antigens from the intestinal lumen (MacPherson et al. 2004). As discussed in Chapter 1. AHR is a ligand activated transcription factor and this contact with the intestinal lumen is likely to expose dendritic cells to diverse AHR ligands.

Classical AHR signalling leads to expression of specific genes. I hypothesised, quantitative measurement of the expression of these AHR regulated genes by RT-qPCR could serve as a surrogate for AHR activity. Previous studies in a human breast cancer cell line and mouse hepatoma cell lines examined which genes with an adjacent AHR binding region were responsive to the AHR agonist TCDD. The largest changes in expression were seen in *CYP1A1* (27 – 40 fold), *CYP1A2* (6.2 fold) and *CYP1B1* (4.9 fold) (Lo R 2012, Nault 2013). These genes all encode cytochrome p450 (CYP) enzymes.

This large family of enzymes have important roles in toxin and drug metabolism, steroid hormone synthesis and fatty acid metabolism. Based on these data, *CYP1A1, CYP1A2* and *CYP1B1* were selected as a potential candidate gene to measure AHR pathway activity.

Tissue and circulating dendritic cells are rare and heterogenous cells. They comprise no more than 1% of circulating or tissue-derived immune cells which makes them a poor choice for optimisation of methodologies and investigating fundamental properties of the AHR pathway. Therefore, an alternative approach was used in this chapter. Monocyte-derived dendritic cells (moDC) are functionally similar to conventional (myeloid) dendritic cells (cDC) (Collin 2018). Importantly, established straightforward methods allow the generation of large numbers of these relatively homogenous cells from circulating monocytes (Romani 1996). Importantly, local data also suggests these cells express AHR (Martha Wildemann thesis).

3.2.3 Selecting AHR agonists and antagonists

The choice of chemicals to stimulate or inhibit the AHR pathway was also carefully considered. AHR ligands can be categorised into synthetic ligands, such as TCDD, a toxic polychlorinated dibenzodioxin, and natural ligands many of which are tryptophan metabolites produced by bacteria, plants or in humans (Denison & Nagy 2003). Many synthetic ligands are toxic. It is thought that synthetic ligands are less susceptible to degradation by the very CYP enzymes induced by AHR activation (Olson 1994). Failure of this physiological negative feedback loop may lead to toxicity through continuous and inappropriate stimulation of AHR. These agents were excluded from our experiments.

One of most potent natural ligands is indolocarbazole (ICZ), derived from I3C. AHR activity is reported at nanomolar ICZ concentrations in rat liver (Gilner M 1993) and murine studies (Bjeldanes LF 1991). FICZ (6-Formylindolo[3,2-b]carbazole) is a related photooxidation product that has considerable structural similarity to ICZ. It is also reported to be a potent AHR agonist and is more widely commercially available. DIM (diindolylmethane) spontaneously forms from plant-derived I3C in the

acidic environment of our stomach. DIM is believed to be a physiological AHR agonist in the gut (Chen I 1998). All these agonists lead to CYP enzyme expression in mice, although importantly species differences and tissue variability are reported with other ligands. Both agonists also have a short biological half-life due to degradation by CYP enzyme within 2 -4 hours (Linda Bergander 2004). These two ligands were selected for analysis in human immune cells.

To confirm that any change in gene expression observed was indeed dependent on AHR an antagonist was identified. CH223191 is a small molecule AHR antagonist that competitively inhibits AHR-DNA binding in response to the AHR agonist TCDD in cells lines from mice, rats, humans and guinea pigs. It shows >90% inhibition of TCDD induced luciferase activity at 10µM concentration with complete inhibition at 100µM (Bin Zhao 2010).

In this chapter monocyte-derived dendritic cells are stimulated with the agents described above. A combination of techniques are used to measure protein and gene expression to identify and validate expression of cytochrome p450 enzymes, particularly *CYP1A1*, as a sensitive quantitative measure of AHR activity. The relative expression of AHR in different peripheral cells is not previously described but is likely to influence the immune cells responsiveness to AHR ligands. This is also explored particularly in circulating dendritic cell subsets.

3.3 Aims

1. Establish the optimal stimulation and inhibition conditions for AHR in human immune cells
2. Confirm candidate CYP genes are regulated by AHR in human immune cells
3. Examine the impact of AHR signalling on human monocyte-derived dendritic cells
4. Compare relative AHR expression in different human peripheral immune cell populations

3.4 Results

3.4.1 Human monocyte-derived dendritic cells express AHR

Monocyte-derived dendritic cells were derived from monocytes which are abundant in peripheral blood. PBMC were isolated and CD14+ monocytes purified using MACS. Monocytes were cultured with IL-4 and GM-CSF for 7 days to generate dendritic cells. The number of monocytes recovered from MACS sorting and the number of moDC generated are shown from 5 experiments below (Table 3.1).

Collection Date	**Volume of whole blood**	**Input monocytes ($x10^6$)**	**moDC recovered ($x10^6$)**	**moDC (% input cells)**
040417	36ml	8.1	0.84	10.4%
230517	45ml	10.0	0.74	7.4%
200718	45ml	8.0	1.08	13.5%
010219	36ml	10.0	2.30	23.0%
050319	36ml	4.7	2.23	47.4%

Table 3.1: Number of moDC generated from monocytes. The range of monocyte numbers and subsequent moDC generated from 5 healthy donors is shown.

DC were derived from purified monocytes by culture with IL-4 and GM-CSF for 7 days. Fixed cells were permeabilised and stained for AHR. DC were identified by FSC and SSC properties. 86.1% of the population were positive for AHR (MFI anti-AHR/MFI Isotype 6.98). The AHR staining of the population appeared homogenous (Figure 3.1B).

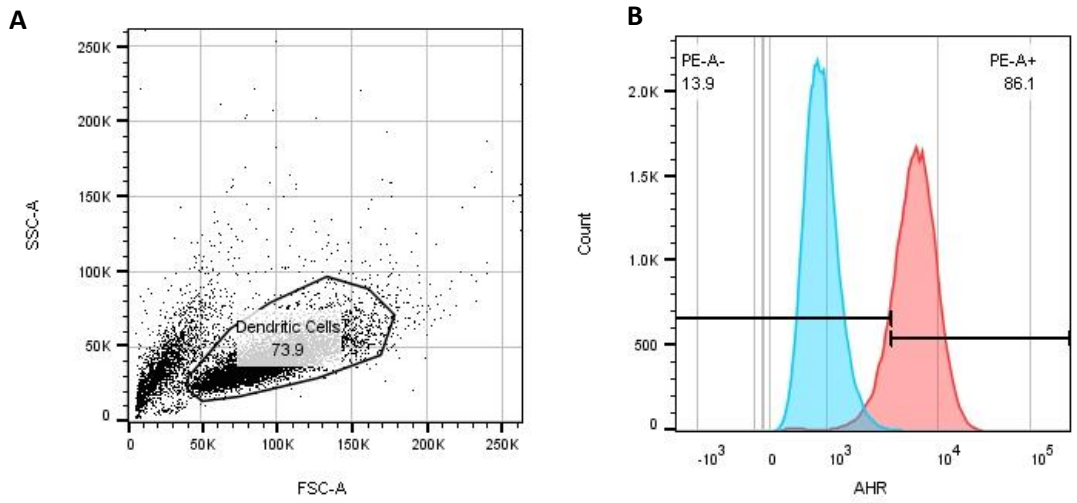

Figure 3.1: AHR is highly expressed in human moDC. moDC were derived from purified monocytes by culture with IL-4 and GM-CSF for 7 days. Cells were permeabilised and labelled with anti-AHR antibodies. **A)** DC were gated based on FSC and SSC properties **B)** Staining with anti-AHR (red histogram) is shown compared with stainng with an isotype-matched control antibody.

3.4.2 Direct visualisation of AHR in moDC

Preceding data using flow-cytometry suggested moDC highly express AHR. To confirm this finding, determine the cellular location of AHR expression and understand if this AHR is functionally active immunohistochemistry was performed. MoDC from healthy donors were stimulated with 100nM FICZ or vehicle control for 4 hours then applied to microscope slides using the Cytospin® method described. Cells were permeabilised with 0.2% Triton and labelled for AHR and mounted with a DAPI nuclear stain.

These images confirmed moDC express AHR (Figure 3.2A). Importantly, staining in the cytoplasm reduced and staining in the nucleus increased after incubation with FICZ, suggesting nuclear translocation after ligand binding (Figure 3.2B). This matches existing understanding of the AHR pathway from previous studies and supports a functional receptor pathway in moDC.

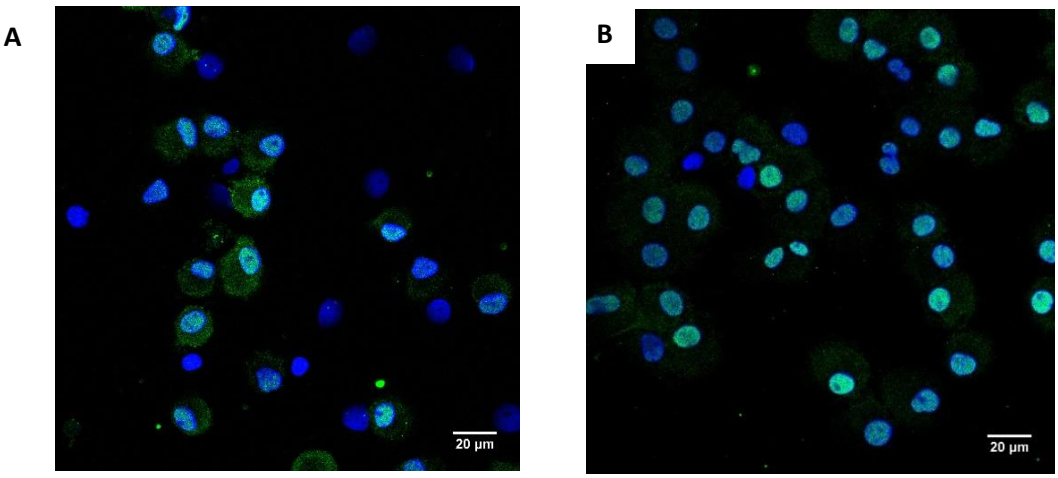

Figure 3.2 AHR staining in moDC is demonstrated by IHC. [Staining seen in the cytoplasma reduced and co-localised with the nucleus after AHR stimulation with FICZ]. moDC from a healthy donor were incubated with 100nM FICZ or complete medium for 4 hours. AHR is green (AF448) and nuclear staining is blue (DAPI). **A**) AHR in unstimulated moDC **B**) AHR in moDC after incubation with FICZ. Images taken at 40X.

3.4.3 Using *CYP1A1* as a quantitative measure of AHR pathway activity

Microscopy suggested the AHR protein was present and functional in moDC based on nuclear translocation in response to agonist. However, a quantitative measure of activation was sought. Previous studies in a breast cancer cell line and mouse hepatoma cell line examined genes responsive to the AHR and found the largest changes in expression were seen in CYP1A1 (27 – 40 fold), CYP1A2 (6.2 fold) and CYP1B1 (4.9 fold) (Lo R 2012, Nault 2013). Based on these results CYP1A1 was selected as a candidate gene to measure AHR pathway activity. To determine if this gene was also highly responsive in human immune cells gene expression in moDC was measured using RT-qPCR in response to AHR agonists and antagonists.

After exposure to FICZ for 4 hours *CYP1A1* expression increased in a concentration dependent manner. Expression increased more than 32-fold even at 2nM. Given this finding, lower concentrations of FICZ

(0.5nM and 1nM) were examined in two additional patients and CYP1A1 expression increased even at this concentration highlighting the potency of FICZ as an AHR ligand FICZ (Figure 3.3). The average EC50 (effective concentration for half maximal CYP1A1 response) was achieved at 5.7nM FICZ.

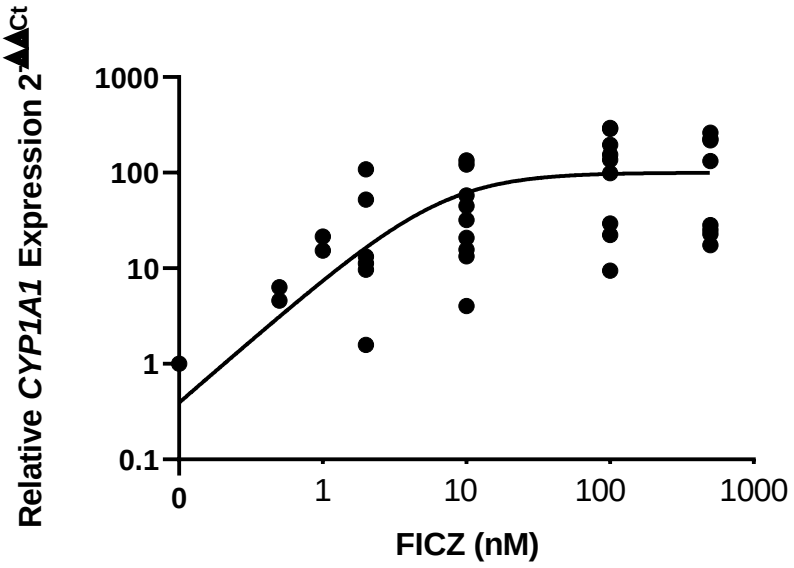

Figure 3.3 Relative *CYP1A1* expression in moDC in response to different concentrations of FICZ. 100,000 moDC derived from healthy donors were incubated for 4 hours with FICZ (6-formylindolo[3,2-b]carbazole) at a range of concentrations (1-500nM) or 0.03% DMSO control made up in fresh complete medium to 100µl. Relative *CYP1A1* expression was measured using RT-qPCR and normalised to expression in DMSO control conditions $2^{-\Delta\Delta Ct}$). Non-linear regression using log(agonist) compared to normalised response give R^2 0.33 and sy.x 71. 9 donors in all conditions except 0.5nM and 1nM which only had 2 repeats.

Considerable inter-individual variation in response was observed. For example, the response to 100nM FICZ varied from 9.42 – 295 fold change, standard deviation 108 (Figure 3.4A). It is not clear what explains this variation between healthy donors. It was considered if this variability in induced response was related to either baseline AHR pathway activity, and thus masked by normalising the data using a standard transformation $2^{-\Delta\Delta Ct}$, or due to differences in the level of AHR expression in cells from different individuals. However, the magnitude of induced *CYP1A1* expression did not correlate with the resting expression of *CYP1A1* (Figure 3.4B) or *AHR* (Figure 3.4C) expression with DMSO control.

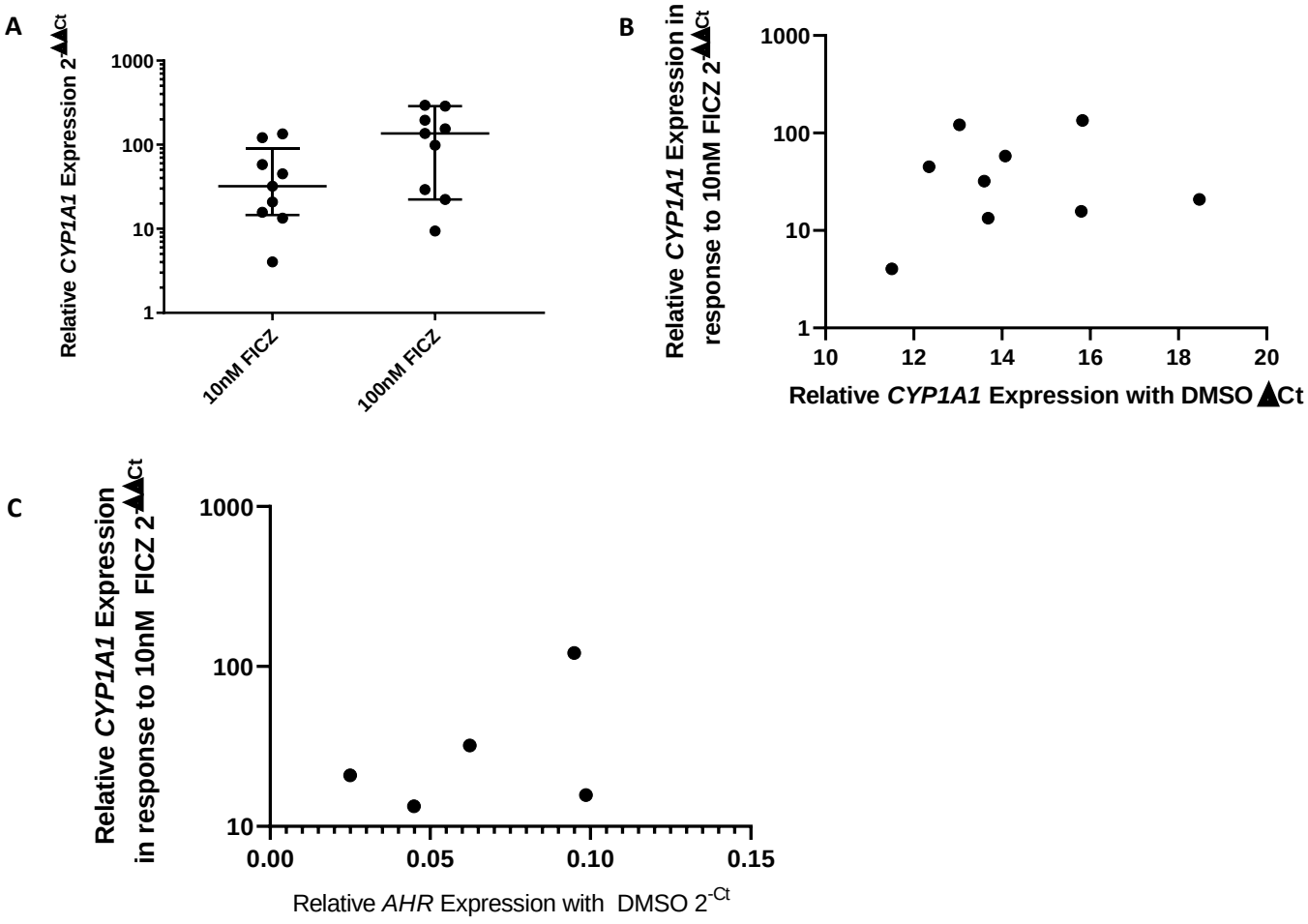

Figure 3.4 Examining the variation in CYP1A1 responses between individuals. A) Relative CYP1A1 expression with 10nM and 100nM FICZ normalised to expression with DMSO control. The variation in induced CYP1A1 expression in response to two difference concentrations of FICZ in moDC from 9 healthy donors. Median and IQR are shown. B) **Relative CYP1A1 expression with 10nM FICZ compared to resting CYP1A1 expression with DMSO control** There is no significant relationship using linear regression between baseline activation of AHR in moDC and the induced response to 10nM FICZ. **C) Relative CYP1A1 expression with 10nM compared to AHR expression with DMSO control**. There is no significant relationship between AHR expression and CYP1A1 response.

To provide further evidence that the induced *CYP1A1* expression seen was directly related to AHR signalling, cells were incubated with the competitive AHR antagonist CH223191 at 10 or 100µM in addition to different concentrations of FICZ or DMSO control. Incubation with 10µM CH223191 inhibited FICZ-induced *CYP1A1* expression at FICZ concentrations below 100nM. The inhibitory effect

could be overcome with the addition of 100nM or 500nM FICZ as would be expected with a competitive antagonist. The EC50 increased significantly from 5.7nM to 301nM FICZ (Figure 3.5 Orange).

Incubation with 100µM CH223191 significantly reduced FICZ-induced *CYP1A1* expression at all FICZ concentrations below 500nM but the inhibitory effect was overcome at this concentration of FICZ. The EC50 for FICZ was increased to 324nM (Figure 3.5 Red).

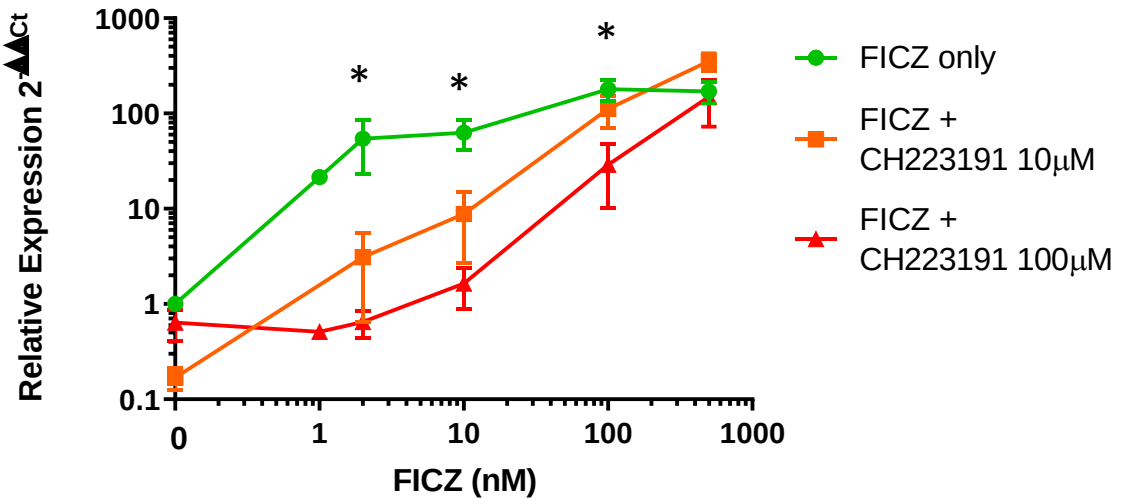

Figure 3.5 [Quantitative] CYP1A1 expression in moDC is induced by FICZ in a dose-dependent manner and is inhibited by CH223191. Human monocyte derived DC were incubated for 4 hours in complete medium with different concentrations of FICZ (nM) (green) in the presence or absence of 10µM (orange) or 100µM (red) CH-223191. Cells were lysed in RLT Buffer®. Relative expression of CYP1A1 was measured using RT-qPCR. Mean and IQR are shown. Dose response curves were analysed using non-linear regression, * $p < 0.05$. n = 6, except 1nM = 1.

These data show that quantitative measurement of *CYP1A1* expression correlates with AHR activation.

3.4.4 CYP1B1 – validating a second AHR dependent gene in moDC

To provide further support for this finding we examined the expression of additional genes reported to be regulated by AHR in other cell types or species using a similar method. CYP1B1 is a cytochrome

p450 enzyme in the same family of enzymes as CYP1A1. *CYP1B1* expression was measured by RT-qPCR using cDNA from moDC derived from 7 healthy donors.

After exposure to FICZ for 4 hours *CYP1B1* expression also increased significantly in a dose-dependent manner (Figure 3.6). However, the magnitude of response was much smaller than *CYP1A1*; the median peak response was 2.57-fold at 100nM FICZ. Mean resting *CYP1B1* expression was 8616x higher than *CYP1A1*. In a subset of patients, the effect of CH223191 was examined. It reduced FICZ-induced *CYP1B1* expression at all concentrations of FICZ below 500nM.

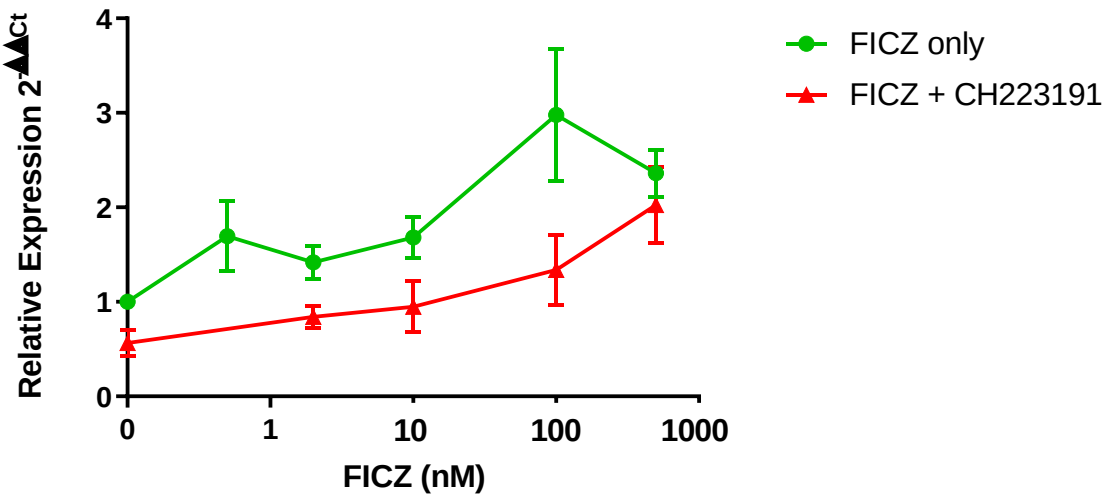

Figure 3.6 *CYP1B1* expression in moDC increases in response to increasing FICZ concentration. Human monocyte derived DC were incubated for 4 hours in complete medium with different concentrations of FICZ (nM) or DMSO control in the absence (green) or presence of CH223191 (100µM) (red). Relative expression of *CYP1B1* was measured using RT-qPCR. 7 donors exposed to FICZ only, 3 donors also exposed to FICZ and CH223191. SEM are shown. Dose response curve was analysed using linear regression. R^2 0.72 $p < 0.05$.

Expression of *CYP1A2*, a third cytochrome p450 enzyme was not detected at rest or in response to incubation with FICZ added at a concentration of up to 500nM in 3 individuals.

3.4.5 Another AHR ligand DIM also induces *CYP1A1* expression in moDC

To support the hypothesis that quantitative measurement of CYP1A1 is a specific measure of AHR activation, an alternative AHR ligand was examined. Diindolylmethane (DIM) is formed in the stomach by acid catalysed condensation of indole-3-carbinol (I3C) which itself is a breakdown product of the glucosinolate glucobrassicin. These compounds are found at high levels in cruciferous vegetables and are reported to be potent AHR ligands (Nagy 2003).

As previously described, moDC were generated from healthy donors then incubated with different concentrations of DIM. Induced *CYP1A1* expression correlated with increasing DIM concentration (R2 0.74 p <0.05). The` peak response, with a mean 18.5-fold increase in expression, was seen at 20uM DIM (Figure 3.7).

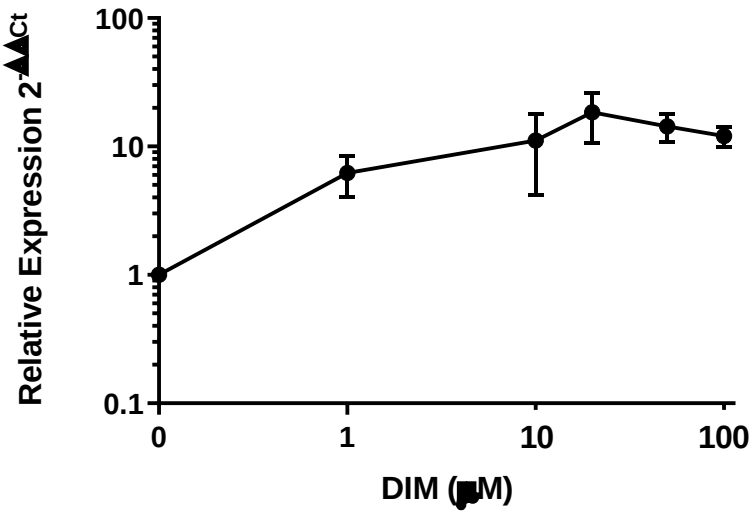

Figure 3.7 Quantitative measurement of *CYP1A1* expression in moDC in response to DIM. Human monocyte derived DC from 3 healthy donors were incubated for 4 hours in complete medium with DIM (μM) Relative expression of *CYP1A1* was measured using RT-qPCR. Mean and SEM are shown. Dose response curves were analysed using linear regression. R^2 0.74 p <0.05.

3.4.6 Examining the impact of AHR signalling on other genes in moDC

3.4.6.1 AHRR is expressed in human moDC and appears to be negatively regulated by AHR

Aryl hydrocarbon receptor repressor (AHRR) suppresses AHR signalling by binding to AHR itself, competing with ARNT and hereby preventing nuclear translocation and gene transcription. In murine studies, expression of AHRR is increased by AHR activation (Bernshausen T 2006). However, in recent studies AHR-independent expression has also been reported in murine model particularly in CD11c+ immune cells. The interaction between AHR and AHRR was more complex than previously described. Of particular relevance to this project, deletion of AHRR led to worsening of DSS colitis similar to deficiency of AHR itself (Brandstatter 2016).

To determine if *AHRR* was expressed in human moDC and directly regulated by AHR activation human moDC were incubated with FICZ or FICZ and CH223191. *AHRR* was expressed at rest, albeit at a very low level ΔCt16.7. Unexpectedly, there was no significant increase in *AHRR* expression in moDC on incubation with FICZ, despite induction of CYP enzyme expression in the same samples. However, incubation with CH223191 significantly increased AHRR expression at rest. This increase in *AHRR* was partially overcome with increasing concentrations of FICZ (Figure 3.8).

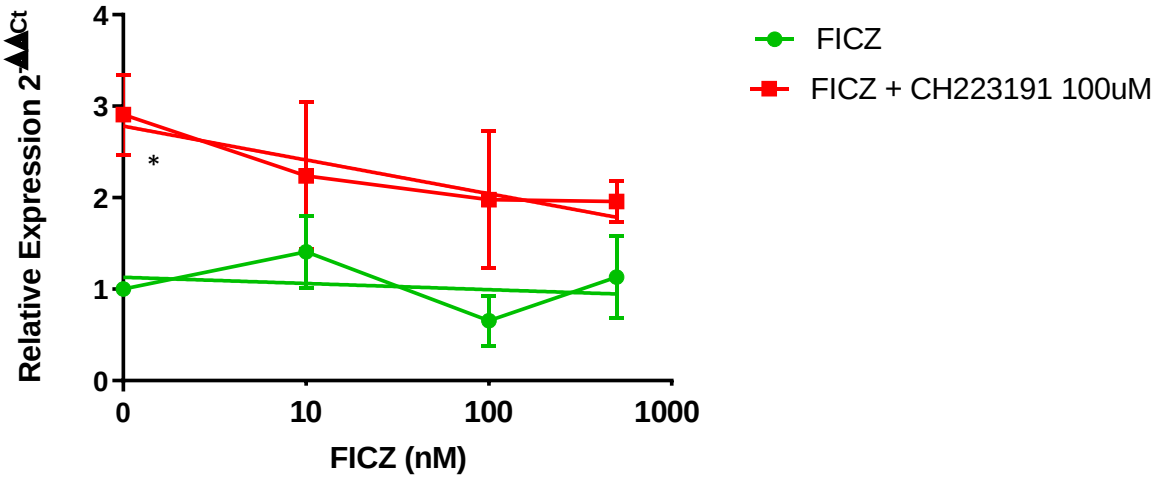

Figure 3.8 *AHRR* expression in human moDC does not increase with AHR activation by FICZ. Human moDC from 3 healthy donors were incubated with FICZ and CH223919 100µM or vehicle control for 4 hours. *AHRR* expression was determined by RT qPCR. Mann-Whitney test * $p < 0.05$.

3.4.6.2 AHR does not regulate CD68 or CD1A1 expression in moDC

CD68 is a transmembrane glycoprotein widely used to identify macrophages and dendritic cells (Ferenback 2008). Increased AHR activation has also been observed in CD68+ cells in viral renal transplant infections and lower activation of AHR has been observed in synovial CD68+ cells in rheumatoid arthritis (Ogando et al. 2016).

CD1A1 is highly expressed in moDC and Langerhan cells but shows very little expression in plasmacytoid DC. *CD1A1* expression characteristically increases as monocytes differentiate into dendritic cells in the culture system used in this study (Collin 2018).

The expression of these genes was measured in moDC exposed to FICZ 100nM or DMSO control. There was no significant difference in expression of either of these markers with FICZ, suggesting these genes are not regulated by AHR in human moDC (Figure 3.9A).

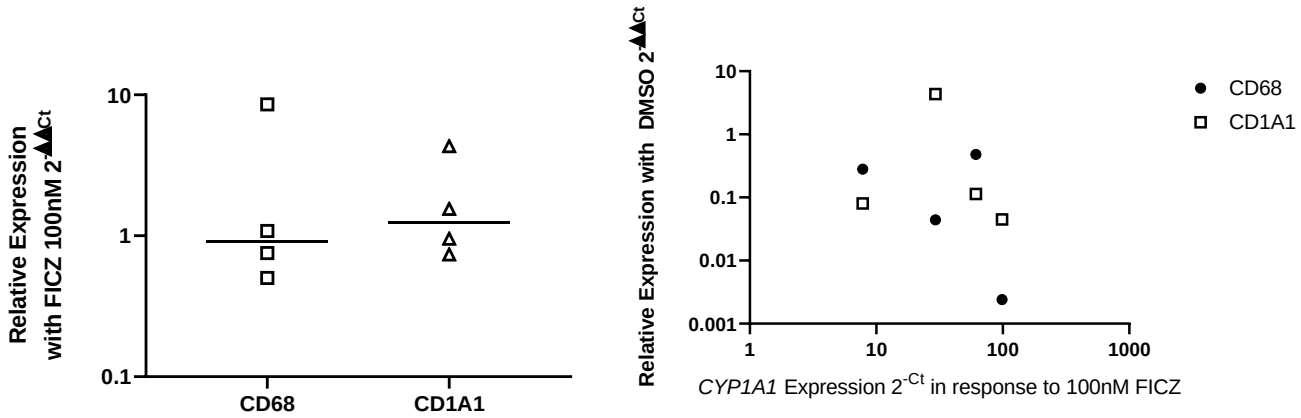

Figure 3.9 A) *CD68* and *CD1A1* expression in moDC does not significantly change with AHR activation by FICZ. Human moDC from 4 healthy donors were incubated with FICZ 100nM or DMSO control. *CD68 and CD1A1* expression was determined by RT qPCR. **B) There is no significant relationship between *CD68* or *CD1A1* expression and *CYP1A1* expression in response to FICZ**. The increase in *CYP1A1* expression with FICZ in the same moDC was determined by RT qPCR

To explore the hypothesis that heterogeneity in monocyte differentiation to dendritic cells could underlie the observed variability in moDC response to the same concentration of AHR ligand (Figure

3.4A), the expression of CD68 and CD1A1 was compared to the CYP1A1 response to FICZ 100nM in the same moDC. There was no clear relationship for either gene (Figure 3.9B). This also suggests variable differentiation from monocyte to dendritic cell does not explain the heterogeneity in *CYP1A1* response to FICZ observed between donors either.

3.4.7 Comparing *AHR* expression in circulating immune cell populations

Monocyte-derived dendritic cells are abundant and homogenous so valuable to optimise methodology. However, these cells are cultured in a synthetic environment *ex-vivo* and do not reflect the diversity of immune cells in the circulation or intestinal tissues. It is also unclear if they have a true *in-vivo* equivalent (Guilliams and van de Laar 2015).

Most intestinal immune cell subtypes including B- and T-lymphocytes, monocytes and DC are derived from cells that undergo trafficking from the circulation to the intestinal mucosa via a tightly regulated process (Habtezion 2017). Some intestinal macrophages are derived from the embryonic yolk sac (Bain 2018). Examination of freshly isolated peripheral immune cells therefore provides an opportunity to examine these precursors, with the major advantage that it is far quicker and easier to isolate PBMC compared to intestinal immune cells.

Peripheral blood mononuclear cells (PBMC) were isolated from 50ml fresh blood from healthy donors using a Ficoll® gradient. Cells were washed with FACS buffer, counted and labelled prior to FACS sorting. Circulating dendritic cells were selected to directly compare with the previous work using moDC. These cells were identified by gating on positive staining with an anti-HLA-DR antibody and negatively staining using a lineage cocktail (CD3, CD14, CD16, CD19, CD20, CD56). Murine literature suggest intestinal gamma delta T-cells depend on AHR signalling (Li 2011) so a γδ T-cell population was isolated using an anti-pan-γδ antibody, as a putative positive control. Finally, in an effort to identify a negative control, B-cells were selected using anti-CD19 antibody based on reports that naïve B-cells express little to no AHR (Lenka Allan, 2005)

Populations of circulating immune cells were isolated using the FACS Aria cell sorter. Relative expression of *AHR* compared to the reference gene *RPL30* (de Jonge 2007) was determined using RT-qPCR.

Gene expression of *AHR* relative to *RPL30* (ΔCt) in each cell population was normalised to expression in unsorted PBMC. *AHR* gene expression was detected in all the examined populations. The highest expression was seen in circulating dendritic cells. However, these cells were rare and represented less than 1% of PBMC in healthy donors. The lowest expression was detected in B-cells.

Cell type	**Gating strategy**	**Mean relative *AHR* Expression (normalised to PBMC)**	**Mean Abundance (%)**
B-Cells	$CD19^+$	0.66	8.1%
γδ-T Cells	γδ-TCR^+	2.37	7.6%
Dendritic cells	$Lineage^-$ $HLA\text{-}DR^+$	5.75	0.6%
PBMC	Not applicable	1	n/a

Table 3.2: *AHR* expression in sorted peripheral immune cell populations. PBMC from 2 healthy donors were washed into FACS buffer and labelled with anti-CD19, anti-γδTCR, anti-HLA-DR and lineage cocktail. Sorted populations were collected into sterile tubes and immediately lysed in RLT Buffer®. *AHR* expression was determined by RT-qPCR.

3.4.8 Comparing AHR protein expression in circulating immune cell populations

Flow cytometry with intracellular staining was used to determine if AHR protein as well as mRNA was present in immune cells and to compare expression between immune cell populations. PBMC from healthy donors were isolated using a Ficoll® gradient and washed into FACS buffer. Cells were labelled with antibodies using PE/Cy7 anti-human HLA-DR antibody and the FITC anti-human lineage cocktail, which includes antibodies for CD3, CD14, CD16, CD19, CD20, CD56. Cells were permeabilised using the eBioscience™ Foxp3/Transcription factor kit and stained for intracellular AHR. The percent of AHR positive cells was determined by comparison to a matched isotype control antibody. The majority of

dendritic cells expressed AHR (58.6%). No AHR protein expression above isotype control was seen in B-cells (Table 3.3). these findings correlate with the gene expression observed.

Cell type	**Gating strategy**	**Mean % AHR$^+$**
All PBMC	None	7.49%
Dendritic cells	Lineage$^-$ HLA-DR$^+$	58.6%
Gamma delta T-Cells	$\gamma\delta$ TCR$^+$	1.20%
Monocytes	CD14$^+$	10.4%
B-Cells	CD19$^+$	0.10%

Table 3.3: Percentage AHR positive compared to isotype control in selected circulating immune cells populations. Different immune cell populations were identified by gating on the surface markers listed. Cells were identified as AHR positive using an isotype control gate set at 0.25%. The percentage of AHR cells in each population is recorded. N = 3 healthy donors.

3.4.9 AHR expression in dendritic cell sub-types

Interestingly, observed AHR expression demonstrated a bimodal distribution in dendritic cells (Figure 3.10E).

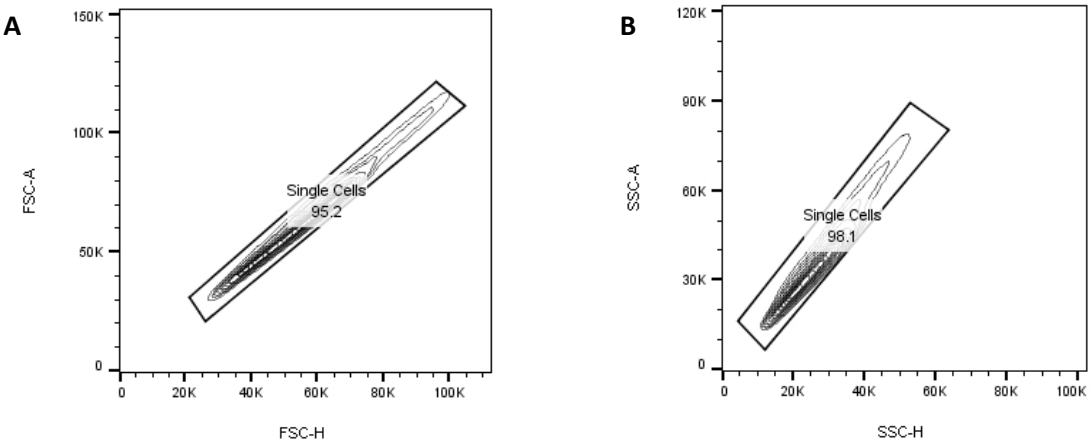

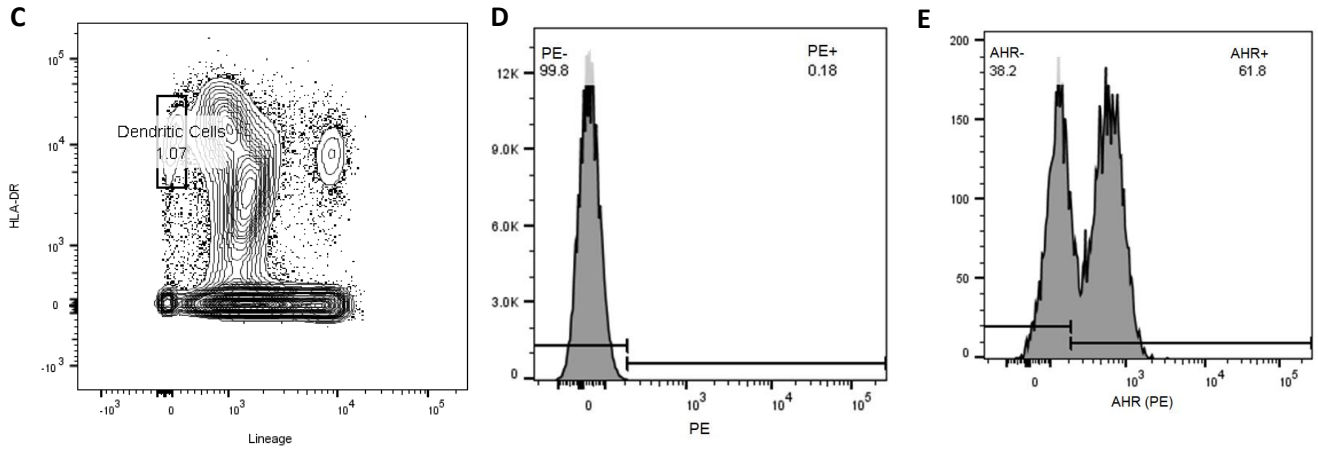

Figure 3.10: **Bimodal AHR expression in circulating human dendritic cells.** Fresh PBMC were labelled with anti-HLA-DR, lineage cocktail and anti-AHR. PBMC were identified using FSC and SSC. **A & B)** Doublet discrimination were performed. C**)** Dendritic cells were identified as HLA-DR positive and lineage negative and represented ~1% PBMC. D**)** PE staining shown with an isotype control antibody **E)** Bimodal distribution of AHR expression was seen in circulating dendritic cells. Single healthy donor shown.

Human dendritic cells can be broadly classified into plasmacytoid DC (pDC) and two types of conventional cDC previously described as myeloid DC (Matthew Collin 2018 Immunology).

Plasmacytoid dendritic cells express high levels of CD123 and CD303 (BDCA2) while conventional DC lack these surface markers and can be defined by expression of CD141 (cDC1) and CD11c (cDC2).

PBMC were isolated and stained for lineage, HLA-DR, CD123, CD303 and CD11c. Doublet discrimination was performed. Dendritic cells were identified as HLA-DR+ and lineage negative and represented 1.1% of PBMC.

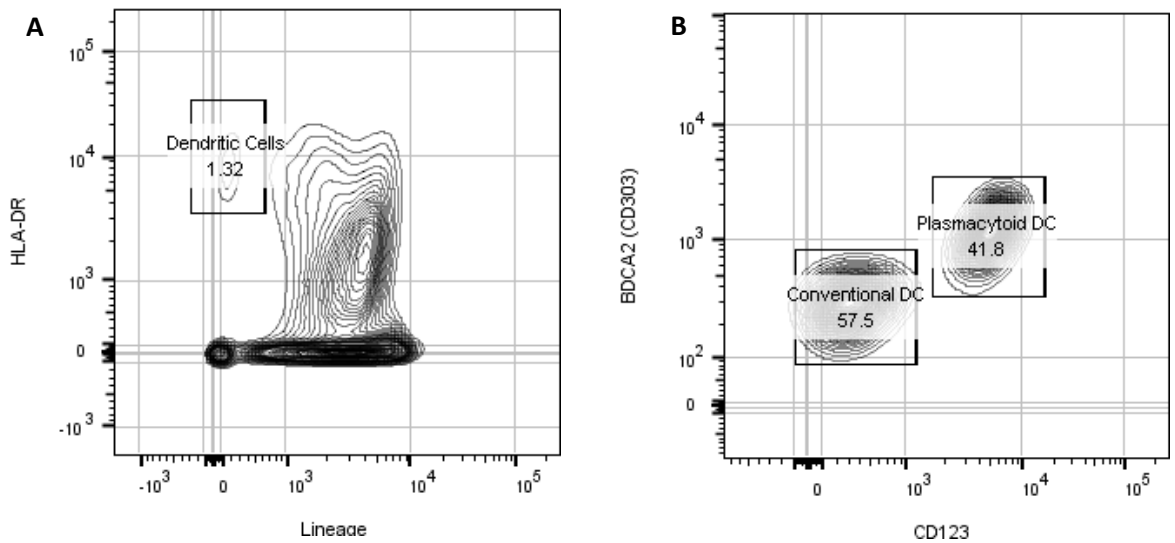

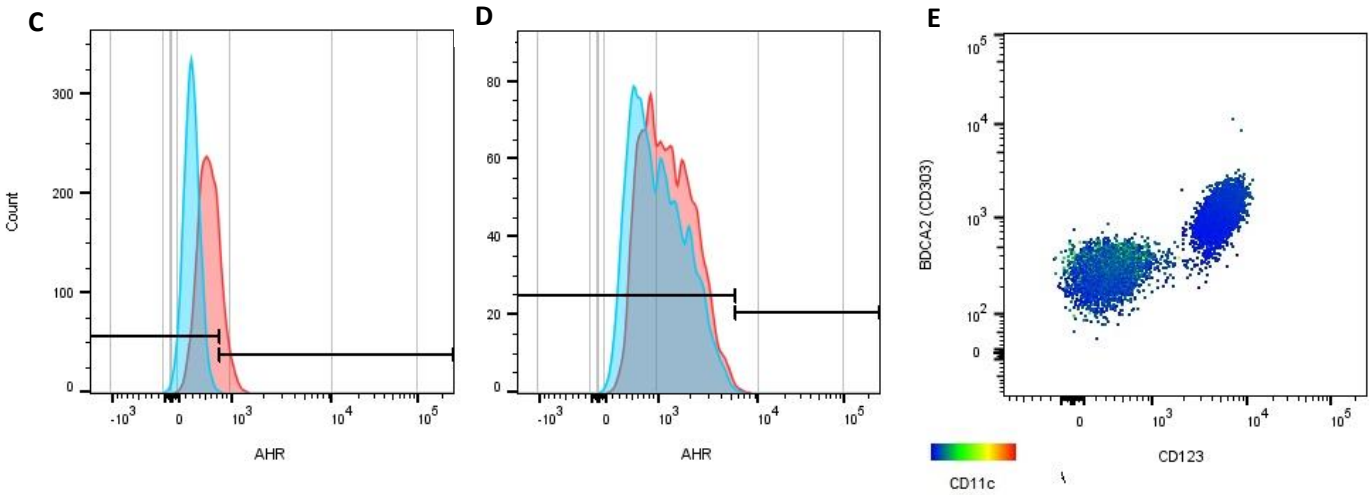

Figure 3.11: AHR expression is restricted to conventional DC sub-types
PBMC were isolated from a healthy donor. Cells were labelled for lineage, HLA-DR, CD123, CD303 and CD11c. Doublet discrimination was performed A**)** Dendritic cells were identified as HLA-DR+ and lineage- **B)** Plasmacytoid DC were identified as CD123+ and CD303+. Conventional DC were CD123- and CD303-. **C)** AHR (red) was detected in 20% cDC compared to isotype control (blue). **D)** Negligible AHR (red) was detected in pDC compared to isotype control (blue). **E)** CD11c staining (yellow-green) was restricted to cDC

Plasmacytoid DC were identified as CD123+ and CD303+ and represented 41.8% of the DC population (Figure 3.11 B). AHR was not detected in this population (Figure 3.2 D). Conventional DC were identified as CD123- and CD303-. CD11c expression was restricted to this population. AHR was expressed in 20.0% of this population (anti-AHR: isotype control MFI ratio 11.2) (Figure 3.11 C). These cells were not further sub-divided into cDC1 or cDC2 populations.

These experiments identified the highest AHR expression in conventional dendritic cells. However, these cells were rare and represented less than 0.5% of circulating PBMC.

3.5 Discussion

This chapter describes the use of a convenient *in-vitro* human immune cell model to explore the relationship between different AHR ligands and AHR dependent gene expression that can be used to inform studies in intestinal tissue.

In this chapter, monocyte-derived dendritic cells (moDC) were generated from monocytes, a cell-type which is abundant in blood. moDC are phenotypically similar to conventional (or myeloid) DC (cDC) (Collin 2018). cDC are particularly implicated in the pathogenesis of IBD (Stagg 2018). For example, cDC isolated from the intestinal tissue of patients with IBD show enhanced recognition of microbes and heightened markers of activation (Hart AL 2005). Whereas plasmacytoid dendritic cells appear dispensable for the pathogenesis of intestinal inflammation, at least in murine models (Sawaii 2018).

In-vitro culture of moDC generated millions of moDC per donor which allowed multiple parallel conditions and optimisation of other methodology (Table 3.1). The yield of DC did vary in this study, donor variation is reported elsewhere (CellXVivo Human Monocyte-derived Dendritic Cell Differentiation Kit), but yield did increase over time during this project which may reflect improvements in basic tissue culture technique during this time period.

Here, these moDC were shown to contain high levels of AHR protein. The narrow distribution of AHR staining also suggested the generation of a homogenous population (Figure 3.1B). High resolution confocal microscopy was used to directly visualise AHR in moDC, and incubation with FICZ lead to nuclear translocation of AHR, visually demonstrating the pathway is functional active in these cells (Figure 3.2). This has previously been reported in hepatoma cell lines (R S Pollenz 1994) and human T-cells (Laurie Prigent 2014) but has not previously been observed in monocytes or moDC.

This information is important to understand the impact of AHR stimulation for a number of reasons. Firstly, to determine if a specific event seen is a direct result of AHR pathway activation it is necessary to compare this event to the expression of a gene known to be directly regulated by AHR at an early time point. Also, a number of target genes induced by AHR activation in previous studies are transcription factors, thus it is likely measuring functional outcomes at a later time point would be influenced by the indirect effect of these downstream transcription factors. Similarly, although classical signalling directly leads to gene transcription, non-classical AHR signalling leads to protein-protein interactions such as enzymatic phosphorylation and ubiquitination. These effects may have different pharmacokinetics.

Prior to analysing intestinal immune cells, where access to tissue and cell numbers are limited, it was necessary to optimise conditions for detection and stimulation of AHR *in vitro*. It was critical to identify specific AHR regulated genes whose expression can be used to quantify AHR signalling.

CYP1 family cytochrome p450 enzymes were identified as strong candidate genes for this role (Lo 2012, Nault 2013)). However, I note with caution other studies found the effects of AHR signalling vary between tissue types (Brandstatter 2016), species (Boitano 2010, Denison 2011, Dere 2011) and the activating ligand used (Mitchell K 2009), highlighting the importance of validating this marker of AHR activity in a relevant human immune cell.

Our results showed that two different AHR ligands (FICZ and DIM) caused a dose-dependent increase in *CYP1A1* expression (Figure 3.3 and Figure 3.7). The fold change in expression seen was higher (108-fold) than reported in mice or breast cancer tissue exposed to TCDD (27 – 40-fold) (Lo R 2012, Nault 2013). Changes in expression were seen at nanomolar concentrations of FICZ, highlighting both the potency of this ligand and the sensitivity of this measure of AHR activity. Expression correlated closely with FICZ concentration (R^2 0.894) (Figure 3.3). Importantly, this effect could be inhibited by a specific small molecule AHR antagonist and the optimal dose for inhibition or stimulation in different experiments can be determined from the drug-response curves generated (Figure 3.5).

For example, 100μM CH223191 of inhibited the highest concentration of AHR stimulation used in this experiment, and would be the optimum concentration in cells exposed to high concentrations of AHR ligands physiologically or experimentally while 100nM FICZ was sufficient to maximally stimulate AHR in similar cells. 10nM FICZ lead to a significant change in expression and would be sufficient concentration to stimulate cells in low AHR ligand experimental conditions.

A second ligand, DIM, was found to be a much less potent activator of AHR. The EC50 required a concentration more than 1000 times greater than FICZ (Figure 3.7). Some reports in the literature suggest no difference in AHR affinity between TCDD and DIM (Hestermann and Brown, 2003). However, DIM has also been shown to be less efficient at recruiting RNA polymerase II to the CYP1A1 gene promoter than other AHR ligands such as β-naphthoflavone (Hestermann 2003). Again, tissue and species-specific difference highlight the importance of validating these agents in a human immune cell. Important differences were indeed seen when examining other cytochrome p450 genes. No *CYP1A2* gene expression was seen at rest or after incubation with FICZ (Appendix) in contrast to previous studies in cancer cell lines (Lo 2012) and mice, where this gene is directly regulated by AHR (Nukaya 2009).

CYP1B1 expression also correlated with FICZ concentration and was inhibited by CH223191 providing further evidence for an AHR specific effect of FICZ. *CYP1B1* expression was very high at rest in unstimulated moDC; close to the expression of the reference gene *RPL30* and while incubation with FICZ did increase *CYP1B1* expression, the magnitude of change was more than 40 times smaller than *CYP1A1* and half the change seen in breast cancer cells (Figure 3.6). This revealed, *CYP1B1* is a less suitable quantitative measure of AHR activation.

One limitation identified was interindividual variation in *CYP1A1* response. While incubating moDC from all donors with FICZ did lead to a significant rise in *CYP1A1* expression in a concentration dependent manner, the magnitude of response and EC50 concentration differed between donors.

I explored whether this was related to the degree of background AHR activation; either a consequence of experimental technique or donor intrinsic properties but there was no significant relationship (Figure 3.4). The blood donors were all healthy individuals, non-smokers, with no significant medical problems in the age range 20 to 40. It is possible variation in environmental exposure to AHR ligands through diet, pollution or otherwise could have influence the monocytes entering culture. However, any physiological AHR ligands should have been metabolised and degraded during the 7-day culture period. Single nucleotide polymorphisms are reported in the AHR gene (e.g. rs6968865) and CYP1A1 and CYP1A2 genes which correlate with altered caffeine and drug metabolism (Sulem 2011). However, these are SNP are rare by definition, and the magnitude of effect does not explain the variation seen.

AHR sensitivity also did not to correlate with expression of markers of moDC differentiation (CD68 and CD1A1) although it would be helpful to examine a larger population (Figure 3.9).

Unexpectedly, AHRR expression in moDC did not increase following incubation with FICZ and in fact, increased following exposure to CH223191. The interplay between AHR, its nuclear partner and ARNT maybe more complex than previously reported. It is possible in this cell type the expression of AHRR is not dependent on AHR signalling. It also is important to acknowledge that only AHRR mRNA was measured and future work should determine if there are also changes in protein expression. It would also be interesting to determine if deletion of the gene either from immortalised immune cell lines or using siRNA has an impact on AHR signalling.

Lastly, here we report the relative expression of AHR protein and mRNA in different sorted circulating immune cell populations, for the first time. *AHR* expression was seen in all cell-types examined. These data identified that the highest AHR gene and protein expression was seen in circulating dendritic cells (Table 3.2 and 3.3). A high level of expression of this environmental sensor certainly seems consistent with the surveillance roles of dendritic cells in contact with our external environment.

A bimodal distribution of protein expression was seen in dendritic cells by flow cytometry which supports previous observations in murine DC (Jennifer C Miller 2012) (Figure 3.10). Conventional DC

and plasmacytoid DC were identified using surface markers (CD123 and CD303). AHR staining was restricted to cDC with negligible AHR detected in pDC (above isotype control) (Figure 3.11). This expression pattern is consistent with our understanding of the different roles of DC: pDC found in peripheral lymphoid tissue play a key role in anti-viral responses while cDC play a major role in antigen presentation and priming T cells and are enriched at barrier sites like the intestine where they are exposed to AHR ligands (K Shortman 2002). The myeloid cDC population could be further subdivided using transcription factor expression (for example, IRF8 is expressed in cDC1 and IRF4 in cDC2). Recent studies in murine lung dendritic cells suggest that although both sub-types express AHR, the impact of AHR signalling differs. AHR signalling in cDC2 was observed to downregulate CD209 expression, a key C-type lectin for viral antigen uptake (Franchini et al. 2019).

3.6 Conclusion

In this chapter moDC are used to optimise methodology to detect the expression of *AHR* and AHR-dependent genes. AHR is directly visualised by flow cytometry and microscopy and a functional receptor is demonstrated through ligand induced nuclear translocation.

Two different classes of AHR specific ligands and a competitive antagonist are used to demonstrate that expression of the cytochrome p450 enzymes *CYP1A1* and *CYP1B1* but not *CYP1A2* are directly regulated by AHR.

The magnitude of *CYP1A1* expression is shown to closely correlate with FICZ concentration and the change in expression seen (>100 fold) identifies the quantitative measurement of this gene as a sensitive and specific measure of AHR activation.

AHR gene and protein expression in circulating in human immune cells is also reported. The highest AHR expression is seen in circulating dendritic cells, specifically conventional DC, which play an important role at the intestinal barrier.

Chapter 4 - Determining the phenotype of AHR expressing cells in the intestinal mucosa

4.1 Chapter Summary

This chapter examines the cellular location and function of the AHR pathway in the human intestine. AHR gene and protein expression is demonstrated in health and inflammatory bowel disease. AHR expression is described spatially using confocal microscopy where it is predominantly restricted to non-immune cells in the lamina propria, with minimal expression in the epithelium. Co-localised staining with CD45 is rare.

In-vivo AHR pathway activity is demonstrated *in-situ* by the expression of *AHR* and the AHR regulated genes *CYP1A1* and *CYP1B1* using immediately processed endoscopic biopsies. Activity is shown to be at a similar level health and IBD.

To determine the presence and activity of AHR in different cell types in the intestinal mucosa a number of sorting strategies are shown. To further explore the novel observation made with con focal microscopy, intestinal cells were divided into an immune (CD45+) and non-immune fraction (CD45-) using magnetic-activated cell sorting. Expression of *AHR* and *CYP1A1* provided further evidence this pathway is already active in both human intestinal immune cells and non-immune cells. Expression of *CYP1A1* is actually shown to be higher in CD45- cells.

In contrast to previous studies suggesting the AHR pathway maybe inactive in Crohn's disease, a trend towards higher *AHR* and *CYP1A1* expression in Crohn's disease is shown.

Another interesting observation is that expression of *AHR* and *CYP1A1* was far higher in intestinal immune cells than circulating PBMC. Although limited by sample size, analysis of the impact of demographic and disease related factors suggests that female sex, ileal location and active inflammation all influence AHR pathway activity. This is particularly important for future study design.

To explore this further and characterise the phenotype of cells with functional AHR activity, two further sorting strategies are described. Using FACS sorting, non-haematopoietic cells are subdivided and *AHR* expression and significant pathway activity *ex-vivo* is demonstrated in epithelial, endothelial

and stromal cell populations. Finally, a novel approach is described to comprehensively characterise AHR expressing cells within the intestinal mucosal immune cell population. Single cell sequencing of sorted CD45+ cells is used to precisely describe the phenotype of AHR positive cells in the intestinal mucosa. This approach reveals that while the majority of AHR expressing cells in the intestinal mucosa are T-lymphocytes, AHR is also expressed in many different immune cell populations where it may exert diverse functional effects.

4.2 Introduction

4.2.1 AHR in the intestinal mucosa: evidence from murine models

Fundamental understanding about the function of the aryl hydrocarbon receptor came from the study of murine models and cancer cell lines. The first studies identifying the receptor as the binding site for dioxin were performed in the widely used C57BL/6 mouse strain (Poland A 1976). Landmark papers demonstrating an important role for AHR in the immune system, particularly at the intestinal barrier followed and used a global homozygous AHR knockout mouse model (AhR-/-) (Fernandez-Salguero P 1995, Veldhoen M 2008, Qui 2012). More recently mice with tissue specific deletion of aryl hydrocarbon receptor (*Ahr*) have been generated, using the Cre-LoxP system, in order to explore the role of AHR in different cell types. However, *Ahr* deletion still take place early in embryonic development meaning that it is not possible to determine if the effects observed are due to the altered immune system throughout early life or accurately represent altered environment, AHR ligand availability and signalling in adult life. There are therefore limitations to extrapolating these data in mice to understand the role of AHR in human health and disease

A limited number of studies have examined the impact of a low AHR activity state by reducing the level of dietary or bacterial AHR ligands on a wildtype genetic background and found that this does not perfectly replicate the phenotype seen in the knockout mice (Li 2011, Qui 2012, Zelante 2013). This is more relevant to human health and disease where homozygous mutations of AHR are not

described in the literature. In a search of a large human genome database of healthy individuals only a single occurrence of a mutation that predicted a loss of function was observed and has not been validated (http://www.genesandhealth.org/).

4.2.2 AHR in the intestinal mucosa: humans

The differences between the human and murine gut immune system are well described (Mestas 2004) and far fewer studies have examined the AHR pathway in human health or intestinal disease. These studies have measured expression in whole biopsies which, given the broad and potentially pleiotropic effects of AHR, is not informative about its activation or role in different intestinal immune cells. Importantly previous studies have also not considered the degree of AHR pathway activity in these cells *in-situ*. It is also not clear at all whether simple quantification of AHR itself provides any information about pathway activation in tissue. This is particularly important when considering the translational implications of murine work showing activation of AHR is protective in models of intestinal inflammation. In most murine models examining the role of AHR in the intestine the pathway is completely inactive due to genetic deletion. It seems unlikely, given the variety of AHR ligands in the environment (Denison MS 2003), that any human would have complete inactivity of this pathway. It is important to determine if relatively low or high activity in this pathway has any meaningful impact on intestinal immune function or whether the phenotype seen in murine models is only recreated by total loss of AHR. The converse question is also important, whether it is possible to augment AHR activity in health or disease to alter immune function for benefit.

Thus, in this chapter I aim to confirm *AHR* is present, and that the pathway is activated *in-situ* in the human intestinal mucosa using the cytochrome p450 genes previously identified as markers of AHR activation in moDC (Chapter 3).

I aim to characterise which cells express AHR, using different techniques. Laser confocal microscopy and immunohistochemistry allow description of the spatial location of AHR in the mucosa. Magnetic

cell sorting and FACS sorting allows the activity and sensitivity of the AHR pathway to be examined *ex-vivo* in immune and well defined non-haematopoetic cells. Finally, a combination of FACS sorting and single cell sequencing is used to precisely describe the phenotype of AHR positive immune cells in the human intestinal mucosa.

In parallel I consider the role of AHR in inflammatory bowel disease. As described in Chapter 1, AHR has been implicated in intestinal inflammation. Polymorphisms in *AHR* are associated with a lower risk of IBD (Liu JZ 2015). Altered *AHR* expression is reported in whole biopsies from patients with UC and, more markedly, in Crohn's disease (Monteleone 2011).

Crohn's disease most commonly affects the terminal ileum and right colon. The ileum is exposed to a variety of dietary and environmental AHR ligands including plant-derived molecules, tryptophan and fat-soluble ligands such as aromatic amines and dioxins (Korecka 2016). The right colon is a site of abundant colonic bacteria with bacterial synthesis of AHR ligands such as indoles and butyrate (Marinelli 2019). For these reasons patients with Crohn's disease were selected for this functional study.

That is not to say study of this pathway in ulcerative colitis would not be valuable. However, there are significant differences between these conditions (Outlined in Chapter 1) and combining them together, as other studies have done previously, would undermine the power to detect any important differences between health and different inflammatory states (Arsenescu 2011).

In this chapter the expression and *ex-vivo* activity of AHR is compared between health and Crohn's disease to answer an important translational question. If AHR activity has regulatory effects in murine models of inflammation, is the AHR pathway less active in Crohn's disease?

4.3 Aims:

1. Determine whether AHR is present and activated *in-situ* in the human intestinal mucosa
2. Identify which cell types express AHR and CYP1A1 in the human intestinal mucosa
3. Compare AHR and AHR-regulated gene expression in health and Crohn's disease

4.4 Results

4.4.1 AHR and AHR-regulated gene expression is detected in intestinal mucosal biopsies in health and IBD

Intestinal mucosal biopsies (approximately $2mm^3$) were collected at the time of scheduled colonoscopy or surgery. Samples were collected from 16 individuals: 8 healthy donors, 6 patients with Crohn's disease and 2 patients with ulcerative colitis (Further details in Appendix 4). Whole biopsies were processed immediately. Biopsies were washed in PBS and transferred to 1.5ml Eppendorf tubes containing RLT Lysis Buffer®. Tissue was then homogenised using an ultrasonic probe sonicator. The sonicator was set to 15W power and applied for up to 3 bursts for 15 seconds with 30 seconds on ice to prevent overheating. After centrifugation the supernatant was aspirated and the lysate immediately stored at -80°C. RNA was extracted using Qiagen RNeasy mini columns. Gene expression was determined using RT-qPCR. Gene expression is shown relative to the reference gene *RPL30*.

AHR expression was detected in 15/16 individuals examined (*AHR* expression was not detected in 1 healthy individual). *CYP1B1* expression was detected in all biopsies examined and *CYP1A1* expression was detected in 14/16 individuals (7/8 healthy and 7/8 IBD). Median *AHR* expression was ΔCt 8.0 and CYP1B1 was expressed at ΔCt 8.8. *CYP1A1* expression was significantly lower than *AHR* or *CYP1B1* expression at ΔCt 16.7 ($p<0.001$). There was a trend towards higher *AHR* expression in IBD (median ΔCt 6.0) compared with health (ΔCt 11.2) but expression of *CYP1A1* and *CYP1B1* were similar (Figure

4.1). There was considerable interindividual variation in expression. Expression of *AHR* and *CYP1A1* was similar in patients with Crohn's (n = 6) and ulcerative colitis (n = 2) (not shown).

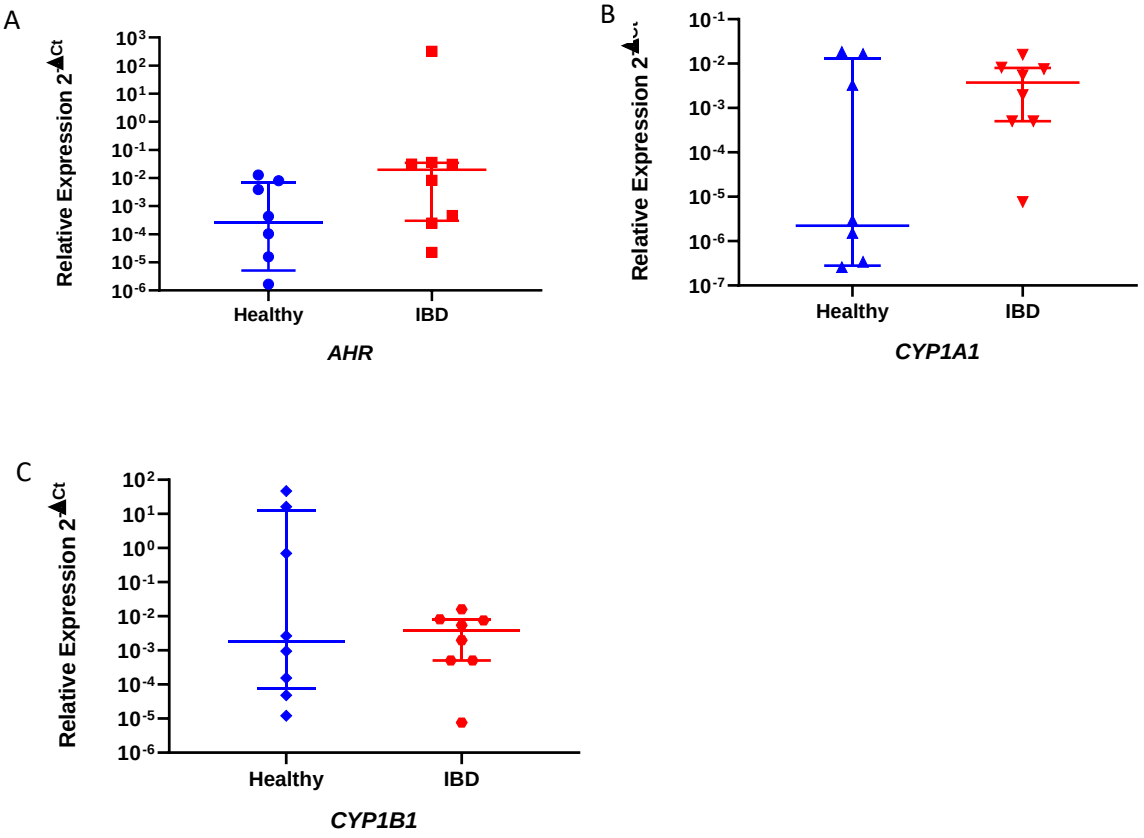

Figure 4.1 Relative gene expression in whole biopsies from the intestinal mucosa. Freshly collected whole intestinal mucosal biopsies (2mm^3) were immediately processed on ice. RNA was extracted using Qiagen RNEasy spin columns. Relative expression of **A) *AHR*** **B) *CYP1A1*** and **C) *CYP1B1*** are shown normalised to *RPL30* ($2^{-\Delta Ct}$). 8 healthy donors and 8 patients with IBD (6 Crohn's, 2 ulcerative colitis). Median with interquartile range shown.

4.4.2 AHR protein expression is highest in non-haematopoetic cells in the intestinal mucosa

4.4.2.1 Determining AHR expression in health colonic mucosa by immunohistochemistry

Gene expression of AHR and AHR regulated genes in whole biopsies showed AHR is present and active *in-situ* in both health and IBD in the human intestinal mucosa. However, lysing whole biopsies mixes the RNA from many different cells. This makes it impossible to know what the activity or impact of AHR signalling is in different cell types. A number of different strategies were used to characterise the

cells in which AHR is present. Firstly, AHR protein expression was examined using immunohistochemistry.

Colonic and ileal mucosa collected at the time of resection for colon cancer or intestinal resection for Crohn's disease was fixed using sucrose and PFA as described (Methods). A crytostat microtome was used to cut 7µm frozen sections. Tissue was stained with antibodies to AHR (green 488nm), CD45 (red 546nm) and a DAPI DNA stain (blue 461nm); the colour of the secondary antibody is shown in brackets. Non-primary controls lacking the primary antibodies were used to exclude non-specific binding of secondary antibodies and determine positive staining. In healthy colonic mucosa AHR staining was infrequent. Bright AHR expression was counted manually in 10 fields at 20x power from 4 healthy donors and on average identified 14 cells per field. Expression was restricted to the lamina propria and was not seen in the surface epithelium (example from two healthy patients shown in Figures 4.2 and 4.3). CD45 staining very rarely appeared to co-localise with AHR (Figure 4.2B).

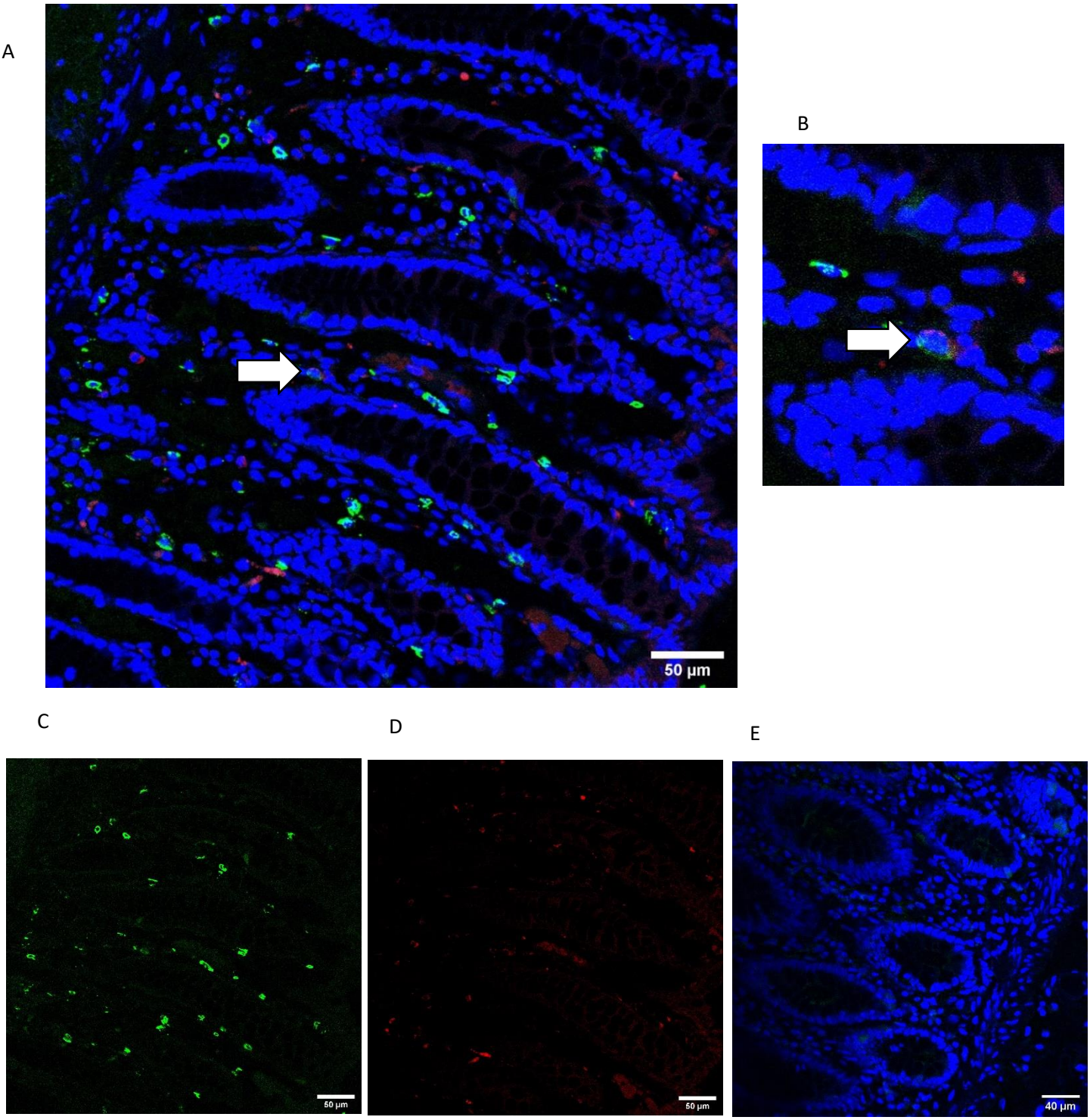

Figure 4.2 AHR and CD45 staining in healthy colonic mucosa. A) Healthy colonic mucosa stained for AHR (Green 488), CD45 (Red 546) and a nuclear stain (Blue DAPI) **B)** A cropped image showing AHR and CD45 co-localisation **C)** AHR staining only **D)** CD45 staining only **E)** No primary antibody control with DAPI only. Cytoplasmic AHR is seen as green rings. Bright AHR staining is seen in 34 cells in 1 20X field of view. Only a single event of co-localised expression is seen. All images taken at 20x power.

A

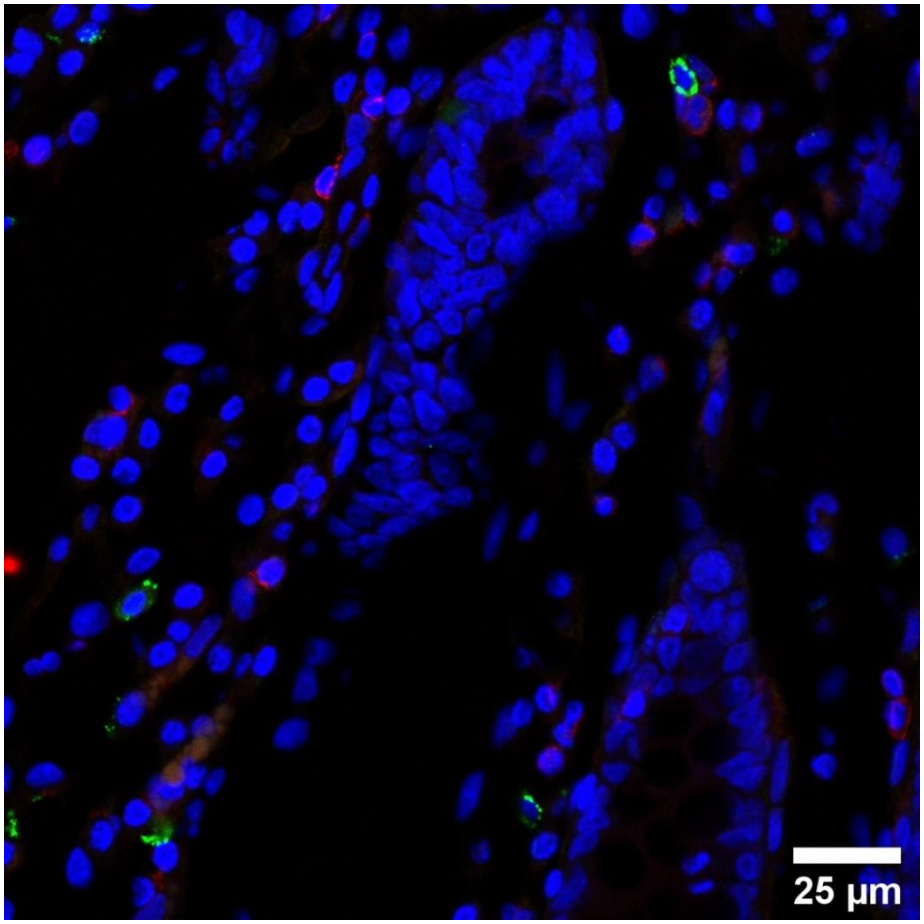

B

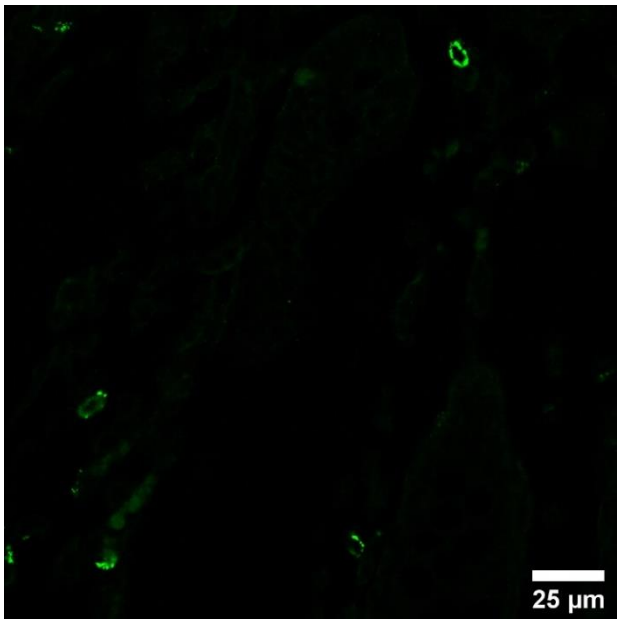

C

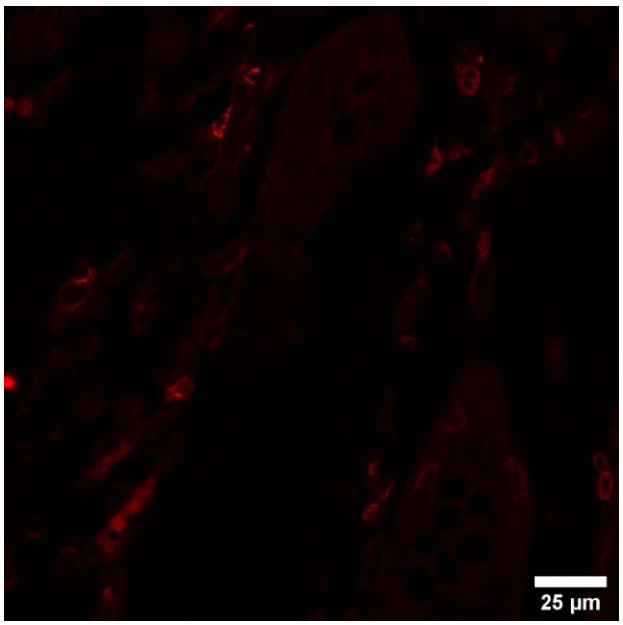

Figure 4.3 AHR and CD45 staining in healthy colonic mucosa from a different patient. A) Healthy colonic mucosa stained for AHR (Green 488), CD45 (Red 546) and a nuclear stain (Blue DAPI). **B)** AHR staining only **C)** CD45 staining only. Cytoplasmic AHR is seen as green rings. Bright AHR staining is seen in 7 cells in 1 40X field of view. No co-localised expression was not seen in this individual. All images taken at 40x power.

4.4.2.2 AHR expression in ileal and colonic mucosa in Crohn's disease by immunohistochemistry

The same methodology was used to examine sections of ileal and colonic mucosa from three patients with Crohn's disease. CD45 expression was significantly increased compared with health confirming that these samples were from inflamed tissue. AHR expression was counted in 10 fields at 20X power from 3 patients with Crohn's disease. On average 44 AHR+ cells were seen per 20X field, which was significantly more than seen in healthy colonic tissue (t-test $p < 0.01$). Expression was restricted to the lamina propria in both colon and ileum. Bright AHR and CD45 rarely co-localised (1 per 20x field) (Figure 4.4B & 4.4C). However, weak AHR staining, just above background, was seen in some areas (Figure 4.5B) which appeared to localise with CD45 staining (Figure 4.5A and 4.5B). However, it is possible this was artefactual.

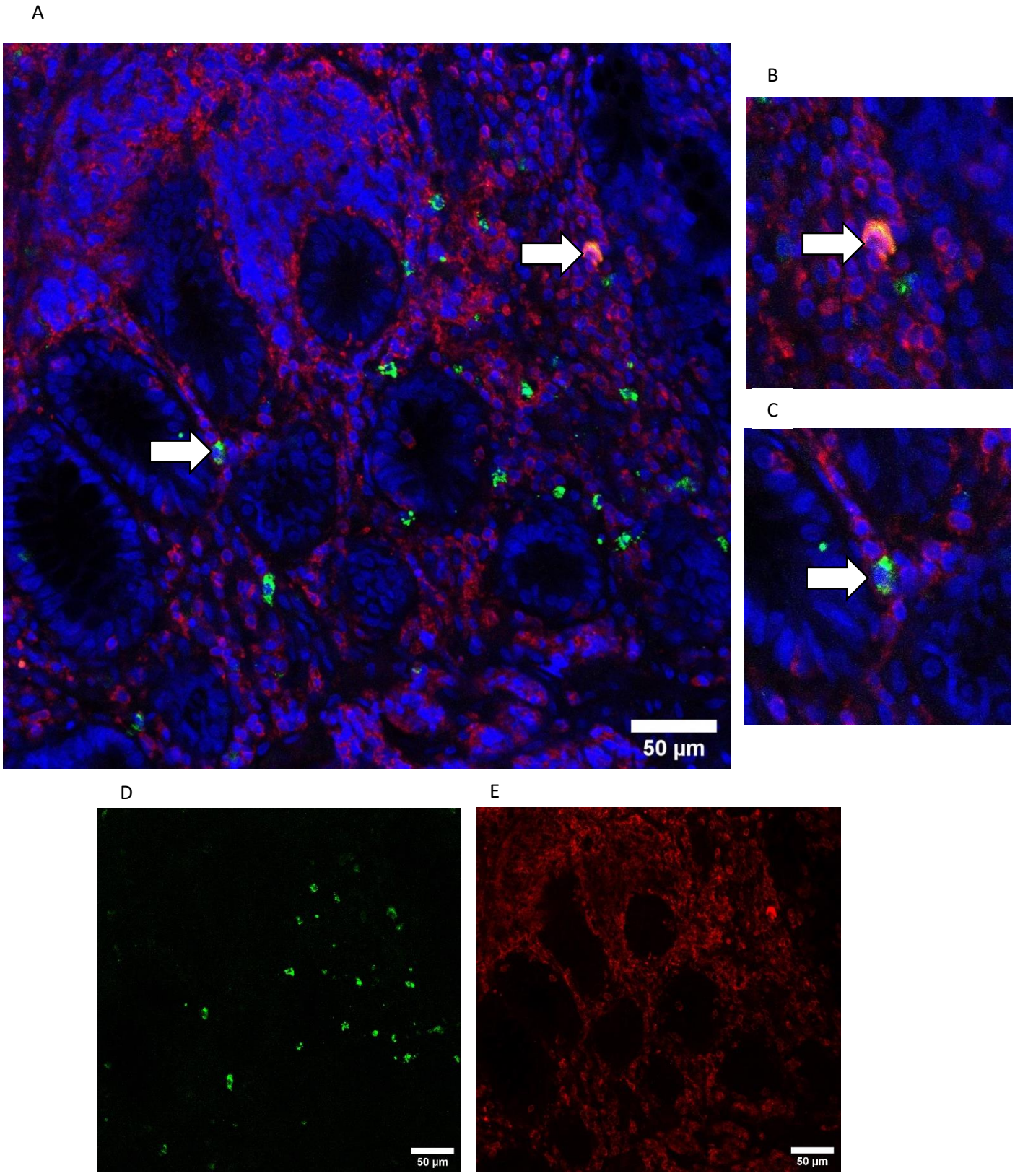

Figure 4.4 A) Inflamed ileal mucosa from a patient with Crohn's disease stained for AHR (Green 488), CD45 (Red 546) and a nuclear stain (Blue DAPI) **B & C)** Cropped images showing AHR and CD45 co-localisation **D)** AHR staining only **E)** CD45 staining only. Bright AHR staining is seen in 31 cells in this 20x field of view. Two events of clear co-localised expression are seen. All images taken at 20x power.

A

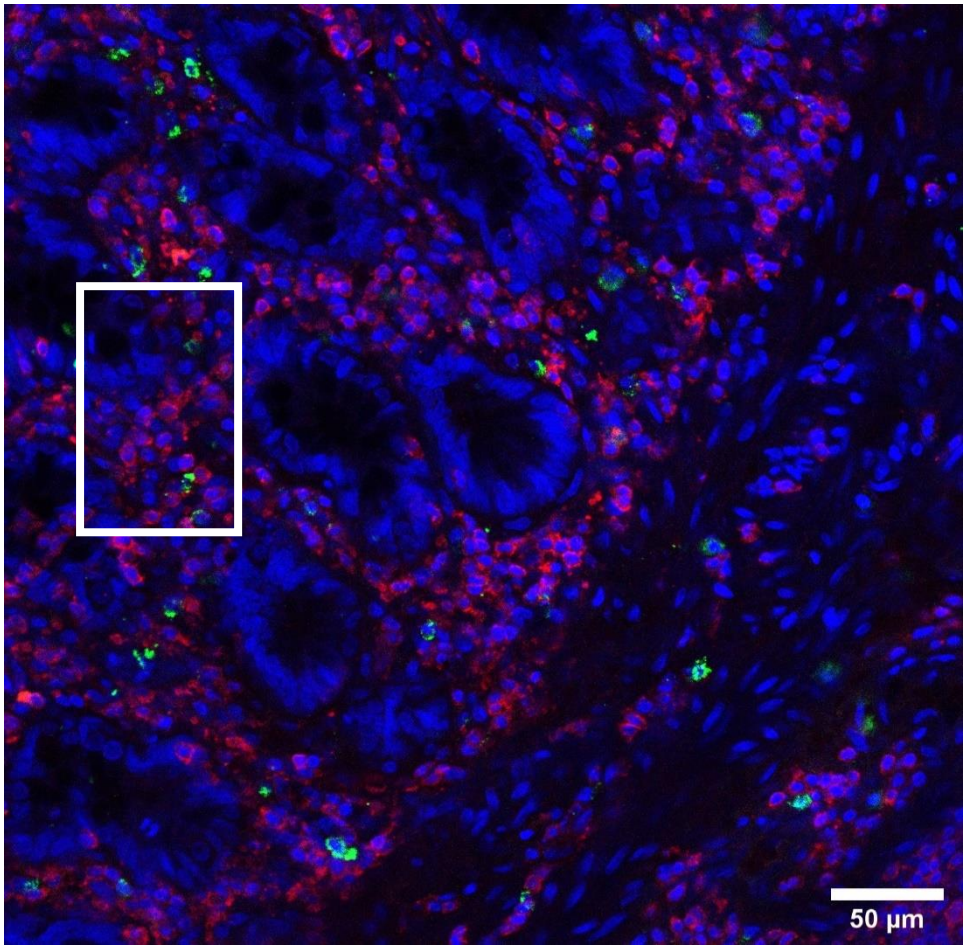

B

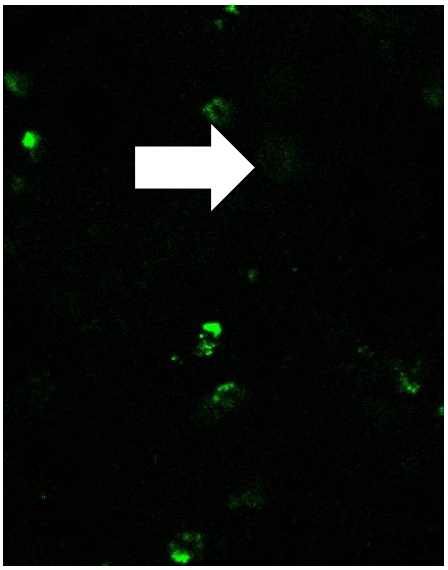

C

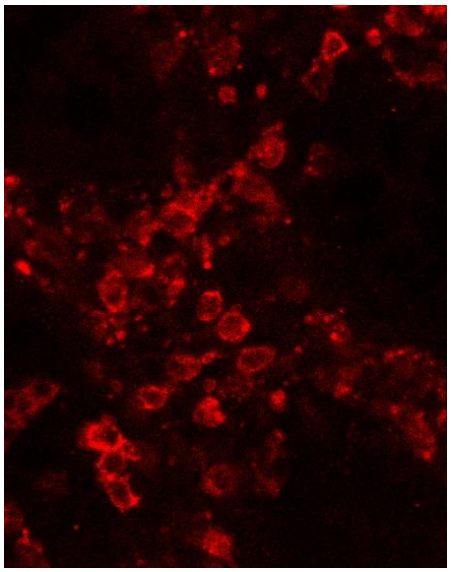

D

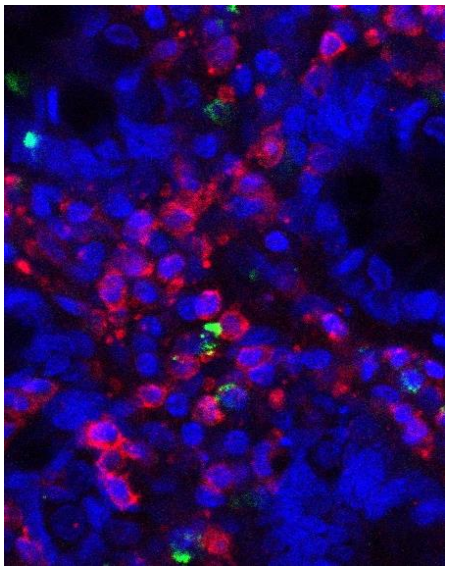

Figure 4.5 A) Inflamed colonic mucosa from a patient with Crohn's disease stained for AHR (Green 488), CD45 (Red 546) and a nuclear stain (Blue DAPI) **B)** A cropped section of the field shows an example of weak AHR staining (Green). **C)** CD45 staining (red) only **D)** A composite image of the cropped area with CD45 and AHR and nuclear staining.
Bright AHR staining is seen in 46 cells in the 20x field of view. Convincing co-localised expression was not seen, although three areas of weak AHR staining did appear to colocalise with CD45.

The microscopy findings were unexpected. My previous observations in circulating immune cells and monocyte-derived dendritic cells showed abundant exression of AHR protein and mRNA. However, in the intestine, even considering the qualitative limitations of microscopy, the brightest AHR staining was actually seen in CD45 negative cells. These cells appeared to be restricted to the lamina propria in both health and disease. CD45- cells in the intestinal mucosa are a mixed population that include fibroblasts, myofibroblasts, vascular endothelial cells and neurons.

To validate this novel observation in fixed tissue it was necessary to isolate live non-haematopoetic cells from the intestinal mucosa. This would enable confirmation that *AHR* is both expressed in these cells but also functionally active in this population and if confirmed, these cells could be characterised further.

4.4.3 Isolating live immune and non-haematopoietic cells from the intestinal mucosa

Reviewing the existing literature suggests AHR is expressed in diverse cell types and it may have different functions in different tissues and cells lineages (discussed in Chapter 1). This may explain some of the variability in measured expression in homogenised whole biopsies. In murine models, conditional deletion of AHR in bone marrow alone does not phenocopy the changes in haematopoietic cells seen in mice with an organism-wide AHR deletion (Bennett 2018) supporting the hypothesis that AHR plays an important role in non-haematopoietic cells.

In this chapter different sorting strategies are used to determine the presence of a functional AHR pathway in different sub-sets of human intestinal mucosal cells.

Firstly, intestinal mucosal cells were separated into haematopoietic and non-haematopoietic cells using the surface marker CD45. CD45, originally called common leucocyte antigen, is an enzyme protein tyrosine phosphatase receptor type C (PTPRC) (McMichael AJ (1987)). This transmembrane protein is found in all differentiated haematopoietic cells except erythrocytes and plasma cells. This

marker was selected to identify intestinal leucocytes. This approach allowed separate and simultaneous examination of the AHR pathway in intestinal immune cells and major non-immune cell types which include epithelial cells and fibroblasts.

Further sub-division into immune cell sub-populations was not performed initially to ensure adequate cell numbers and allow sorting using a single parameter. In addition, given the unexpected microscopy findings, it was important to determine AHR is present and functional in this population at all before considering multiple parameter sorting.

Mucosal biopsies were obtained at the time of planned colonoscopy from a 21 individuals: 10 healthy patients and 11 patients with Crohn's disease (Further details in Appendix 5). The inclusion criteria are detailed below (4.4.6).

Intestinal tissue was immediately digested using the collagenase method to generate a single cell suspension. $CD45^+$ cells were labelled and positively selected using MACS® cell separation columns from Miltenyi Biotec. This technique allows sterile enrichment of the cells on the bench independently which allowed freshly collected samples to be processed at any time of day. The purity of a representative sample was assessed using flow cytometry. The positive and negative fraction were divided and washed into FACS buffer. The cells were relabelled with Pacific Blue™ anti-human CD45 or isotype control. 83.4% MACS selected CD45+ cells were CD45+ following re-staining and 7.1% MACS selected CD45- cells were CD45+ by FACS meaning 92.9% of the CD45- cells were truly CD45- (Figure 4.6).

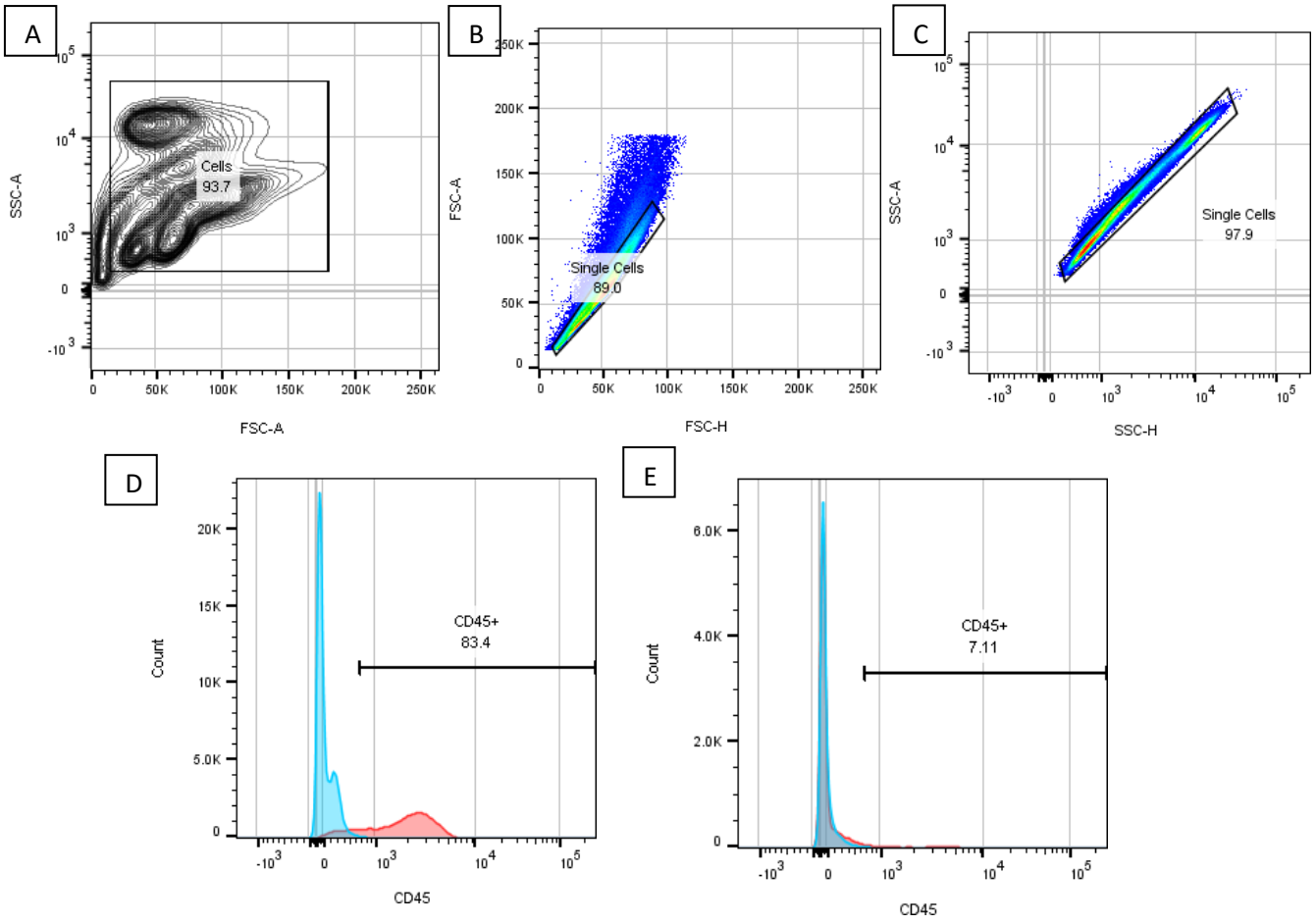

Figure 4.6 Assessment of CD45 purity after MACS selection. 8 intestinal biopsies from 1 patient were digested using a collagenase method. Cells were labelled for CD45 and magnetically separated using MS columns. The positive and negative fraction were divided and washed into FACS buffer. The cells were relabelled with anti-CD45 (in red) or isotype-matched control antibody (in blue). **A-C)** Single cells were identified (CD45+ fraction shown). **D)** 83.4% MACS selected CD45+ cells showed CD45+ staining by FACS. **E)** 7.1% MACS selected CD45- cells were CD45+ by FACS.

4.4.4 Determining *AHR* and *CYP1A1* expression in intestinal immune cells and non-haematopoietic cells in health and Crohn's disease

AHR expression in ex-vivo MACS sorted intestinal immune cells (CD45+) and non-haematopoietic cells (CD45-) was determined by RT-qPCR. Similar to the results observed in whole biopsies, there was a trend towards higher expression of *AHR* in Crohn's disease in both CD45+ and CD45-, but this difference was not statistically significant (Figure 4.7). Inter-individual variation was higher in Crohn's

disease than health (standard deviation 0.04 in health and 0.08 in Crohn's disease). Unexpectedly, *AHR* gene expression was similar in immune and non-haematopoietic cells.

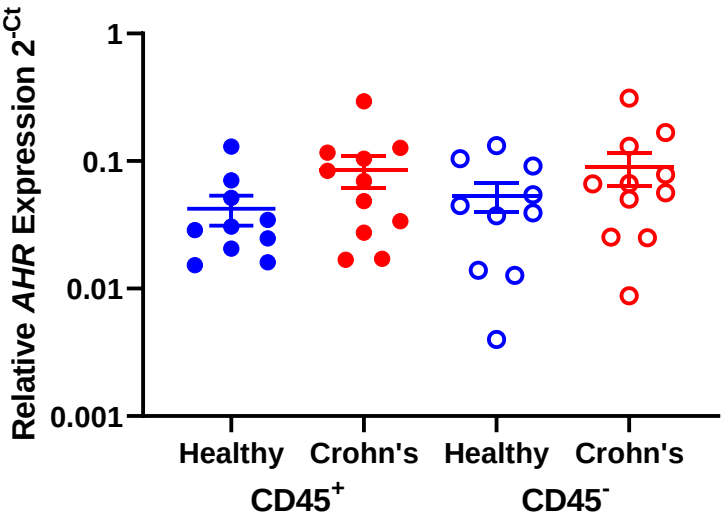

Figure 4.7 *AHR* expression in CD45 positive and negative cells from the intestinal mucosa. Intestinal biopsies were digested with collagenase. Positive selection for CD45+ cells was performed using MACS. Expression of *AHR* was determined by RT-qPCR and is shown relative to *RPL30* ($2^{-\Delta Ct}$). n = 10 healthy and 11 Crohn's disease. There were no significant differences by Kruskal–Wallis.

In a paired comparison, *AHR* expression was similar in CD45- cells and CD45+ overall (Figure 4.8A) (Wilcoxon paired test, p = 0.54). There was a trend towards higher expression of *AHR* overall in Crohn's disease compared to health but this difference was not statistically significant (Mann-Whitney, p = 0.07) (Figure 4.8B).

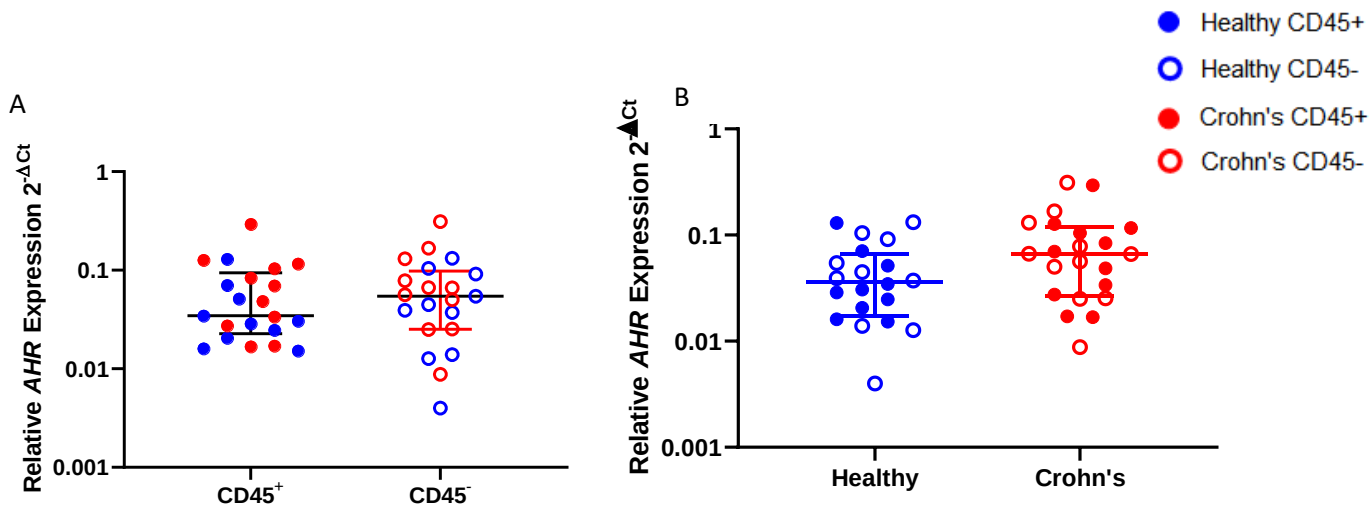

Figure 4.8 A) *AHR* expression compared between CD45+ and CD45- cells and B) compared between healthy patients and Crohn's disease. Expression of *AHR* in MACS separated CD45+ (filled circles) and CD45- cells (hollow circles) is shown relative to RPL30 ($2^{-\Delta Ct}$); n = 10 healthy (blue) and 11 Crohn's (red) disease. Median with interquartile range shown for each group. Expression between CD45+ and CD45- was compared using Wilcoxon paired signed-rank test. There was no significant difference in AHR expression between CD45+ and CD45- cells (p = 0.54). There was a trend towards higher *AHR* expression in Crohn's disease compared to healthy donors but this difference was not significant (p = 0.07; Mann Whitney U-test).

Resting *CYP1A1* expression was measured as a surrogate for AHR signalling activity. In both CD45+ cells and CD45- cells there was a trend towards higher *CYP1A1* expression in Crohn's disease however this difference was not significant using Kruskal–Wallis test. CYP1A1 expression was significantly higher in CD45- cells from patients with Crohn's compared to CD45+ cells from healthy donors using Kruskal–Wallis (Figure 4.9). The variation (standard deviation) in unstimulated *CYP1A1* expression was 5.8 times higher in Crohn's disease.

Unexpectedly *CYP1A1* expression was also detected in non-immune cells in both health and Crohn's disease confirming the AHR pathway is also active in these cells. It was previously believed human stromal cells were not responsive to AHR ligands (Gradin et al. 1993). However, more recent studies also provide evidence of a functional AHR pathway in epithelial cells and fibroblasts (Monteleone, Zorzi, Marafini, Di Fusco, Dinallo, Caruso, Izzo, Franzè, et al. 2016; Schiering et al. 2017).

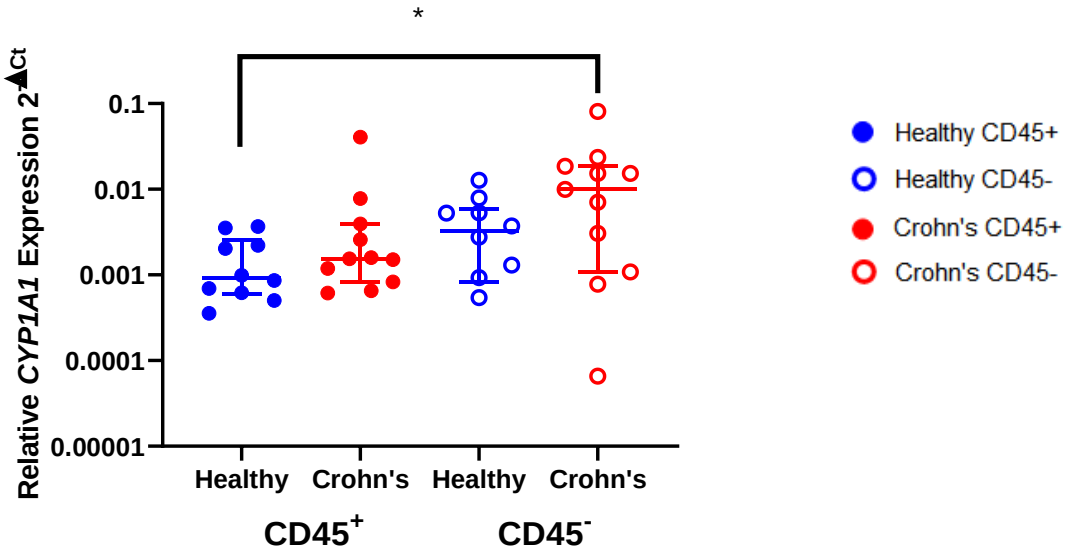

Figure 4.9 *CYP1A1* expression in CD45+ and CD45- cells from the intestinal mucosa. Expression of *CYP1A1* in MACS separated CD45+ and CD45- cells was determined by RT-qPCR and is shown relative to RPL30 ($2^{-\Delta Ct}$); n = 10 healthy and 11 Crohn's disease. There was a trend towards higher CYP1A1 expression in both CD45- cells compared to CD45+ cells and Crohn' disease compared to health, although these differences were not significant. CYP1A1 was significantly higher in CD45- cells in Crohn's compared to CD45+ cells from healthy donors p = 0.05 Kruskal–Wallis.

In a paired comparison, *CYP1A1* expression was significantly higher in CD45- cells than CD45+ overall (p = 0.026 Wilcoxon paired signed-rank test) (Figure 4.10A). There was no significant difference in expression of *CYP1A1* (at rest) overall in health compared to Crohn's disease (Figure 4.10B).

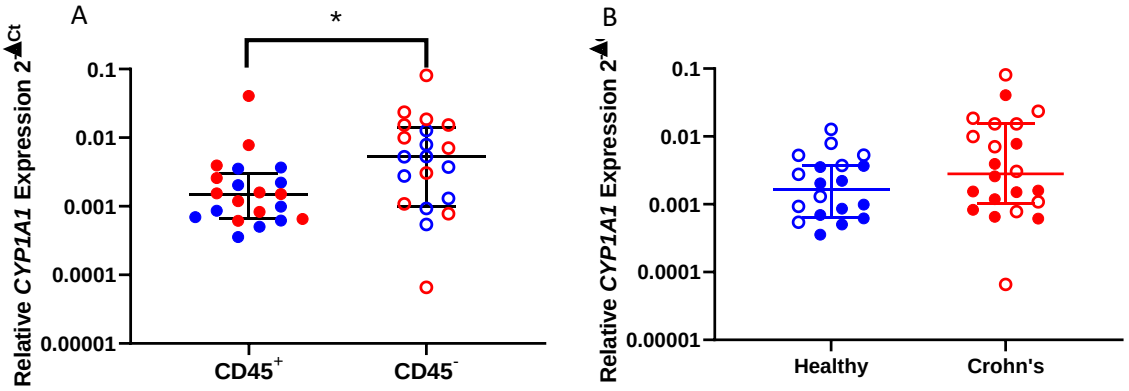

Figure 4.10 A) *CYP1A1* expression compared between CD45+ and CD45- cells and B) compared between healthy patients and Crohn's disease. Expression of *CYP1A1* in MACS separated $CD45^+$ and $CD45^-$ cells is shown relative to RPL30 ($2^{-\Delta Ct}$); n = 10 healthy and 11 Crohn's disease. Median with interquartile range shown for each group. Expression between CD45+ and CD45- cells was compared using Wilcoxon paired signed-rank test. Expression between health and Crohn's was compared using Mann-Whitney test. *CYP1A1* expression was significantly higher in $CD45^-$ cells than $CD45^+$ overall. p = 0.026.

Overall, these data provide a number of important insights. Firstly, AHR is expressed and AHR signalling active in both immune and non-haematopoietic cells in the human intestinal mucosa, a key novel finding. Secondly, these data demonstrate that the pathway is neither inactive in Crohn's disease nor less active in Crohn's disease than health. This helps us dismiss an important translational hypothesis: that Crohn's is a state of AHR inactivity.

4.4.5 The relationship between *AHR* and *CYP1A1* expression in intestinal mucosal immune and non-haematopoietic cells

To explore if there is a relationship between *AHR* expression and *CYP1A1* activity *ex-vivo* in unstimulated cells, the relative expression of these two genes in cells from the same individual was compared. Linear regression showed a significant positive relationship between *AHR* and *CYP1A1* expression in both CD45+ cells (R^2 0.75 p <0.001) and CD45- cells (R^2 0.66 p <0.001), suggesting there is a direct association between the magnitude of expression these genes (Figure 4.11).

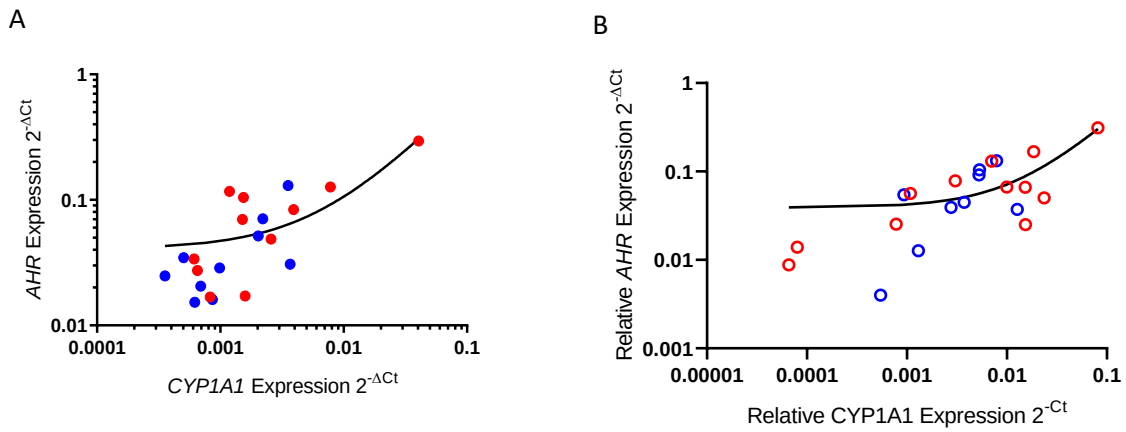

Figure 4.11 A) *AHR* expression compared to *CYP1A1* in unstimulated intestinal CD45+ cells B) and CD45- cells. The relationship between *AHR* and *CYP1A1* expression measured by RT-qPCR was examined using linear regression. n = 10 healthy individuals, 11 Crohn's disease. A positive relationship was seen in CD45+ cells (R^2 0.75, p <0.001). A weaker but significantly positive relationship was also seen in CD45- cells (R^2 0.66 p <0.001).

4.4.6 Comparing expression of AHR pathway genes with demographic parameters

The following analyses explore the relationship between different clinical and demographic parameters (recorded in Appendix) and AHR pathway gene expression. It is important to acknowledge that the number of patients in each sub-grouping is small and the study was not prospectively designed to consider these relationships.

There was no significant relationship between AHR expression and age (by linear regression).

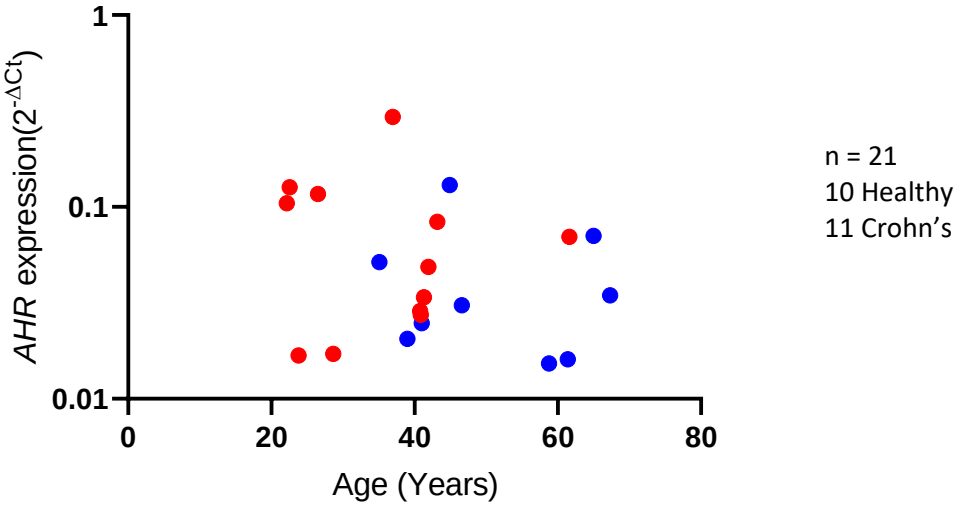

Figure 4.12 *AHR* expression compared to age in intestinal CD45+. The relationship between *AHR* measured by RT-qPCR and age was examined using linear regression. n = 10 healthy individuals, 11 Crohn's disease. There was no significant correlation.

Overall *AHR* expression was significantly higher in CD45+ cells from female patients (Figure 4.13A). However, more Crohn's patients were female (73%) compared with healthy controls (30%). A trend towards this observation was preserved in each sub-group (health and Crohn's disease) but was not significant (Appendix 6). A trend towards higher *CYP1A1* expression was seen in female patients but this difference was also not significant; p = 0.08 (Figure 4.13B).

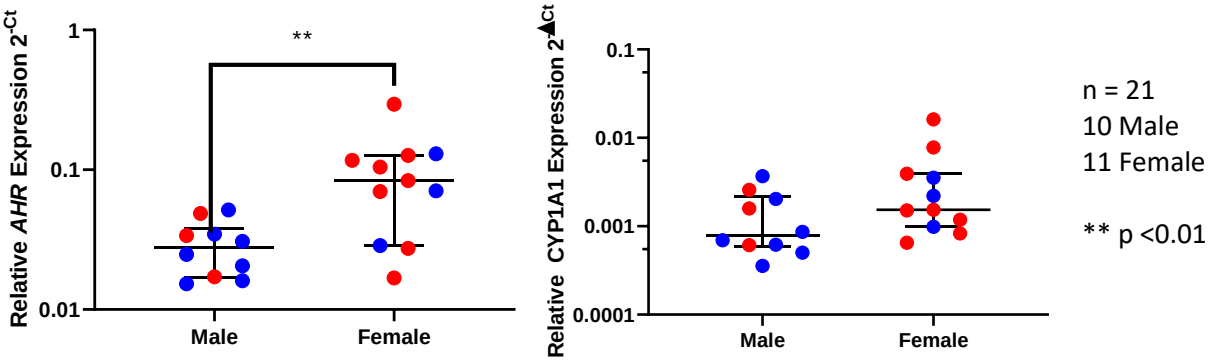

Figure 4.13 Relative *AHR* and *CYP1A1* expression in intestinal CD45⁺ cells from female and male patients. **A) *AHR* expression** in CD45+ cells exposed to medium control normalised to RPL30 ($2^{-\Delta Ct}$). *AHR* expression was significantly higher in female patients overall; p <0.01 (Mann Whitney test). **B) *CYP1A1* expression** in CD45+ cells exposed to medium control normalised to RPL30 ($2^{-\Delta Ct}$). CYP1A1 expression not significantly different between the sexes; p = 0.08 (Mann Whitney). Healthy in blue (n = 10), Crohn's disease in red (n = 11). Median expression with interquartile range shown.

The population of immune cells present and the expression profiles are very different in the inflamed mucosa. Previous reports suggest different *AHR* expression in areas of inflammation (Monteleone 2011). Therefore, the impact of Crohn's disease activity on *AHR* and *CYP1A1* expression was considered. *CYP1A1* and *AHR* expression were both higher in samples from inflamed mucosa but this difference was not significant (not shown). The limitations of comparing these variables in isolation is discussed below.

4.4.7 Comparing expression of AHR pathway genes with anatomical location and disease activity

AHR and *CYP1A1* expression is also reported to vary along the gastrointestinal tract (Mowat 2014). Considering all samples (n = 21) *AHR* and *CYP1A1* expression in was higher in the ileum than tissue from the right colon. However, ileal tissue was not collected from healthy donors in this study so it was not possible to disentangle if this represents a difference in disease or anatomical location. Sub-analysis of patients with Crohn's disease did not reveal any significant regional differences in AHR expression however was limited by small numbers (not shown).

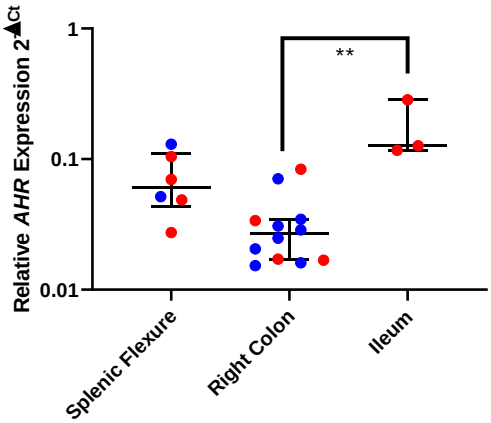

Figure 4.14 Relative *AHR* expression in intestinal CD45+ cells grouped by anatomical location. *AHR* expression in CD45+ cells is shown normalised to RPL30 ($2^{-\Delta Ct}$). *AHR* expression was significantly higher

in cells from the ileum compared to the right colon; p <0.01 (Kruskal Wallace). Healthy in blue (n = 10), Crohn's disease in red (n = 11). Median expression with interquartile range shown.

The composition of immune cells from inflamed intestinal mucosa is different from inactive, non-inflamed tissue. Relative *AHR* and *CYP1A1* expression was compared between cells from macroscopically inflamed tissue to macroscopically normal tissue from patients with Crohn's disease. There was no difference in *AHR* expression in CD45+ cells from actively inflamed mucosa compared to non-inflamed tissue (Figure 4.15A). There was a trend towards higher *CYP1A1* expression in actively inflamed tissue, however this difference was not significant; p = 0.08 (Mann-Whitney test) (Figure 4.15B).

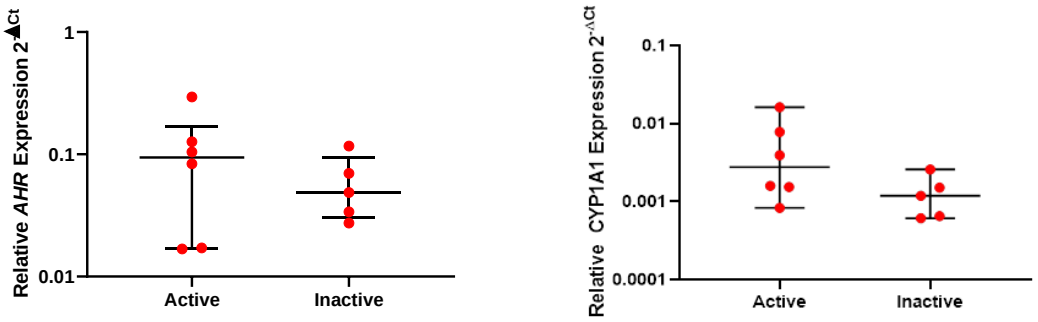

Figure 4.15 Relative gene expression in intestinal CD45+ cells grouped by Crohn's disease activity. A) *AHR* expression in CD45+ cells is shown normalised to RPL30 ($2^{-\Delta Ct}$). *AHR* expression was not significantly different in cells from actively inflamed tissue compared to inactive. **B)** *CYP1A1* expression in CD45+ cells is shown normalised to RPL30 ($2^{-\Delta Ct}$). There was a trend towards higher CYP1A1 expression in cells from actively inflamed tissue compared to inactive, but this difference was not significant; p = 0.08 (Mann-Whitney test). N = 11 patients with Crohn's disease. Median expression with interquartile range shown.

4.4.8 *AHR* expression and activity is higher in the intestinal mucosa compared with circulating immune cells

Relative *AHR* expression in MACS purified intestinal CD45+ and CD45- cells was compared with relative expression in moDC and circulating immune cells (mean expression in PBMC). *AHR* expression was significantly higher in isolated intestinal mucosal immune cells compared with circulating immune cells

(PBMC). Quantitative expression was similar to moDC which have the highest *AHR* expression observed in any *peripheral* immune cell type and was more than 20-fold higher than average expression in PBMC.

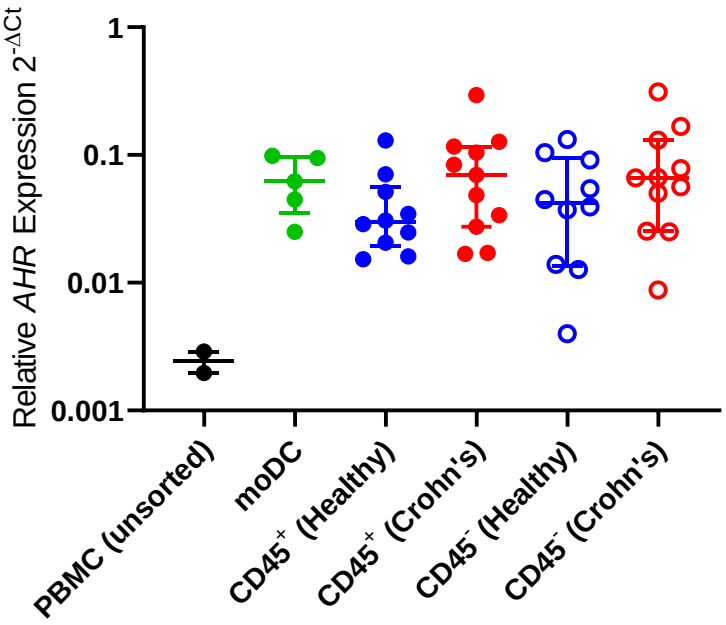

Figure 4.16 Relative *AHR* expression in sorted intestinal mucosal cells compared with moDC and PBMC. Unstimulated cells were lysed in RLT Buffer®. RNA was extracted using Qiagen spin columns. Gene expression was measured by RT-qPCR. Median relative *AHR* expression is shown normalised to *RPL30* ($2^{-\Delta Ct}$) ± interquartile range. 2 healthy donor PBMC, 5 moDC, 10 healthy and 11 Crohn's disease CD45+ and CD45- cells. Kruskal-Wallis test $p < 0.001$, groups differences not significant after correcting for multiple comparisons with Dunn's test.

Relative *CYP1A1* expression in MACS purified intestinal CD45+ and CD45- cells was compared with relative expression in moDC and circulating immune cells (mean expression in PBMC). *CYP1A1* expression was significantly higher in intestinal cells than observed in moDC or PMBC, where no expression was detected.

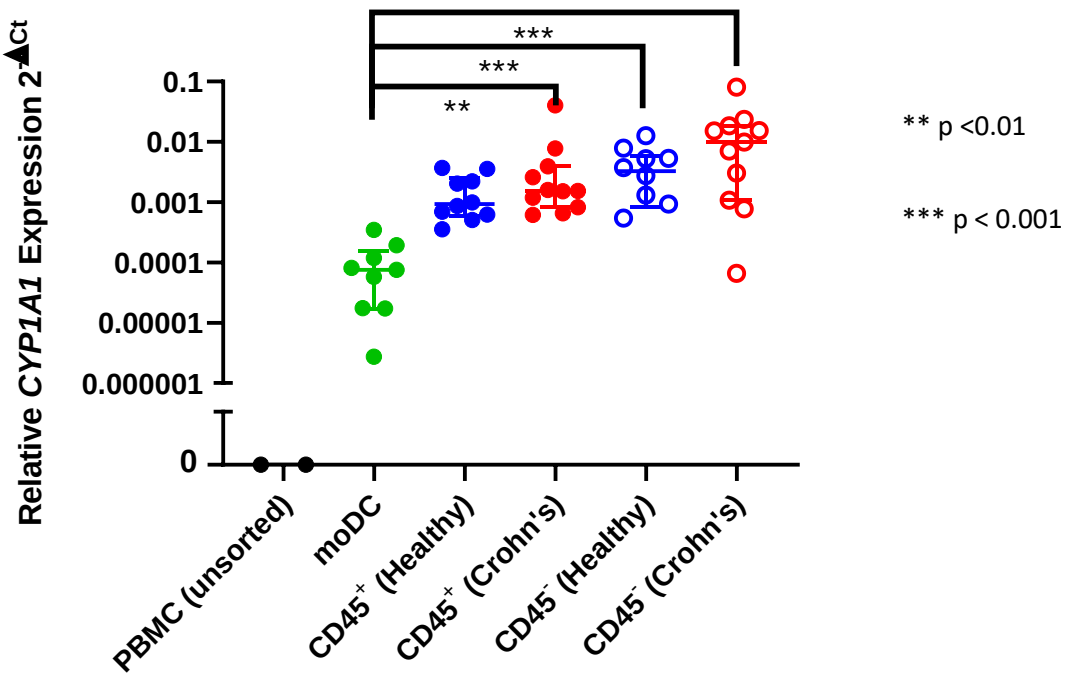

Figure 4.17 Relative *CYP1A1* expression in sorted intestinal mucosal cells compared with moDC and PBMC. Unstimulated cells were lysed in RLT Buffer®. RNA was extracted using Qiagen spin columns. Gene expression was measured by RT-qPCR. Median relative *CYP1A1* expression is shown normalised to *RPL30* ($2^{-\Delta Ct}$) ± interquartile range. 2 healthy donor PBMC, 9 moDC, 10 healthy and 11 Crohn's disease CD45+ and CD45- cells. *CYP1A1* was expression was significantly higher in intestinal derived cells compared to PBMC (where no expression was seen) and moDC. Kruskal-Wallis test p <0.001, correction for multiple comparisons with Dunn's test.

Unlike snap lysed biopsies, cells extracted from digested and sorted intestinal biopsies are exposed to hours of processing in a variety of laboratory reagents. To determine if the process of cell separation and sorting could influence the important observations above, resting *CYP1A1* expression was compared in whole biopsies and sorted cells. *CYP1A1* expression in sorted cells was not significantly different to expression in whole biopsies from similar patients. Although, as stated previously, there was considerable heterogeneity in biopsies from healthy donors (Figure 4.18).

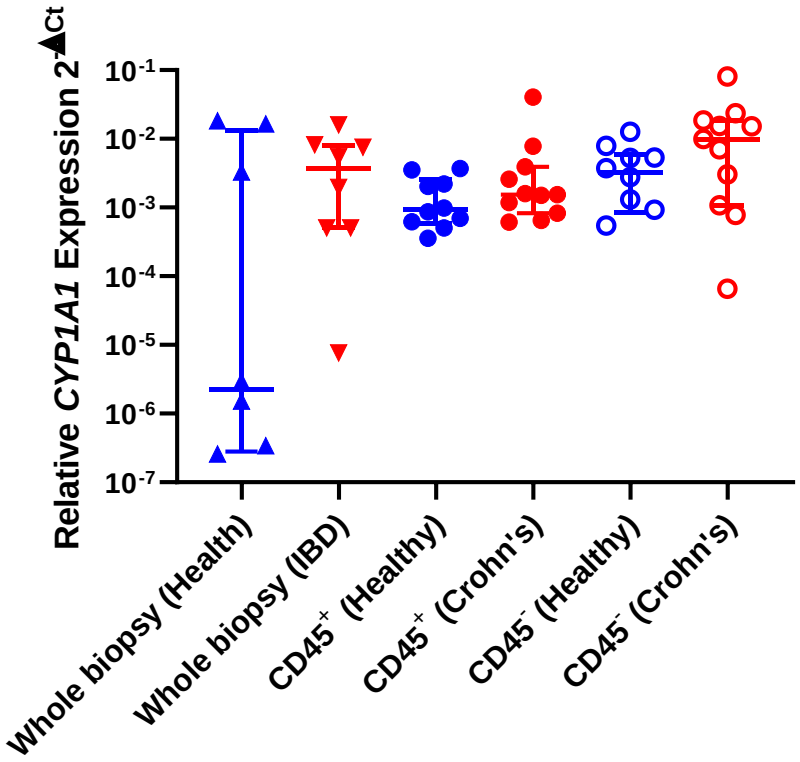

Figure 4.18 Relative *CYP1A1* expression in sorted intestinal mucosal cells compared with whole biopsies. MACS separated intestinal cells or whole biopsies were lysed in RLT Buffer®. RNA was extracted using Qiagen spin columns. Gene expression was measured by RT-qPCR. Median relative *CYP1A1* expression is shown normalised to *RPL30* ($2^{-\Delta Ct}$) ± interquartile range. 8 healthy and 8 IBD whole biopsies, 10 healthy and 11 Crohn's disease CD45+ and CD45- cells are shown. *CYP1A1* was expression was not significantly different in processed cells to expression in whole biopsies from similar patients.

4.4.9 Characterising the CD45 negative fraction using FACS sorting

These data demonstrate for the first time, that the AHR pathway is also active in non-immune cells in the human intestinal mucosa. However, the CD45- MACS fraction is inherently a very heterogenous population of cells. The composition of the CD45- population can be affected by a number of variables. Starting with the collection of the biopsy which can vary in depth and location, variation is also introduced through variable depletion of epithelial cells by the EDTA wash and variable contamination with CD45+ following MACS selection. FACS sorting offers the advantage of purity and sophisticated

selection based on multiple variables at the cost of convenience and availability. A sorting strategy was devised to sub-divide live mucosal cells into major groups (Table 4.4).

Surface Marker	Function	Cell Type
CD45	Protein tyrosine phosphatase, receptor type C	Al haemopoietic immune cells (except plasma cells)
CD31	Platelet endothelial cell adhesion molecule	Endothelial cells (also expressed on platelets, neutrophils and some monocytes)
EpCAM	Epithelial cell adhesion molecule	Epithelial cells
None of the above ('triple negative')	-	Stromal cells (Fibroblasts, myofibroblast) (Also erythrocytes)

Table: 4.4. Surface markers used to sub-divide digested mucosal biopsies after live/dead gating using Zombie NIR™

Eight biopsies were collected at the time of colonoscopy. The tissue was washed with DTT and immediately digested with collagenase, the EDTA washes were omitted to preserve the epithelial layer and reduce variability. Cells were stained using the surface markers above (Table 4.4) and a viability dye (Zombie NIR™). Cells were resuspended in sterile, azide-free FACS buffer. 4 populations of live cells were separated using an Aria III Cell sorter (CD45+, CD45- CD31+, CD45- EpCAM+, CD45- CD31- EpCAM-).

On average 61% cells remained live as determined by dye staining. The number of cells recovered in each population varied. A mean 126,000 $CD45^{+}$ cells, 516,000 epithelial cells and 910,000 triple negative cells were recovered from each patient. On average far fewer endothelial cells were recovered (5300) than any other cell type, reflecting the collection of superficial biopsies without major blood vessels (Figure 4.19).

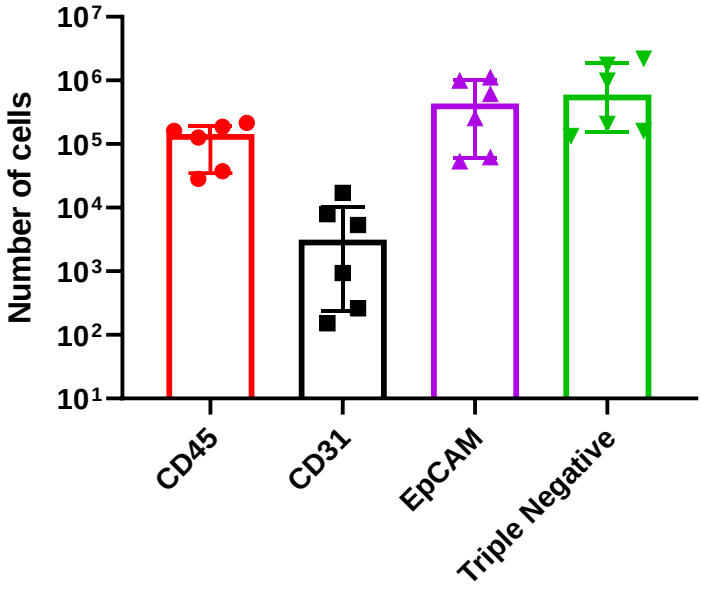

Figure 4.19 The number of cells recovered in each population from sorted colonic mucosal cells. Intestinal biopsies were washed with DTT then digested with collagenase. After incubation with a viability dye and surface staining, cells were FACS sorted. The median number of live CD45+, CD31+ CD45-, EpCAM+ CD45- and CD45- CD31- EpCAM- cells recovered from each patient is shown ± interquartile range. n = 6 (4 healthy donors, 2 UC).

Gene expression in the sorted cell populations was determined by RT-qPCR. In epithelial (EpCAM), endothelial (CD31) and CD45+ cells expression of the reference gene *RPL30* correlated with the cell counts from the FACS sorter. However, *RPL30* expression was much lower in triple negative cells than expected by cell count (Appendix 7). This mismatch is likely to be partly explained by erythrocyte contamination in this gate; red blood cells contain less RNA and do not contain ribosomes (Kabanova 2009). Also, µm size debris could auto-fluoresce at 780nm and are more likely to appear as cells in the triple negative fraction on the FACS machine. This means the true number of triple negative mucosal cells recovered were much less than estimated by the cell counts.

4.4.10 The AHR pathway is most active in colonic stromal and epithelial cells

Resting expression of *AHR* and *CYP1A1* in each of the sorted mucosal cell populations was determined by RT-qPCR relative to *RPL30*. *AHR* expression was detected in all three populations of CD45- cells. Mean expression of *AHR* was highest in the triple negative cells (ΔCt 4.4). This was at a similar level to that observed in CD45+ cells. (ΔCt 5.0). Mean expression in epithelial cells was lowest (Δ8.1). *AHR* expression in endothelial cells (CD31+) was only detected in 2/6 patients (ΔCt 6.7). However, in 4/6 patients no *AHR* expression was detected in CD31+ cells (Figure 4.20). It is worth highlighting that because very few of these cells were recovered from each patient even reference gene expression (*RPL30*) was detected at a very low level (>34/40 cycles). This limited the sensitivity of this test because qPCR accuracy declines after 35 cycles and only relatively high gene expression would be detectable with very low amount of total RNA input.

CYP1A1 expression mirrored the findings obtained with MACS sorted cells. When detected, the highest expression was seen in CD31+ (ΔCt 0.56). and triple negative cells (ΔCt -0.45). Expression in CD45+ and EpCAM+ cells was numerically lower (Figure 4.20B). However, no *CYP1A1* expression was detected in 8/24 samples (2 CD45, 3 CD31, 3 triple negative).

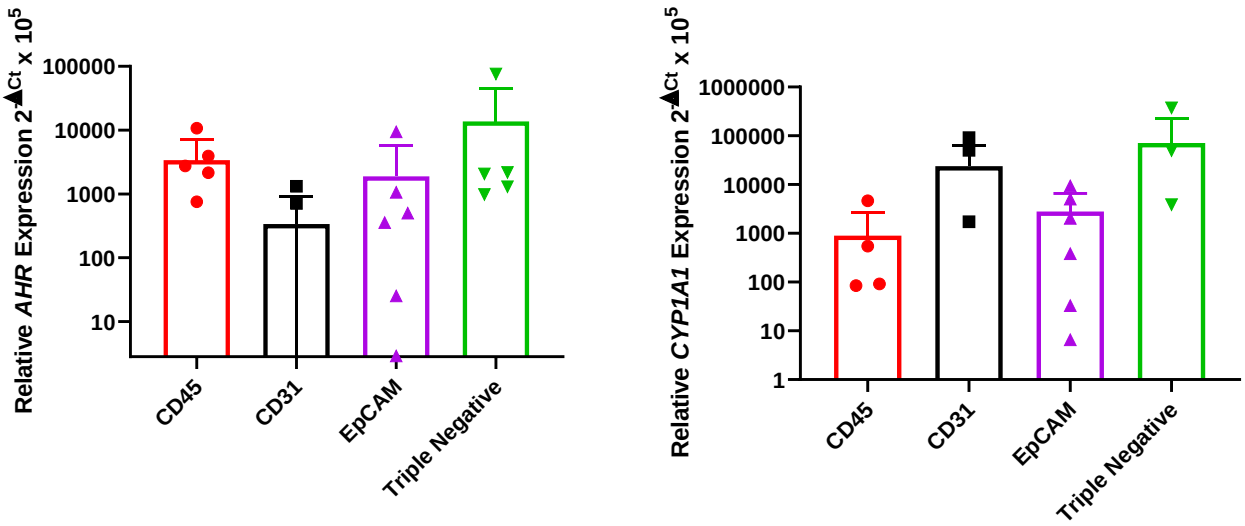

Figure 4.20 Relative gene expression in sorted mucosal cells. Intestinal mucosal biopsies were digested with collagenase, stained and FACS sorted for live cells using the surface markers CD45, CD31 and EpCAM. **A) Mean relative *AHR* expression** is shown normalised to *RPL30* expression ($2^{-\Delta Ct}$) ±

standard deviation. *AHR* was detected in all cell types examined. The highest expression was observed in the triple negative population. **B) Mean relative *CYP1A1* expression** is shown normalised to *RPL30* expression ($2^{-\Delta Ct}$) ± standard deviation. *CYP1A1* expression was detected in all cell types examined. The highest expression was again observed in the triple negative population. n = 6 (4 Healthy, 2 UC).

FACS sorting allows highly pure population of cells to be selected using surface markers. However, there are limitations to this approach, only 4 different populations can be collected simultaneously and not all cell populations are easy to define by surface protein expression (for example ILC) and intra-cellular staining necessitates cell fixation. In addition, whilst isolation of rare sub-populations of cells is clearly possible using this technique, as demonstrated here by the isolation of <1000 CD31+ cells from >1.5 million cells, low cell numbers means low input RNA which approaches the limits of current RNA extraction and qPCR kits. Finally, another a key limitation of this technique is that RT-qPCR only measures average expression in a population of cells which, despite sorting, will inevitably be heterogenous.

4.4.11 Characterising AHR positive cells in the intestinal mucosa at single cell resolution

The Chromium Single Cell Gene Expression Solution® from 10X Genomics is a new platform that allows simultaneous gene expression profiling of thousands of cells. The platform is discussed in more detail in Chapter 2. Briefly, using microfluidic partitioning individual cells are captured in a small droplet. The cells are lysed and the RNA labelled with a unique barcode known as the unique molecular identifier (UMI). When subsequent sequencing is performed this genetic barcode allows the cell of origin to be deconvoluted meaning gene expression can be examined on a single cell level.

4.4.11.1 Single cell acquisition

Intestinal biopsies from a healthy donor were prepared as described in Chapter 2. A target of 1000 cells with a read depth of 50,000 reads per cell was selected for this experiment to allow a comparison of cell populations representing at least 5% of the CD45+ cells while keeping costs within budget. Cell

acquisition and sequencing was more efficient than predicted. In total, 1,305 CD45+ cells were collected from the sample with a mean read per cell of 63,419. Gene expression was determined using Cell Ranger 3.0 with the assistance of Eva Wozniak, QMUL Genome Centre. A median 1875 genes were detected per cell with a median 8,832 UMI per cell. 93.8% of reads mapped to the known genome (reference genome GRCh38).

4.4.11.2 Cell clustering using Loupe cell browser

10X Genomics provide free software called Loupe Cell Browser® which can be used to visualise single cell gene expression data. The software uses an algorithm called t-SNE (t-distributed stochastic neighbor embedding) to reduce the dimensionality of the data and divide the cells into clusters with similar features using closed-source algorthims.

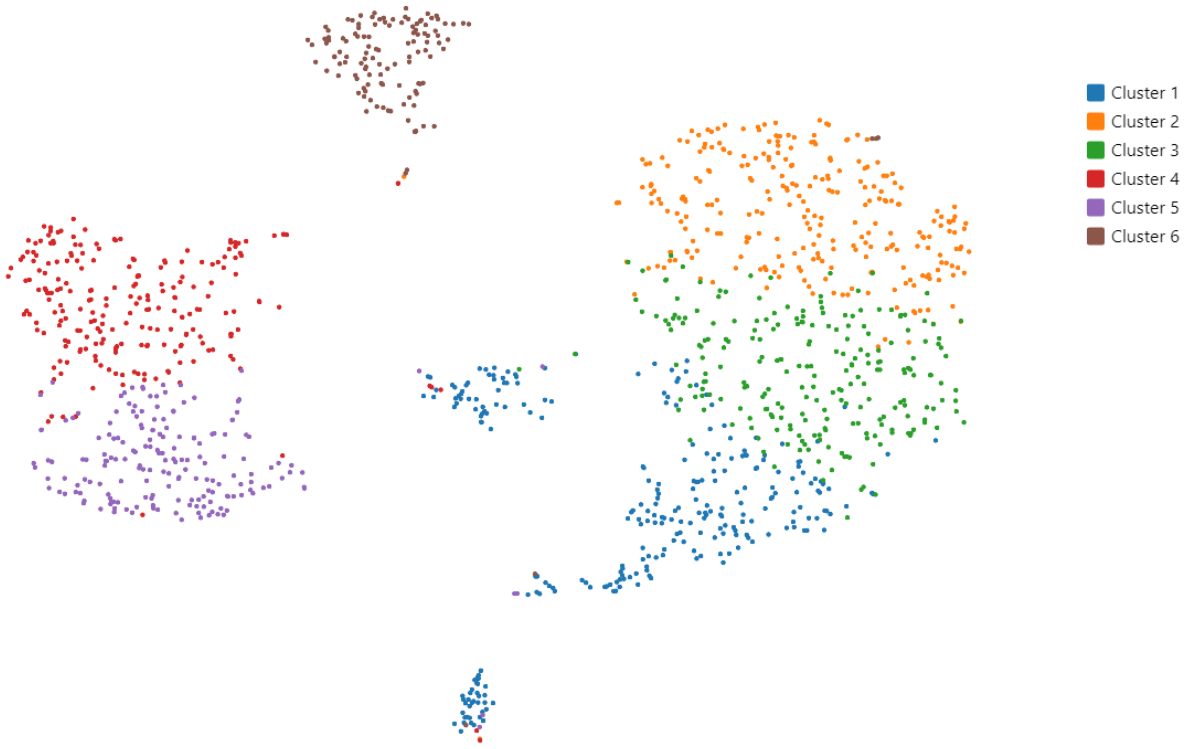

Figure 4.21 t-SNE plot showing 1305 intestinal CD45+ cells clustered by gene expresion. 6 clusters automatically defined by 10X Genomics Loupe Cell browser are colour coded.

6 clusters were defined automatically. However, visually it was apparent that the separation between some clusters e.g. 4 & 5 is weak while others such as cluster 6 are well separated. Cluster 1 appears to include three different populations of cells which remain spatialy separated.

To explore the phenotype of these clusters I examined the up-regulated genes that defined each cluster. The top 10 up-regulated genes per cluster are shown in Table 4.5.

Cluster	**1**	**2**	**3**	**4**	**5**	**6**
1	IGLC2	IGLL5	IGHGP	GNLY	LEF1	MS4A1
2	IGLC3	IGLV2-14	IGHG2	ITGA1	PASK	MARCH1
3	HSPA1B	GADD45A	IGHG4	KLRD1	SATB1	CCL22
4	HSPA6	IGLC6	IGKV4-1	NKG7	TCF7	ARHGAP24
5	IGHM	CCL3	IGHG3	GZMK	CAMK4	HLA-DQB1
6	IGHA2	HSPA5	IGHG1	CCL5	GIMAP7	HLA-DRA
7	IGKC	DUSP5	IGHV3-7	JAML	GIMAP1	HLA-DQA1
8	IGHA1	LMNA	IGKC	CD8A	FYB1	LINC00926
9	SSR4	ATF5 (Tf	SPINK2	BATF	LTB	BCL11A
10	HSPA1A	CCPG1	IGLC6	CST7	GIMAP2	HLA-DRB1
Proposed cell type	B-cell lineage (Under stress)	B-cell / Mixed population	B-cell lineage	NK / Effector T-cell	T- Lymphocytes	Antigen presenting cells

Key:

Immunoglobulin family genes	
Heat shock protein & cellular stress	
NK / Effector T-cell defining	
T-lymphocyte defining	
Antigen presentation	

Table 4.5 Top 10 up-regulated genes are shown for each cluster with colour coding to identify cell type or features. Clusters 1,2 and 3 all show high expression of immunoglobulins which are exclusively expressed by B-cells. Cluster 4 and 5 appear to represent lymphocytes with higher expression of NK and effector T-cell genes in cluster 4 and different T-lymphocyte family genes in cluster 5. The spatially distinict cluster 6 shows high levels of expression of genes critical antigen presentation and MS4A1 (which encodes the protein CD20).

The Loupe cell browser also allows cells to be identified based on the quantitative expression of any human gene. To illustrate this expression of the gene *CD3E* is shown below. *CD3E* encodes CD3-epsilon, a component of the T-cell receptor complex and thus is exclusively expressed on T-cells. The

expression of this gene again highlights the strenghts and limitations of the t-SNE clustering. The majority of CD3E expression is restricted to clusters 4 and 5. However, there are 7 cells in cluster 1, spatially close to cluster 4 and 5 and a 5 more distant cells with CD3E expression within other clusters (Figure 4.22).

Figure 4.22 CD3E gene expression on a single cell level superimposed on the global clusters. CD3E expression is shown in yellow to red with darker colours representing higher expression. CD3E is almost entirely restricted to clusters 4 and 5 but 7 cells spatially close by have CD3E expression but are allocated to other clusters and another 5 distant cells show CD3E expression.

The gene browser was also used to more accurately sub-divide the spatiality separated cluster 1. TPSAB1, encodes tryptase beta-1, the main tryptase isoenzyme expressed in mast cells. Expression of this gene entirely overlaps with a spatially distinct part of cluster 1. Complete separation in original t-SNE plot may not have occurred due to insufficient power due to low cell numbers (Figure 4.23). Finally, the gene brower was used to examine sample purity. Although a FACS sort was performed to select CD45+ cells, 9 cells were included that showed EPCAM expression (0.69%). There were no cells included expressing collagen genes (eg. COL1A2; COL3A1).

Figure 4.23 TPSAB1 gene expression on a single cell level superimposed on the global clusters. TPSAB1 expression is shown in yellow to red with darker colours representing higher expression. TPSAB1 is entirely restricted to a spatially distinct sub-group of cluster 1. It is likely these cells are mast cells. It highlights the potential and limitations of statistical clustering.

4.4.12 *AHR* is expressed in diverse intestinal immune cells

Similar approaches were used in reverse to determine the characteristics of cells expressing *AHR*. 84/1305 (6.4%) cells had any detectable *AHR* expression. The distribution of *AHR* expression is shown below superimposed on the original clusters (Figure 4.24). 48/84 cells are in the lymphocyte clusters (4 &5) with the largest number of *AHR* expressing cells (39) in cluster 4. However, scattered expression is seen in all other clusters.

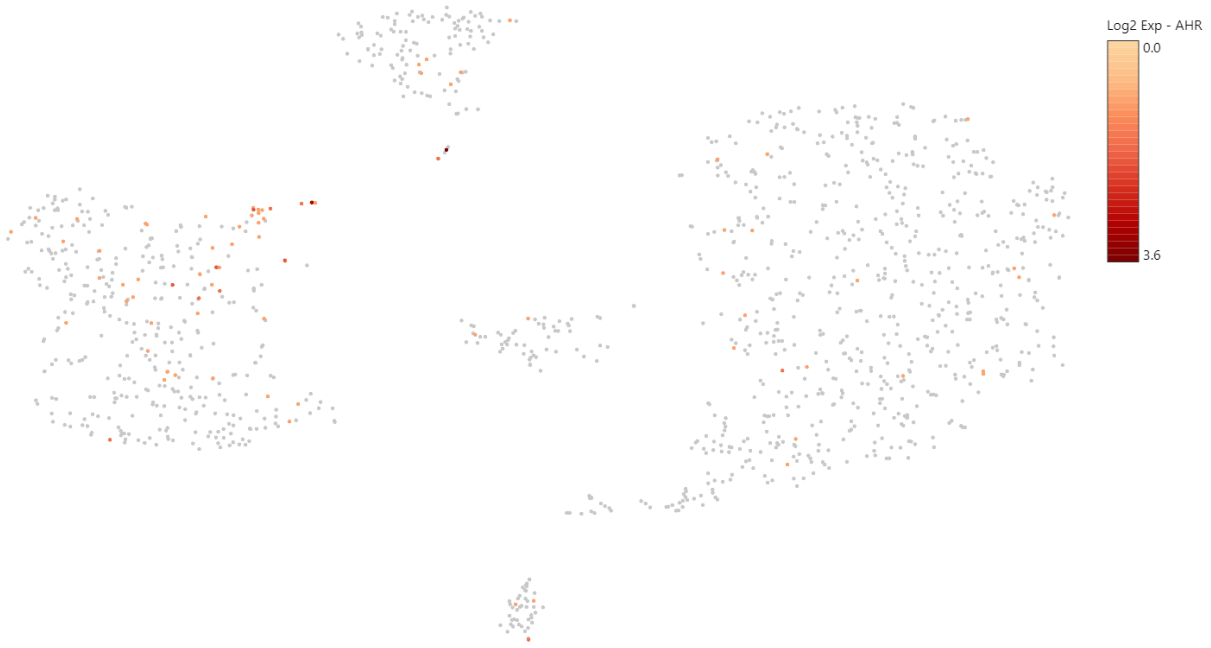

Figure 4.24 AHR gene expression on a single cell level superimposed on the global clusters. AHR expression is shown in yellow to red with darker colours representing higher expression. The greatest number of AHR expressing cells are T-cells but AHR positive cells are seen throughout the intestinal immune system.

The loupe cell browsers also allows examination of gene expression in defined cell populations. Gene expression was compared across the 1305 cells between cells expressing or not expressing AHR. Using a p-value threshold of 0.05, 36 genes showed significant upregulation in AHR expressing cells. The top 10 genes showing the largest difference are shown below (Table 4.6); the full list is included in Appendix 8.

Gene	Log2 fold difference	Function
IL22	10.1	Cytokine
CXCL8	5.87	Chemokine
MMP9	4.79	Enzyme involved in ECM degradation
C15orf48	4.49	Unknown -? NADH activity
CCL3L1	3.98	Chemokine
BATF	3.96	Transcription factor (Th17 differentiation)
SOD2	3.70	Antioxidant
SLC7A11	2.99	Cysteine/Glutamine transporter (antioxidant)
KLF6	2.65	Tumour suppressor gene
ANXA1	2.52	Inhibits phospholipase A2

Table 4.6 Top 10 up-regulated genes in AHR+ intestinal CD45$^+$ cells compared to AHR- CD45$^+$ cells. This gene list identifies a target that is known to be expressed in AHR+ cells (*IL22*) but also highlights novel gene targets which have not previously been associated with AHR and warrant exploration.

It is possible to make a number of observations using this list. Firstly, a number of genes in this list are already known to be associated with AHR such as *IL22*. Secondly, as expected from the distribution of AHR expressing cells, many of the genes are characteristically expressed in T-cells and NK-cells. However, genes commonly expressed in other cell types, including three HLA genes are also higher in AHR expressing cells reflecting AHR expression in antigen presenting cells.

Thus, this approach can both help determine the immune phenotype of AHR expressing cells and help design functional experiments based on the targets identified. Finally, another important observation is that transcripts of *CYP1A1* were not detected in any cells and *CYP1B1* was only detected in 11 cells. This again highlights a potential limitation of this technique (discussed below).

4.5 Discussion

4.5.1 Detecting AHR and AHR regulated genes in the human intestinal mucosa

Before considering pathway activity or function it was important to independently confirm if the aryl hydrocarbon receptor pathway is active *in-vivo* in the human intestinal mucosa. Whole biopsies were immediately processed on ice to extract RNA meaning measurement of gene expression reflected *in-situ* gene expression as closely as possible. In both healthy donors, Crohn's and ulcerative colitis *AHR* gene expression was detected. More importantly the previously validated genes of *AHR* activation, *CYP1A1* and *CYP1B1*, were also expressed in both health and IBD (Figure 4.1) showing this pathway is activated *in-vivo*. Unexpectedly there was no significant difference in expression of these three genes between health and IBD. However, there was considerable inter-individual variation in gene expression. This may reflect the true normal distribution of AHR pathway activation in the human gut but other factors will undoubtedly contribute to this variation. Whole biopsies contain a mixed cell population with a variable composition of immune, stromal and other specialised cells.

A key step to understanding the role of AHR signalling in the intestinal mucosa is to determine in which cell types AHR is present and activated. In this chapter immunohistochemistry and confocal microscopy demonstrates expression of AHR protein in the intestinal mucosa in health and Crohn's disease. Unexpectedly the brightest AHR staining was seen in non-immune cells (lacking CD45 staining). Bright AHR staining was relatively scanty and restricted to the lamina propria (Figure 4.2 and 4.3). Co-localisation with CD45 staining was very rare. The number of AHR+ cells by manual counts was higher in Crohn's disease compared to health. These findings were in contrast to some published literature (Monteleone et al. 2011) but similar to findings in other studies (Arsenescu et al. 2011). Previous data in chapter 3 showed AHR staining and gene expression in circulating immune cells while almost no AHR expression in CD45+ cells was seen by microscopy. The absolute number of AHR positive cells was also relatively low given the observed gene expression.

It was not initially clear what explains this difference. One contributing factor maybe that microscopy is a qualitative technique and there a number of challenges to generate quantitative data. For example, to keep an image in focus and appropriately exposed it is often necessary to adjust the exposure time or laser power even within the same slide on the microscope or adjust the contrast of the captured image using software. This makes comparing between images problematic. In addition, the in-focus portion of tissue was only a fraction of the full thickness of the cut sections (Z-axis). Staining was observed to vary throughout this axis but due to time and data storage constraints the entire field could not be imaged throughout the Z-axis and only a single slice was captured. Finally, it is also possible the primary antibody stained the target (AHR) poorly. Although experiments were always designed to include a no-primary antibody control to exclude non-specific binding of the secondary antibody, each experiment did not include positive controls. In effect, positive controls were used to optimise the immunohistochemistry methodology (specifically cytospun moDC),

however stained tissue cannot be stored for weeks due to degradation in fluorophore brightness and it was not practical to simultaneously generate these cells for each tissue experiment. Without a positive control it is more difficult to determine the threshold for positive staining. If the threshold for positive was set too high this may explain the relatively few AHR positive cells observed via microscopy compared to expression. Although gene expression via qPCR, only considers average expression in a population of cells (where expression maybe very high in a small number of cells), single cell expression data suggested 6.4% CD45+ cells do express AHR. There may of course be post-translational mechanisms which mean gene and protein expression do not correlate.

4.5.2 AHR is present and active in both intestinal immune and non-haematopoietic cells

To validate this unexpected observation by microscopy and determine whether *AHR* expression was indeed higher in non-immune cells in the intestinal mucosa, and to characterise these cells further, two sorting strategies were used.

Firstly, MACS purification was employed to separate CD45+ and CD45- cells. This broad marker was selected to avoid bias in any further selection and maximise the number of cells recovered.

MACS sorting had significant practical advantages for these experiments. It can be performed independently at any time of day meaning patients could be recruited throughout the whole working day and cell sorting could take place after hours if required. However, it is important to highlight that MACS purification of digested intestinal mucosal cells is results in lower sample purity than FACS sorting PBMC. 83.4% of MACS selected CD45+ cells were actually CD45+ cells by FACS and 96.9% of the CD45- fraction was CD45- (Figure 4.6). FACS sorting typically achieves a purity above 98% but unfortunately the Aria cell sorter in our facility has limited availability which would have made patient recruitment much more difficult. It is likely these impurities contribute to the variation in the data presented.

Gene expression was measured in these MACS sorted intestinal mucosal cells. Expression of *AHR* and the dependent gene *CYP1A1* was detected in both CD45+ and CD45- cells. However, unlike the findings at microscopy, although *AHR* expression was higher on average in CD45- cells in both health and Crohn's disease this difference was not significant (Figure 4.9). However, it is important to acknowledge that microscopy allowed the number of cells expressing AHR protein to be determined where as qPCR measured the average amount of RNA of each transcript across a population of cells.

Again, unlike the findings at microscopy in this study and a previously published study which showing higher numbers of AHR positive cells (Arsenescu 2011), there was no clear difference in *AHR* gene expression between health and Crohn's disease in isolated cells. There was an trend towards higher *AHR* expression in Crohn's disease overall, that did not reach statistical signifcance compared to health ($p = 0.07$ Mann-Whitney) (Figure 4.8B) or comparing CD45+ or CD45- cells alone (Figure 4.7).

CYP1A1 expression was significnatly higher in CD45- cells compared with CD45+ cells (Figure 4.10A) supporting the idea that the AHR pathway is more active in non-immune cells but there was no difference in expression of this gene between health and Crohn's disease overall (Figure 4.10B) or considering each cell popualtion separately (CD45+ or CD45-), although CYP1A1 expression was significnatly higher in CD45- cells in Crohn's disease compared to CD45+ in health.

The variation in expression of these genes was higher in Crohn's disease; the standard deviation was more than twice as high as in healthy controls. In some individuals, expression completely overlapped the range of expression seen in normal individuals while in 3/11 Crohn's patients the expression of *CYP1A1* was above that seen in health. There were no individuals where the expression of *AHR* or *CYP1A1* was below that seen in health. This distribution of expression is not unexpected, Crohn's is a very heterogenous condition.

It is likely other patient factors also contribute to this variation, such as differing exposure to dietary or bacterial ligands, not measured in this study, or intrinsic differences in the pathway such as, SNP variation in AHR or CYP genes which have been associated with IBD (Liu 2015) and altered drug metabolism (Alessandrini et al., 2013).

Overall, what is clear from these data is that the AHR pathway is not ***less*** active in Crohn's disease and is more active in non-immune CD45- cells than CD45+ cells. This means the simple paradigm developed in murine models where low AHR activity leads to intestinal inflammation does not explain intestinal inflammation in Crohn's disease.

4.5.3 Major demographic and clinical factors may influence AHR

Interestingly there does also seem to be a close relationship between relative expression of *AHR* and *CYP1A1* unrelated to disease in both CD45+ and CD45- cells (Figure 4.11). This creates a circular problem; does observing higher *CYP1A1* in a particular cell type reflect higher AHR activation or higher AHR receptor availability. These variables may be colinear. Without simultaneous measurement of the AHR ligand concentration it is difficult to untangle this relationship, this is explored further in chapter 5. However, it does also suggest that in most cell types observed, any downstream negative feedback loops are not sufficiently different between cell type to prevent stimulation of CYP1A1 in any specific cell types observed.

Human samples can never match the homogeneity of murine models where the genetic background, diet, gut bacteria and inflammatory state can all be controlled. The demographics of the 21 patients included in the MACS experiments were recorded. Despite efforts to match the patient groups differences were observed. Healthy patients were older on average and more likely to be male (Table 4.1). No significant relationship between age and AHR expression was observed in this cohort (Figure 4.12). However, other groups have reported a positive correlation between age, AHR expression and vascular stiffness (Eckers 2016).

In this cohort *AHR* expression was significantly higher in females than males but there was no significant difference in *CYP1A1* expression. Basal expression of *AHR* has been reported to be higher in female rats (Lu 2006) and there are sex differences in the response to AHR activation in mice which may in part be due to interactions between AHR and oestrogen signalling (Lee 2015). The AHR/ARNT complex can function as a coactivator for the oestrogen receptors (ERα and ERβ) (Ohtake 2003 Nature). CYP1A1 and CYP1B1 are also implicated in estradiol metabolism (Lee 2003 Endocrinology) and there may be specific feedback loops present in females. This is an important confounder which should be considered in future studies and is also discussed in Chapter 6.

Crohn's disease is a heterogenous condition and it is challenging to recruit individuals with exactly the same clinical characteristics. Another limitation of these findings is that previous surgery or targeting disease activity meant the anatamoical location of intestinal biopsies varied. It is reported that *AHR* and *CYP1A1* expression varies along the length of the gastrointestinal tract (Le Ferrec 2002, Mowat 2014). In the colon, there is a high density of anaerobic bacteria compared with the ileum (Hillman 2017). If bacterial metabolism plays an important role in the generation of AHR ligands in humans it is likely to affect the colon more than the ileum. Conversely components of the diet are largely processed and absorbed by the end of the ileum meaning these factors will have a diminishing effect along the gastrointestinal tract.

In this cohort it did appear that ileal expression of *AHR* was higher than expression in the right colon. However, to understand the importance of this confounder additional samples need to be collected particularly from healthy ileum, which were not included in this study. Previous studies have also shown differences in *AHR* expression in areas of active inflammation compared to uninflammed tissues in Crohn's disease, albiet with opposite findings (Monteleone 2011, Arsenescu 2011). In this study there was no signfiicant difference in *AHR* expression between actively inflammed and inactive disease. An important limitation of this observation and all previous studies is that disease activity was

only determined based on macroscopic appearance. It is recognised that a proportion of patients have microscopic disease activity without macroscopically normal colon, meaning that tissue labelled as inactive could include patients who actually have histological inflammation. To address this in future paired samples could be taken for histologically analysis.

In this chapter the expression of both *CYP1A1* and *AHR* were compared to a number of different variables including age, sex, diagnosis, disease activity, cell type and anatomical location. Comparing each variable individually introduces the possiblity of a Type I error through multiple comparisons. A regression model was considered to determine the impact of these potentially independent variables on *AHR* and *CYP1A1* expression. However, the sample size in each group in this study was below the number of variables considered, meaning any model would not be adequately powered to detect significant relationships.

4.5.4 AHR is enriched in the intestinal mucosa compared to circulation

Another striking observation from this cohort is that *AHR* expression is higher in both immune and non-immune cells in the intestinal mucosa compared to circulating immune cells. In fact, average expression of these mixed intestinal cell populations is as high as the expression seen in monocyte derived dendritic cells generated *in vitro,* the highest level of expression observed in this project (Figure 4.16). This suggest that cells at the intestinal barrier may acquire higher expression of *AHR* after trafficking from the circulation. It is not clear if this happens in other organs such as the skin or lungs.

Expression of *CYP1A1* was even higher than the level observed in unstimulated moDC (Figure 4.17) but this may reflect *in-vivo* or experimental exposure to AHR ligands during the processing of gut tissue. A comparison with whole biopsy gene expression suggests the former explanation plays an important role, expression of *AHR* was observed at a similar level in MACS sorted CD45+ and CD45- cells and freshly processed whole biopsies (Figure 4.18).

4.5.5 AHR is present and active in epithelial, endothelial and stromal cells in the intestinal mucosa

To further explore the observation that AHR is active in non-immune cells in the intestinal mucosa FACS sorting was used in order to better characterise the CD45 negative population. Live endothelial, epithelial, immune and stromal cells were identified in digested colonic biopsies. Although very few endothelial cells were recovered (Figure 4.19), consistent with superficial sampling of the mucosa, *AHR* and *CYP1A1* expression was seen in all the populations examined confirming that the pathway is present in a far wider subset of cells in the intestinal mucosa than previously appreciated. This is another important finding.

Again, supporting previous work, the highest expression of *AHR* and *CYP1A1* was seen in the negatively selected fraction likely to represent stromal fibroblasts and myofibroblasts. However, it is important to acknowledge differences in expression between populations were not statistically significant in part due to low numbers of patients and in part due to heterogeneity in number of cells recovered from each individual.

These data also highlighted the limitation of a combined FACS sort and RT-qPCR approach. Very few endothelial (CD31+) cells were recovered from each individual meaning input RNA approached or was below the limit of detection for qPCR. The reproducibility and sensitivity of qPCR significantly reduces after 35 cycles. Reference gene, by definition, a highly expressed gene was only detected close to this threshold meaning that only other genes also expressed at a high level could have been detected by this approach. Whilst it is tempting to consider further sub-division of the examined populations any assessment of gene expression, let alone function, will become more difficult.

4.5.6 Characterising AHR+ intestinal immune cells at single cell resolution

A different approach was used to characterise the CD45+ population. A new single cell sequencing platform was used to sequence the mRNA in 1305 intestinal immune cells that had undergone FACS sorting to select live CD45+ cells. Clustering using tSNE identified 6 different immune cell populations (Figure 4.21).

Analysis of differentially expressed genes revealed that the clusters did not correspond directly to classical immune cell groups. For example, B-cell lineage immunoglobulin genes were expressed in cells within clusters 1,2 and 3. Nonetheless, it was possible to identify the phenotype of the major spatial clusters and identify major immune cell groups within the sample. T-cell receptor genes were expressed in both clusters 4 and 5, APC in cluster 6 and a mast cell defining gene was only expressed in a sub-group of cluster 1.

There are a number of limitations to the statistical approach used to analyse this data. Firstly, both the CellRanger software used to align read data to the reference genome and the Loupe visualisation software are proprietary. The tSNE algorithm used to identify clusters is not visible to or modifiable by the end user. Variables such as perplexity which determine the balance of local and global relationships in the data are not modifiable. Different data sets can require different numbers of iterations to converge which also cannot be adjusted.

There are also fundamental limitations to the tSNE method itself (van Maaten and Hinton 2008). tSNE is computationally demanding and is hard to scale to larger datasets. Importantly, the addition of any data, for example additional samples, requires complete re-analysis. Repeated runs can produce different clustering using tSNE. Although apparently stable, repeated analyses were not systematically compared for the clusters presented in this chapter.

Other dimensionality reduction techniques exist such as UMAP (McInnes et al. 2018). This technique has won favour in single cell data analysis. Analysis of large data sets is significantly faster, unlike tSNE

the spatial distance between clusters is meaningful and it is much faster to repeat analysis after the addition of additional samples.

In 6.4% cells at least one *AHR* transcript was detected. By comparing this expression to the characterised clusters, it was possible to determine that the greatest number of AHR expressing cells were in the T-cell cluster. However, AHR+ cells were seen in all populations of intestinal immune cells.

Comparing the genes differentially expressed in *AHR* expressing cells with *AHR* negative cells identified known AHR-associated genes such as *IL22*, which is expressed in lymphocytes. This also highlighted a number of novel genes which have not previously been associated with AHR such as *MMP9, CXCL8* and *CCL3L1* (Table 4.6) which are expressed in innate immune cells like macrophages

Expression of both CXCL8 (also known as IL-8) and MMP9 is elevated in IBD (Daig et al. 1996). However, clinical studies have not found benefit from directly inhibiting MMP9 (de Bruyn and Ferrante 2018). BATF was also associated with AHR expression. Deletion of this transcription factor in mice leads to loss of Th17 cells (Schraml 2009).

It is not clear if these novel genes identified are directly dependent on AHR signalling or simply define the cell-types where *AHR* expression is highest but this warrants further investigation. It is also worth noting that *CYP1A1* transcripts were not detected in any cells and *CYP1B1* was only expressed in <1% cells. This highlights the limitations of this technology which currently is less sensitive than single gene PCR or bulk RNASeq, due to variable capture efficiency and high dropouts meaning scRNA-seq produces nosier and more variable data and is less able to detect the expression of a genes at a low level (Geng Chen, Ning, and Shi 2019). Nonetheless, this very powerful tool has provided unrivalled highly parallel information about the characteristics of *AHR* expressing intestinal immune cells which will inform the rational design of future functional studies.

4.6 Conclusion

In this chapter AHR protein and gene expression is demonstrated in both intestinal immune cells and in non-haematopoietic cell types including epithelial cells, stromal cells and endothelial cells. In contrast to some previous studies, there is a trend to higher AHR expression and activation in Crohn's disease, and importantly is more active in non-haematopoietic cell types, inviting important questions about the function of AHR in these newly recognised AHR expressing cell. AHR expression is shown to be enriched in immune cells at the intestinal barrier compared to circulating immune cells in keeping with its role as an environmental sensor. Single cell sequencing is used to precisely characterise the intestinal immune cells expressing AHR. More than half of these cells are lymphocytes. AHR expression was also seen in innate immune cells and there is an association between many of the identified genes and IBD. It remains to be determined if these genes are co-expressed in cells with AHR or directly regulated by this pathway.

Chapter 5 - AHR pathway activity in the human intestinal mucosa in health and Crohn's disease

5.1 Chapter Summary

In this chapter the activity and responsiveness of the AHR pathway to stimulation in the human intestine is determined. Intestinal immune cells are separated from non-haematopoietic cells and incubated with AHR agonist or antagonists. Quantitative measurement of cytochrome p450 gene expression is used to determine the magnitude of AHR signalling *ex-vivo* and importantly the responsiveness to further stimulation.

Intestinal immune cells show modest activation on incubation with FICZ, suggesting although the pathway can be activated further, AHR is already near maximally activated. Importantly, there were no differences in AHR activity *ex vivo* or responsiveness *in-vitro* in between intestinal immune cells from Crohn's disease patients and healthy subjects. This allows us to reject the hypothesis that the AHR pathway is either inactive or less responsive to stimulation in Crohn's disease.

There was a weak correlation between the degree of prior activation and responsiveness but other factors determining inter-individual variation in AHR pathway sensitivity remain unknown.

Mucosal non-haematopoietic cells were more responsive to AHR stimulation than immune cells and these cells were even more responsive to AHR stimulation in Crohn's disease than health.

The non-haematopoietic population was fractionated using flow-cytometry but attempts to examine pathway activity and responsiveness in these purified populations was limited by the low number of cells recovered.

Cultured intestinal-fibroblasts were therefore used as an alternative approach to examine human intestinal stromal cells. The AHR pathway is shown to be functional in these cells. A potential impact of this pathway is also highlighted: human intestinal fibroblasts are shown to have the capacity to degrade the AHR ligand FICZ and restrict activation of the AHR pathway in human immune cells. This stromal-immune cell interaction could have an important role regulating AHR ligand availability to immune cell at the intestinal barrier.

Finally, single gene approaches are used to determine the impact of AHR on selected immune signalling genes in intestinal immune and non-immune cells.

5.2 Introduction

5.2.1 Determining AHR pathway responsiveness in health and Crohn's disease

In the previous chapter, AHR activity in unstimulated isolated intestinal mucosal cells was determined *ex-vivo*. In contrast to some published data, AHR expression and activity was not lower in Crohn's disease compared with health (Monteleone et al. 2011). However, an important translational question remains. Is it possible to augment AHR activity in health or Crohn's disease or is the pathway already maximally stimulated *in-vivo*?

These pharmacological questions are particularly relevant now clinical trials of AHR agonists are underway for conditions including ulcerative colitis (Naganuma et al. 2018) and trials of AHR antagonists have begun for colorectal cancer (https://clinicaltrials.gov/ct2/show/NCT04069026).

It has previously been reported that polymorphisms (rs1077773) in AHR are associated with an altered risk of IBD (OR 0.93) (Liu JZ 2015). However, the impact of AHR polymorphisms on gene function is not known; is the pathway less responsive in disease? This is particularly important if considering a dietary or pharmacological intervention to stimulate the pathway in IBD with the goal of promoting the anti-inflammatory effects as seen in murine models of colitis (Li 2011).

Previous studies to examine the AHR pathway in humans have been very limited. CYP1A1 expression, a surrogate for AHR pathway activation, has only previously been reported in homogenised whole biopsies from poorly characterised IBD donors (Arsenescu et al. 2011). This limited study, also only reported a qualitative assessment of AHR expression in haematopoietic cells by microscopy (Arsenescu et al. 2011). However, in Chapter 4 quantitative assessment of AHR expression (by

microscopy and qPCR) and activation (measured by *CYP1A1* expression) was determined and found to be higher in non-immune cells particularly epithelial and stromal populations. This highlighted a novel avenue of exploration.

Gene expression at rest and in stimulated sorted live cells has not previously been reported. Measuring dynamic changes with stimulation or blockade will allow it to be determined if AHR activity varies in different tissue types and importantly, through incubation with biologically relevant agonists and antagonists, will provide the first assessment of *in-vivo* activation and pathway responsiveness.

In the experiments presented in this chapter, the techniques refined in the work described in chapter 3 were used to stimulate and inhibit AHR signalling in cells isolated from the intestinal mucosa. Firstly, in intestinal immune and non-immune cells and subsequently in better defined sub-populations of these non-immune cells to determine whether the pathway can be significantly activated above baseline.

5.2.2 Determining the impact of AHR signalling – a targeted strategy

In the second part of this chapter, the consequences of AHR signalling are examined using a targeted strategy. Potential targets of AHR in the sorted cell types were identified in the literature.

Interleukin 22 is a key signal molecule produced by immune cells at the intestinal barrier. It promotes epithelial barrier repair supporting LGR5+ epithelial stem cell regeneration (Lindemans, Calafiore, Mertelsmann, O'Connor, et al. 2015) and the synthesis of innate immune peptides by epithelial cells (Parks 2016).

In murine models, loss of AHR is associated with reduced IL-22 (both protein and gene expression) (Veldhoen et al. 2008). In mice, a number of AHR response elements have been identified at the Il22 locus and direct binding of AHR has been observed (Qiu et al. 2012).

The role of IL-22 in human IBD is unclear. The observed effects on epithelial barrier repair have led to a clinical trial evaluating the role of recombinant IL-22 therapy in patients with active IBD (Stefanich et al. 2018). However, another emerging therapy for both UC and Crohn's disease is blockade of IL-23, a key upstream cytokine which drives IL-22 production. In fact, phase 2 clinical studies have suggested serum levels of IL-22 predict response to anti-IL23 therapy (Sands et al. 2017). Given the close association between *AHR* and *IL22* expression in murine models it is important to understand this relationship in human intestinal immune cells.

In this study the impact of AHR activation on *IL22* expression in human intestinal immune cells is examined.

A literature review was performed to identify potentially important targets of AHR in fibroblasts with focus on genes expressed in fibroblasts with an established role in the intestinal immune response (Owens 2015; Owens et al. 2013). CXCL10 and IL-1β were selected for further study:

- **CXCL10** is a chemokine secreted by fibroblasts. It can function as a chemoattractant for immune cells including monocytes, macrophages and T-cells via interaction with CXCR3 (West 2019 Front Imm) . Expression of CXCL10 is upregulated in IBD and coeliac disease (Ostvik A 2013 IBD, Bondar 2014 PlosOne).
- **IL-1β** is a cytokine classically produced by macrophages that is an important mediator of inflammation with a wide variety of cellular effects in the intestinal mucosa (Mao L 2018 Front Imm). Fibroblasts are also reported produce IL-1β (Tardif 2004 J Cell Phy).

These proteins represent important immune mediators produced by stromal cells at the intestinal barrier. Following the novel demonstration of significant AHR pathway activity in this cell type these targets were selected to examine the functional impact of AHR on the immune function of these cells.

Although these genes are not previously established AHR targets, the impact of AHR on the expression of these genes is examined in human intestinal fibroblasts.

Finally, the complex relationship between AHR signalling in different immune cell populations found in the intestinal mucosa is explored. Recent high impact papers suggest the AHR pathway in non-haematopoietic cells may have a critical role in regulating the availability of AHR ligands to mucosal immune cells (Schiering 2017, Metidji 2019). In these murine models' epithelial cells were shown to have the potential to perform this function. In this chapter we present novel data showing intestinal stromal cells could also perform this regulatory function in the human intestine.

5.3 Aim

Determine if there is a difference in AHR pathway activity in intestinal mucosal cells in Crohn's disease compared to health

Objectives

1. Compare AHR responses in intestinal mucosal immune cells to ligand and antagonist in health and Crohn's disease
2. Compare AHR responses in intestinal mucosal non-haematopoietic cells to ligand and antagonist in health and Crohn's disease
3. Determine AHR pathway activity in purified populations of stromal, epithelial and endothelial cells
4. Determine if AHR is functional in cultured human intestinal fibroblast cell lines
5. Examine the functional consequences of AHR signalling in human intestinal fibroblasts

5.4 Results

5.4.1 Dynamic measurement of AHR pathway responses in intestinal CD45+ cells reveals the AHR pathway is already significantly activated in both health and Crohn's disease

To further examine the pre-existing activation of the AHR pathway, and to determine the sensitivity of the pathway to further activation, intestinal biopsies were digested using collagenase and separated into an immune (CD45+) and non-immune fraction (CD45-) using MACS as described previously.

The patient characteristics & clinical features are recorded in Appendix 5. 10 healthy controls and 11 patients with confirmed Crohn's disease were included. Active intestinal inflammation was seen at the time of endoscopy in 6/11 patients with Crohn's disease. Control patients were only included if the colon was macroscopically normal, less than 4 adenomatous polyps all below 1cm were permitted. Patients with major comorbidities, as described previously were excluded.

Isolated MACS sorted cells were then incubated for 4 hours with culture medium alone or with the addition of the AHR antagonist CH223191 (100µM), the agonist FICZ (10nM) or both chemicals. RNA was isolated and expression of *CYP1A1* was measured, as a surrogate for AHR activation.

The concentration of each reagent was selected based on the change in *CYP1A1* expression observed in moDC reported in Chapter 3 (Figure 3.5). 10nM was the minimum concentration of FICZ that cause a significant increase in *CYP1A1* expression (almost 100-fold) but was still fully blocked by co-incubation with CH223191 at 100µM.

There were two striking observations. Firstly, in both health and Crohn's disease, the AHR pathway already shows considerable activation in intestinal immune cells. Median *CYP1A1* expression reduced to 0.09X DMSO control in health and 0.21X in Crohn's disease following incubation with 100µM

CH223191. Conversely, in response to FICZ 10nM, although *CYP1A1* expression did significantly increase compared to DMSO control, expression only increased 1.70-fold in health and 1.76-fold in Crohn's disease (compared to the ~100-fold increase observed moDC). There were no significant differences in the magnitude of response to FICZ or CH223191 in health compared to Crohn's disease (by ANOVA) suggesting the AHR pathway in intestinal immune cells is similarly sensitive in Crohn's disease as health.

When cells were incubated with both 10nM FICZ and 100µM CH223191, the antagonist effect was dominant and *CYP1A1* expression was reduced (Figure 5.1).

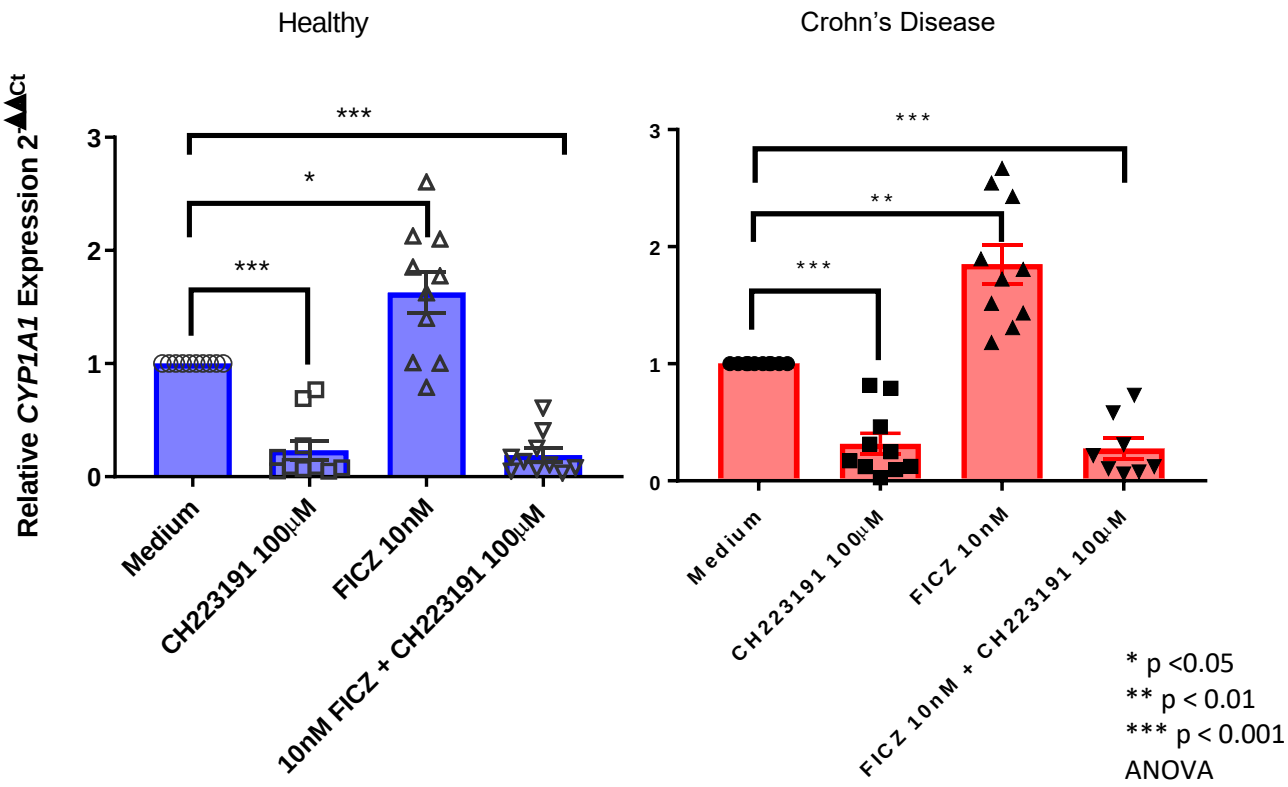

Figure 5.1 Relative *CYP1A1* expression in intestinal CD45+ cells from healthy donors or patients with Crohn's cultured with FICZ, CH223191 or both compared with culture in medium alone. Intestinal biopsies were digested using collagenase. CD45+ cells were purified using MACS sorting. Cells were incubated with medium, FICZ (10nM), CH223191 (100μM) or both drugs for 4 hours. Cells were lysed and RNA was extracted using Qiagen spin columns. Gene expression was measured by RT-qPCR relative to *RPL30*. Mean relative *CYP1A1* expression is shown normalised control conditions +/- SEM.

n = 10 healthy and 11 Crohn's disease. Expression was compared between incubation conditions and health and Crohn's disease using two-way ANOVA.

In Chapter 3, I showed that in dendritic cells a second cytochrome p450 enzyme (*CYP1B1*) is also regulated by AHR activity, although the magnitude of change was smaller (Figure 3.6). Expression of *CYP1B1* by intestinal CD45+ cells was also measured in a subset of 3 patients with Crohn's by RT-qPCR. In contrast to moDC, *CYP1B1* expression did not significantly increase above the level observed with DMSO following incubation with FICZ, but did reduce significantly following incubation with CH223191. Again, the antagonist was dominant at these concentrations (Figure 5.2). These data provide further support to the AHR-specific effects of these reagents and importantly provides further support to the hypothesis that the AHR pathway is already significantly activated in immune cells in the intestine in both health and Crohn's disease.

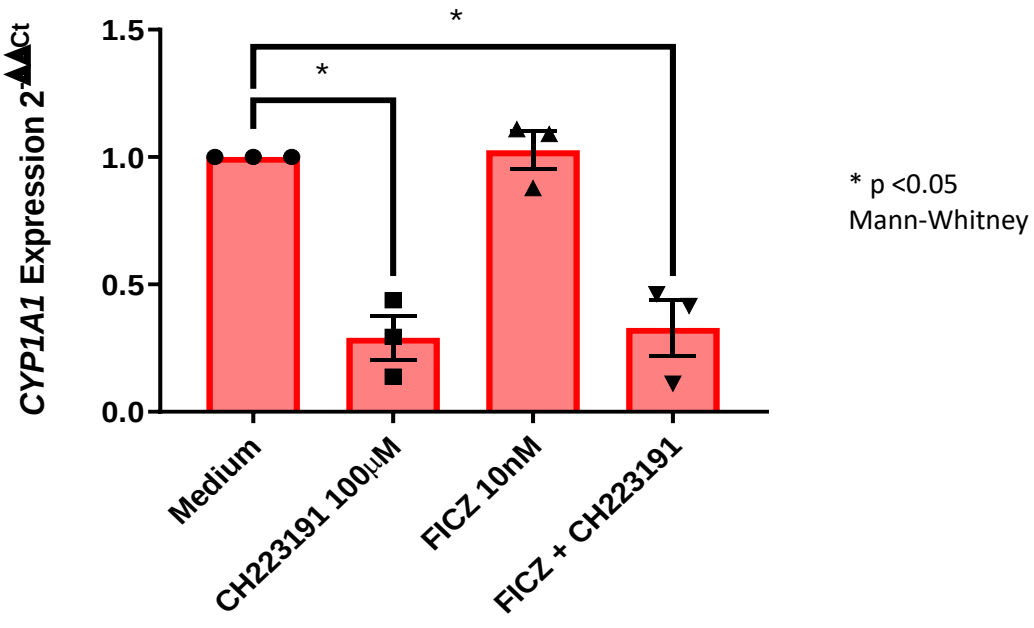

Figure 5.2 Relative *CYP1B1* expression in intestinal CD45$^+$ cells from 3 patients with Crohn's disease cultured with FICZ, CH-223191, or both compared with culture in medium alone. Gene expression was measured by RT-qPCR relative to *RPL30*. Relative *CYP1B1* expression is shown normalised to medium control ($2^{-\Delta\Delta Ct}$) +/- SEM. N = 3. Two-group comparisons using Mann-Whitney <0.05.

5.4.2 Predictors of AHR pathway responses in intestinal CD45+ cells

5.4.2.1 Expression of CYP1A1 and AHR in unstimulated cells is poorly predictive of response to AHR agonist

Considerable inter-experimental variation in the *CYP1A1* response to FICZ was observed in both health and Crohn's disease. This could be explained by biological inter-individual differences in pathway activation prior to FICZ stimulation *in-vivo* or experimentally induced variation which led to the pathway being closer to maximal stimulation in some individuals than others.

CYP1A1 expression in response to FICZ was compared to resting *CYP1A1* expression (with DMSO control). However, no significant relationship was found (Figure 5.3), suggesting AHR activation at baseline does not contribute to the inter-individual variation in response to FICZ observed.

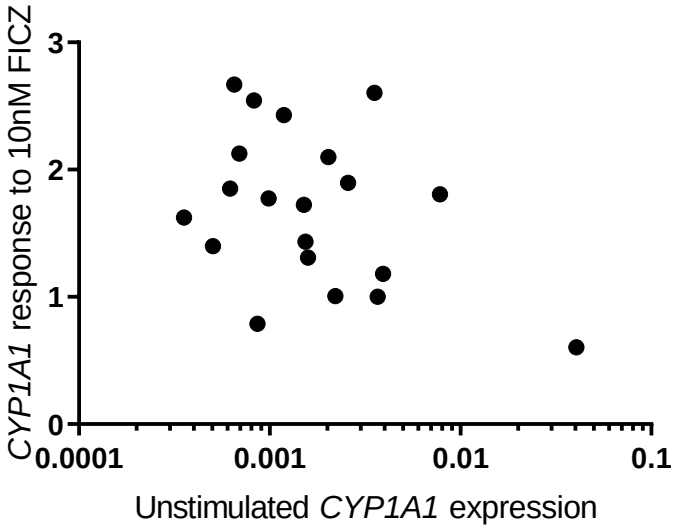

Figure 5.3 *CYP1A1* expression in medium alone compared with FICZ induced CYP1A1 expression in the same patient. *CYP1A1* expression in unstimulated CD45+ cells was determined by RT-qPCR and expressed as $2^{-\Delta Ct}$ was compared to the magnitude of induced *CYP1A1* response by FICZ 10nM in the same donor, expressed as $2^{-\Delta\Delta Ct}$. There was no significant relationship $p = 0.057$, $R^2 = 0.19$.

Alternatively, the amount of AHR itself could influence the magnitude of the *CYP1A1* response to FICZ. Therefore, expression of AHR was compared to the response to FICZ. Again, the *CYP1A1* response to

FICZ did not correlate with expression of *AHR* overall (Figure 5.4), or considering heath and Crohn's disease separately (not shown).

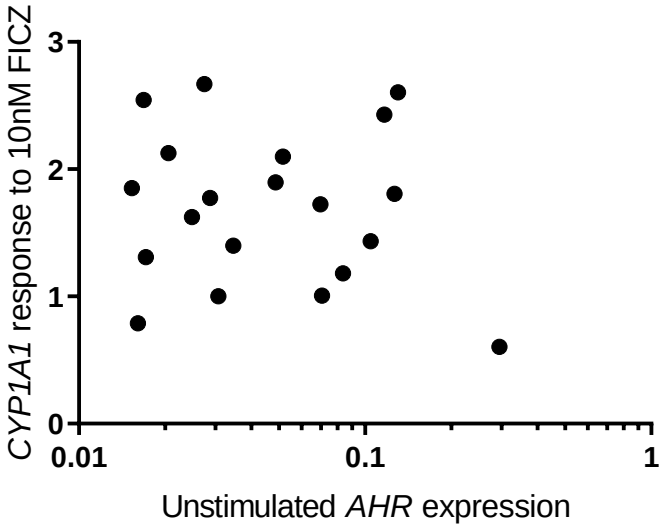

Figure 5.4 ***CYP1A1* expression in response FICZ compared with *AHR* expression in the same patient.** *CYP1A1* expression in cells stimulated with 10nM FICZ was determined by RT-qPCR and expressed as $2^{-\Delta\Delta Ct}$ was compared to relative AHR expression in the same donor, expressed as $2^{-\Delta Ct}$. There was no significant relationship.

5.4.2.2 The reduction in *CYP1A1* in response to CH223191 (reflecting the magnitude of prior activation) does correlate with the increase in *CYP1A1* in response to FICZ in health

Finally, the *CYP1A1* response to CH223191 could reflect the degree of prior AHR pathway activation better than simple measurement of *CYP1A1* in control conditions. A large reduction in *CYP1A1* expression with CH223191 may predict a cell is in a less responsive state to AHR ligands.

Overall, there was no significant relationship between the magnitude of reduction in *CYP1A1* in to the presence of CH223191 and the rise in *CYP1A1* in response to FICZ in the same individuals overall (not shown). However, there was a weak, but significant relationship in healthy individuals but not in Crohn's disease (Figure 5.5). This may reflect true differences is *in-vivo* activation or a Type I error from multiple comparisons.

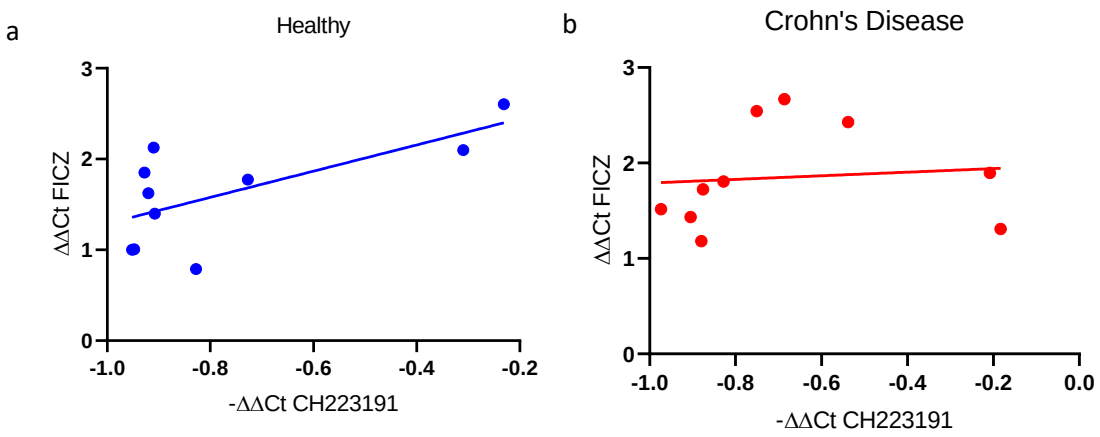

Figure 5.5 *CYP1A1* expression in response FICZ compared with the reduction in CYP1A1 expression with CH223191 in (a) health and (b) Crohn's disease. *CYP1A1* expression in cells stimulated with 10nM FICZ was determined by RT-qPCR and expressed as $2^{-\Delta\Delta Ct}$ was compared to the reduction in CYP1A1 expression with CH223191 in the same donor, expressed as $2^{-\Delta Ct}$. There was a weak but significant relationship by linear regression in healthy donors ($p = 0.03$, R^2 0.45) but not in Crohn's disease ($p = 0.78$, $R^2 = 0.01$).

5.4.2.3 Variation in response to AHR agonists and antagonists in different anatomical locations in the intestine

The concentration and composition of gut bacteria varies between the ileum, caecum and left colon (Marteau P 2001). Although unknown, it is likely this variation combined with variation in nutrient concentrations leads to different availability of AHR ligands. To examine this the *CYP1A1* response to AHR agonist and antagonist was compared between intestinal CD45+ cells isolated from the splenic flexure (left colon), caecum and ileum.

CD45+ cells from the splenic flexure were significantly more responsive to FICZ (compared to DMSO) than cells from the right colon (Figure 5.6a), whilst cells from the right colon showed the largest drop in *CYP1A1* expression after incubation with CH223191 (Figure 5.6b) (although this difference was not significant when considering multiple comparisons using ANOVA). This observation may reflect a different level of *in-vivo* activation and corresponding reduced responsiveness to AHR agonists in the right colon. Resting (unstimulated) *CYP1A1* expression was highest in the ileum (Appendix 9).

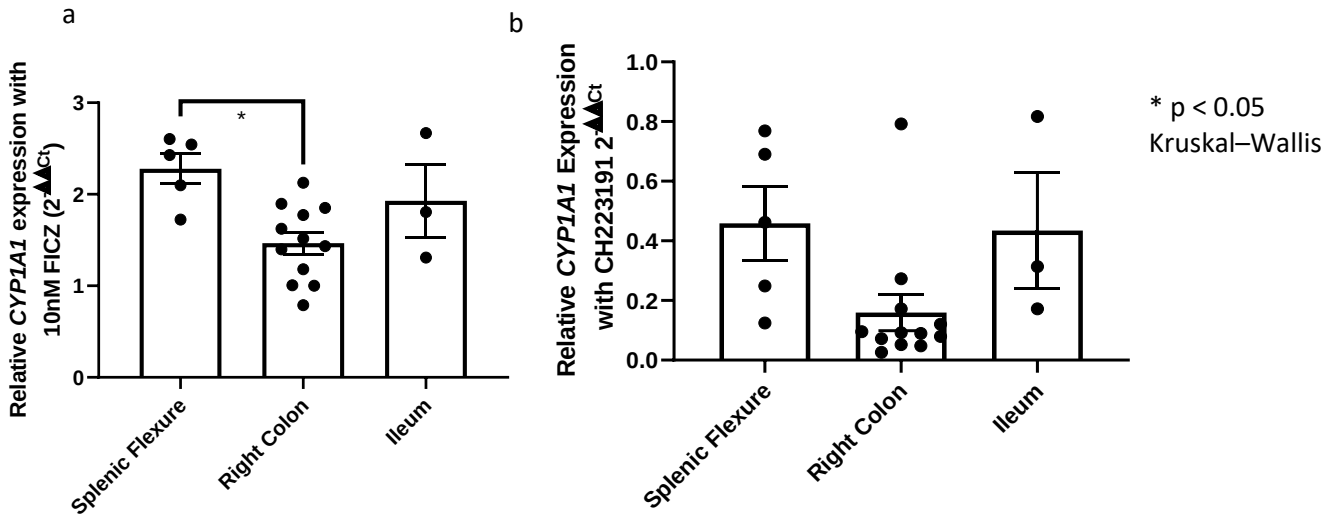

Figure 5.6 Relative *CYP1A1* expression in response to FICZ (a) and CH223191 (b) in CD45+ cells from different anatomical locations. CD45+ cells from the right colon showed a smaller increase in CYP1A1 in response to FICZ and a small drop in CYP1A1 in response to CH223191 (n = 21; analysis using Kruskal–Wallis test).

5.4.3 AHR pathway is more responsive in non-haematopoietic cells than haematopoietic cells from the intestinal mucosa

In the previous chapter, I showed resting *CYP1A1* expression was higher in non-immune cells from the intestinal mucosa compared to immune cells (Figure 4.10).

Using the previously described methodology, MACS enriched intestinal CD45- cells were incubated for 4 hours with DMSO alone or with the addition of CH223191 (100μM), FICZ (10nM) or both FICZ and CH223191. RNA was isolated and gene expression determined using RT-qPCR. Expression of *CYP1A1* was measured as a surrogate for AHR activation compared to the reference gene *RPL30*.

The AHR pathway was highly responsive in intestinal CD45- cells. There was a large increase in *CYP1A1* expression in response to FICZ and this induced expression was again inhibited by co-incubation with CH223191, supporting the hypothesis that this is a specific effect of AHR activation. The response to

FICZ was greater in CD45- from patients with Crohn's compared to health. This difference was just below statistical significance after correcting for multiple comparisons using a one-way ANOVA (p = 0.054). Unlike CD45+ cells there was no significant reduction in *CYP1A1* after incubation with CH223191 compared to DMSO control alone (Figure 5.7). This may simply reflect that AHR is less stimulated *in-vivo* in these cells or altered intrinsic properties.

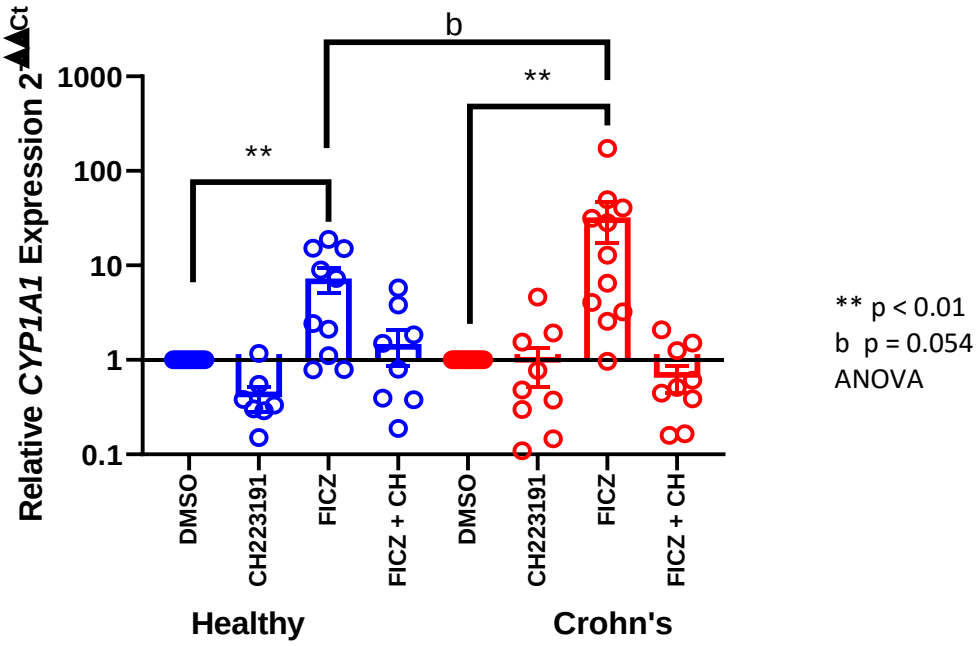

Figure 5.7 Relative *CYP1A1* expression in intestinal CD45$^-$ cells from healthy donors or patients with Crohn's cultured with FICZ, CH223191 or both compared to DMSO control. CD45$^-$ cells were purified using MACS sorting. Cells were incubated with DMSO 0.16%, FICZ 10nM, CH223191 100μM or both drugs for 4 hours. Gene expression was measured by RT-qPCR. Mean relative *CYP1A1* expression is shown normalised to control conditions +/- SEM ($2^{-\Delta\Delta Ct}$). n = 10 healthy and 11 Crohn's disease. *CYP1A1* expression was significantly higher with FICZ in both health and disease (p <0.01). CH223191 completely inhibited the effect of FICZ (p <0.01) there was no significant reduction compared with unstimulated cells. Expression between conditions and disease was compared using ANOVA.

The response to FICZ in CD45 positive and negative cells was also directly compared. In both health and Crohn's disease CD45- were far more responsive to FICZ than CD45+ immune cells (Figure 5.8).

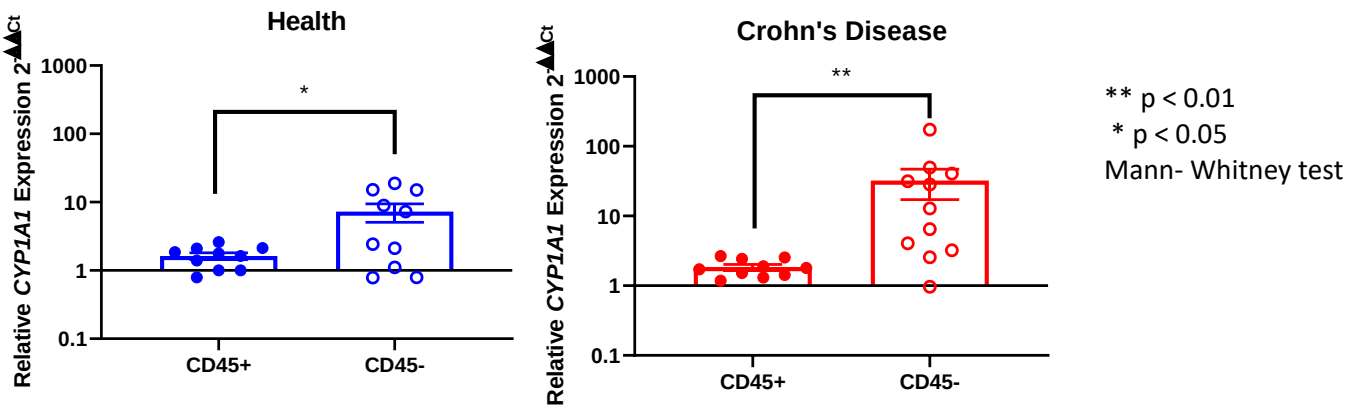

Figure 5.8 The change in *CYP1A1* expression in response to 10nM FICZ in CD45+ and CD45- cells in health and Crohn's disease. Mean relative *CYP1A1* expression is shown normalised to respective control conditions +/- SEM ($2^{-\Delta\Delta Ct}$). n = 10 healthy and 11 Crohn's disease. The increase in *CYP1A1* expression in response to FICZ was significantly greater in non-haematopoietic cells and this difference was even more marked in Crohn's disease. Paired comparisons using Mann- Whitney test.

5.4.4 Predictors of AHR pathway responses in intestinal CD45⁻ cells

There was even wider variation between individual's response to FICZ in CD45- cells than CD45+ cells. To explore if this was partly explained by differences in pathway activation prior to FICZ stimulation, *CYP1A1* expression in response to FICZ was compared to resting *CYP1A1* expression (with DMSO control). However, no significant relationship was found (Figure 5.9).

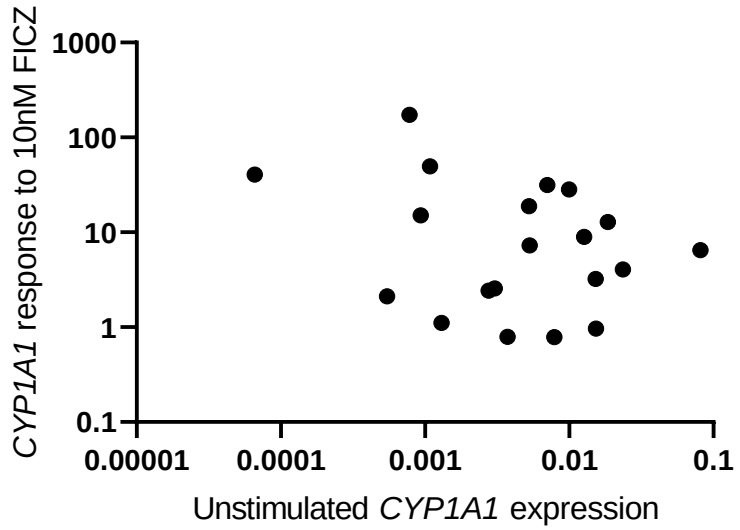

Figure 5.9 *CYP1A1* expression in DMSO alone compared with FICZ induced *CYP1A1* expression in CD45- cells from the same patient. CYP1A1 expression in unstimulated CD45- cells was determined by RT-qPCR and expressed as $2^{-\Delta Ct}$ was compared to the magnitude of induced *CYP1A1* response by FICZ 10nM in the same donor, expressed as $2^{-\Delta\Delta Ct}$. There was no significant relationship by linear regression.

Similar to findings in $CD45^{+}$ cells, the expression of *AHR* did not correlate with CYP1A1 response to FICZ (Figure 5.10). Suggesting differences in the amount of AHR did not explain the differences observed between individuals.

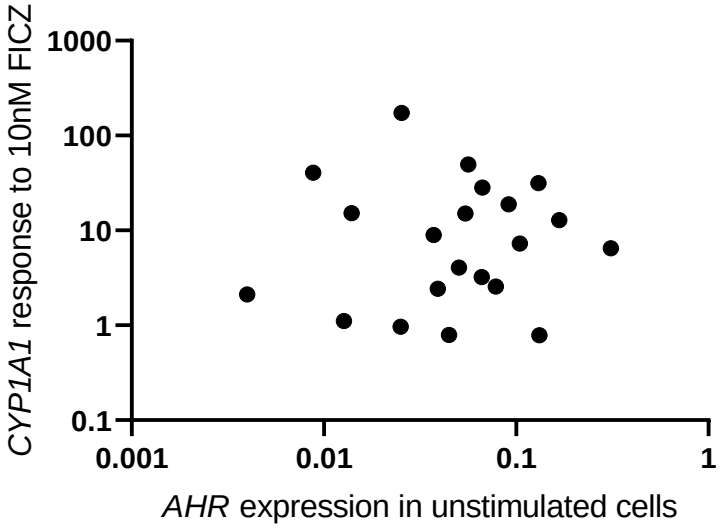

Figure 5.10 *AHR* expression in medium alone compared with FICZ induced *CYP1A1* expression in CD45- cells from the same patient. *AHR* expression in unstimulated CD45- cells was determined by RT-qPCR and expressed as $2^{-\Delta Ct}$ was compared to the magnitude of induced *CYP1A1* response by FICZ 10nM in the same donor, expressed as $2^{-\Delta\Delta Ct}$. There was no significant relationship by linear regression.

Finally, the *CYP1A1* response to CH223191, which could reflect the degree of prior AHR pathway activation, was compared to the rise in *CYP1A1* in response to FICZ in the same individuals. An interesting pattern was observed: in some individuals a marked reduction in *CYP1A1* with CH223191 was associated with an attenuated response to FICZ, but not all. Conversely, no reduction in *CYP1A1* expression with CH223191 was always associated with a large magnitude response to FICZ (Figure

5.11). However, overall, or considering health and disease separately (not shown), there was no significant relationship between the CYP1A1 response to agonist (FICZ) and antagonist (CH223191).

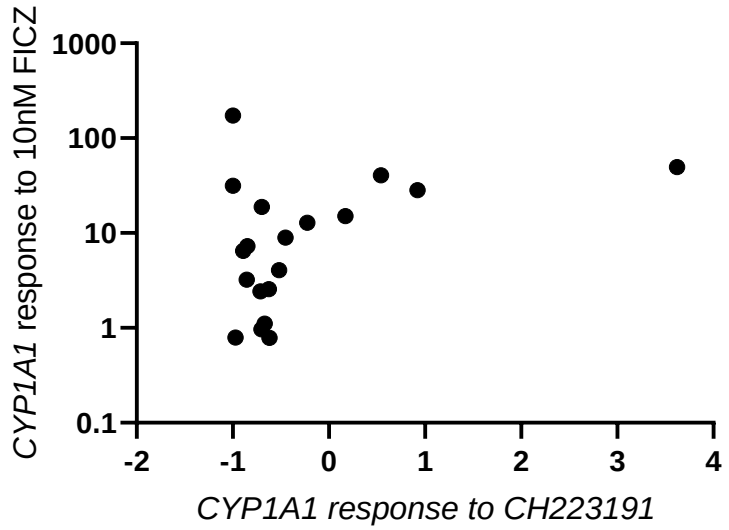

Figure 5.11 *CYP1A1* expression in response FICZ compared with the reduction in CYP1A1 expression with CH223191 in CD45- cells from 9 healthy donors and 10 Crohn's disease. *CYP1A1* expression in cells stimulated with 10nM FICZ was determined by RT-qPCR and expressed as $2^{-\Delta\Delta Ct}$ was compared to the reduction in *CYP1A1* expression with CH223191 in the same donor, expressed as $2^{-\Delta Ct}$. There was no significant relationship by linear regression.

5.4.5 AHR is more active in intestinal epithelial and stromal cells than CD45+ cells

As previously acknowledged, the CD45- fraction is a heterogenous population of cells. FACS sorting offers the advantage of purity and more sophisticated selection. A sorting strategy described in Chapter 4 (Table 4.4) was used to isolate epithelial and endothelial cells as well as a triple negative (stromal) fraction. Cells were incubated with DMSO (0.02%), FICZ (100nM) and/or CH223191 (100μM) for 4 hours. RNA was isolated and expression of CYP1A1 determined using RT-qPCR with RPL30 as the reference gene.

As previously reported, few CD31 cells were recovered and *CYP1A1* expression was below the limit of detection in samples incubated with FICZ and CH223191.The highest induced *CYP1A1* expression at rest was seen in the triple negative (stromal) fraction. *CYP1A1* expression at rest and with FICZ was

higher in both epithelial and triple negative cells than CD45+ cells. Although incubation with FICZ did not significantly change CYP1A1 expression in the triple negative cells, perhaps due to prior significant activation. *CYP1A1* expression was reduced by CH223191 in epithelial and triple negative cells supporting a degree of pre-existing AHR activation in non-haematopoietic cells in the intestinal mucosa (Figure 5.12).

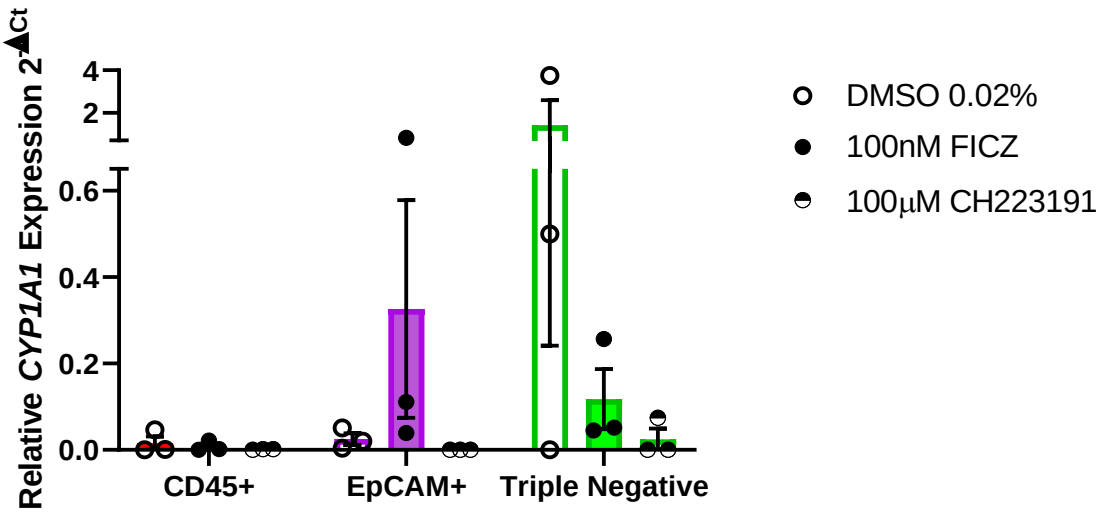

Figure 5.12 *CYP1A1* expression in stimulated sorted mucosal cells. Intestinal mucosal biopsies were digested and FACS sorted into live CD45+, EpCAM+, CD31+ (not shown) or triple negative populations. Cells were cultured with DMSO, FICZ or CH223191 for 4 hours. Relative *CYP1A1* expression normalised to RPL30 expression ($2^{-\Delta Ct}$) was determined by RT-qPCR. n = 3 patients.

These data help us further understand the findings previously described in MACS separated CD45- cells. The AHR pathway is indeed more active and responsive in CD45- cells than immune cells, particularly in epithelial cells and stromal cells. The latter have not previously been shown to have a functional AHR pathway.

However, this approach also highlights practical obstacles to cell sorting intestinal biopsies and the number of cells recovered in each population is relatively low. Too few cells were recovered from some individuals to perform these studies, which could introduce a selection bias. In addition, the low cell numbers limit the ability to perform any functional studies to examine the role of AHR in these cell types.

Because of these limitations, an alternative approach was identified to examine the AHR pathway in intestinal stomal cells.

A number of nominally healthy semi-immortalised human colonic fibroblasts are commercially available. CCD-18Co (from ATCC®) is a human colonic fibroblast cell derived from a paediatric patient. In the appropriate culture conditions, it will adhere and divide. However, it is not an immortal cancer cell line and will senesce after 40-42 passages. This cell was selected to represent the stromal cell fraction and explore the AHR pathway in human fibroblasts further.

5.4.6 The AHR pathway is functional in cultured human colonic fibroblasts

Intestinal fibroblasts were cultured in 25cm^2 Falcon™ tissue-culture treated flasks in fibroblast culture medium for at least 3 passages after defrosting before use in functional experiments. 5000 fibroblasts were transferred to each well of a 96-well tissue-culture treated plate and left overnight to adhere. Fibroblasts were then incubated for 4 hours with 0.02% DMSO, FICZ 100nM, CH223191 10µM or both, with at least 4 wells (20,000 cells) per condition.

Similar to sorted intestinal stromal cells, AHR was highly expressed in cultured fibroblasts and was expressed at a significantly higher level than in MACS sorted CD45+ or CD45- cells (Figure 5.13).

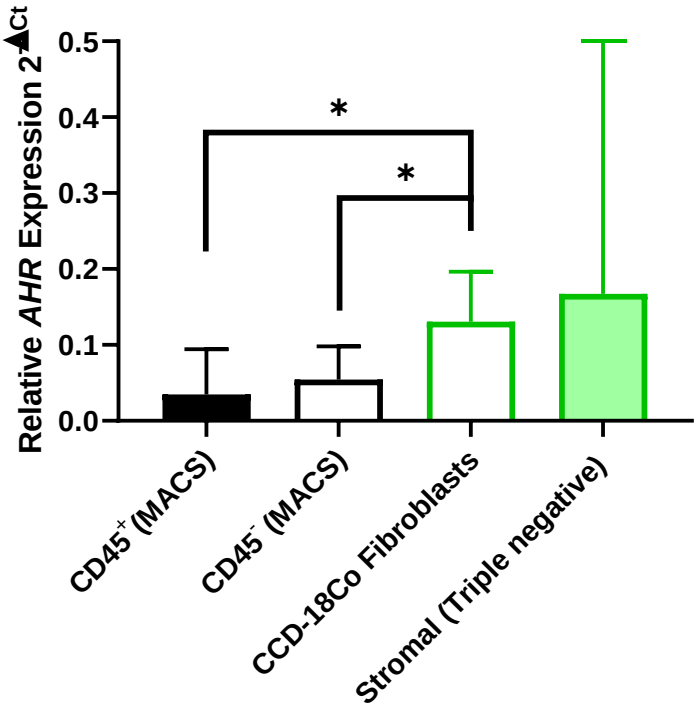

Figure 5.13 Relative *AHR* expression in MACS sorted intestinal mucosal cells compared with cultured fibroblasts and FACS sorted stromal cells. Unstimulated cells were lysed in RLT Buffer®. RNA was extracted using Qiagen spin columns. Gene expression was measured by RT-qPCR. Median relative *AHR* expression is shown normalised to *RPL30* ($2^{-\Delta Ct}$) ± interquartile range. n =21 CD45+ and CD45- cells, n= 5 fibroblasts, n = 6 stromal (triple negative cells).

Importantly, the AHR pathway is functional in cultured fibroblasts. The expression of *CYP1A1* and *CYP1B1* significantly increased in response to AHR ligands and this activity was inhibited by CH223191 (Figure 5.14). There was no significant background activation of the AHR pathway in these cultured cells (determined by the change in expression with CH223191 alone) presumably reflecting low availability of AHR ligands in the culture medium. The magnitude of FICZ induced induction of *CYP1A1* and *CYP1B1* was less than that observed in ex-vivo stromal cells or CD45- cells. There was no relationship between passage number and responsiveness to AHR stimulation (not shown).

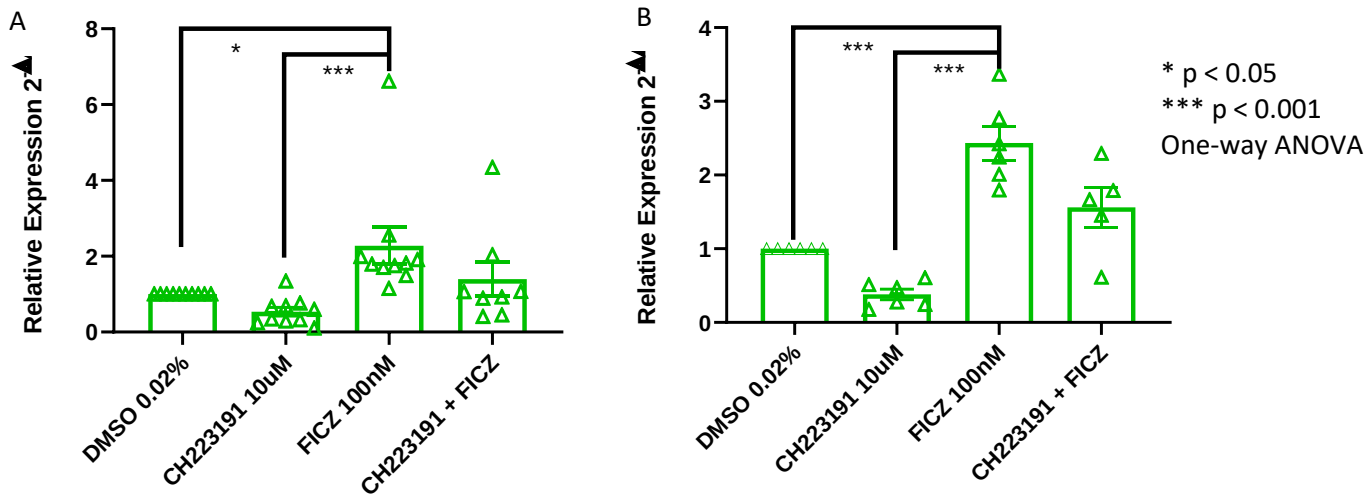

Figure 5.14 Relative gene expression in stimulated cultured colonic fibroblasts. A) *CYP1A1* B) *CYP1B1*. 5000 fibroblasts were then incubated for 4 hours with 0.02% DMSO, FICZ 100nM, CH223191 10µM or both with at least 4 wells per condition. RNA was collected and gene expression determined using RT-qPCR relative to *RPL30*. **A)** Relative *CYP1A1* expression is shown normalised to expression with DMSO ($2^{-\Delta\Delta Ct}$) n = 10 **B)** Relative *CYP1B1* expression is shown normalised to DMSO expression ($2^{-\Delta\Delta Ct}$). n = 6.

5.4.7 Intestinal stromal cells metabolise AHR ligands preventing stimulation of immune cells

Recent high impact papers suggest the AHR pathway in non-haematopoetic cells may have a critical role in regulating the availability of AHR ligands to mucosal immune cells (Schiering 2017, Metidji 2019). In these murine models, epithelial cells were identified as a key population with this activity.

The data presented in this chapter demonstrated that intestinal stromal cells from the human colon have the highest induced *CYP1A1* expression in response to exposure to the AHR agonist FICZ. Cytochrome p450 enzymes are known to metabolise physiological AHR ligands in a classic negative feedback loop. To determine if this function could also be important in the human intestine two established models were combined. Firstly, cultured fibroblasts were exposed to FICZ. A 25cm^2 flask of 80-90% confluent fibroblasts was incubated with 2ml of fibroblast medium containing 100nM FICZ overnight. The fibroblast exposed medium was aspirated and the supernatant collected after centrifugation. Monocyte-derived dendritic cells were then incubated for 4 hours in either fibroblast medium with 0.005% DMSO, fibroblast medium with 100nM FICZ left overnight exposed or unexposed

to fibroblasts, or fibroblast exposed FICZ with the addition of fresh FICZ 100nM (to test for any inhibitory factors produced by fibroblasts). The activation of the AHR receptor in moDC was determined using quantitative measurement of *CYP1A1* expression by RTqPCR.

CYP1A1 expression increased a mean 26-fold in moDC incubated with 100nM FICZ. However, in moDC incubated with fibroblast exposed FICZ *CYP1A1* expression only increased 18-fold. This did not appear to be due to the production of any factors that inhibit AHR, because addition of fresh FICZ increased *CYP1A1* expression even further (a mean 33-fold) (Figure 5.15).

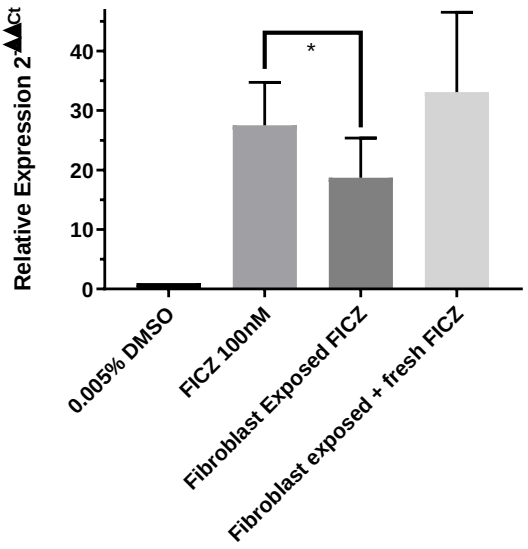

* p = 0.057 (t-test)

Figure 5.15 Relative *CYP1A1* expression in moDC exposed to different media.
Monocyte-derived dendritic cells from healthy donors were incubated for 4 hours with DMSO, 100nM FICZ, fibroblasts-exposed 100nM FICZ or fibroblast-exposed FICZ with the addition of fresh FICZ. The RNA from moDC was extracted and gene expression determined by RT-qPCR using the reference gene *RPL30.* Relative *CYP1A1* expression is shown normalised to expression in DMSO control media ($2^{-\Delta\Delta Ct}$). *CYP1A1* expression was reduced in moDC incubated in medium containing 100NM and exposed to fibroblast compared with fresh FICZ 100nM. Paired t-test p = 0.057, not significantly different by ANOVA p = 0.20. n = 10 donors except addition of fresh FICZ where n = 7.

5.4.8 Examining the impact of AHR signalling – single gene approaches

5.4.8.1 The AHR pathway does not regulate CXCL10 or IL-1β expression in colonic fibroblasts

A literature review was performed to identify potentially important targets of AHR in fibroblasts with focus on genes expressed in fibroblasts with an established role in the intestinal immune response (Owens 2015; Owens et al. 2013). CXCL10 and IL-1β were selected for further study:

- **CXCL10** is a chemokine secreted by fibroblasts. (West 2019 Front Imm)
- **IL-1β** is a cytokine classically produced by macrophages, also produced by fibroblasts (Tardif 2004 J Cell Phy).

To determine if these genes are expressed in human fibroblasts, and whether this gene expression is regulated by AHR, the expression of these genes was measured in fibroblasts incubated with FICZ and CH223191.

Expression of both *CXCL10* and *IL-1β* was detected in colonic fibroblasts. However, the expression of these genes in unstimulated colonic fibroblasts did not significantly change following incubation with FICZ or CH223191 (Figure 5.16). Protein expression was not measured in this study.

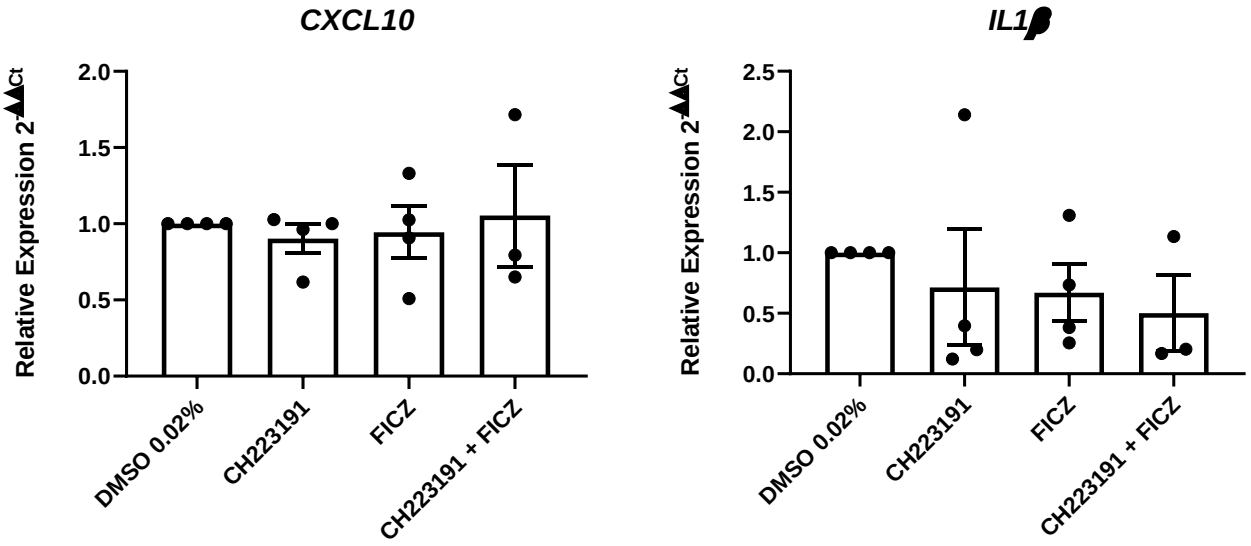

Figure 5.16 Relative *CXCL10* and *IL-1β* expression in stimulated cultured colonic fibroblasts. A) Relative *CXCL10* expression is shown normalised to DMSO expression ($2^{-\Delta\Delta Ct}$) and did not change with AHR modulation. **B)** Relative IL-1β expression is shown normalised to DMSO expression ($2^{-\Delta\Delta Ct}$) and did not change with AHR modulation (n = 4).

5.4.8.2 AHR does not directly regulate *IL22* expression in human intestinal CD45+ cells

Interleukin 22 is a key signal molecule produced by immune cells at the intestinal barrier. It promotes epithelial barrier repair and the synthesis of innate immune peptides by epithelial cells. AHR binding sites (DRE) are reported upstream of the *IL22* gene (Qui J 2012) and in murine models genetic deletion of AHR is associated with reduced IL-22 protein production and gene expression (Veldhoen et al. 2008).

To determine whether *IL22* expression in *ex-vivo* human intestinal immune cells was regulated by AHR, expression of *IL22* was measured by RT-qPCR in the MACS sorted CD45+ cells which were stimulated with FICZ, CH223191 or both as described previously.

Baseline expression of *IL22* was numerically higher but not significantly different in unstimulated CD45+ cells in health compared to Crohn's disease (Mann Whitney test p =0.12) (Figure 5.17).

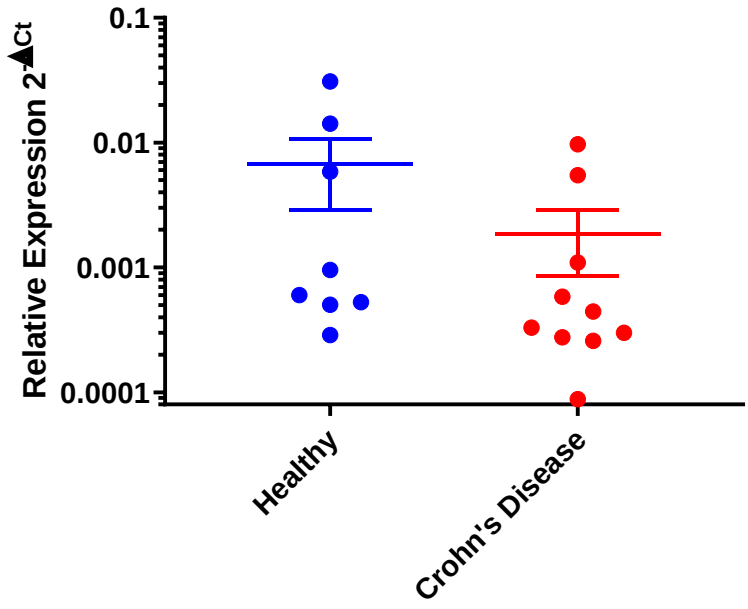

Figure 5.17 Relative *IL22* expression in unstimulated intestinal CD45$^+$ cells. Intestinal biopsies were digested with collagenase. CD45$^+$ cells were isolated using MACS. *IL22* expression was measured in unstimulated cells directly *ex-vivo* by RT-qPCR. Relative *IL22* expression is shown normalised to *RPL30* ($2^{-\Delta Ct}$) +/- SEM. n = 8 Healthy 10 Crohn's. *IL22* expression was lower Crohn's disease but this difference was not significant (Mann Whitney test p =0.12).

The effect of AHR pathway manipulation with either CH223191 or FICZ on *IL22* expression was highly variable in health and Crohn's disease. However overall, there were no significant differences in *IL22* expression in cultures supplemented with either AHR agonist or antagonist compared with medium alone (Figure 5.18).

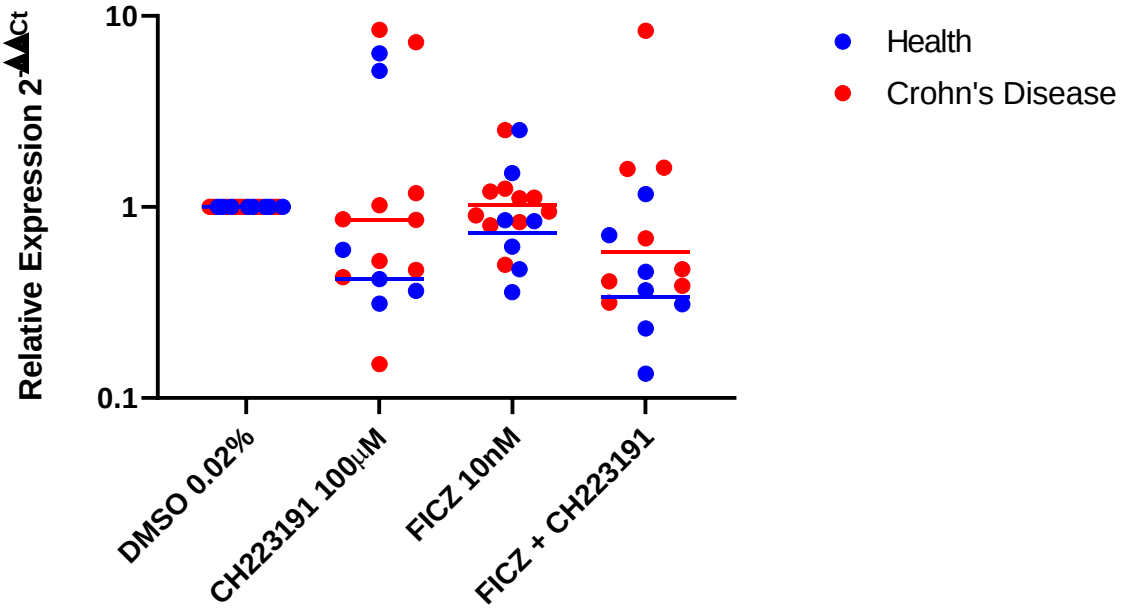

Figure 5.18 Relative *IL22* expression in intestinal CD45+ cells cultured with FICZ 10nM, CH223191 100µM or both compared with the DMSO control. Gene expression was measured by RT-qPCR. Mean relative *IL22* expression in health (blue) and Crohn's disease is shown normalised to control ($2^{-\Delta\Delta Ct}$). n = 8 Healthy 10 Crohn's. There was considerable inter-individual variation and no significant difference by Friedman test between conditions in health or Crohn's disease.

To understand if variation in *ex-vivo* pathway activation explained this variation the change in *IL22* seen, the *IL22* response to FICZ was firstly compared to the change in *CYP1A1* expression in response to CH223191 (a large reduction would suggest a significant degree of prior activation) and secondly,

the *CYP1A1* response to FICZ (a large increase suggesting an AHR responsive state). However, there was no significant relationship between the change in *CYP1A1* and *IL22* expression (not shown). IL-22 protein expression was not measured in this study.

5.5 Discussion

5.5.1 AHR is near-maximal activation in intestinal immune cells *ex-vivo* in both health and Crohn's disease

In this chapter a previously validated measure of AHR activity (quantitative measurement of *CYP1A1* expression) was used to examine AHR pathway activation and responsiveness in *ex-vivo* intestinal mucosal cells.

The first key finding of this chapter was that the AHR pathway is indeed responsive to manipulation with specific ligands and antagonists in both intestinal immune cells (CD45+) and divided non-haematopoietic mucosal populations. In both health and Crohn's disease incubating cells with FICZ significantly increased *CYP1A1* expression while incubation with CH223191 reduced *CYP1A1* expression. However, the magnitude of change was surprising. There was only a modest increase in CYP1A1 expression in response to FICZ 10nM (1.70 – 1.76x) in intestinal immune cells. This compared to a ~50-fold increase in *CYP1A1* expression in moDC at this concentration.

There a number of possible explanations for this difference. Firstly, the expression data derived from single cell sequencing showed only a minority of intestinal immune cells (<8%) expressed AHR. It is likely cells which highly express AHR, such as moDC are more responsive to AHR ligands, whereas the effect of FICZ on AHR responsive intestinal immune cells is diluted by the presence of cells which are not expressing AHR.

It is also important to note that moDC are cultured for 7 days ex-vivo before stimulation. Any AHR ligands present are likely to be degraded over this time whereas intestinal cells are exposed to numerous AHR ligands in the lumen of the bowel and were processed and examined immediately *ex-vivo* in this study. Supporting this is the observation that unstimulated *CYP1A1* expression in moDC is very low mean ΔCt 14.3 whereas the pathway is more activated in all intestinal cell types ΔCt 9.4 for CD45+ cells and 8.3 for CD45- cells and whole biospies.

Further support for prior activation is seen when incubating with an antagonist. A much greater drop in *CYP1A1* expression (5.5 – 11 x) was seen with the antagonist CH223191 compared to the rise with the agonist (Figure 5.1). In moDC the reduction in *CYP1A1* expression seen with CH223191 was less than 40% (0.6X) and was not significantly different compared to DMSO control. This strongly supporting the hypothesis that the pathway is already significantly activated.

Prior to stimulation intestinal cells underwent repeated washes. It is possible small amounts of AHR ligand carried over from the intestine or were already present in the culture media, although the same culture media was used to incubated moDC. It would be helpful to compare gene expression in cells prior to and after 4 hours of incubation in control conditions to determine if AHR was activated.

This could reflect true differences in *in-vivo* AHR activation, or intrinsic differences in the ability of these cells to metabolise and degrade AHR ligands over the course of the tissue digestion and sorting process prior to stimulation. Digestion of tissue may liberate AHR ligands and other lab reagents like fetal calf serum, used in culture medium, are also reported to contain AHR ligands (Adachi J 2001).

No significant difference in *AHR* or *CYP1A1* expression between health and IBD was seen in freshly processed whole biopsies. Importantly, mean quantitative expression of *CYP1A1* in freshly processed whole biopsies was not significantly different from *CYP1A1* expression in CD45+ cells derived from digested and sorted intestinal biopsies (Appendix 10), and was significantly higher than expression seen in moDC providing some evidence that experimental *ex-vivo* activation of AHR is not a major factor.

It is also possible that the reversibility of AHR stimulation may depend on the nature of the stimulating ligand in the gut. For example, inorganic pollutants are highly resistant to degradation and may persistently activate the receptor while the effect of organic ligands is reversible and short lived

(Wheeler et al. 2014). One way to overcome this would be to simultaneously collect stool samples with intestinal biopsies to measure AHR ligands either through mass spectroscopy or using an AHR reporter cell line.

It was interesting to compare AHR pathway activity and responses in cells taken from different sites in the gastrointestinal tract. Cells from the splenic flexure were more responsive to FICZ than the right colon, which conversely showed the biggest reduction in *CYP1A1* activity following incubation with CH223191 suggesting the pathway is more active *in-vivo* in the right colon. This could reflect the high bacterial load in the right colon, particularly of obligate anaerobes, and different dietary metabolites which may lead to a higher exposure to bacteria-derived AHR ligands (Marteau et al. 2001).

When comparing the response to FICZ or CH223191 in intestinal immune cells there was no difference between health and Crohn's disease. This answers a particularly important translational question; intestinal immune cells from patients with Crohn's disease do not display any inherent defects in AHR pathway responsiveness, suggesting this pathway is not insensitive to AHR activation in Crohn's disease or indeed inactivated. However, it also suggests a strategy attempting to supra-stimulate this pathway using additional pharmacological or dietary AHR ligands might have little impact. This is of particular relevance given a number of open clinical trials are already attempting this strategy (https://clinicaltrials.gov/ct2/show/NCT04069026; and NCT03059862).

It worth nothing that a recent study did show significant clinical benefit from the natural AHR ligand, indigo naturalis, in ulcerative colitis (Naganuma et al. 2018). However, it is important to highlight that the functional studies in this chapter only included IBD patients with Crohn's disease. It would be interesting to both examine the pathway sensitivity in ulcerative colitis and consider whether the

response to treatment correlated with baseline AHR activation, particularly given the wide variation in *ex-vivo* AHR activation.

5.5.2 The AHR pathway is more responsive in non-haematopoietic cells in Crohn's disease compared to health

A key novel finding in this chapter was that non-haematopoietic cells from the intestinal mucosa are significantly more responsive to AHR ligands than immune cells (Figure 5.8). *CYP1A1* expression increased 20-fold with 10nM FICZ compared to 1.7-fold in CD45+ cells on average.

It is not clear what explains this difference. It is possible intestinal epithelial and stromal cells have a higher capacity to respond to and degrade AHR ligands. Studies in mice have shown enzymatic activity in these cells forms a functional barrier which regulates the exposure of intestinal immune cells to AHR ligands (Schiering et al. 2017) (Metidji et al. 2018).

It is also likely that different genes change in response to AHR activation in different tissues. Therefore, other genes, not *CYP1A1*, may show a greater magnitude of change in intestinal immune cells. However, work in human moDC found large magnitude changes which does not support this.

Interestingly, incubation with CH223191 did not lead a significant reduction in *CYP1A1* expression in health or Crohn's disease but did inhibit the response to FICZ. This suggests there may be differences in the relative contribution of *in-vivo* or experimental activation of these cells. This adds support to the hypothesis that differences in the ability of CD45+ and CD45- to degrade AHR ligands explains some of these observed differences but also raises the possibility of inherent differences in ligand-independent AHR activity which has been reported in other cell types, for example keratinocytes (Xiao et al. 2015).

Of particular note, when examining the response of CD45- cells from the intestinal mucosa, it was clear that unlike CD45+, there is a large difference in the response of these cells to FICZ. In health CYP1A1 expression in these cells increased 7.3-fold while in Crohn's disease it increased 35-fold with FICZ (Figure 5.7). This difference was borderline significant (p =0.054) after correcting for multiple comparisons using ANOVA. It is not known if this difference is also present in ulcerative colitis or infectious pathology, and thus a physiological feature of intestinal inflammation, or whether this finding is specific to the pathology of Crohn's disease. This remains an opportunity for future research.

It would also be interesting to compare AHR ligand concentration in the faeces of these individuals to determine if the more responsive pathway observed in Crohn's disease reflected a lower *in-vivo* activation, with consequent reduction in negative feedback responses. Different concentrations of AHR ligand are report in IBD and discussed previously (Lamas et al. 2016).

A large inter-individual variation in response was observed. This was not completely explained by baseline activation. In CD45+ cells from healthy donors, there was a weak correlation between the reduction in *CYP1A1* with CH223191 and the response to FICZ. However, this was not seen in Crohn's disease or CD45- cells. Difference in ligand exposure *in-vivo* could be measured directly using an AHR reporter cell line (www.invivogen.com/hepg2-lucia-ahr) or estimated by dietary or other environmental exposure surveys, although none of these indirect approaches have been validated.

Intrinsic factors may also underlie these differences such as AHR pathway gene polymorphisms (N Ezzeldin 2017, JZ Liu 2015) which may alter either ligand metabolism or the affinity of AHR ligand binding. Future work could explore the impact of the reported SNP in AHR associated with IBD on ligand responsiveness. Experimental variation is also likely to be a contributing factor. Collecting and processing human samples on different days introduces variability. Variable carry over of intestinal

AHR ligands from the biopsy to cell suspension (JM Natividad 2018) and variability in cell numbers recovered, particularly epithelial cells which are variable depleted by EDTA could all contribute to a Type II error.

5.5.3 AHR is highly expressed and active in sorted intestinal stromal and epithelial cells and cultured human fibroblasts

Following the unexpected finding of significant AHR activity in CD45- cells, intestinal biopsies were digested and FACS sorted into pure populations of epithelial and endothelial cells as well as a negatively selected stromal fraction (For more detail see Chapter 4). In 3 individuals enough cells were recovered to stimulate AHR with parallel control, agonist and antagonist conditions. A dynamic AHR pathway was demonstrated in epithelial cells (Figure 5.12) and resting *CYP1A1* expression was highest in stromal cells. However, attempting to purify and stimulate mucosal cell populations revealed the limit of this RT-qPCR based approach to measuring AHR activity. Too few CD31 cells were recovered to detect *CYP1A1* expression. The number of samples with Ct values above 35 also increased. Too few cells were recovered from some individuals to include these studies which could introduce a selection bias.

To examine the stromal fraction further but avoid the limitations of using primary tissue a semi-immortal fibroblast cell line was identified. This cell line also showed high levels of AHR expression (similar to sorted stromal and epithelial cells) Figure 5.13. Importantly, stimulation of these cells showed AHR is functional and leads to predictable changes in *CYP1A1* and *CYP1B1* as observed in other cell types. There are limitations to using *in-vitro* cell lines. It is not clear how well they reflect the *in-vivo* behaviour, environment and interactions (Pan C 2009). However, there are practical advantages such as homogeneity, abundance, time and cost savings which allow more complex experiments to be performed than would be possible with primary cells from mucosal biopsies.

For the first time, this study demonstrates that AHR is indeed highly expressed and functional human intestinal fibroblasts which opens the door to a variety of potential functional experiments. An important example is discussed next.

5.5.4 Human intestinal fibroblasts metabolise AHR ligands restricting AHR activation in human immune cells

Murine models suggest epithelial cells play a role in AHR ligand metabolism in the murine intestine (Schiering 2017, Metidji 2019). Degradation of AHR ligands by enzymes like CYP1A1 in these cells was shown to regulate the availability of AHR ligands to intestinal immune cells, forming a functional barrier. This influenced cell numbers and responses to inflammatory stimuli (Schiering et al. 2017).

In digested human intestinal biopsies there are a large number of CD45-CD31-EpCAM- ('triple negative') cells which include stromal fibroblasts and myofibroblasts. It had not previously been reported whether AHR expressed by these cells could perform a regulatory role similar to that identified in murine epithelial cells.

To address this question, the metabolic capacity of human intestinal fibroblasts was examined. Semi-immortal human intestinal fibroblasts were incubated with medium containing FICZ 100nM overnight in the dark. Prior incubation with fibroblasts attenuated the increase in *CYP1A1* in moDC exposed to culture media with FICZ (Figure 5.15). This did not appear to be due to the production of any toxic or AHR inhibitory factors because this reduction in stimulation was overcome by adding fresh FICZ back to the fibroblast exposed media. Instead, the reduction appears to be due to a reduction in AHR ligand concentration. The change in concentration of FICZ could be measured directly using mass-spectrometry.

The dosimetry of this process is very important. It is important to note that a reduction in stimulation was seen despite a high starting concentration of FICZ (100nM), which could have saturated the

metabolic capacity of the fibroblasts. Would a lower ligand concentration lead to an even greater effect?

It is also not clear whether these AHR ligand concentrations are relevant to the levels found in the human intestinal mucosa. The impact of this reduction could also be even more marked in the intestinal mucosa where the stromal cells from part of a continuous barrier structure rather than the cell suspension used in this experiment where ligand moves between cells. A murine model using fibroblast selective deletion or over-expression of *CYP1A1* would be useful to determine whether modifying *CYP1A1* expression in these cells also impacts ILC3 numbers and responses to inflammatory stimuli (Schiering et al. 2017). A comparison could also be made between cultured human fibroblasts and epithelial cells. Finally, it would also be interesting measure the metabolic activity of sorted *ex-vivo* stromal and epithelial cells, which would give a better estimate of metabolic activity *in-vivo*.

5.5.5 The challenge of a single gene approach

A literature review was undertaken to identify molecules produced by intestinal fibroblasts that have established effects of the immune system in order determine whether their production can be regulated by AHR (Kelly, Meade, and O'Farrelly 2019; Tardif, Ross, and Rouabhia 2004; West et al. 2017). CXCL10 and IL-1β were selected for further investigation. However, although expression of both genes was detected in the cultured fibroblasts, confirming previously published work (West et al. 2017), it did not change with AHR modulation (Figure 5.17).

It is possible that AHR only modifies the expression of these targets when their expression is stimulated by an inflammatory stimulus as has been observed in other cell types (Piccioli and Rubartelli 2013). It is also important to acknowledge that only mRNA expression not protein expression was measured. Post-transcriptional effects via non-canonical signalling could theoretically impact protein expression alone.

Using a similar strategy another gene *IL22* was examined in intestinal immune cells. Altered IL-22 production by intestinal immune cells is implicated in many murine models of colitis which show AHR deletion or reduced activation is harmful (Y Li 2011). *IL22* gene expression in CD45+ cells was not significantly affected by AHR agonists or antagonists (Figure 5.18). These agents had diverse effects in different individuals in both health and Crohn's disease and no clear relationship between *IL22* expression and AHR state was identified. This may be because other factors play a dominant role in this model such as c-Maf, Notch and other interleukins (Ouyang 2019). It is also possible that the sterile *in-vitro* culture system lacked other necessary stimuli to promote *IL22* expression. In murine models showing altered *IL22* expression in AHR null mice, cells were stimulated with the potent phorbol dibutyrate and ionomycin or model of systemic inflammation was used (Qiu et al. 2012; Veldhoen et al. 2008). In future studies IL-23 or IL-6, which stimulate RORC via STAT3 (Zenewicz 2018), could be included in the cell culture.

It is also important to acknowledge that throughout these experiments only RNA was measured which may not reflect differences in protein due to post-translational modification effects, including glycosylation and phosphorylation which are which are described for *IL22* (L Hardle 2015, https://www.genecards.org/cgi-bin/carddisp.pl?gene=IL22).

These examples highlight the limitations of selecting single genes and extrapolating murine data to human samples. To comprehensively understand the impact of AHR in particular cells an alternative approach is required without selection bias and with broad coverage. The design and outcome of such a strategy, RNASeq, is described in detail in the next chapter.

5.6 Conclusion

In this chapter I demonstrate that major non-haematopoetic cell lineages, as well as immune cells in the human intestinal mucosa, possess a functional AHR pathway. In *ex-vivo* intestinal immune cells this pathway is already nearly maximally activated in both health and Crohn's disease. In contrast *ex-*

vivo non-haematopoetic cells are highly responsive to AHR ligands, and in fact these cells are more sensitive to AHR ligands in Crohn's disease than health. A potentially regulatory role for the AHR pathway in these cells is demonstrated by the ability to metabolise AHR ligands and restrict the activation of immune cells.

Chapter 6 – Determining which genes are regulated by AHR in human intestinal immune cells

6.1 Chapter Summary

In previous chapters AHR was found to be expressed, activated and responsive to stimulation in intestinal immune cells. Murine studies suggest AHR is an attractive target for IBD therapy. However, the impact of AHR in human intestinal immune cells in not known.

In this chapter RNA-Seq is used to comprehensively determine which genes are regulated by AHR in human intestinal immune cells. This is the first study to measure AHR-dependent gene expression in ex-vivo human cells. CD45+ cells from 20 patients are isolated and incubated with FICZ, CH223191 or DMSO. After rigorous quality control 30 samples from 10 patients are sequenced and AHR-dependent gene expression is determined.

53 genes show significantly altered expression with FICZ and 166 genes show altered expression with CH223191. Gene ontology analysis is performed using a variety of tools to determine the impact of altered expression of multiple genes in the same pathway.

These approaches reveal AHR-dependent regulation of many novel genes and pathways including haematopoietic cell adhesion, antioxidant metabolism, cytoskeletal and microtubule functions and Rap 1 Signalling. A number of genes known to be altered or associated with IBD including LPXN, GPR35, GPR68 were also shown to be regulated by AHR for the first time.

This work provides many opportunities for future research and should prove a useful reference now therapies targeting AHR are beginning human studies

6.2 Introduction

RNA-Seq is a technique used to identify all the RNA molecules in a biological sample (also known as the transcriptome). RNA-Seq can measure all the mRNA transcripts in a sample or the total RNA including small RNA such as microRNA, transfer RNA and ribosomal RNA. Ribosomal RNA actually constitutes the majority of cellular RNA. RNA-Seq is described in more detail in Chapter 1 and 2.

In chapters 4 and 5 a literature search was employed to identify candidate genes of functional importance which may be regulated by AHR. However, I found evidence for these genes were influenced by AHR in the models used. It would be costly and inefficient even to increase the number of genes or conditions examined significantly.

RNA-Seq has a number of potential advantages over single gene approaches. It removes bias in gene selection, which also remains an issue for arrays. It can comprehensively detect all the genes expressed in a sample across a wide dynamic range even for rare or low-abundance transcripts.

These qualities meant RNA-Seq was selected as an approach to answer another key translational question in this project: What genes does AHR regulate in human intestinal immune cells?

The input cell type was carefully considered. In Chapter 4, I showed *AHR* expression was enriched in intestinal CD45+ cells compared to circulating immune cells. This population is inevitably mixed and heterogenous. However, there is an inherent compromise when designing RNA-Seq experiments. A purified population of cells may fall below the amount of input RNA required for sequencing. In addition, considerable cost could be spent on a cell population that turns out not to be influenced by AHR.

It would also be interesting to know if the genes regulated by AHR are different in IBD compared with health. However, an initial power calculation performed with the assistance of David Watson, *post-doctoral data scientist at QMUL*, suggested that this would not be possible without very large sample numbers. David used PROPER (PROspective Power evaluation for RNASeq) and previously published

comparisons of expression between health and Crohn's disease and AHR-dependent gene expression in cancer cell lines to show that if a 2 x 2 design were used to compare the effect of an AHR modulating drugs in health and Crohn's disease over 100 patients would be required in each group to achieve a generous false discovery rate (FDR) of 10% with only 80% power to detect differential expression.

The design of the experiment was informed by this finding. Only healthy donors were included and instead of a disease group to reduce heterogeneity and focus on the physiological role of AHR. Two opposing treatment groups were included; a control group (DMSO 0.167%), an AHR agonist (FICZ 100nM) and an AHR antagonist (CH223191 100µM). It was predicted 10 samples per group would be required to detect differential expression with 80% power and FDR below 5%.

This study design has a number of advantages: removing patients with Crohn's disease reduces heterogeneity, which increases the power to detect any AHR effect. Adding two AHR modulating agents also takes into consideration my previous findings showing the AHR pathway is already considerably activated in these cells *ex-vivo*. It maybe some effects are only revealed by incubation with an antagonist. However, including an agonist condition will allow this study to determine the if expression of genes changes in the opposite direction in the opposite AHR condition which would add strength to a claim the observed effects are directly due to AHR.

6.3 Aims

1. Determine if adequate RNA quantity and quality can be obtained from mucosal biopsies acquired at colonoscopy for RNA Sequencing
2. Determine AHR regulated gene expression in human intestinal mucosal CD45 cells
3. Characterise differentially expressed genes using gene ontology and pathway analysis tools
4. Validate differentially expressed gene candidates using qPCR

6.4 Results

6.4.1 Assessment of RNA quantity and quality

RNA was extracted using Qiagen RNEasy Micro Columns. To check adequate RNA quality and quantity, the 12 samples from the first 4 patients recruited were assessed using the NanoDrop™ and Agilent bioanalyzer by the Genome Centre, QMUL.

The RIN values for the first 6 samples assessed were all low suggesting the samples were of low quality (Table 6.1). The electrophoretic pattern suggested DNA contamination was the cause of this. The RNeasy Micro kit uses an in solution enzymatic genomic DNA digest (DNase) which is anecdotally reported to be less efficient than an on-column approach to remove genomic DNA.

RNA quantity after standard extraction (ng)	**RIN after standard extraction**	**RNA quantity after clean-up (ng)**	**RIN after clean-up**
199.2	2.6	144.8	5.9
125.3	Unrecordable	90.5	8.0
82.0	3.7	85.7	6.9
1000.2	5.7	278.3	9.4
640.2	Unrecordable	262.0	9.2
768.2	6.1	223.0	8.6

Table 6.1: Determining the quality and quantity of RNA recovered. Initial RNA recovery appeared adequate (>100ng/sample) for 5/6 samples test. However, RIN values were poor due to contamination with gDNA. After following a clean-up protocol to remove gDNA RIN values improved (>6 acceptable) but *true* RNA quantity was reduced

To remove gDNA and any other contaminants samples were re-processed using the RNA clean-up protocol provided by Qiagen (RNeasy Mini Handbook 2012). This protocol includes an on-column DNase digestion step and a number of wash steps).

The RNA quality was reassessed after completing this protocol. RIN values increased significantly to an average of 8.0 from 3.7 (Figure 6.2, Table 6.1). RIN values above 8.0 are ideal but values >6.0 are acceptable (Pereira 2017 Applications of RNA-Seq and Omic Strategies).

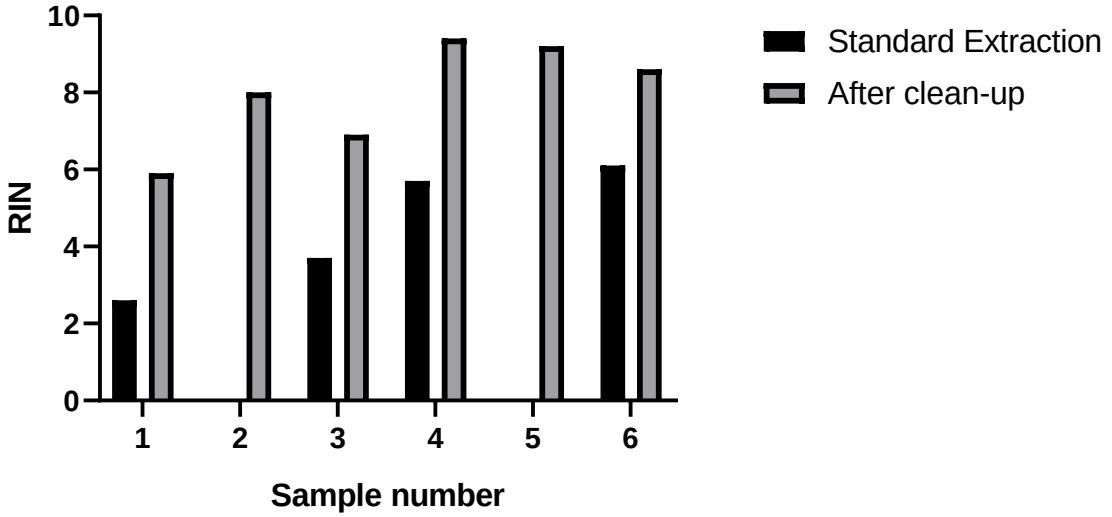

Figure 6.2 RIN values before and after RNA clean-up protocol. RIN values determined by the Agilent bioanalyzer are shown for the same samples before and after completing the Qiagen RNeasy clean-up protocol. First, the volume of the RNA samples was adjusted to 100µl by the addition of RNase free water. 350µl Buffer RLT was added and mixed. Then 250µl 100% ethanol was added and mixed by pipetting. The samples were transferred to spin columns and centrifuged for 15 seconds at 8000g. The flow through was discarded. The samples were washed with 350µl RW1. Then 80µl of the pre-prepared DNAse mix was added to each sample and left at room temperature for 15 minutes to digest genomic DNA. The samples were then washed with 350µl RW1 and then twice with 500µl RPE. After each wash the flow through was discarded. The spin column was transferred to a new collection tube and spun at full speed to dry. Finally, 30µl RNase free water was added directly to elute the RNA. The samples were then stored at -80°C. RIN values improved significantly.

The quantity of RNA in the sample was reassessed using the Nanodrop after clean-up. The reported value of RNA was lower and was only above 100ng in 4 out of 6 samples.

To enable expression to be normalised to baseline (unstimulated) expression it was necessary to have all three samples from a donor of adequate quality and quantity. After this initial assessment was performed a decision was made to collect at least 20 samples with the goal that all three samples from each condition from 10 donors could be sequenced.

6.4.2 Pilot sequencing

In total 20 patients were recruited. All biopsies were collected from a standardised location, 10cm distal to the ileocaecal valve, in the right colon. One patient was subsequently excluded from the analysis because histological assessment of his biopsies subsequently showed microscopic inflammation. A second patient was excluded because his sample developed an infection in culture. After RNA extraction and clean-up was performed quality and quantity was assessed as described above.

There was no difference in RNA quantity or quality (RIN value) between culture conditions. The local genome centre (QMUL) protocol recommended using at least 100ng per sample. However, the Illumina NGS library preparation kit protocol suggests it can be used with RNA input above 50ng. Only 6 patients had 3 samples of adequate quality at the higher threshold (100ng). However, using the threshold of 50ng would mean 11 patients had 3 adequate samples.

To ensure successful sequencing at this lower threshold I decided to sequence 3 pilot samples (using samples where there was sufficient RNA to discard 50ng).

Sample	**Duplication Rate %**	**Alignment %**	**Input RNA**
HC1	10.39	91.79	50ng
HC2	14.84	80.89	50ng
HC3	15.71	92.86	50ng
Local Control RNA	9.25	97.38	50ng
Local Control RNA	10.04	97.31	100ng

Table 6.2: Assessment of pilot RNA sequencing quality. FastQC and Bamtools were used by the QMUL Genome centre to assay the quality of sequencing data generated. The duplication rate and alignment rates were consistent and within reported rates for similar studies (Bansal 2017; Conesa et al. 2016).

Pilot sequencing was successful. The duplication rate, a measure of PCR duplicates, a common problem with low input RNA, was acceptable (average 13.6%). Similarly, alignment, a measure of how well the sequences map to the known transcriptome, was also acceptable (average 88.5%). Following this 33 (11 x 3) samples were taken forwards for sequencing. Samples from 1 patient did not produce a useable library; less than 2% of the mRNA aligned to the human transcriptome and therefore these samples were also excluded from analysis.

6.4.3 Demographics and sample properties of patients included in RNASeq

The RNA sample properties of the 10 patients taken forward to analysis are shown in Table 6.2. The demographic details and medical history are included in Appendix 11. 70% of participants were male. Median age was 53.8 years. 4 patients had incidental colonic adenomas. This reflects the population undergoing colonoscopy. 50ng RNA was used from each condition. RIN values were excellent, median 8.6 overall, with no difference between culture conditions. A median 124,000 CD45+ cells were included in each culture condition.

Patient	CD45⁺ Cells per well	RIN Value		
		DMSO	FICZ	CH223191
RNASeq 1	60200	8.8	9.0	9.0
RNASeq 2	234000	8.1	8.2	7.8
RNASeq 3	124000	8.7	8.7	8.8
RNASeq 4	Not recorded	7.6	9.1	8.6
RNASeq 5	111000	8.5	8.8	8.6
RNASeq 6	256500	8.2	8.6	8.4
RNASeq 7	90250	8.3	8.9	8.8
RNASeq 8	500000	9.4	9.2	8.6
RNASeq 9	228000	8.6	8.8	8.6
RNASeq 10	114000	8.6	8.7	8.6

Table 6.2 RNA sample characteristic of patients included in final RNASeq analysis

6.4.4 RNA-Seq initial analysis

The analysis of the RNASeq was performed with assistance from David Watson and Prof. Michael Barnes both at the QMUL Centre for Bioinformatics and is described in Chapter 2 and Appendix 2. Briefly I used the QMUL high performance computing cluster to perform a pseudo-alignment using kallisto (https://github.com/COMBINE-lab/salmon/releases) using the reference genome GRCh38.p10 (Bray et al. 2016).

Transcript-level reads were aggregated to gene-level using the tximport package giving counts per gene. Normalisation was performed using dds from the DESeq2 pipeline (Love et al., 2014). Gene counts were normalised to account for library size using DESeq2. Following the recommendations of Robinson et al. (2010), genes with fewer than 1 normalised count in at least 10 libraries were removed. This approach identified 19,061 different genes expressed in this experiment.

Diagnostic plots and dimensionality reduction techniques were then used to check for outliers. DESeq2 was used to fit expression data to negative binomial generalised linear models.

Different dimensionality reduction techniques were used to visually inspect for outliers and clustering. A principle component analysis showed three samples were extreme outliers (Figure 2.8). These three samples were removed from the subsequent analysis. Subsequent analysis showed the samples clustering by donor.

A novel program written by David (rdrr.io/github/dswatson/bioplotr/man/plot_drivers.html) was used to visualise the key drivers of variation in the dataset (Figure 6.3). It considers the relationship between the demographic and sample variables listed in Table 6.2 and the top principal components of gene expression.

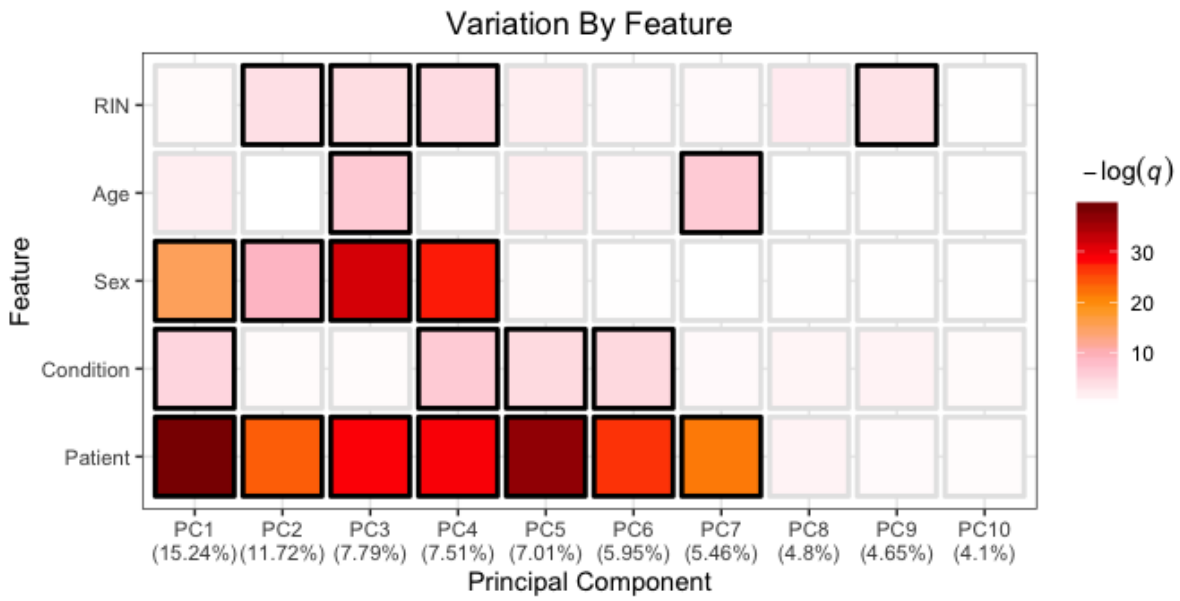

Figure 6.3 Heatmap showing drivers of variation in gene expression in this study. The patient is the greatest contributor to variation in transcriptomic data in this study.

Similar to the PCA, this plot shows by far the greatest driver of variation in gene expression was inter-individual variation between patients. After controlling for patients as a variable there were associations between the drug condition (DMSO/FICZ/CH223191) and the sex of the donor. Age was less predictive. RIN was correlated with principal components 2-4 suggesting variation in quality may have some effect on variation in recorded gene expression (Figure 6.3).

6.4.5 Differential gene expression analysis

David Watson wrote custom R code that used the results and lfcShrink functions within DESeq2 (Chapter 2) to test for differential expression between agonist and control and then antagonist and control with a target false discovery rate at ≤5%. Results are shown visually here in a volcano plot which compares $\log_2$ fold change with $-\log_{10}$ (p).

In both comparisons the genes which showed the largest fold change in expression on average were not significant after correction (q-value) due to inter-individual variation, whereas the majority of genes that were significantly different showed a small fold change below ±0.5 $\log_2$ fold change (equivalent to a 58% change) (Figure 6.4A and B). There was a symmetric distribution of significant genes with both increased and decreased gene expression with both agonist and antagonist.

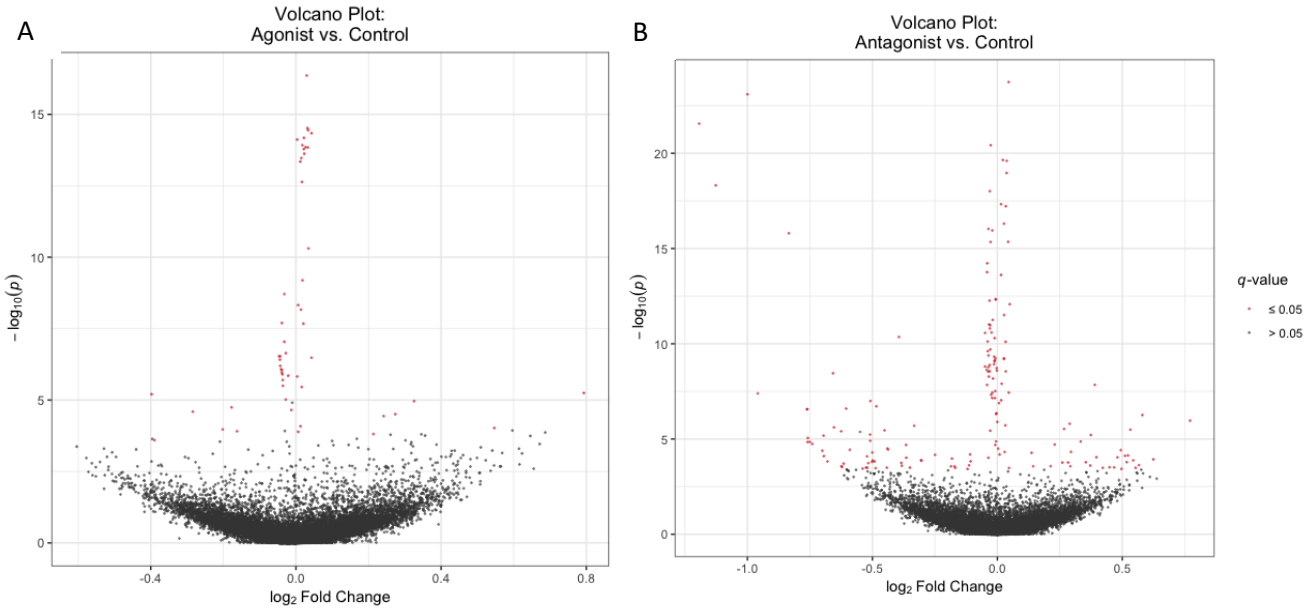

Figure 6.4 Volcano plot showing the log2 fold change in expression with agonist (A) and antagonist (B) compared to control conditions compared to -log10 (p). Adjusted significance below 0.05 (q) is show in red. There is a symmetric distribution of significant genes with both positive and negative changes observed in both conditions. Most significant changes are for genes with a small fold change.

A heat map of the top 500 gene was generated using unsupervised clustering. There was poor separation by condition, although a clustering based on treatment is partially visible in the antagonist comparison (Figure 6.5B), the dominant effect on clustering remains the donor (Figure 6.5 A & B).

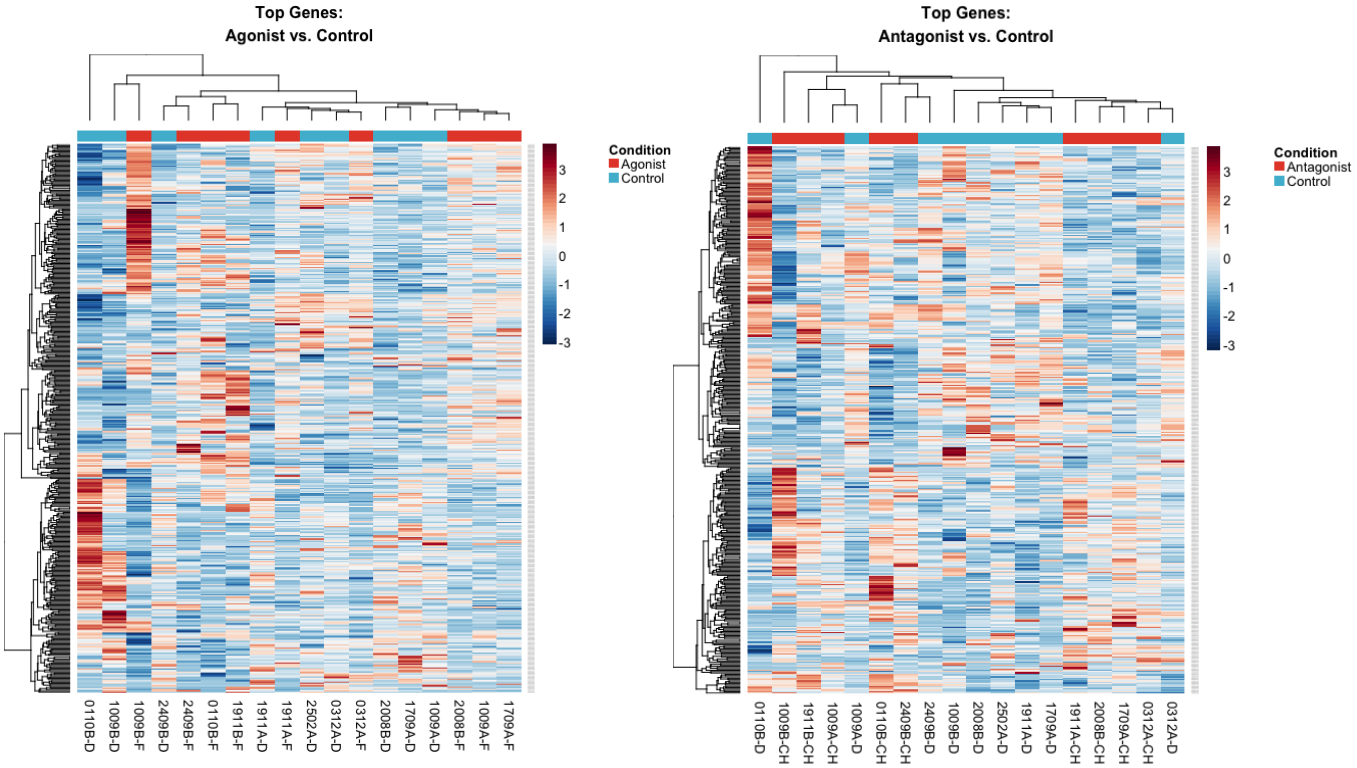

Figure 6.5 Heat map showing the log_2 fold change in expression of the 500 highest expressed genes (rows) in each sample (columns) with FICZ (agonist) (A) and CH223191 (antagonist) (B) compared to control conditions. The dominant effect on clustering is the patient. Partial clustering based on condition is seen with CH223191 (antagonist).

6.4.6 Single gene analysis of differentially expressed genes

Gene expression of 29565 different transcripts was detected in this experiment. Using false discovery rate 5% (q <0.05) 53 differentially expressed genes between the agonist (FICZ) and control condition and 166 differential expressed genes between the antagonist (CH223191) and control condition were identified (Full list in Appendix 12 and 13). Widening the FDR to 10% increased the significantly differentially expressed genes to 67 with agonist (FICZ) and 211 with the antagonist (CH223191).

I considered the function of differentially expressed genes individually and I also used pathway and gene otology tools to describe the changes seen. I searched public databases such as Genecards.org to characterise the top differentially expressed transcripts in each gene list.

Gene Code	Gene Name	Proposed Functions	Fold change with FICZ	Fold change with CH223191 (q >0.05)
GCFC2	GC-Rich Sequence DNA-Binding Factor 2	Factor that reportedly represses transcription Regulates pre-mRNA splicing	1.73	1.17
SLAMF1	Signaling Lymphocytic Activation Molecule Family Member 1	Inhibits INFγ production in T-cells Role in Tfh cells and B-cells iNKT differentiation	1.46	1.05
LPXN	Leupaxin	Haematopoietic cell adhesion, integrin mediated signalling Lower protein expression in UC (Drobin et al. 2019)	1.25	0.93
GTF2IP7	General Transcription Factor IIi Pseudogene 7	Pseudogene Aligns to many gene families (Johnson 2019 GigaScience)	1.21	0.93
ZNF610	Zinc Finger Protein 610	DNA binding protein Unknown function	1.18	1.13
SDC1	Syndecan 1	Transmembrane heparan sulfate proteoglycan SDC1 knockout mice show increased colitis with DSS (Floer 2010)	1.16	0.97
AC078927.1	Novel transcript	Novel transcript with homology to transmembrane BAX inhibitor motif-containing protein 4 Golgi protein that regulates apoptosis	1.03	1.00
ASCL5	Achaete-Scute Family BHLH Transcription Factor 5	A basic helix-loop-helix transcription factors of unknown function	1.03	1.00
AC110275.1	Combined transcript	Novel transcript with homology to HOOK3; a microtubule protein and FNTA; a farnesyltransferase	1.02	1.01
AC091849.1	Pseudogene	Possible Coiled-Coil Domain Containing 127 pseudogene	1.02	1.01

Table 6.9 The top 10 genes with the largest increase in expression with FICZ. Differentially expressed genes with q<0.05 were sorted by fold change increase in expression with FICZ compared to DMSO (control). Gene name and proposed function are shown. Differential expression in the opposite condition (with CH223191) was only seen in 4/10 genes (highlighted orange).

Although the expression of 53 genes was significantly different with FICZ, the majority of these genes only showed very small magnitude differences over the time of this experiment. 40/53 differentially expressed genes changed by less than ±3%. In isolation these changes are of unclear significance. The additive impact of small changes in multiple related genes is considered below. Interestingly, although expression of *CYP1A1* was observed to increase 1.10-fold, this increase was not statistically significant.

Another important observation is that only 3 of the top 10 genes with the largest change in expression with FICZ show opposite changes with CH223191. Nonetheless, interesting novel candidates for AHR-dependent genes are identified; Leupaxin is important in immune cell adhesion. Lower protein levels of leupaxin have recently been observed in patients with ulcerative colitis (Drobin et al. 2019).

Syndecan acts as a co-receptor to G-protein coupled receptors and is important in recruitment of leucocytes to inflamed endothelium (Voyvodic et al. 2014). GCFC2 is a factor which suppresses transcription and may serve an autoregulatory function.

Gene Code	**Gene Name**	**Proposed Functions**	**Fold change with FICZ**	**Fold change with CH223191**
FBXL5	F-box/LRR-repeat protein 5	Ubiquitin protein ligase complex Iron sensing gene	0.76	0.94
SYMPK	Symplekin	Regulation of polyadenylation and gene expression	0.76	0.86
SRXN1	Sulfiredoxin 1	Antioxidant metabolism Resolves disulphide bonds	0.82	1.06
FAM186B	Family with sequence similarity 186 member B	Unknown	0.87	0.93
RAB4B-EGLN2	Combined transcript	RAB4B is a small GTPase and EGLN2 is a hypoxia inducible factor	0.88	0.93
PTX3	Pentraxin 3	Released by cells in response to inflammatory signals, activates complement	0.89	0.89
CKMT1B	Creatine kinase, mitochondrial 1B	Ubiquitous mitochondrial creatine kinase	0.97	0.97
RPS15AP12	Pseudogene	Pseudogene for 40S ribosomal protein	0.97	0.97

AC003002.1	Novel transcript	Novel transcript in the region of zinc finger proteins ZNF547 and ZNF548	0.97	0.97
H2AFB3	H2A Histone Family Member B3	Basic histone protein	0.97	0.97

Table 6.10 The top 10 genes with the largest reduction in expression with FICZ. Differentially expressed genes with q<0.05 were sorted by fold change reduction in expression with FICZ compared to DMSO (control). Gene name and proposed function are shown. Differential expression in the opposite biological condition (with CH223191) was only seen in one gene (highlighted orange).

Only 6 of genes that showed decreased expression with FICZ, decrease more than 5% and only Sulfiredoxin 1 showed opposite changes in expression with CH223191. This may reflect the fact that the AHR pathway is already activated *in-situ*.

FBXL5 is an e3 ubiquitin ligase which showed the largest reduction in expression with FICZ. It is also predicted to contain an AHR binding site in the promotor region (GeneCard.org). Cytoplasmic AHR is also bound in a complex with E3 ubiquitin ligases which promote proteolysis (Ohatake 2009). FBXL5 may play an important role in AHR-dependent non-classical protein-protein signalling.

Sulfiredoxin 1 (SRXN1) is an important enzyme which contributes to oxidative stress resistance by reducing cysteine-sulfinic acid formation by resolving disulphide bonds (genecards.org).

Gene Code	**Gene Name**	**Proposed Functions**	**Fold change with CH223191**	**Fold change with FICZ**
TIPARP	TCDD-inducible poly ADP-ribose polymerase	TIPARP negatively regulates AHR (Matthews J 2017 Curr Op Tox)	0.44	1.31
CYP1B1	Cytochrome P450 Family 1 Subfamily B Member 1	Detoxifying enzyme involved in drug and lipid metabolism	0.46	1.13
SEMA6B	Semaphorin 6B	Semaphorins play a major role in axon guidance. May have a role in cytoskeleton organisation in APC (Gautier 2006)	0.50	1.04
GPR68	G Protein-Coupled Receptor 68 (also known as OGR1)	pH sensor. Receptor for sphingosyl-phosphorylcholine (SPC). Calcium and ERK signalling (Hutter S 2019)	0.51	1.42

		Higher expression in IBD (de Vallière et al. 2016)		
P2RY8	P2Y Receptor Family Member 8	Purine receptor Role in B-cell germinal centre formation	0.56	1.16
ASB2	Ankyrin Repeat and SOCS Box Containing 2	Role in SOCS suppression of cytokine signalling, inhibits inflammation	0.59	1.20
SLC16A6	Solute Carrier Family 16 Member 6	Catalyses the transport of many monocarboxylates such as lactate, pyruvate	0.59	1.0
F2RL3	F2R Like Thrombin Or Trypsin Receptor 3	Leucocyte rolling and adherence	0.59	1.27
HLA-DPA1	Major histocompatibility complex class II, DP α1	Antigen binding and presentation	0.59	1.22
LRG1	Leucine-rich alpha-2-glycoprotein 1	Intracellular signalling Granulocyte differentiation	0.59	0.96

Table 6.11 The top 10 genes with the largest decrease in expression with CH223191. Differentially expressed genes with q<0.05 were sorted by fold change reduction in expression with CH223191 (antagonist). Where differential expression was seen in the opposite biological condition the cell is highlighted orange. The antagonist caused a biggest magnitude change in gene expression and the opposite effect was seen with FICZ in the majority of these genes.

More genes changed significantly with the antagonist CH223191 than agonist, and the magnitude of change in expression was also greater. The two genes that showed the biggest reduction in expression were *CYP1B1*, which has already been shown in this study to be an AHR dependent gene in gut immune cells and moDC. The other gene, *TIPARP*, is an AHR ligand dependent poly ADP-ribose polymerase which has recently been shown to negatively regulate AHR (Matthews J 2017). The reduction in expression of these two AHR dependent gene confirms that these cells were indeed incubated in with an AHR inhibitory agent adding weight to the conclusion the other observed changes are directly to the same drugs impact on AHR. Adding further evidence to this argument is the observation that 8/10 genes showing the biggest fall in expression with CH223191 also show a rise in expression with FICZ. The other 2/10 genes do not change, which may reflect the prior activation I have already demonstrated previously. Interestingly, although expression of *CYP1A1* was observed to decrease 0.79-fold, again this reduction was not statistically significant or large in magnitude. Differentially expressed genes identified in this study reveal a number of novel gene targets associated with AHR with fundamental roles in the immune system.

Gene Code	Gene Name	Proposed Functions	Fold change with CH223191	Fold change with FICZ
ABCG1	ATP-binding cassette (ABC) transporters	Involved in macrophage, cholesterol and lipids transport. Regulates cellular lipid homeostasis	1.71	0.90
BBS4	Bardet-Biedl Syndrome 4	Intracellular trafficking and microtubule transport	1.54	0.93
ST3GAL6	ST3 Beta-Galactoside Alpha-2,3-Sialyltransferase 6	Sialyl transferase enzyme Important in intestinal mucus (Arike 2017 Glycobiology)	1.49	0.84
MYLIP	Myosin Regulatory Light Chain Interacting Protein	Ubiquitin ligase that ubiquinates LDL receptors in endosomes	1.48	1.05
CHD8	Chromodomain Helicase DNA Binding Protein 8	Transcriptional regulation, epigenetic regulation	1.47	1.21
PLIN2	Perilipin 2	Perilipin family members coat intracellular lipid storage droplets	1.46	0.97
PLK3	Polo like kinase 3	Serine/threonine kinase involved in cell cycle and stress response	1.45	1.29
SGK1	Serum/Glucocorticoid Regulated Kinase 1	Serine/threonine kinase regulated by glucocorticoids and insulin Also highly expressed in colonic epithelial cells	1.44	0.96
RANBP3	Ran-binding protein 3	Regulates nuclear transport	1.43	1.24
LRRC8D	Leucine-rich repeat-containing protein 8D	Part of a volume-regulated anion channel; osmotic stress	1.42	1.34

(Genecards.org)

Table 6.12 The top 10 genes with the largest increase in expression with CH223191. Differentially expressed genes with q<0.05 were sorted by fold change increase in expression. Full gene name, proposed functions and observed fold-change in expression with antagonist (CH223191) and agonist (FICZ) are shown. Where differential expression was seen in the opposite biological condition the cell is highlighted orange.

Unexpectedly, the direction of change in gene expression that occurred in cells cultured with CH223191 was balanced. There were a number of genes which showed increased expression after incubation with CH223191 including an ABC transporter, microtubule transport genes and RANBP3 which regulated nuclear transport which may counter the effects of CH223191 and favour the delivery

of more AHR ligand to the cells. Another ubiquitin ligase was identified and important genes involved in lipid transport and storage.

6.4.7 Gene ontology and pathway analysis

A number of free bioinformatic resources have been developed to provide functional grouping of large lists of genes. These tools can identify biological themes based on public efforts to annotate function. These tools can also consider interacting proteins in a pathway and highlight reported gene-disease associations.

DAVID (the database for annotation, visualization and integrated discovery) is a free online resource that includes many of these capabilities.

Gene Ontology (GO) is an open biological database managed by a large consortium. The projects aim is to annotate genes and provide tools to examine functional analysis of complex. The defined terms are organised into three domains; cellular component, molecular function and biological process.

Genes were uploaded to DAVID 6.8 and the annotations were assigned. The same tool was used to examine the Kyoto Encyclopaedia of Genes and Genomes (KEGG), another database which pools diverse bioinformatic data from genomics, metabolomics as well as analyses of disease and drug research into different groupings.

6.4.7.1 Using GO Terms to characterise differentially expressed genes with CH223191 (Antagonist)

I uploaded a list of the differentially expressed genes in the antagonist condition to DAVID and analysed these using GO. The results are shown below. The number of genes within each category and percentage of these genes out of all the genes within that category are shown.

GO Term (Cellular Component)	Gene count	%
integral component of membrane	41	29.9
plasma membrane	35	25.5
integral component of plasma membrane	15	10.9
cytoplasmic vesicle	5	3.6
NADPH oxidase complex	3	2.2
myosin complex	3	2.2

Table 6.13 GO (Cellular Component) annotation for differentially expressed genes (q<0.05) with CH223191 (antagonist). 78.8% genes had defined ontology. Membrane proteins were the most common grouping.

GO Term (Biological process)	Gene count	%
inflammatory response	8	5.8
oxidation-reduction process	8	5.8
intracellular signal transduction	7	5.1
extracellular matrix organization	5	3.6
positive regulation of catalytic activity	4	2.9
positive regulation of angiogenesis	4	2.9
respiratory burst	3	2.2
superoxide metabolic process	3	2.2
positive regulation of JAK-STAT cascade	3	2.2
positive regulation of Rho protein signal transduction	3	2.2
positive regulation of cytosolic calcium concentration involved in PLC-activating G-protein coupled signalling pathway	3	2.2
cellular response to heat	3	2.2
response to unfolded protein	3	2.2
heterophilic cell-cell adhesion via plasma membrane cell adhesion molecules	3	2.2
hemopoiesis	3	2.2
response to endoplasmic reticulum stress	3	2.2
sodium ion transport	3	2.2

Table 6.14 GO (Biological Process) annotation for differentially expressed genes (q<0.05) with CH223191 (antagonist). 75.9% genes had defined ontology. Inflammatory response genes and oxidation-reduction processes were the most common grouping. There was wide diversity with small numbers of genes in diverse gene groups.

GO Term (Molecular Function)	Gene Count	%
phosphatidylinositol binding	5	3.6
superoxide-generating NADPH oxidase activator activity	3	2.2
superoxide-generating NADPH oxidase activity	3	2.2
phosphatidylinositol-3,4-bisphosphate binding	3	2.2
phosphatidylcholine transporter activity	2	1.5
actin-dependent ATPase activity	2	1.5

Table 6.15 GO (Molecular function) annotation for differentially expressed genes (q<0.05) with CH223191 (antagonist). 73.7% genes had defined ontology. Phosphatidylinositol and lipid signalling and again, oxidation-reduction processes were the most common grouping. There was wide diversity with fewer than 3 genes in most groups.

6.4.7.2 Using GO Terms to characterise differentially expressed genes with FICZ (Agonsit)

Differentially expressed genes with FICZ were uploaded to DAVID using the same approach. The gene ontology is shown below. However, 23 genes could not be mapped to known GO terms.

GO Term (Cellular Component)	Gene count	%
focal adhesion	3	8.1
nuclear nucleosome	2	5.4
Transcriptionally active chromatin	2	5.4

Table 6.16 GO (Cellular Component) annotation for differentially expressed genes (q<0.05) with FICZ (agonsit). Only 56.8% genes had defined ontology. Few GO terms had more than 1 gene assigned.

GO Term (Biological process)	Gene count	%
Innate immune response	3	8.1
Chromatin silencing	2	5.4
Negative regulation of viral entry to cell	2	5.4

Table 6.17 GO (Biological Process) annotation for differentially expressed genes (q<0.05) with FICZ (agonist). 56.8% genes had defined ontology. A small number of immune pathway genes were highlighted but few GO terms had multiple genes assigned.

GO Term (Molecular Function)	Gene Count	%
DNA Binding	6	16.2
Protein heterodimerization activity	3	8.1

Table 6.18 GO (Molecular function) annotation for differentially expressed genes (q<0.05) with FICZ (agonist). Only 54.1% genes had defined ontology. Few GO terms had multiple genes assigned. DNA binding fits with AHR known role as a ligand activated transcription factor.

6.4.7.3 Kegg pathway analysis

I also used KEGG pathway analysis as an alternative approach to characterise the differentially expressed genes. KEGG analysis of the differentially expressed gene with CH223191 are shown in Table 6.19. A number of important inflammatory pathways and disease associations were seen.

7 genes were identified in the Rap1 signalling pathway. Rap1 is a small GTPase that functions like a cellular switch and is important for signal transduction, particularly T-cell receptor signalling to integrins to promote stable contact with antigen presenting cells (Burbach 2007 Immunological Reviews). No significant terms were identified using the differentially expressed genes with FICZ.

Kegg Term	Gene count	%
Rap 1 Signalling pathway	7	5.1%
Neuroactive ligand-receptor interaction	6	4.4%
Phagosome	5	3.6%
Aldosterone-related sodium reabsorption	3	2.2%
Staphylococcus aureus infection	3	2.2%
Viral Myocarditis	3	2.2%

Table 6.19 KEGG pathway analysis of differentially expressed genes (q<0.05) with CH223191 (antagonist). Rap1 is a small GTPase that functions like a cellular switch and is important for signal transduction particularly T-cell receptor signalling to integrins to promote stable contact with antigen presenting cells (Burbach 2007 Immunological Reviews)

6.4.7.4 Metascape

Metascape (metacape.org) is recently developed tool for analysing large data sets to determine enriched biological pathways or protein complexes within a list of differentially expressed genes (Zhou Y 2019). Unlike DAVID where each tool is used individually, Metascape combines multiple different resources to generate visual maps of protein-protein interaction and lists of enriched terms.

The q-value is a widely used statistical method in the analysis of genome-wide expression data to estimate false discovery rate. Conventionally an arbitrary threshold of 0.05 is often used which can under or overestimate the false discovery (Yinglei Lai 2017). It is common practice to adjust this value and examine differential gene expression. This is particularly useful when considering multiple genes

in a pathway may not change significantly individually but when using pathway analysis tools may still reveal information about the pathways that are changing in particular experimental conditions.

Differentially expressed gene lists were determined using the q threshold 0.05 or 0.10. 166 and 211 genes were differentially expressed with CH223191 compared to control, using the 0.05 and 0.10 threshold respectively. Lists of HUGO standard gene symbols were uploaded to Metascape for pathway analysis. Protein-protein interaction maps and terms were similar with both thresholds but more relationships were identified at the higher q threshold and these are shown below because they provide a more comprehensive picture of the pathways impacted by AHR inhibition.

The gene pathways that change with the AHR antagonist (CH223191) are shown below (Figure 6.20). The lower number of differentially expressed genes in cells incubated with FICZ limited the use of these analysis tools in that condition.

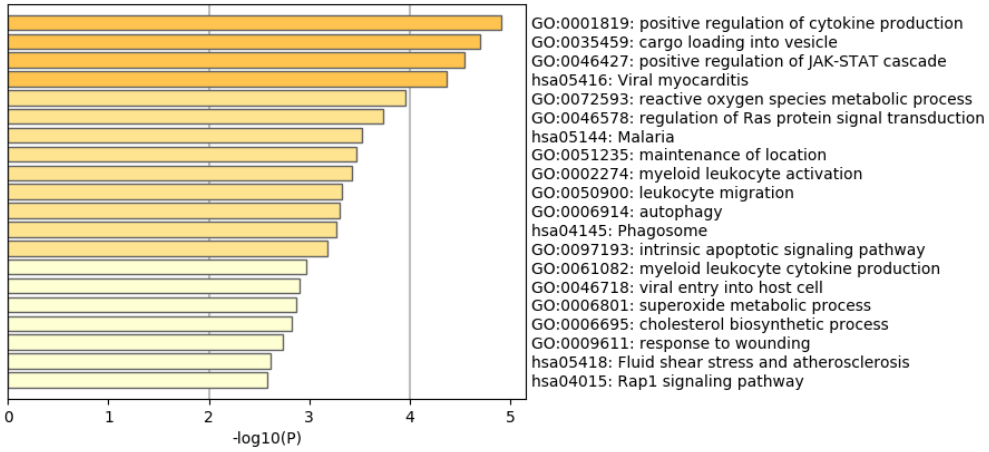

Figure 6.20 Metascape enrichment analysis of differentially expressed genes (q<0.10) with CH223191 Differentially expressed gene lists were determined using the q threshold 0.10. 211 genes were differentially expressed in the antagonist condition compared to control. Lists of HUGO standard gene symbols were uploaded to Metascape for pathway analysis. A bar graph of the top 20 clusters was generated by Metascape (metascape.org)

It was observed that antagonising AHR led to enrichment of genes which are involved in cytokine production, vesicle loading, various metabolic processes and positive regulation of JAK-STAT pathways

(Figure 6.20). This observation is consistent with observations of anti-inflammatory effects from activating AHR in murine models.

Any given gene is associated with a set of multiple gene annotation terms. If genes share similar set of those terms, it is proposed they are more likely to be involved in similar biological mechanisms. Kappa statistics quantitatively measures the degree of the agreement or overlap in annotation terms. The Kappa result ranges from 0 to 1 (McHugh 2012).

Cytoscape includes a tool called Metscape which can visualise the relationship between enriched terms that considers this overlapping annotation. Enriched annotation is rendered as a network plot where terms with Kappa similarity >0.3 is connected by edges. Terms are arbitrarily colour coded by cluster and spatially separated closer together based on similarity of terms (Figure 6.21). The spatially overlapping enriched terms showed overlap between those previously described particularly cytokine production and myeloid leucocyte activation and leukocyte migration.

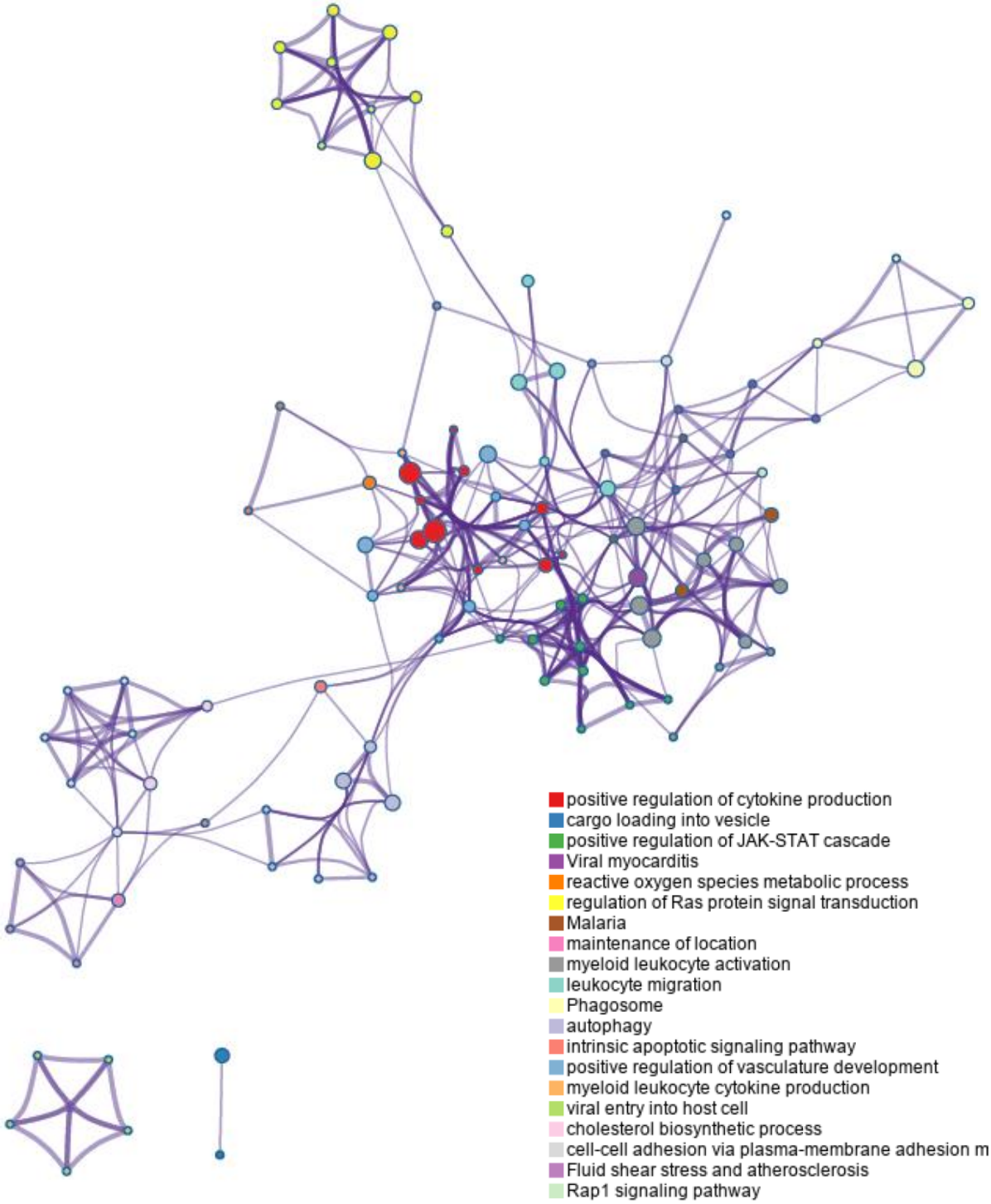

Figure 6.21 Network of enriched terms coloured by cluster ID for differentially expressed genes (q<0.10) with CH223191 Enrichment terms shown in key. A list of differentially expressed genes in the antagonist (CH223191) condition compared to control (q<0.01) was uploaded to Metascape. Network analysis was performed using Cytoscape. Terms were arbitrarily colour coded by cluster and spatially separated closer together by Kappa similarity of terms.

Protein-protein interaction enrichment analysis with Metascape can also generate a network using multiple reference databases (BioGrid, InWeb_IM and OmniPath) to determine groups of proteins that are predicted to physically interact with other members in groups, rather than using gene ontogeny alone to group terms. The Molecular Complex Detection (MCODE) algorithm is used to apply a pathway and process enrichment analysis term to the interacting proteins (Bader and Hogue 2003).

Most terms had fewer than two members. However, 4 proteins and 8 related proteins were identified in the class A/1 rhodopsin-like receptors sub-family. This sub-family is part of a large family of G-protein couple receptors and interestingly this includes the chemokine receptors CCR1-5 CCR8 and CCRL2 which are proposed therapeutic targets in IBD.

6.4.8 Single gene qPCR to validate targets identified in RNASeq

Analysis of RNASeq data uses multiple statistical procedures on very large data sets. Confidence limits are known, but limited by sample number, the magnitude of differential expression between conditions and inter-individual variability. Throughout this study q values of 5% and 10% were used to determine differentially expressed genes.

It is important to determine if these observations were false positives. Thus, the expression of selected genes was examined individually by qPCR.

Target genes were selected based on a number of characteristics. Firstly, genes that demonstrated opposite changes in expression in the agonist and antagonist conditions in the RNASeq were examined to identify genes which are more likely to be directly impacted by AHR activation. The magnitude of change was also considered. The reported function and potential translational impact of the differentially expressed genes was considered and the potential to measure a functional impact in *ex vivo* experiments. Two candidate genes were selected and are described in here (Table 6.23)

Gene code	Change with AHR agonist (FICZ)	Change with AHR antagonist (CH223191)	Description and proposed functions	Future Experimental opportunities
HLA-DPA1	0.59	1.22	Alpha subunit of HLA-DP Cell surface receptor for foreign or self-antigen Key role in antigen presentation	Flow cytometry antibody commercially available Antigen presentation co-culture models
GPR35	1.12	0.62	SNP variations associated with IBD (Jostins et al. 2012) Orphan receptor Proposed role in intestinal mucosal repair via fibronectin and ERK1 (MacKenzie et al. 2011)	Pharmacological agonists and antagonists commercially available

Table 6.23 Gene candidates identified in RNASeq for validation at single gene level Candidate genes of relevance to intestinal immune responses in IBD and bi-directional change with FICZ and CH223191 were selected from differentially expressed gene lists.

Due to time constraints and tissue availability peripheral immune cells rather than intestinal immune cells were selected to provide supporting evidence that HLA-DPA1 and GPR35 are truly regulated by AHR.

PBMC were isolated from healthy donors and stimulated with DMSO, 100nM FICZ or 100µM CH223191 for 16 hours. A longer incubation was selected to increase the likelihood of also detecting changes in protein expression, which take longer to occur than changes in mRNA. Paired samples were analysed for gene expression by RT-qPCR .

Effective *in-vitro* stimulation of AHR was confirmed by the measurement of *CYP1A1* expression which showed an average 14-fold increase in expression with FICZ and 7-fold reduction in expression with CH223191 compared to DMSO control (Figure 6.23A).

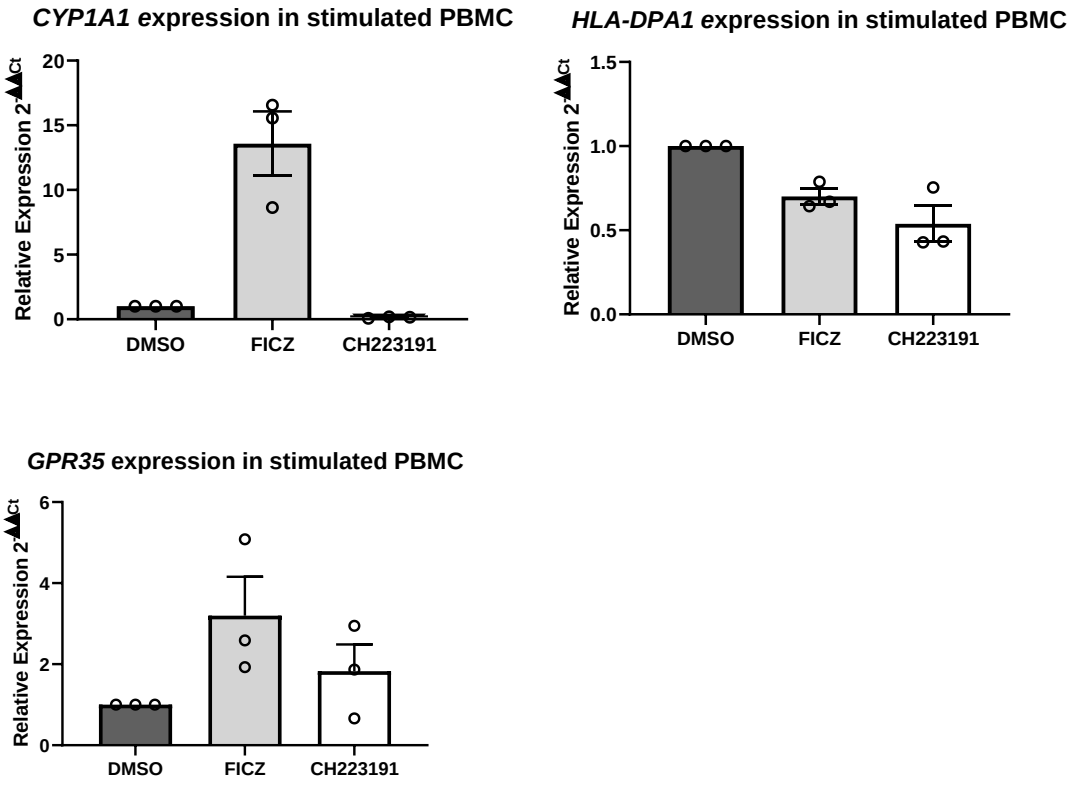

Figure 6.23 Gene expression in PBMC exposed to DMSO, FICZ of CH223191 determined by RT-qPCR (n = 3). A) *CYP1A1* Expression **B)** *HLA-DPA1* expression **C)** *GPR35* expression. *CYP1A1* expression confirmed AHR was effectively stimulated and inhibited. *GPR35* expression did appear to increase in response to FICZ but did not reduce with CH223191. *HLA-DPA1* expression was lower with both drugs.

HLA-DPA1 expression in PBMC reduced following incubation with both FICZ and CH223191 but these differences were not significant (Figure 6.23B). GPR35 expression increased with FICZ but also slightly increased with CH223191 (Figure 6.23C), these differences were also not significant albeit with 3 repeats.

To summarise, these results describe how a systematic approach was used to isolate intestinal immune cells from colonic biopsies, specifically stimulate AHR in these cells and extract RNA. The techniques used to improve RNA quality for bulk RNA sequencing are reported. Using this strategy more than 200 novel candidates for AHR-dependent genes in the human intestine are described in details along with the limitations of this approach.

6.5 Discussion

6.5.1 Quantitative and qualitative findings from this study could inform future sequencing studies in human intestinal tissues

The role of the aryl hydrocarbon receptor in the human intestinal immune system is not well described. This information is an important part of the process of developing any dietary, pharmacological or bacterial intervention designed to modify this pathway, to ensure the effects are predictable, measurable and likely to be safe.

The vast majority of previous studies of gene expression in human intestinal tissue have only examined gene expression in whole biopsies (Haberman et al. 2019; Holgersen et al. 2015; Leonard et al. 2019). These studies have allowed broad-brush comparisons of health or disease states but are undermined by the diluting effects of an enormously heterogenous mix of cell types.

To improve the power to detect differential gene expression dependent on AHR a bulk RNASeq was performed on a sorted population of intestinal immune cells freshly isolated from colonic mucosal biopsies. The anatomical location of sampling, demographic details and comorbidities were standardised in an effort to reduce inter-individual variation.

Within the last year, the availability of single cell sequencing has allowed other groups to report intestinal gene expression at single cell resolution (Martin et al. 2019). However, this technology is currently far more expensive than conventional 'bulk' RNASeq and the statistical analysis is challenging. In this chapter a successful strategy using bulk RNASeq combined with sorting and pharmacological stimulation is described.

Due to time, ethical and safety constraints only 8 colonic biopsies could be collected from each donor. After digestion and cell sorting a median 372,000 CD45+ cells were recovered from each patient and

divided into 3 culture conditions. This practical information is often difficult to find in the literature but will be invaluable for future experiment design.

The RNA recovered from these cells was initially poor quality, with RIN values below the desired level for high quality sequencing. There was no relationship between donor demographic and the quantity or quality of RNA recovered. Electrophoretic examination revealed high levels of genomic DNA contamination in most samples.

An additional on-column gDNA digestion step was performed which anecdotally has been reported to be more effective than in-solution enzymatic digestion (researchgate.net) but I can find no scientific comparison of these methods. A subsequent pilot RNA sequencing of 3 samples was successful and importantly demonstrated that none of the reagents used (DMSO, FICZ, CH223191) or any other intestinally derived compounds inhibited the PCR or sequencing process.

It is also important to note that the RNA quality (RIN value) or quantity also did not vary between experimental conditions supporting the argument that FICZ and CH223191 do not cause differential gene expression through indirect effects on cell proliferation or cell death.

However, it is worth noting that the total RNA recovered from these cells approached the limit of the Illumina sequencer. Only 10 of the 21 recruited patients had more than 50ng RNA in all three paired samples. This is also informative for future experiment design; sorting a population of cells any less abundant would not be possible without also reducing the number of parallel conditions. It also suggests, using this approach to measure gene expression in a rare intestinal immune population would not be successful.

Dimensionality reduction techniques and bespoke software analysis revealed the dominant drivers of variation in the cohort were inter-individual differences in gene expression. These differences accounted for the majority of variation between samples despite considerable efforts to ensure similar

demographic profiles, standardised anatomic location and homogenous sample processing and stimulation. This inevitably limits the power of the experiment to detect changes in gene expression due to experimental conditions alone.

However, this information can be used to generate an estimate of dispersion (a measure of the variance) which is a critical component of any power calculation for RNASeq studies (Yu, Fernandez, and Brock 2017) (bioconductor.org/packages/release/bioc/vignettes/PROPER/inst/doc/PROPER.pdf). Most experiments, including this project use previously published values from different tissues or species. These data can inform power calculations for future RNASeq studies in human intestinal immune cells.

6.5.2 Novel candidate AHR-dependent genes

The key findings of this chapter which further our understanding of AHR biology are the identification of more than 200 novel genes which are strong candidates for genes where expression is truly regulated by AHR.

This is the first time AHR dependent expression has been measured in any healthy human tissue or the intestine of any species (Lo and Matthews 2012; Nault et al. 2013; Sartor et al. 2009). Although some of the AHR regulated genes identified were similar to those seen in other species or cancer call lines (TIPARP, GPR35), many of the genes identified were different, highlighting the importance of examining gene expression in the relevant human tissue. Despite examining purified intestinal immune cells, the genes identified are highly diverse highlighting the pleiotropic effects of AHR signalling on human immune cells.

It is worth acknowledging an important limitation of bulk RNASeq is that this technique measures the average gene expression in a population of cells. Single cell RNASeq findings presented in Chapter 4

have already highlighted AHR is expressed in diverse intestinal immune cells including T-cell, myeloid antigen presenting cells and other immune cell types It is possible that very large magnitude changes in gene expression restricted to a single population of cells is not detected through this approach.

However, single cell approaches are not without drawbacks. There is more variation between similar cells and a higher level of technical noise. Transcripts expressed at a low level are also less likely to be detected but may have important cellular effects (Haque et al. 2017).

The number of significantly differentially expressed genes was far greater when comparing the antagonist condition (CH223191) with control. It is tempting to speculate why this difference was seen. The magnitude of change in gene expression with the agonist (FICZ) for each gene was also less.

It is possible this difference reflects a degree of prior AHR pathway activation as demonstrated in Chapter 5. If the pathway is already near maximally activated, then the addition of 100nM FICZ may not lead to further changes in gene expression. It is possible a higher concentration of FICZ would lead to a greater difference, however moDC incubated with 100nM FICZ showed more than 100-fold changes in CYP1A1 expression within 4 hours. That said, continuous exposure of intestinal immune cells to AHR ligands could alter the pathway sensitivity or kinetics.

It was also interesting to observe that although expression of *CYP1A1* did change in the expected direction (increasing with FICZ and decreasing with CH223191) the average magnitude of change observed was very small and non-significantly different from control conditions.

This observation highlights a limitation of this approach, given significant alterations of this gene have been seen using single gene qPCR. However, it is also possible that the genes which show the greatest magnitude change in expression vary between tissues.

The change expression of two key genes with CH223191 (*CYP1B1* and *TPARP*) provided validation that the experimental conditions in this study did create an AHR antagonised state. The expression of both

of these genes has long been reported to depend on AHR (Ma et al. 2001; Savas and Jefcoate 1994). It is possible that these two genes may serve as a better measure of AHR activity than *CYP1A1* in intestinal tissues (also considered in Chapter 5). Although in this study gene expression was only measured in CD45+ cells from the right colon. These findings may not be generalisable to other cell types or locations in the intestine.

It is also worth highlighting the time-course of this experiment, a 4 hour stimulation, was designed to optimise the detection of altered gene expression through canonical signalling while limiting alteration in gene expression through non-canonical signalling or secondary effects from the first differentially-expressed genes. It may be possible to more definitively untangle this using selective AHR modulators (Safe et al. 2018) or anti-sense DRE to inhibit AHR binding.

A variety of approaches were used to identify AHR-dependent genes. Not all the genes that showed significantly different expression necessarily directly depend on AHR signalling. Many of the genes showing the largest magnitude reduction in expression with CH223191 also showed a reciprocal increased expression with FICZ. However, genes such as SLC16A6 (Solute Carrier Family 16 Member 6) and LRG1 (Leucine-rich alpha-2-glycoprotein 1) showed a reduction in expression with CH223191 but no change with FICZ. These alterations in expression may reflect indirect effects; although the time course of the experiment was restricted to 4 hours to minimise this. It may also reflect the complexity of the AHR negative feedback mechanisms or non-canonical signalling. AHR signalling may not exert a simple binary effect on every gene it regulates.

Important novel single genes were identified by this study and warrant further review. Semaphorin 6B have a well-characterised role in guiding developing axons but have recently been recognised to

play a role in immune responses including regulation of antigen presenting cell migration and thymocyte development (Nishide and Kumanogoh 2018).

GPR68, is a pH sensor and receptor for sphingosyl-phosphorylcholine (SPC) which influences calcium and ERK signalling. This protein has also recently been reported to impact lymphocyte proliferation (Hutter S 2019). Importantly, expression of GPR68 has been shown to be higher in the colonic mucosa of patients with IBD and expression is enhanced by TNF and hypoxia (de Vallière et al. 2016).

The majority of these genes have not previously been recognised to be regulated by AHR. They are reported here together for the first time.

It was interested to observe an increase in expression of ABCG1. This protein family is known to export a variety of medication and is associated with multi-drug resistance in cancer (Iwasaki et al. 2010). It is possible the induction of this gene by CH223191 leads to the export of this chemical from cells. This finding may also present a translational opportunity; activation of AHR may lead to a reduction in this protein and therefore inhibit one mechanism of chemotherapy escape by cancerous cells.

A number of different strategies were used to group genes by ontogeny. These approaches confirmed a key role for AHR in the inflammatory response and cytokine production as previously reported. However, it did reveal a number of other important pathways which have been less studied including a role in oxidation-reduction processes and leucocyte migration.

Predicted protein interactions reveal multiple genes coding class A1 rhodopsin-like receptors were regulated by AHR. Interestingly this sub-group of G-protein coupled includes the chemokine receptors CCR1-5 CCR8 and CCRL2. These receptors play a fundamental role in regulating mucosal immunity and a number of receptors and their ligands have been targeted in clinical trials of treatment for IBD (Trivedi and Adams 2018).

A number of genes known to be altered in specific diseases also appear affected by AHR including genes altered in viral myocarditis and malaria. These present novel avenues for AHR translational research.

6.5.3 Validation and future work

It is important to validate the findings of transcriptomic studies at a single gene and protein level and this work is not complete. Peripheral immune cells were used to examine the effects of AHR manipulation on HLA-DPA1 (an important MHC Class II protein) and GPR35 (an orphan receptor implicated in IBD aetiopathogenesis). The expression of GPR35 did increase with FICZ as observed in the RNASeq study. However, this pilot study did not include sufficient samples to determine if there is any significant difference in expression of these genes. Importantly, this model is also not a perfect strategy to validate the observations in intestinal tissue, particularly given the tissue variation in AHR reported (Chapter 1). It is also important to examine the effect on AHR signalling on the relevant protein and design suitable experiments to determine if it has a significant impact on function. Fortunately, many of the proteins encoded by the genes identified in this study have widely available reagents to allow this work in the future.

ChIP-seq combines chromatin immunoprecipitation (ChIP) with DNA sequencing to identify the binding sites of DNA-associated proteins. Previously published studies have in human cancer cell lines (Lo and Matthews 2012, Yang et al. 2018) identified thousands of putative AHR, ARNT and AHRR binding sites. It would add support to the findings in this study if the genes identified were also observed AHR binding sites. In addition, comparing the binding of ARNT and AHRR at these sites may provide insights into the behaviour of inhibitory pathways and relationships with other transcription factors. Similarly, genome-wide computational analysis has identified the distribution of AHR response elements (also known as DRE) in the human genome (Dere et al 2011). Identification of AHRE

upstream of the 5’ end of the gene would add further supporting evidence that the genes identified here are AHR regulated.

6.6 Conclusion

In this chapter I present a well-powered RNA-Seq study which allows AHR-dependent gene expression to be determined in human intestinal immune cells. This is the first study to examine this pathway in *ex-vivo* human cells. Thorough RNA quality and quantitative assessment was performed prior to sequencing and highlighted a number of challenges to obtaining adequate samples for sequencing studies from human colonic biopsies.

Analysis of the RNA-Seq revealed AHR influences a wide range of cellular processes in intestinal immune cells, many of which have not previously be described; including pH sensing, cytoskeletal and microtubule arrangement, Rap 1 Signalling and rhodopsin receptors.

Importantly a number of genes associated with IBD were identified as regulated by AHR for the first time. These findings require further validation but provide many exciting opportunities for future research

Chapter 7 - Discussion and future work

The work presented in this thesis provides new understanding about aryl hydrocarbon receptor signalling in the human intestine in both health and Crohn's disease.

A number of earlier studies have provided indirect evidence the AHR pathway plays an important role in intestinal inflammation and is altered in IBD. Polymorphisms in AHR are associated with a small but significantly altered risk of IBD (Liu et al. 2015). Faecal samples from patients with IBD contain lower concentrations of AHR ligands, particularly tryptophan derivatives (Lamas et al. 2016). The impact of environmental risk factors such as dietary fibre, smoking and breastfeeding on IBD risk could be explained, at least in part, by AHR-dependent mechanisms (Ananthakrishnan et al. 2013; Gomez de Agüero et al. 2016; Parkes, Whelan, and Lindsay 2014).

Supporting evidence also comes from murine studies which have also shown that a complete loss of AHR signalling is associated with profound alteration in intestinal immune function. These changes include the loss of specific subsets of immune cells, ILC3 and γδ T-cells (Kiss et al. 2011; Li et al. 2011), and the failure to produce antimicrobial peptides such as a Reg3γ and calprotectin leading to impaired barrier function (Metidji et al. 2018). Importantly loss of AHR signalling is associated with worse outcomes in models of colitis.

However, a major limitation of these studies is that an extremely low AHR state was artificially generated either through genetic deletion of AHR or models which highly restricted AHR ligand availability through major alterations to diet, intestinal microbiota or altered AHR ligand metabolism (Kiss et al. 2011; Li et al. 2011; Schiering et al. 2017). It was not clear whether the extreme inhibition of AHR signalling used in these models is relevant to human physiology or IBD when natural and man-made AHR ligands are present almost ubiquitously in the modern environment (Denison and Nagy 2003).

This highlights the first important unanswered question in the field. Is there a difference in AHR pathway activation in IBD?

If the AHR pathway is less active in IBD then it is plausible that stimulating the pathway may have beneficial effects. However, studies to date that have examined aspects of the AHR pathway in the human intestine have not measured AHR activation or indeed whether it is responsive to stimulation (Arsenescu et al. 2011; Monteleone et al. 2011).

The second fundamental unanswered question is much broader in scope. What is the impact of AHR signalling in the human intestine both in physiological conditions and IBD? This question is of particular importance now clinical studies of pharmacological agents or diets design to impact the AHR pathway have commenced (Naganuma et al. 2018)clinicaltrials.gov/ct2/show/NCT03059862) and in fact have shown potential adverse effects including pulmonary hypertension and intestinal intussusception from what may be hyper-stimulation of the AHR pathway (Naganuma et al. 2019).

These questions could only be adequately addressed by examination of AHR in human intestinal tissue. Previous studies have shown variation in AHR regulated expression between tissue and species (Brandstätter et al. 2016; Fraccalvieri et al. 2013; Schroeder et al. 2010) meaning it is not possible to extrapolate findings from transcriptomic studies in murine models or cancer cell lines (Lo and Matthews 2012; Nault et al. 2013).

In Chapter 3 the optimal stimulation and inhibition conditions for human immune cells were determined using monocyte-derived dendritic cells as an accessible and abundant model.

The expression of cytochrome p450 genes (CYP1A1 and CYP1B1) was selected, as a candidate for a quantitative and specific measure of AHR activation based on previous transcriptomic studies. To confirm gene expression was dependent on AHR a small molecule inhibitor (CH223191) was used to demonstrate *CYP1A1* and *CYP1B1* expression could be inhibited. In addition, two different AHR ligands

were used to stimulate the moDC. Both ligands were selected on the basis of their similarity to physiological ligands (FICZ is a tryptophan derived ligand and DIM is a condensation produce of indole-3-carbinol found in Brassica vegetables (Denison and Nagy 2003)).

In Chapter 3 the expression of *CYP1A1* and *CYP1B1* in moDC was shown to be highly responsive to AHR stimulation; an increase in expression up to 295-fold was observed. Importantly this effect was inhibited by the competitive inhibitor CH223191 (Zhao et al. 2010). This effect was overcome at the highest dose of FICZ.

Further supporting evidence of this AHR specific stimulation was seen using microscopy to directly visualise the translocation of AHR protein from the cytoplasm to the nucleus following incubation with FICZ.

One limitation of this approach is that moDC are not freshly isolated human immune cells but derived by culture in-vitro. This approach was both convenient and reproducible but this cell type should be regarded as a model of an intestinal immune cell rather than identical to the observations that maybe seen in an intestinal immune cell.

For the first time in this study the relative expression of AHR was compared in circulating immune cells. Peripheral blood dendritic cells also had high *AHR* expression and protein expression compared with other peripheral blood mononuclear cells, supporting the value of the moDC model. conventional DC (cDC) showed the highest AHR expression and B-cells showed low AHR expression. This novel observation is consistent with the function of these cells; cDC play a critical role in antigen presentation and T-cell activation and are enriched at barrier sites where they are exposed to AHR ligands.

As an exploratory end-point, the impact of AHR stimulation on the expression of AHRR was examined. Unexpectedly, AHRR expression increased with blockade of AHRR and did not increase with FICZ as expected. This is counter to the prevailing view that AHRR expression increases in response to AHR

stimulation and functions as a classical negative feedback loop (Brandstätter et al. 2016). It is important to acknowledge that only AHRR mRNA was measured and future work should determine if there are also changes in protein expression. It would also be interesting to determine if deletion of the gene either from immortalised immune cell lines or using siRNA has an impact on AHR signalling.

Single gene qPCR was also used to examine expression of *CD68* and *CD1A* in moDC, which did not change with AHR stimulation. The availability and falling cost of bulk and single cell sequencing technology, even during this project has made these technologies more attractive than oligogenic approaches particularly when examining the impact of a transcription factor such as AHR.

In Chapter 4 the techniques optimised in moDC were used to examine AHR in the human intestinal mucosa. Microscopy and qPCR of freshly isolated tissue were used to demonstrate that AHR is both present and activated *in-situ* in the intestinal mucosa in both health and IBD.

Unexpectedly, the majority of AHR staining did not co-localise with CD45 and was located in the lamina propria rather than epithelial layer. This finding was not unexpected at the outset of this project; stromal cells are the predominant CD45- cell in this space and previous studies had not reported AHR expression or activity in non-haematopoietic cells in the human intestinal mucosa. However, this finding does correlates with similar observations which show AHR expression in epithelial cells in the murine intestine (Metidji et al. 2018) and human intestinal epithelial and fibroblast cell lines (Marinelli et al. 2019, Zhou et al. 2014).

The technical limitations of microscopy may explain the mismatch between observed *AHR* mRNA and protein in CD45+ cells but does not detract from this bright staining observed in CD45- cells.

In an attempt to obtain further evidence for AHR expression by the intestinal CD45- population, live cells were isolated using MACS selection. A key advantage of this methodology is the ability to select

for a particular surface marker at the bench with complete time flexibility which is important when processing freshly collected patient samples. However, it is important to highlight a number of limitations, firstly selection is only binary and the purity of selected populations is lower than other approaches such as FACS sorting. In this study around 7% cells selected as CD45- were actually CD45+ which will undermine the power to detect differences between these groups.

AHR expression and activation (inferred by *CYP1A1* expression) was detected in both health and Crohn's disease. There was a borderline significant trend towards higher *AHR* expression in Crohn's disease in CD45+ and CD45- cells supporting the findings of one previous study (Arsenescu et al. 2011). There was also significantly higher *CYP1A1* expression in CD45- cells. This provides information about AHR activity in purified live intestinal cell populations for the first time. Unexpectedly these results show that despite the majority of studies examining the impact of AHR in the intestine focusing on the impact on intestinal immune cells, there is also significant AHR activity in non-haematopoietic cells in the human intestinal mucosa.

There was considerable heterogeneity and overlap between gene expression observed in both health and Crohn's disease and in CD45+ and CD45- cells. Some of this difference may be explained by regional variation in AHR activation along the intestine, although this analysis was limited by small numbers and a lack of ileal tissue from healthy donors.

Another consistent, novel but not unexpected finding was that *AHR* expression and activation was much higher in isolated intestinal immune cells in both health and Crohn's disease than peripheral immune cells. This is likely to reflect differences in exposure to AHR ligand *in-vitro* although could also reflect differential ligand-independent activation during isolation or the presence of a different variety of immune cells with variable AHR responsiveness. A key limitation of this entire project is that AHR ligands either in stool or serum were not measured. It is plausible that differences in diet or bacterially derived ligands explain this difference in activation and may also explain some of the observed differences between patients. There are a number of methods to measure AHR ligands. An unbiased

option is to use a luciferase reporter cell line to quantify the total amount of AHR ligand in a sample agnostic to the nature of the ligand (www.invivogen.com/hepg2-lucia-ahr). Other studies have used liquid chromatography coupled to mass spectrometry to identify specific AHR ligands (Lamas et al. 2016). It would also be possible to prospectively collect dietary information or determine the composition of the microbiota using 16S sequencing to integrate these environmental variables into the analysis.

To further characterise the non-haematopoietic fraction a 4-way FACS sorter was used to separate live intestinal immune, epithelial, endothelial and stromal cells. Very few endothelial cells were recovered from each patient. This observation is useful for future experiment design; it is possible surgical specimens rather than endoscopic biopsies would yield higher cell numbers. AHR expression and activation (*CYP1A1* expression) was detected in all cell types examined. It is not possible to determine from these studies whether AHR is expressed uniformly in each of these non-haematopoietic populations, or similar to observations in CD45+ cells, expression of AHR is confined to subsets of stromal or epithelial cells within heterogeneous populations. Although these cell types are less well characterised than immune cells, a number of important sub-divisions are recognised such as Paneth cells (a secretory epithelial cells) or myofibroblasts (which support the developing epithelial crypts). In fact, murine studies have found AHR is abundantly expressed in Paneth cells (Kawajiri et al. 2009).

It is worth highlighting the observed gene expression in <10,000 CD31 cells approached the limit of detection using qPCR to measure gene expression and highlights the limits of using FACS sorting technology to further sub-divide these populations.

In this thesis, a single cell sequencing approach is presented which was used to overcome this challenge in the CD45+ fraction but could be used to characterise the stromal or epithelial cells in future experiments. Studies in murine skin fibroblasts suggests these cells do tolerate microfluidic sorting and reveal a high degree of heterogeneity (Guerrero-Juarez et al. 2019).

Chapter 4 also prsented the findings from a single cell sequencing study in colonic CD45+ cells from a healthy donor. For the first time, comprehensive picture of AHR expression in the intestinal immune compartment is revealed. Only 6.4% intestinal immune cells had detectable *AHR* expression. The sensitivity of 10X single cell sequencing is lower than single gene PCR which can theoretically detect a single transcript so some cells may not be included but nonetheless, this approach allows the cells with the highest AHR expression to be characterised.

More than 50% of AHR expressing cells were lymphocytes, although AHR expression was also seen within all other major clusters including antigen presenting cells. Consistent with previous observations AHR+ cells were more likely to express *IL22*. AHR expression was also associated with CXCL8 and MMP9, both of which show elevated expression in IBD and BATF, which is essential for Th17 cell differentiation. Importantly, genes involved in cell metabolism particularly anti-oxidant responses were associated with AHR. The growing field of immunometabolism has recently highlighted how important hypoxia and metabolic switching is to inflammation (Van Welden, Selfridge, and Hindryckx 2017). It would be fascinating to examine how AHR stimulation or blockade affected hypoxia-induced signalling in intestinal immune cells.

It is not clear if the genes identified merely define the cell type (for example as IL22 producing or a Th17 cell) or whether AHR plays a direct role in the expression of the gene and impacts on function.

It would be more straightforward to answer the first question using a comparison of gene expression in immune cells exposed to CH223191 or control. It would also be possible to determine if AHR directly impacts the production of the identified cytokines and chemokines but it may be more challenging to identify the conditions in which these proteins are produced if there is no difference in resting cells, as seen later in this project.

It is worth acknowledging that looking at separated cells in isolation inherently involves a degree of stimulation as the tissue is digested and this stimulation is not well defined and may affect different cell types variably. Importantly, this approach also cannot reveal the interactions between different

cell types which have already been shown to be critical to normal barrier function in murine models. For example, deletion of AHR in CD11c expressing cells (dendritic cells and other APCs) leads to impaired epithelial barrier repair; overexpression of Cyp1a1 in epithelial cells impairs mucosal immune responses (Chng et al. 2016; Schiering et al. 2017).

In Chapter 5, building on the observations in unstimulated intestinal immune cells, the cell culture conditions optimised in moDC were used to compare AHR pathway activity and response to stimulation in health and Crohn's disease. For the first time, these studies provided direct evidence that AHR signalling is functional in intestinal immune cells. Unexpectedly, in both health and disease the pathway was already near-maximally stimulated in CD45+ cells. Incubation with the AHR ligand FICZ only increased CYP1A1 expression 1.7-fold, far less than the ~100-fold increase observed in moDC. This may reflect a high level of stimulation *in-situ* or experimental stimulation.

This also provides evidence that the AHR pathway is neither inactive or unresponsive in Crohn's disease refuting the hypothesis that chronic inflammation in Crohn's disease is due to lower AHR activation (either through lack of ligand exposure due to altered environment, or inherent defect in AHR). It is important to contrast this with observations in murine models where worse inflammation was seen in models of colitis with loss of AHR. In Crohn's inflammation is seen despite AHR activity.

Another novel and unexpected finding was seen when examining responses in CD45- cells. These cells proved far more responsive to AHR activation than intestinal immune cells and importantly this difference was more marked in Crohn's disease. Incubation with FICZ led to a logarithmically greater increase in CYP1A1 expression in CD45- cells from patients with Crohn's compared to health. Recently published murine data has shown a role for AHR in epithelial cells. AHR directly regulates core functions of these cell including proliferation and barrier repair (Metidji et al. 2018). However, these

cells also plays second regulatory role and metabolise AHR ligands, controlling the exposure of intestinal immune cells to luminal AHR ligands (Schiering et al. 2017).

In this study *AHR* expression and activity was demonstrated in human intestinal epithelial and stromal cells. At microscopy most AHR was located in CD45- cells in the lamina propria. The dominant cell type in this compartment is intestinal fibroblasts.

To provide evidence that a similar process of ligand degradation by non-immune cells could be occurring in the human intestine, intestinal fibroblasts were examined. A functional AHR pathway was demonstrated in these cells and in fact *AHR* expression was significantly higher than seen in CD45+ cells. Crucially, when fibroblasts were incubated with FICZ these cells were able to degrade this ligand and reduce subsequent stimulation of moDC using this fibroblast-exposed media compared to unexposed FICZ.

These cells were not derived from patients and future work should explore whether cultured fibroblasts from patients with IBD also possess this capacity, and whether their ability to degrade AHR ligands is altered compared to healthy controls. This mechanism may explain why no difference in AHR responsiveness was seen in CD45+ cells but was observed in CD45- cells. It maybe there is no deficit in the ability of intestinal immune cells to respond to AHR ligands in Crohn's disease but instead there is an enhanced capacity to degrade AHR ligands by the surrounding stromal cells.

The scope of these experiments was intentionally restricted to patients with Crohn's disease. Previous studies had suggested AHR expression was more significantly altered in Crohn's disease (Monteleone et al. 2011), while other studies did not sub-divide IBD (Arsenescu et al. 2011). In addition Crohn's disease most commonly affects the ileum and colon which are exposed to a wide variety of dietary and environmental AHR ligands including those derived from the abundant colonic bacteria found in the caecum (Korecka et al. 2016; Marinelli et al. 2019).

I considered the merits of also including patients with ulcerative colitis. However, there are considerable differences between these diseases and I was concerned increasing heterogeneity by mixing two different diagnoses would undermine the power to detect any differences between health and disease. In future work, it would be valuable to examine this pathway in UC, particularly as trials of recombinant IL-22 and AHR agonists such as indigo naturalis are only recruiting patients with this condition.

These finding also highlight the value of *CYP1A1* expression as a biomarker of AHR activation for clinical studies in IBD. It would be interesting to explore whether quantification in *CYP1A1* expression could explain differences in the response to many IBD drugs particularly anti-IL23 therapies which influence IL-17 and IL-22 expression. Only 50-60% patients respond to these therapies and an association between IL-22 and response has already been reported (Feagan et al. 2018; Sands et al. 2017). AHR activation may also influence the response to treatment and measurement of *CYP1A1* expression could easily be incorporated into studies as a biomarker.

Similarly, many dietary therapies and bacterial are in development for diseases such as Crohn's disease and IBS (Cox et al. 2020; Levine et al. 2019). Usually dietary intake alone is recorded in studies. However, CYP gene expression could serve as a more accurate surrogate for AHR pathway activation and could be combined with other markers downstream of SCFA or glucose receptors to provide information about intake and host response agnostic of particular food ligand or probiotic intake. For example, it may be possible to indirectly determine intake of Brassica vegetables or tryptophanase expressing probiotics through the measurement of *CYP1A1* expression.

In this thesis a number of single genes, selected following a review of the literature were examined to determine if their expression was regulated by AHR. This strategy largely showed no difference in expression with AHR manipulation. It is possible the genes selected were not controlled by AHR or that the culture conditions were not optimal to detect a difference.

In Chapter 6 a transcriptomic approach is used to comprehensively determine AHR regulated gene expression in intestinal mucosal CD45+ cells. A careful quality control process was carried out before sequencing all the samples. This study provides clear and novel information about the quantity and quality of RNA that can be recovered from colonic biopsies using the latest technology available. It also provides useful information for future RNASeq using mucosal cells particularly the coefficient of variation (Voyvodic et al. 2014) which is a key component of power calculations (Schurch et al. 2016)and should help inform future study design.

In this study, 219 differentially expressed genes ($p<0.05$) were identified. Pathway analysis revealed a wide variety of cellular effects. This dataset will be an invaluable resource for future research in the field. For example, AHR regulates 4 genes which positively regulate angiogenesis and 5 genes important in ECM organisation as well as genes like Syndecan 1 which play a role in leucocyte adhesion to the endothelium. An impact of AHR signalling on expression of these genes could help us understand the mechanism underlying the development of pulmonary hypertension that was observed in some ulcerative colitis patients treated with the ligand indigo naturalis (Naganuma et al. 2019).

Specific genes identified such as GPR68, GPR35 and a number of chemokine receptors have been associated with IBD. It would be useful to confirm this relationship and determine the functional effect of manipulating AHR on these receptors. It may be that targeting AHR with medication allows a number of pathways implicated in IBD to be modified simultaneously.

An important limitation of these studies, but particularly relevant to this transcriptomic study is that patient genotype was not determined and AHR ligand exposure *in-vivo* was not measured. AHR polymorphisms have been reported although loss of function mutations are extremely rare even in large human genome databases (www.genesandhealth.org/). High throughput commercial assays

have now been developed to measure AHR ligands in biological samples and coupled with detailed environmental history could allow multi-omic analysis in future studies.

It is important to validate the findings of transcriptomic studies at a single gene and protein level and this work is not complete. The expression of *GPR35* did increase in PMBC exposed to FICZ as observed in the RNASeq analysis of intestinal cells. However, I plan to confirim this observation in intestinal tissue and measure protein expression using flow cytometry.

Many avenues for investigation were opened by this work and I am only sad that I will not be able to follow all of these leads myself.

Summary

In this study of AHR in the human intestine, the intestinal immune cells expressing *AHR* are characterised. The gene expression directly regulated by AHR in these cells is comprehensively described highlighting novel consequences of AHR stimulation in the human gut. Importantly, a quantitative measure of AHR activation, *CYP1A1* expression is validated and used to demonstrate that Crohn's disease is not a state of AHR inactivity. However, AHR is shown to be expressed and highly responsive in mucosal stromal cells in Crohn's disease. One potential impact of this is shown to be the regulation of AHR ligand availability.

References

Abbott, B D et al. 1999. “AhR, ARNT, and CYP1A1 MRNA Quantitation in Cultured Human Embryonic Palates Exposed to TCDD and Comparison with Mouse Palate in Vivo and in Culture.” *Toxicological Sciences* 47(1): 62–75. https://doi.org/10.1093/toxsci/47.1.62.

Agbor, Larry N et al. 2014. “Role of CYP1A1 in Modulating the Vascular and Blood Pressure Benefits of Omega-3 Polyunsaturated Fatty Acids.” *The Journal of pharmacology and experimental therapeutics* 351(3): 688–98. https://pubmed.ncbi.nlm.nih.gov/25316121.

Alenghat, Theresa et al. 2013. “Histone Deacetylase 3 Coordinates Commensal-Bacteria-Dependent Intestinal Homeostasis.” *Nature* 504(7478): 153–57. https://pubmed.ncbi.nlm.nih.gov/24185009.

Ali, Nasir, Rita de Cássia Pontello Rampazzo, Alexandre Dias Tavares Costa, and Marco Aurelio Krieger. 2017. “Current Nucleic Acid Extraction Methods and Their Implications to Point-of-Care Diagnostics.” *BioMed research international* 2017: 9306564. https://pubmed.ncbi.nlm.nih.gov/28785592.

Altmann, Daniel M. 2018. “A Nobel Prize-Worthy Pursuit: Cancer Immunology and Harnessing Immunity to Tumour Neoantigens.” *Immunology* 155(3): 283–84. https://pubmed.ncbi.nlm.nih.gov/30320408.

Amre,Devendra; D’Souza, Savio; Morgan, Kenneth. 2007. “Imbalances in Dietary Consumption of Fatty Acids, Vegetables, and Fruits Are Associated With Risk for Crohn’s Disease in Children.” *Am. J. Gastroenterol.* 102: 2016–25.

Ananthakrishnan, Ashwin N. et al. 2013. “A Prospective Study of Long-Term Intake of Dietary Fiber and Risk of Crohn’s Disease and Ulcerative Colitis.” *Gastroenterology* 145(5): 970–77. http://linkinghub.elsevier.com/retrieve/pii/S0016508513011402.

Ananthakrishnan, Ashwin N et al. 2012. “Aspirin, Nonsteroidal Anti-Inflammatory Drug Use, and Risk for Crohn Disease and Ulcerative Colitis: A Cohort Study.” *Annals of internal medicine* 156(5): 350–59. https://pubmed.ncbi.nlm.nih.gov/22393130.

Andreu-Ballester, J C et al. 2012. “Values for Aβ and Γδ T-Lymphocytes and CD4+, CD8+, and CD56+ Subsets in Healthy Adult Subjects: Assessment by Age and Gender.” *Cytometry Part B: Clinical Cytometry* 82B(4): 238–44. https://doi.org/10.1002/cyto.b.21020.

Apetoh, Lionel et al. 2010. “The Aryl Hydrocarbon Receptor Interacts with C-Maf to Promote the Differentiation of Type 1 Regulatory T Cells Induced by IL-27.” *Nature immunology* 11(9): 854–61. http://dx.doi.org/10.1038/ni.1912.

Arsenescu, Razvan et al. 2011. “Role of the Xenobiotic Receptor in Inflammatory Bowel Disease.” *Inflammatory Bowel Diseases* 17(5): 1149–62.

Bader, Gary D, and Christopher W V Hogue. 2003. “An Automated Method for Finding Molecular Complexes in Large Protein Interaction Networks.” *BMC Bioinformatics* 4(1): 2. https://doi.org/10.1186/1471-2105-4-2.

Bain, C C et al. 2013. “Resident and Pro-Inflammatory Macrophages in the Colon Represent Alternative Context-Dependent Fates of the Same Ly6Chi Monocyte Precursors.” *Mucosal immunology* 6(3): 498–510. https://pubmed.ncbi.nlm.nih.gov/22990622.

Bankoti, Jaishree et al. 2010. “Functional and Phenotypic Effects of AhR Activation in Inflammatory Dendritic Cells.” 246(406): 18–28.

Bansal, Vikas. 2017. “A Computational Method for Estimating the PCR Duplication Rate in DNA and RNA-Seq Experiments.” *BMC Bioinformatics* 18(3): 43. https://doi.org/10.1186/s12859-017-1471-9.

Barnhoorn, M C et al. 2020. “Stromal Cells in the Pathogenesis of Inflammatory Bowel Disease.” *Journal of Crohn’s and Colitis*. https://doi.org/10.1093/ecco-jcc/jjaa009.

Baron, S et al. 2005. “Environmental Risk Factors in Paediatric Inflammatory Bowel Diseases: A Population Based Case Control Study.” *Gut* 54(3): 357 LP – 363. http://gut.bmj.com/content/54/3/357.abstract.

Beedanagari, Sudheer R, Robert T Taylor, and Oliver Hankinson. 2010. “Differential Regulation of the Dioxin-Induced Cyp1a1 and Cyp1b1 Genes in Mouse Hepatoma and Fibroblast Cell Lines.” *Toxicology letters* 194(1–2): 26–33. https://www.ncbi.nlm.nih.gov/pubmed/20116417.

Behnsen, Judith et al. 2014. “The Cytokine IL-22 Promotes Pathogen Colonization by Suppressing Related Commensal Bacteria.” *Immunity* 40(2): 262–73.

Belkaid, Yasmine, and Oliver J Harrison. 2017. “Homeostatic Immunity and the Microbiota.” *Immunity* 46(4): 562–76. http://dx.doi.org/10.1016/j.immuni.2017.04.008.

Bell, Sally J et al. 2001. “Migration and Maturation of Human Colonic Dendritic Cells.” *The Journal of Immunology* 166(8): 4958 LP – 4967. http://www.jimmunol.org/content/166/8/4958.abstract.

Benson, Jenna M, and David M Shepherd. 2011. “Aryl Hydrocarbon Receptor Activation by TCDD Reduces Inflammation Associated with Crohn’s Disease.” *Toxicological sciences : an official journal of the Society of Toxicology* 120(1): 68–78. http://europepmc.org/articles/PMC3044199/?report=abstract.

Beresford, Alan P. 1993. “CYP1A1: Friend or Foe?” *Drug Metabolism Reviews* 25(4): 503–17. https://doi.org/10.3109/03602539308993984.

Berger, Joel, and David E Moller. 2002. “The Mechanisms of Action of PPARs.” *Annual Review of Medicine* 53(1): 409–35. https://doi.org/10.1146/annurev.med.53.082901.104018.

Beriou, Gaelle et al. 2009. “IL-17 Producing Human Peripheral Regulatory T Cells Retain Suppressive Function.” *Blood* 113(18): 4240–50.

Bernardo, D et al. 2018. “Human Intestinal Pro-Inflammatory CD11chighCCR2+CX3CR1+

Macrophages, but Not Their Tolerogenic CD11c−CCR2−CX3CR1− Counterparts, Are Expanded in Inflammatory Bowel Disease." *Mucosal Immunology* 11(4): 1114–26. https://doi.org/10.1038/s41385-018-0030-7.

Bernink, Jochem H et al. 2013. "Human Type 1 Innate Lymphoid Cells Accumulate in Inflamed Mucosal Tissues." *Nature Immunology* 14(3): 221–29. https://doi.org/10.1038/ni.2534.

Bernshausen, Thorsten et al. 2006. "Tissue Distribution and Function of the Aryl Hydrocarbon Receptor Repressor (AhRR) in C57BL/6 and Aryl Hydrocarbon Receptor Deficient Mice." *Archives of Toxicology* 80(4): 206–11. https://doi.org/10.1007/s00204-005-0025-5.

Bessede, Alban et al. 2014. "Aryl Hydrocarbon Receptor Control of a Disease Tolerance Defense Pathway." *Nature* 511(7508): 184–90.

Bhutia, Yangzom D, Ellappan Babu, and Vadivel Ganapathy. 2015. "Interferon- γ Induces a Tryptophan-Selective Amino Acid Transporter in Human Colonic Epithelial Cells and Mouse Dendritic Cells." *BBA - Biomembranes* 1848(2): 453–62.

Biagioli, Michele et al. 2017. "The Bile Acid Receptor GPBAR1 Regulates the M1/M2 Phenotype of Intestinal Macrophages and Activation of GPBAR1 Rescues Mice from Murine Colitis." *The Journal of Immunology* 199(2): 718 LP – 733. http://www.jimmunol.org/content/199/2/718.abstract.

Bingham, Sheila a et al. 2003. "Dietary Fibre in Food and Protection against Colorectal Cancer in the European Prospective Investigation into Cancer and Nutrition (EPIC): An Observational Study." *The Lancet* 361(9368): 1496–1501.

van den Bogaard, Ellen H et al. 2013. "Coal Tar Induces AHR-Dependent Skin Barrier Repair in Atopic Dermatitis." *The Journal of clinical investigation* 123(2): 917–27. http://www.pubmedcentral.nih.gov/articlerender.fcgi?artid=3561798&tool=pmcentrez&rendertype=abstract.

Boitano, Anthony E et al. 2010. “Aryl Hydrocarbon Receptor Antagonists Promote the Expansion of Human Hematopoietic Stem Cells.” *Science* 329(5997): 1345–48.

Bowers, Owen J et al. 2006. “2, 3, 7, 8 Tetrachlorodibenzo-P-Dioxin (TCDD) Reduces Leishmania Major Burdens in C57BL / 6 Mice.” *Am. J. Trop. Med. Hyg.* 75(4): 749–52.

Brandstätter, Olga et al. 2016. “Balancing Intestinal and Systemic Inflammation through Cell Type-Specific Expression of the Aryl Hydrocarbon Receptor Repressor.” *Scientific Reports* 6(26091): 1–17. http://dx.doi.org/10.1038/srep26091.

Bray, Nicolas L, Harold Pimentel, Páll Melsted, and Lior Pachter. 2016. “Near-Optimal Probabilistic RNA-Seq Quantification.” *Nature Biotechnology* 34(5): 525–27. https://doi.org/10.1038/nbt.3519.

de Bruyn, Magali, and Marc Ferrante. 2018. “Failure of MMP-9 Antagonists in IBD: Demonstrating the Importance of Molecular Biology and Well-Controlled Early Phase Studies.” *Journal of Crohn’s and Colitis* 12(9): 1011–13. https://doi.org/10.1093/ecco-jcc/jjy102.

Bulus, H et al. 2019. “Expression of CYP and GST in Human Normal and Colon Tumor Tissues.” *Biotechnic & Histochemistry* 94(1): 1–9. https://doi.org/10.1080/10520295.2018.1493220.

Carbo, Adria et al. 2014. “Computational Modeling of Heterogeneity and Function of CD4+ T Cells.” *Frontiers in cell and developmental biology* 2(July): 31. http://www.ncbi.nlm.nih.gov/pubmed/25364738%5Cnhttp://www.pubmedcentral.nih.gov/articlerender.fcgi?artid=PMC4207042.

Catalan-Serra, Ignacio, Arne Kristian Sandvik, Torunn Bruland, and Juan Carlos Andreu-Ballester. 2017. “Gammadelta T Cells in Crohn’s Disease: A New Player in the Disease Pathogenesis?” *Journal of Crohn’s and Colitis* 11(9): 1135–45. https://doi.org/10.1093/ecco-jcc/jjx039.

Chang, Pamela V, Liming Hao, Stefan Offermanns, and Ruslan Medzhitov. 2014. “The Microbial Metabolite Butyrate Regulates Intestinal Macrophage Function via Histone Deacetylase

Inhibition." *Proceedings of the National Academy of Sciences of the United States of America* 111(6): 2247–52. https://pubmed.ncbi.nlm.nih.gov/24390544.

Chen, Dan et al. 2009. "Association of Human Aryl Hydrocarbon Receptor Gene Polymorphisms with Risk of Lung Cancer among Cigarette Smokers in a Chinese Population." *Pharmacogenetics and Genomics* 19(1). http://journals.lww.com/jpharmacogenetics/Fulltext/2009/01000/Association_of_human_aryl_hydrocarbon_receptor.3.aspx.

Chen, Geng, Baitang Ning, and Tieliu Shi. 2019. "Single-Cell RNA-Seq Technologies and Related Computational Data Analysis ." *Frontiers in Genetics* 10: 317. https://www.frontiersin.org/article/10.3389/fgene.2019.00317.

Chen, Guangxin et al. 2018. "Sodium Butyrate Inhibits Inflammation and Maintains Epithelium Barrier Integrity in a TNBS-Induced Inflammatory Bowel Disease Mice Model." *EBioMedicine* 30: 317–25. https://pubmed.ncbi.nlm.nih.gov/29627390.

Chng, Song Hui, Parag Kundu, Carmen Dominguez-brauer, and Wei Ling Teo. 2016. "Ablating the Aryl Hydrocarbon Receptor (AhR) in CD11c + Cells Perturbs Intestinal Epithelium Development and Intestinal Immunity." *Nature Publishing Group* (October 2015): 2–3. http://dx.doi.org/10.1038/srep23820.

Cleynen, Isabelle et al. 2016. "Inherited Determinants of Crohn's Disease and Ulcerative Colitis Phenotypes: A Genetic Association Study." *The Lancet* 387(10014): 156–67. https://doi.org/10.1016/S0140-6736(15)00465-1.

Cole, Philip et al. 2003. "Dioxin and Cancer: A Critical Review." *Regulatory Toxicology and Pharmacology* 38(3): 378–88. http://www.sciencedirect.com/science/article/pii/S027323000300103X.

Conesa, Ana et al. 2016. "A Survey of Best Practices for RNA-Seq Data Analysis." *Genome biology* 17:

13. https://pubmed.ncbi.nlm.nih.gov/26813401.

Cox, Selina R et al. 2020. “Effects of Low FODMAP Diet on Symptoms, Fecal Microbiome, and Markers of Inflammation in Patients With Quiescent Inflammatory Bowel Disease in a Randomized Trial.” *Gastroenterology* 158(1): 176-188.e7. https://doi.org/10.1053/j.gastro.2019.09.024.

D’Haens, Geert et al. 2015. “A Phase II Study of Laquinimod in Crohn’s Disease.” *Gut* 64(8): 1227 LP – 1235. http://gut.bmj.com/content/64/8/1227.abstract.

Dai, Wei. 1990. “Regulation of Indoleamine Human Fibroblasts by Interferon-y Gene Expression.” 265(32): 19871–77.

Daig, R et al. 1996. “Increased Interleukin 8 Expression in the Colon Mucosa of Patients with Inflammatory Bowel Disease.” *Gut* 38(2): 216–22. https://pubmed.ncbi.nlm.nih.gov/8801200.

Dang, Eric V et al. 2011. “Control of TH 17/Treg Balance by Hypoxia-Inducible Factor 1.” *Cell* 146(5): 772–84.

Darcy, Christabelle J et al. 2011. “An Observational Cohort Study of the Kynurenine to Tryptophan Ratio in Sepsis: Association with Impaired Immune and Microvascular Function.” *PLOS ONE* 6(6): e21185. https://doi.org/10.1371/journal.pone.0021185.

Denison, Michael S., and Scott R. Nagy. 2003. “Activation of the Arylhydrocarbon Receptor by Structurally Diverse Exogenous and Endogenous Chemicals.” *Annual Review of Pharmacology and Toxicology* 43(1): 309–34. http://www.annualreviews.org/doi/abs/10.1146/annurev.pharmtox.43.100901.135828.

Díaz-Díaz, Carol J et al. 2016. “The Aryl Hydrocarbon Receptor Is a Repressor of Inflammation-Associated Colorectal Tumorigenesis in Mouse.” *Annals of surgery* 264(3): 429–36. http://www.ncbi.nlm.nih.gov/pubmed/27433903.

Drobin, Kimi et al. 2019. “Targeted Analysis of Serum Proteins Encoded at Known Inflammatory Bowel Disease Risk Loci.” *Inflammatory bowel diseases* 25(2): 306–16. https://pubmed.ncbi.nlm.nih.gov/30358838.

Duckworth, Carrie A et al. 2013. “Progastrin-Induced Secretion of Insulin-like Growth Factor 2 from Colonic Myofibroblasts Stimulates Colonic Epithelial Proliferation in Mice.” *Gastroenterology* 145(1): 197-208.e3. https://pubmed.ncbi.nlm.nih.gov/23523669.

Dudakov, Jarrod A et al. 2015. “Interleukin-22: Immunobiology and Pathology.” *Annual Review of Immunology* 21(33): 747–85.

van den Elsen, Lieke W J, Johan Garssen, Remy Burcelin, and Valerie Verhasselt. 2019. “Shaping the Gut Microbiota by Breastfeeding: The Gateway to Allergy Prevention?” *Frontiers in pediatrics* 7: 47. https://pubmed.ncbi.nlm.nih.gov/30873394.

Eltom, S E, M C Larsen, and C R Jefcoate. 1998. “Expression of CYP1B1 but Not CYP1A1 by Primary Cultured Human Mammary Stromal Fibroblasts Constitutively and in Response to Dioxin Exposure: Role of the Ah Receptor.” *Carcinogenesis* 19(8): 1437–44. https://doi.org/10.1093/carcin/19.8.1437.

Facchin, Sonia et al. 2020. “Microbiota Changes Induced by Microencapsulated Sodium Butyrate in Patients with Inflammatory Bowel Disease.” *Neurogastroenterology & Motility* n/a(n/a): e13914. https://doi.org/10.1111/nmo.13914.

Fallarino, Francesca et al. 2006. “The Combined Effects of Trypptophan Starvation and Tryptophan Catabolites Down-Regulate T Cell Receptor -Chain and Induce a Regulatory Phenotype in Naive T Cells.” *J. Immunol* 176: 6752–61.

Feagan, Brian G et al. 2018. “Risankizumab in Patients with Moderate to Severe Crohn’s Disease: An Open-Label Extension Study.” *The Lancet Gastroenterology & Hepatology* 3(10): 671–80. https://doi.org/10.1016/S2468-1253(18)30233-4.

Fernandez-Salguero, P et al. 1995. “Immune System Impairment and Hepatic Fibrosis in Mice Lacking the Dioxin-Binding Ah Receptor.” *Science (New York, N.Y.)* 268(5211): 722–26.

Fraccalvieri, Domenico et al. 2013. “Comparative Analysis of Homology Models of the AH Receptor Ligand Binding Domain: Verification of Structure-Function Predictions by Site-Directed Mutagenesis of a Nonfunctional Receptor.” *Biochemistry* 52(4): 714–25. https://pubmed.ncbi.nlm.nih.gov/23286227.

Franchini, Anthony M et al. 2019. “Genome-Wide Transcriptional Analysis Reveals Novel AhR Targets That Regulate Dendritic Cell Function during Influenza A Virus Infection.” *ImmunoHorizons* 3(6): 219–35. https://pubmed.ncbi.nlm.nih.gov/31356168.

Franzosa, Eric A et al. 2019. “Gut Microbiome Structure and Metabolic Activity in Inflammatory Bowel Disease.” *Nature Microbiology* 4(2): 293–305. https://doi.org/10.1038/s41564-018-0306-4.

Fritsche, Ellen et al. 2007. “Lightening up the UV Response by Identification of the Arylhydrocarbon Receptor as a Cytoplasmatic Target for Ultraviolet B Radiation.” *Proceedings of the National Academy of Sciences* 104(21): 8851 LP – 8856. http://www.pnas.org/content/104/21/8851.abstract.

Fujino, S et al. 2003. “Increased Expression of Interleukin 17 in Inflammatory Bowel Disease.” *Gut* 52(1): 65–70. https://pubmed.ncbi.nlm.nih.gov/12477762.

Furumatsu, Keisuke et al. 2011. “A Role of the Aryl Hydrocarbon Receptor in Attenuation of Colitis.” *Digestive Diseases and Sciences* 56(9): 2532–44. http://link.springer.com/10.1007/s10620-011-1643-9.

Gagliani, Nicola et al. 2015. “Th17 Cells Transdifferentiate into Regulatory T Cells during Resolution of Inflammation.” *Nature* 523(7559): 221–25.

Gaitanis, Georgios et al. 2012. “The Malassezia Genus in Skin and Systemic Diseases.” *Clinical*

Microbiology Reviews 25(1): 106–41.

Gargaro, M, M Pirro, R Romani, and T Zelante. 2016. “Aryl Hydrocarbon Receptor – Dependent Pathways in Immune Regulation.” *American Journal of Transplantation* (7): 2270–76.

Geginat, Jens et al. 2014. “Plasticity of Human CD4 T Cell Subsets.” *Frontiers in Immunology* 5(December): 1–10.

Giani Tagliabue, Sara et al. 2019. “Modeling the Binding of Diverse Ligands within the Ah Receptor Ligand Binding Domain.” *Scientific Reports* 9(1): 10693. https://doi.org/10.1038/s41598-019-47138-z.

Gisbert, Javier P, and María Chaparro. 2019. “Predictors of Primary Response to Biologic Treatment [Anti-TNF, Vedolizumab, and Ustekinumab] in Patients With Inflammatory Bowel Disease: From Basic Science to Clinical Practice.” *Journal of Crohn’s and Colitis*. https://doi.org/10.1093/ecco-jcc/jjz195.

Go, Ryeo-Eun, Kyung-A Hwang, and Kyung-Chul Choi. 2015. “Cytochrome P450 1 Family and Cancers.” *The Journal of Steroid Biochemistry and Molecular Biology* 147: 24–30. http://www.sciencedirect.com/science/article/pii/S0960076014002581.

Golan, David, Eric S Lander, and Saharon Rosset. 2014. “Measuring Missing Heritability: Inferring the Contribution of Common Variants.” *Proceedings of the National Academy of Sciences* 111(49): E5272 LP-E5281. http://www.pnas.org/content/111/49/E5272.abstract.

Gomez de Agüero, Mercedes et al. 2016. “The Maternal Microbiota Drives Early Postnatal Innate Immune Development.” *Science* 351(6279): 1297–1302.

Gonzalez, Frank J, and Pedro Fernandez-salguero. 1998. “THE ARYL HYDROCARBON RECEPTOR Studies Using the AHR-Null Mice.” *Pharmacology* 26(12): 1194–98.

Gophna, Uri et al. 2006. “Differences between Tissue-Associated Intestinal Microfloras of Patients

with Crohn's Disease and Ulcerative Colitis." *Journal of clinical microbiology* 44(11): 4136–41. https://pubmed.ncbi.nlm.nih.gov/16988016.

Gordon, Hannah, Frederik Trier Moller, Vibeke Andersen, and Marcus Harbord. 2015. "Heritability in Inflammatory Bowel Disease: From the First Twin Study to Genome-Wide Association Studies." *Inflammatory bowel diseases* 21(6): 1428–34. https://pubmed.ncbi.nlm.nih.gov/25895112.

Goto, Yoshiyuki et al. 2014. "Innate Lymphoid Cells Regulate Intestinal Epithelial Cell Glycosylation." *Science* 345(6202): 1–24.

Goudot, Christel et al. 2017. "Aryl Hydrocarbon Receptor Controls Monocyte Differentiation into Dendritic Cells versus Macrophages." *Immunity* 47(3): 582-596.e6. https://doi.org/10.1016/j.immuni.2017.08.016.

Gradin, K, A Wilhelmsson, L Poellinger, and A Berghard. 1993. "Nonresponsiveness of Normal Human Fibroblasts to Dioxin Correlates with the Presence of a Constitutive Xenobiotic Response Element-Binding Factor." *Journal of Biological Chemistry* 268(6): 4061–68. http://www.jbc.org/content/268/6/4061.abstract.

Graham, Daniel B, and Ramnik J Xavier. 2020. "Pathway Paradigms Revealed from the Genetics of Inflammatory Bowel Disease." *Nature* 578(7796): 527–39. https://doi.org/10.1038/s41586-020-2025-2.

Guerrero-Juarez, Christian F et al. 2019. "Single-Cell Analysis Reveals Fibroblast Heterogeneity and Myeloid-Derived Adipocyte Progenitors in Murine Skin Wounds." *Nature Communications* 10(1): 650. https://doi.org/10.1038/s41467-018-08247-x.

Guilliams, Martin, and Lianne van de Laar. 2015. "A Hitchhiker's Guide to Myeloid Cell Subsets: Practical Implementation of a Novel Mononuclear Phagocyte Classification System." *Frontiers in immunology* 6: 406. https://pubmed.ncbi.nlm.nih.gov/26322042.

Gury-BenAri, Meital et al. 2016. "The Spectrum and Regulatory Landscape of Intestinal Innate

Lymphoid Cells Are Shaped by the Microbiome." *Cell* 166(5): 1231-1246.e13.

Gutiérrez-Vázquez, Cristina, and Francisco J Quintana. 2018. "Regulation of the Immune Response by the Aryl Hydrocarbon Receptor." *Immunity* 48(1): 19–33. https://doi.org/10.1016/j.immuni.2017.12.012.

Haberman, Yael et al. 2019. "Ulcerative Colitis Mucosal Transcriptomes Reveal Mitochondriopathy and Personalized Mechanisms Underlying Disease Severity and Treatment Response." *Nature communications* 10(1): 38. https://pubmed.ncbi.nlm.nih.gov/30604764.

Hahn, Mark E et al. 2017. "Diversity as Opportunity: Insights from 600 Million Years of AHR Evolution." *Current Opinion in Toxicology*: 58–71.

Halfvarson, Jonas et al. 2003. "Inflammatory Bowel Disease in a Swedish Twin Cohort: A Long-Term Follow-up of Concordance and Clinical Characteristics." *Gastroenterology* 124(7): 1767–73. https://doi.org/10.1016/S0016-5085(03)00385-8.

Haque, Ashraful, Jessica Engel, Sarah A Teichmann, and Tapio Lönnberg. 2017. "A Practical Guide to Single-Cell RNA-Sequencing for Biomedical Research and Clinical Applications." *Genome Medicine* 9(1): 75. https://doi.org/10.1186/s13073-017-0467-4.

Harbord, Marcus et al. 2016. "ECCO Guideline / Consensus Paper The First European Evidence-Based Consensus on Extra-Intestinal Manifestations in Inflammatory Bowel Disease." : 239–54.

Harusato, Akihito, Duke Geem, and Timothy L Denning. 2016. "Macrophage Isolation from the Mouse Small and Large Intestine." *Methods in molecular biology (Clifton, N.J.)* 1422: 171–80. https://www.ncbi.nlm.nih.gov/pubmed/27246032.

Hayes, Mark D et al. 2014. "The Aryl Hydrocarbon Receptor: Differential Contribution to T Helper 17 and T Cytotoxic 17 Cell Development." *PloS one* 9(9): e106955. http://www.pubmedcentral.nih.gov/articlerender.fcgi?artid=4159274&tool=pmcentrez&rendertype=abstract.

Hedin, C. R. et al. 2014. “Altered Intestinal Microbiota and Blood T Cell Phenotype Are Shared by Patients with Crohn’s Disease and Their Unaffected Siblings.” *Gut* 63(10): 1578–86. http://gut.bmj.com/cgi/doi/10.1136/gutjnl-2013-306226.

Hedin, Charlotte, Kevin Whelan, and James O Lindsay. 2007. “Evidence for the Use of Probiotics and Prebiotics in Inflammatory Bowel Disease: A Review of Clinical Trials.” *Proceedings of the Nutrition Society* 66(3): 307–15. https://www.cambridge.org/core/article/evidence-for-the-use-of-probiotics-and-prebiotics-in-inflammatory-bowel-disease-a-review-of-clinical-trials/19DC1E6B2BDBCDA420DB56CA72B39866.

Hernandez, Ana et al. 2007. “Inhibition of NF-Kappa B during Human Dendritic Cell Differentiation Generates Anergy and Regulatory T-Cell Activity for One but Not Two Human Leukocyte Antigen DR Mismatches.” *Human immunology* 68(9): 715–29. http://www.sciencedirect.com/science/article/pii/S0198885907001322.

Hill, Jonathan A et al. 2007. “Foxp3 Transcription-Factor-Dependent and -Independent Regulation of the Regulatory T Cell Transcriptional Signature.” *Immunity* 27: 786–800.

Ho, Nhan T et al. 2018. “Meta-Analysis of Effects of Exclusive Breastfeeding on Infant Gut Microbiota across Populations.” *Nature communications* 9(1): 4169. https://pubmed.ncbi.nlm.nih.gov/30301893.

Holgersen, Kristine et al. 2015. “High-Resolution Gene Expression Profiling Using RNA Sequencing in Patients With Inflammatory Bowel Disease and in Mouse Models of Colitis.” *Journal of Crohn’s and Colitis* 9(6): 492–506. https://doi.org/10.1093/ecco-jcc/jjv050.

Hoorweg, Kerim et al. 2012. “Functional Differences between Human NKp44(-) and NKp44(+) RORC(+) Innate Lymphoid Cells.” *Frontiers in immunology* 3: 72. https://pubmed.ncbi.nlm.nih.gov/22566953.

Hou, Jason K, Bincy Abraham, and Hashem El-serag. 2011. “Dietary Intake and Risk of Developing

Inflammatory Bowel Disease : A Systematic Review of the Literature." *The American Journal of Gastroenterology* 106(4): 563–73. http://dx.doi.org/10.1038/ajg.2011.44.

Huang, Zhen et al. 2013. "3,3-Diindolylmethane Alleviates Oxazolone-Induced Colitis through Th2/Th17 Suppression and Treg Induction." *Molecular Immunology* 53(4): 335–44. http://dx.doi.org/10.1016/j.molimm.2012.09.007.

Hugot, Jean-Pierre et al. 2001. "Association of NOD2 Leucine-Rich Repeat Variants with Susceptibility to Crohn's Disease." *Nature* 411(6837): 599–603. https://doi.org/10.1038/35079107.

IARC Handbook of Cancer Prevention Volume 9. 2004. "Cruciferous Vegetables." 9.

Ikuta, Togo et al. 2013. "ASC-Associated Inflammation Promotes Cecal Tumorigenesis in Aryl Hydrocarbon Receptor-Deficient Mice." *Carcinogenesis* 34(7): 1620–27.

Inouye, Kuniyo, Raku Shinkyo, Teisuke Takita, Miho Ohta, and Sakaki Toshiyuki. 2002. "Metabolism of Polychlorinated Dibenzo-p-Dioxins (PCDDs) by Human Cytochrome P450-Dependent Monooxygenase Systems." *J. Agric. Food Chem*: 5496–5502.

Inouye, Kuniyo, Raku Shinkyo, Teisuke Takita, Miho Ohta, and Toshiyuki Sakaki. 2002. "Metabolism of Polychlorinated Dibenzo-p-Dioxins (PCDDs) by Human Cytochrome P450-Dependent Monooxygenase Systems." *Journal of Agricultural and Food Chemistry* 50(19): 5496–5502. https://doi.org/10.1021/jf020415z.

Ishida, Takumi et al. 2005. "2,3,7,8-Tetrachlorodibenzo-p-Dioxin-Induced Change in Intestinal Function and Pathology: Evidence for the Involvement of Arylhydrocarbon Receptor-Mediated Alteration of Glucose Transportation." *Toxicology and Applied Pharmacology* 205(1): 89–97. http://www.sciencedirect.com/science/article/pii/S0041008X04004375.

Ito, Go et al. 2013. "Lineage-Specific Expression of Bestrophin-2 and Bestrophin-4 in Human Intestinal Epithelial Cells." *PLOS ONE* 8(11): e79693. https://doi.org/10.1371/journal.pone.0079693.

Iwasaki, Hironori et al. 2010. “Down-Regulation of Lipids Transporter ABCA1 Increases the Cytotoxicity of Nitidine.” *Cancer Chemotherapy and Pharmacology* 66(5): 953–59. https://doi.org/10.1007/s00280-010-1247-7.

James Lind Alliance. 2015. *IBD Research Priorities from the IBD Priority Setting Partnership 2015*. http://www.jla.nihr.ac.uk/__data/assets/pdf_file/0003/158016/IBD-PSP-Top-10-with-detail.pdf.

Jeffers, Michael et al. 2002. “A Novel Human Fibroblast Growth Factor Treats Experimental Intestinal Inflammation.” *Gastroenterology* 123(4): 1151–62. https://doi.org/10.1053/gast.2002.36041.

Jeuken, Anoek et al. 2003. “Activation of the Ah Receptor by Extracts of Dietary Herbal Supplements , Vegetables , and Fruits.” *J. Agric. Food Chem* (51): 5478–87.

Ji, Tao et al. 2015. “Aryl Hydrocarbon Receptor Activation Down-Regulates IL-7 and Reduces Inflammation in a Mouse Model of DSS-Induced Colitis.” *Digestive Diseases and Sciences* 60(7): 1958–66. https://doi.org/10.1007/s10620-015-3632-x.

Jiang, Wenyu et al. 2014. “Elevated Levels of Th17 Cells and Th17-Related Cytokines Are Associated with Disease Activity in Patients with Inflammatory Bowel Disease.” *Inflammation Research* 63(11): 943–50. https://doi.org/10.1007/s00011-014-0768-7.

Jin, Un-Ho et al. 2014. “Microbiome-Derived Tryptophan Metabolites and Their Aryl Hydrocarbon Receptor-Dependent Agonist and Antagonist Activities.” *Molecular Pharmacology* 85(May): 777–88. http://dx.doi.org/10.1124/mol.113.091165.

Jones, Gareth-Rhys et al. 2019. “IBD Prevalence in Lothian, Scotland, Derived by Capture–Recapture Methodology.” *Gut* 68(11): 1953 LP – 1960. http://gut.bmj.com/content/68/11/1953.abstract.

de Jong, D J et al. 2003. “Genetic Polymorphisms in Biotransformation Enzymes in Crohn’s Disease: Association with Microsomal Epoxide Hydrolase.” *Gut* 52(4): 547–51. http://www.pubmedcentral.nih.gov/articlerender.fcgi?artid=1773587&tool=pmcentrez&rende

rtype=abstract.

de Jonge, Hendrik J M et al. 2007. “Evidence Based Selection of Housekeeping Genes.” *PLOS ONE* 2(9): e898. https://doi.org/10.1371/journal.pone.0000898.

Jostins, Luke et al. 2012. “Host-Microbe Interactions Have Shaped the Genetic Architecture of Inflammatory Bowel Disease.” *Nature* 491(7422): 119–24.

Julliard, Walker et al. 2017. “Amelioration of Clostridium Difficile Infection in Mice by Dietary Supplementation With Indole-3-Carbinol.” *Annals of surgery* 265(6): 1183–91. https://www.ncbi.nlm.nih.gov/pubmed/27280500.

Kadivar, Mohammad, Julia Petersson, Lena Svensson, and Jan Marsal. 2016. “CD8αβ+ Γδ T Cells: A Novel T Cell Subset with a Potential Role in Inflammatory Bowel Disease.” *Journal of immunology (Baltimore, Md. : 1950)* 197(12): 4584–92. http://europepmc.org/abstract/MED/27849165.

Kadow, Stephanie et al. 2011. “Aryl Hydrocarbon Receptor Is Critical for Homeostasis of Invariant Γδ T Cells in the Murine Epidermis.” *The Journal of Immunology* 187(6): 3104 LP – 3110. http://www.jimmunol.org/content/187/6/3104.abstract.

Kamada, Nobuhiko, and Gabriel Núñez. 2013. “Role of the Gut Microbiota in the Development and Function of Lymphoid Cells.” *Journal of immunology (Baltimore, Md. : 1950)* 190(4): 1389–95. https://pubmed.ncbi.nlm.nih.gov/23378581.

Kaplan, Gilaad G, and Siew C Ng. 2017. “Understanding and Preventing the Global Increase of Inflammatory Bowel Disease.” *Gastroenterology* 152(2): 313-321.e2. http://dx.doi.org/10.1053/j.gastro.2016.10.020.

Kawajiri, Kaname et al. 2009. “Aryl Hydrocarbon Receptor Suppresses Intestinal Carcinogenesis in ApcMin/+ Mice with Natural Ligands.” *Proceedings of the National Academy of Sciences of the United States of America* 106(32): 13481–86.

Kawamoto, Shimpei et al. 2014. “Foxp3^{+} T Cells Regulate Immunoglobulin A Selection and Facilitate Diversification of Bacterial Species Responsible for Immune Homeostasis.” *Immunity* 41(1): 152–65. https://doi.org/10.1016/j.immuni.2014.05.016.

Kaye, Joel et al. 2016. “Laquinimod Arrests Experimental Autoimmune Encephalomyelitis by Activating the Aryl Hydrocarbon Receptor.” *Proceedings of the National Academy of Sciences of the United States of America* 113.

Kelly, Paul, Kieran G Meade, and Cliona O’Farrelly. 2019. “Non-Canonical Inflammasome-Mediated IL-1β Production by Primary Endometrial Epithelial and Stromal Fibroblast Cells Is NLRP3 and Caspase-4 Dependent .” *Frontiers in Immunology* 10: 102. https://www.frontiersin.org/article/10.3389/fimmu.2019.00102.

Kerger, Brent et al. 2006. “Age- and Concentration-Dependent Elimination Half-Life of 2,3,7,8-Tetrachlorodibenzo-p-Dioxin in Seveso Children.” *Environmental Health Perspectives* 1596(10): 1596–1602.

Kimura, Akihiro et al. 2009. “Aryl Hydrocarbon Receptor in Combination with Stat1 Regulates LPS-Induced Inflammatory Responses.” *The Journal of experimental medicine* 206(9): 2027–35. http://www.ncbi.nlm.nih.gov/pmc/articles/PMC2737163/pdf/JEM_20090560.pdf.

Kinchen, James et al. 2018. “Structural Remodeling of the Human Colonic Mesenchyme in Inflammatory Bowel Disease.” *Cell* 175(2): 372-386.e17. https://doi.org/10.1016/j.cell.2018.08.067.

Kiss, E. A. et al. 2011. “Natural Aryl Hydrocarbon Receptor Ligands Control Organogenesis of Intestinal Lymphoid Follicles.” *Science* 334(6062): 1561–65. http://www.sciencemag.org/cgi/doi/10.1126/science.1214914.

Komatsu, Noriko et al. 2014. “Pathogenic Conversion of Foxp3+ T Cells into TH17 Cells in Autoimmune Arthritis.” *Nature Medicine* 20(1): 62–68.

http://www.ncbi.nlm.nih.gov/pubmed/24362934.

Korecka, Agata et al. 2016. “Bidirectional Communication between the Aryl Hydrocarbon Receptor (AhR) and the Microbiome Tunes Host Metabolism.” *npj Biofilms and Microbiomes* 16014. http://dx.doi.org/10.1038/npjbiofilms.2016.14.

Korn, Thomas. 2010. “How T Cells Take Developmental Decisions by Using the Aryl Hydrocarbon Receptor to Sense the Environment.” *Proceedings of the National Academy of Sciences of the United States of America* 107(48): 20597–98. http://www.pubmedcentral.nih.gov/articlerender.fcgi?artid=2996416&tool=pmcentrez&rendertype=abstract.

Korn, Thomas, Estelle Bettelli, Mohamed Oukka, and Vijay K Kuchroo. 2009. “IL-17 and Th17 Cells.” *Annual Review of Immunology* 27(1): 485–517. https://doi.org/10.1146/annurev.immunol.021908.132710.

van de Laar, Lianne et al. 2010. “A Nonredundant Role for Canonical NF-KB in Human Myeloid Dendritic Cell Development and Function.” *Journal of immunology* 185(12): 7252–61. http://www.ncbi.nlm.nih.gov/pubmed/21076069.

Lai, Yinglei. 2017. “A Statistical Method for the Conservative Adjustment of False Discovery Rate (q-Value).” *BMC Bioinformatics* 18(3): 69. https://doi.org/10.1186/s12859-017-1474-6.

Lai, Yunjia et al. 2019. “Serum Metabolomics Identifies Altered Bioenergetics, Signaling Cascades in Parallel with Exposome Markers in Crohn’s Disease.” *Molecules* 24(3).

Lamas, Bruno et al. 2016. “CARD9 Impacts Colitis by Altering Gut Microbiota Metabolism of Tryptophan into Aryl Hydrocarbon Receptor Ligands.” *Nature Medicine* (April).

de Lange, Katrina M et al. 2017. “Genome-Wide Association Study Implicates Immune Activation of Multiple Integrin Genes in Inflammatory Bowel Disease.” *Nature genetics* 49(2): 256–61. https://www.ncbi.nlm.nih.gov/pubmed/28067908.

Lee, Alexander et al. 2014. “IDO1 and IDO2 Non-Synonymous Gene Variants: Correlation with Crohn’s Disease Risk and Clinical Phenotype.” *PloS one* 9(12): e115848–e115848. https://www.ncbi.nlm.nih.gov/pubmed/25541686.

Lee, H B et al. 1997. “Differences in Immunophenotyping of Mucosal Lymphocytes between Ulcerative Colitis and Crohn’s Disease.” *The Korean journal of internal medicine* 12(1): 7–15. https://pubmed.ncbi.nlm.nih.gov/9159031.

Lee, Sung Hee. 2015. “Intestinal Permeability Regulation by Tight Junction: Implication on Inflammatory Bowel Diseases.” *Intestinal research* 13(1): 11–18. https://pubmed.ncbi.nlm.nih.gov/25691839.

Leonard, Maureen M et al. 2019. “RNA Sequencing of Intestinal Mucosa Reveals Novel Pathways Functionally Linked to Celiac Disease Pathogenesis.” *PLOS ONE* 14(4): e0215132. https://doi.org/10.1371/journal.pone.0215132.

Levine, Arie et al. 2019. “Crohn’s Disease Exclusion Diet Plus Partial Enteral Nutrition Induces Sustained Remission in a Randomized Controlled Trial.” *Gastroenterology* 157(2): 440-450.e8. https://doi.org/10.1053/j.gastro.2019.04.021.

Lewis, Robert A. 1998. *Lewis’ Dictionary of Toxicology*. Braintree Scientific.

Li, Daochuan et al. 2014. “AhR Is Negatively Regulated by MiR-203 in Response to TCDD or BaP Treatment †.” *Toxicology Research* 3: 142–51.

Li, Jian, Andria Doty, and Sarah C Glover. 2016. “Aryl Hydrocarbon Receptor Signaling Involves in the Human Intestinal ILC3/ILC1 Conversion in the Inflamed Terminal Ileum of Crohn’s Disease Patients.” *Inflammation and cell signaling* 3(3): e1404. https://www.ncbi.nlm.nih.gov/pubmed/28286805.

Li, Shiyang et al. 2018. “Aryl Hydrocarbon Receptor Signaling Cell Intrinsically Inhibits Intestinal Group 2 Innate Lymphoid Cell Function.” *Immunity* 49(5): 915-928.e5.

https://www.ncbi.nlm.nih.gov/pubmed/30446384.

Li, Ying et al. 2011. “Exogenous Stimuli Maintain Intraepithelial Lymphocytes via Aryl Hydrocarbon Receptor Activation.” *Cell* 147(3): 629–40. http://dx.doi.org/10.1016/j.cell.2011.09.025.

Lichtenstein, Paul. 2000. “Environmental and Heritable Factors in the Causation of Cancer.” *NEJM* 343(2): 78–85.

Lin, Sheng-Cai, and D Grahame Hardie. 2018. “AMPK: Sensing Glucose as Well as Cellular Energy Status.” *Cell Metabolism* 27(2): 299–313. https://doi.org/10.1016/j.cmet.2017.10.009.

Lindemans, Caroline A, Marco Calafiore, Anna M Mertelsmann, Margaret H O’Connor, et al. 2015. “Interleukin-22 Promotes Intestinal-Stem-Cell-Mediated Epithelial Regeneration.” *Nature* 528(7583): 560–64. https://pubmed.ncbi.nlm.nih.gov/26649819.

Lindemans, Caroline A, Marco Calafiore, Anna M Mertelsmann, H Margaret, et al. 2015. “Interleukin-22 Promotes Intestinal Stem Cell-Mediated Epithelial Regeneration.” *Nature* 528(7583): 560–64.

Lipchock, Sarah V, Julie A Mennella, Andrew I Spielman, and Danielle R Reed. 2013. “Human Bitter Perception Correlates with Bitter Receptor Messenger RNA Expression in Taste Cells.” *The American journal of clinical nutrition* 98(4): 1136–43. https://www.ncbi.nlm.nih.gov/pubmed/24025627.

Liu, Jimmy Z et al. 2015. “Association Analyses Identify 38 Susceptibility Loci for Inflammatory Bowel Disease and Highlight Shared Genetic Risk across Populations.” *Nature Genetics* 47(9): 979–89. http://dx.doi.org/10.1038/ng.3359.

Liu, Ta-chiang et al. 2018. “Interaction between Smoking and ATG16L1 T300A Triggers Paneth Cell Defects in Crohn’s Disease Triggers Paneth Cell Defects in Crohn’s Disease.” *JCI* 128(11): 5110–22.

Livak, K J, and T D Schmittgen. 2001. “Analysis of Relative Gene Expression Data Using Real-Time Quantitative PCR And.” *Methods* 25: 402–8.

Lo, Raymond, and Jason Matthews. 2012. “High-Resolution Genome-Wide Mapping of AHR and ARNT Binding Sites by ChIP-Seq.” *Toxicological sciences : an official journal of the Society of Toxicology* 130(2): 349–61. http://www.ncbi.nlm.nih.gov/pubmed/22903824.

Long, Millie D et al. 2016. “Role of Nonsteroidal Anti-Inflammatory Drugs in Exacerbations of Inflammatory Bowel Disease.” *Journal of clinical gastroenterology* 50(2): 152–56. https://pubmed.ncbi.nlm.nih.gov/26485106.

Longhi, Maria Serena et al. 2017. “Bilirubin Suppresses Th17 Immunity in Colitis by Upregulating CD39.” *JCI Insight* 2(9): 1–15.

Luther, Jay, Maneesh Dave, Peter D R Higgins, and John Y Kao. 2010. “Association between Helicobacter Pylori Infection and Inflammatory Bowel Disease: A Meta-Analysis and Systematic Review of the Literature.” *Inflammatory bowel diseases* 16(6): 1077–84. https://pubmed.ncbi.nlm.nih.gov/19760778.

Ma, Qiang et al. 2001. “TCDD-Inducible Poly(ADP-Ribose) Polymerase: A Novel Response to 2,3,7,8-Tetrachlorodibenzo-p-Dioxin.” *Biochemical and Biophysical Research Communications* 289(2): 499–506. http://www.sciencedirect.com/science/article/pii/S0006291X0195987X.

MacDonald, Bryan T, Keiko Tamai, and Xi He. 2009. “Wnt/Beta-Catenin Signaling: Components, Mechanisms, and Diseases.” *Developmental cell* 17(1): 9–26. https://pubmed.ncbi.nlm.nih.gov/19619488.

MacDonald, T T. 1990. “The Role of Activated T Lymphocytes in Gastrointestinal Disease.” *Clinical & Experimental Allergy* 20(3): 247–52. http:https://doi.org/10.1111/j.1365-2222.1990.tb02679.x.

MacKenzie, Amanda et al. 2011. “GPR35 as a Novel Therapeutic Target .” *Frontiers in Endocrinology* 2: 68. https://www.frontiersin.org/article/10.3389/fendo.2011.00068.

MacPherson, Gordon et al. 2004. “Uptake of Antigens from the Intestine by Dendritic Cells.” *Annals of the New York Academy of Sciences* 1029(1): 75–82. https://doi.org/10.1196/annals.1309.010.

Mangan, Paul R et al. 2006. “Transforming Growth Factor-Beta Induces Development of the T(H)17 Lineage.” *Nature* 441(7090): 231–34.

Mangin, Irène et al. 2004. “Molecular Inventory of Faecal Microflora in Patients with Crohn’s Disease.” *FEMS Microbiology Ecology* 50(1): 25–36. https://doi.org/10.1016/j.femsec.2004.05.005.

Mann E, Landy J, D. Bernardo, H. Omar Al-Hassi, S. Peake, R. Man, G. Han Lee, N. Yassin, S. Knight, A. Hart. 2013. “A Novel Therapeutic Target Linking Diet to Disease Pathogenesis in Ulcerative Colitis: The Aryl Hydrocarbon Receptor.” *ECCO Congress*: P100.

Marinelli, Ludovica et al. 2019. “Identification of the Novel Role of Butyrate as AhR Ligand in Human Intestinal Epithelial Cells.” *Scientific reports* 9(1): 643. https://www.ncbi.nlm.nih.gov/pubmed/30679727.

Marks, Daniel J B et al. 2006. “Defective Acute Inflammation in Crohn’s Disease: A Clinical Investigation.” *The Lancet* 367(9511): 668–78. https://doi.org/10.1016/S0140-6736(06)68265-2.

Marteau, P et al. 2001. “Comparative Study of Bacterial Groups within the Human Cecal and Fecal Microbiota.” *Applied and environmental microbiology* 67(10): 4939–42. https://pubmed.ncbi.nlm.nih.gov/11571208.

Martin, Jerome C et al. 2019. “Single-Cell Analysis of Crohn’s Disease Lesions Identifies a Pathogenic Cellular Module Associated with Resistance to Anti-TNF Therapy.” *Cell* 178(6): 1493-1508.e20. http://www.sciencedirect.com/science/article/pii/S0092867419308967.

Maxwell, Joseph R. et al. 2015. “Differential Roles for Interleukin-23 and Interleukin-17 in Intestinal

Immunoregulation." *Immunity* 43(4): 739–50. https://doi.org/10.1016/j.immuni.2015.08.019.

McCarthy, N. E. et al. 2013. "Proinflammatory V 2+ T Cells Populate the Human Intestinal Mucosa and Enhance IFN- Production by Colonic T Cells." *The Journal of Immunology* 191(5): 2752–63. http://www.jimmunol.org/cgi/doi/10.4049/jimmunol.1202959.

McHugh, Mary L. 2012. "Interrater Reliability: The Kappa Statistic." *Biochemia medica* 22(3): 276–82. https://pubmed.ncbi.nlm.nih.gov/23092060.

Metidji, Amina et al. 2018. "The Environmental Sensor AHR Protects from Inflammatory Damage by Maintaining Intestinal Stem Article The Environmental Sensor AHR Protects from Inflammatory Damage by Maintaining Intestinal Stem Cell Homeostasis and Barrier Integrity." *Immunity* 49(2): 353-362.e5. https://doi.org/10.1016/j.immuni.2018.07.010.

Mitchell, Kristen A., and Cornelis J. Elferink. 2009. "Timing Is Everything: Consequences of Transient and Sustained AhR Activity." *Biochemical Pharmacology* 77(6): 947–56.

Moayyedi, Paul et al. 2015. "Fecal Microbiota Transplantation Induces Remission in Patients With Active Ulcerative Colitis in a Randomized Controlled Trial." *Gastroenterology* 149(1): 102-109.e6. https://doi.org/10.1053/j.gastro.2015.04.001.

Mohinta, S. et al. 2015. "Differential Regulation of Th17 and T Regulatory Cell Differentiation by Aryl Hydrocarbon Receptor Dependent Xenobiotic Response Element Dependent and Independent Pathways." *Toxicological Sciences* 23(2): 1–11. http://www.toxsci.oxfordjournals.org/cgi/doi/10.1093/toxsci/kfv046.

Moini, Maryam et al. 2017. "Association Study of Glutathione S-Transferases Gene Polymorphisms (GSTM1 and GSTT1) with Ulcerative Colitis and Crohn's Disease in the South of Iran." *Advanced biomedical research* 6: 67. https://www.ncbi.nlm.nih.gov/pubmed/28626742.

Molodecky, Natalie A et al. 2012. "Increasing Incidence and Prevalence of the Inflammatory Bowel Diseases." *Gastroenterology* 142: 46–54. http://dx.doi.org/10.1053/j.gastro.2011.10.001.

Molodecky, Natalie A, and Gilaad G Kaplan. 2010. “Environmental Risk Factors for Inflammatory Bowel Disease.” *Gastroenterology & hepatology* 6(5): 339–46. http://www.pubmedcentral.nih.gov/articlerender.fcgi?artid=2886488&tool=pmcentrez&rendertype=abstract.

Monteleone, Ivan et al. 2011. “Aryl Hydrocarbon Receptor-Induced Signals Up-Regulate IL-22 Production and Inhibit Inflammation in the Gastrointestinal Tract.” *Gastroenterology* 141(1): 237-248.e1. http://linkinghub.elsevier.com/retrieve/pii/S0016508511005166.

Monteleone, Ivan, Francesca Zorzi, Irene Marafini, Davide Di Fusco, Vincenzo Dinallo, Roberta Caruso, Roberta Izzo, Eleonora Franz, et al. 2016. “Aryl Hydrocarbon Receptor-Driven Signals Inhibit Collagen Synthesis in the Gut.” *European Journal of Immunology* 46(4): 1047–57.

Monteleone, Ivan, Francesca Zorzi, Irene Marafini, Davide Di Fusco, Vincenzo Dinallo, Roberta Caruso, Roberta Izzo, Eleonora Franzè, et al. 2016. “Aryl Hydrocarbon Receptor-Driven Signals Inhibit Collagen Synthesis in the Gut.” *European Journal of Immunology* 46(4): 1047–57. https://doi.org/10.1002/eji.201445228.

Monteleone, Ivan, Irene Marafini, et al. 2016. “Smad7 Knockdown Restores Aryl Hydrocarbon Receptor-Mediated Protective Signals in the Gut.” *Journal of Crohn’s and Colitis* 10(6): 670–77.

Moura-Alves, P et al. 2014. “AhR Sensing of Bacterial Pigments Regulates Antibacterial Defence.” *Nature* 512(7515): 387–92. http://www.ncbi.nlm.nih.gov/pubmed/25119038%5Cnhttp://www.nature.com/nature/journal/v512/n7515/pdf/nature13684.pdf.

Murray, Iain A et al. 2016. “Expression of the Aryl Hydrocarbon Receptor Contributes to the Establishment of Intestinal Microbial Community Structure in Mice.” *Nature Publishing Group* (May): 1–14. http://dx.doi.org/10.1038/srep33969.

Murray, Iain A, and Gary H Perdew. 2017. “Ligand Activation of the Ah Receptor Contributes to

Gastrointestinal Homeostasis." *Current opinion in toxicology* 2: 15–23. https://pubmed.ncbi.nlm.nih.gov/28944314.

Murthy, Aditya et al. 2014. "A Crohn's Disease Variant in Atg16l1 Enhances Its Degradation by Caspase 3." *Nature* 506(7489): 456–62. https://doi.org/10.1038/nature13044.

Mylonaki, Maria et al. 2005. "Molecular Characterization of Rectal Mucosa-Associated Bacterial Flora in Inflammatory Bowel Disease." *Inflammatory bowel diseases* 11: 481–87.

Naganuma, Makoto et al. 2018. "Efficacy of Indigo Naturalis in a Multicenter Randomized Controlled Trial of Patients With Ulcerative Colitis." *Gastroenterology* (February): 1–13.

———. 2019. "Adverse Events in Patients with Ulcerative Colitis Treated with Indigo Naturalis: A Japanese Nationwide Survey." *Journal of Gastroenterology* 54(10): 891–96. https://doi.org/10.1007/s00535-019-01591-9.

Nakahama, Taisuke et al. 2013. "Aryl Hydrocarbon Receptor-Mediated Induction of the MicroRNA-132/212 Cluster Promotes Interleukin-17-Producing T-Helper Cell Differentiation." *Proceedings of the National Academy of Sciences of the United States of America* 110(29): 11964–69. http://www.pubmedcentral.nih.gov/articlerender.fcgi?artid=3718186&tool=pmcentrez&rendertype=abstract.

Nakano, Naoko et al. 2020. "Dissociation of the AhR-ARNT Complex by TGF-β-Smad Signaling Represses CYP1A1 Gene Expression and Inhibits Benze[a]Pyrene-Mediated Cytotoxicity." *Journal of Biological Chemistry* . http://www.jbc.org/content/early/2020/05/14/jbc.RA120.013596.abstract.

Nault, Rance, Agnes Forgacs, Edward Dere, and Timothy Zacharewski. 2013. "Comparisons of Differential Gene Expression Elicited by TCDD, PCB126, BNF, or ICZ in Mouse Hepatoma Hepa1c1c7 Cells and C57BL/6 Mouse Liver." *Toxicol Lett.* 223(1): 52–59.

Ng, Siew C et al. 2015. "Environmental Risk Factors in Inflammatory Bowel Disease: A Population-

Based Case-Control Study in Asia-Pacific." *Gut* (64): 1063–71.

———. 2017. "Worldwide Incidence and Prevalence of Inflammatory Bowel Disease in the 21st Century : A Systematic Review of Population-Based Studies." *The Lancet* 390(10114): 2769–78. http://dx.doi.org/10.1016/S0140-6736(17)32448-0.

Nguyen, Nam Trung et al. 2010. "Aryl Hydrocarbon Receptor Negatively Regulates Dendritic Cell Immunogenicity via a Kynurenine-Dependent Mechanism." *Proceedings of the National Academy of Sciences of the United States of America* 107(46): 19961–66.

Nielsen, Morten M, Deborah A Witherden, and Wendy L Havran. 2017. "Γδ T Cells in Homeostasis and Host Defence of Epithelial Barrier Tissues." *Nature reviews. Immunology* 17(12): 733–45. https://www.ncbi.nlm.nih.gov/pubmed/28920588.

Nikfar, Shekoufeh, Solmaz Ehteshami-Ashar, Roja Rahimi, and Mohammad Abdollahi. 2010. "Systematic Review and Meta-Analysis of the Efficacy and Tolerability of Nicotine Preparations in Active Ulcerative Colitis." *Clinical Therapeutics* 32(14): 2304–15. https://doi.org/10.1016/j.clinthera.2011.01.004.

Nikolaus, Susanna et al. 2017. "Increased Tryptophan Metabolism Is Associated With Activity of Inflammatory Bowel Diseases." *Gastroenterology* (153): 1504–16.

Nishide, Masayuki, and Atsushi Kumanogoh. 2018. "The Role of Semaphorins in Immune Responses and Autoimmune Rheumatic Diseases." *Nature Reviews Rheumatology* 14(1): 19–31. https://doi.org/10.1038/nrrheum.2017.201.

O'Connor Jr, William et al. 2009. "A Protective Function for Interleukin 17A in T Cell-Mediated Intestinal Inflammation." *Nature immunology* 10(6): 603–9. https://pubmed.ncbi.nlm.nih.gov/19448631.

Öberg, Mattias et al. 2005. "Identification of the Tryptophan Photoproduct 6-Formylindolo[3,2-b]Carbazole, in Cell Culture Medium, as a Factor That Controls the Background Aryl

Hydrocarbon Receptor Activity." *Toxicological Sciences* 85(2): 935–43.

Ogando, Jesús et al. 2016. "Notch-Regulated MiR-223 Targets the Aryl Hydrocarbon Receptor Pathway and Increases Cytokine Production in Macrophages from Rheumatoid Arthritis Patients." *Scientific reports* 6: 20223. https://pubmed.ncbi.nlm.nih.gov/26838552.

Ogino, Takayuki et al. 2013. "Increased Th17-Inducing Activity of CD14+ CD163low Myeloid Cells in Intestinal Lamina Propria of Patients With Crohns Disease." *Gastroenterology* 145(6): 1380-1391.e1. https://doi.org/10.1053/j.gastro.2013.08.049.

Oh-oka, Kyoko et al. 2017. "Induction of Colonic Regulatory T Cells by Mesalamine by Activating the Aryl Hydrocarbon Receptor." *Cmgh* 4(1): 135–51. http://dx.doi.org/10.1016/j.jcmgh.2017.03.010.

Ohtake, Fumiaki, Yoshiaki Fujii-Kuriyama, and Shigeaki Kato. 2009. "AhR Acts as an E3 Ubiquitin Ligase to Modulate Steroid Receptor Functions." *Biochemical pharmacology* 77(4): 474–84. http://www.ncbi.nlm.nih.gov/pubmed/18838062.

Olivares-Villagómez, Danyvid, and Luc Van Kaer. 2018. "Intestinal Intraepithelial Lymphocytes: Sentinels of the Mucosal Barrier." *Trends in Immunology* 39(4): 264–75. https://doi.org/10.1016/j.it.2017.11.003.

Oshima, Motohiko. 2007. "Molecular Mechanism of Transcriptional Repression of AhR." *BBRC* 364: 276–82.

Owens, Benjamin M.J., and A Simmons. 2012. "Intestinal Stromal Cells in Mucosal Immunity and Homeostasis." 6(2): 224–34. http://dx.doi.org/10.1038/mi.2012.125.

Owens, Benjamin M J et al. 2013. "CD90 + Stromal Cells Are Non-Professional Innate Immune Effectors of the Human Colonic Mucosa." *Frontiers in Immunology* 4(September): 1–11.

———. 2015. "Inflammation, Innate Immunity, and the Intestinal Stromal Cell Niche: Opportunities

and Challenges." *Frontiers in immunology* 6: 319. https://www.ncbi.nlm.nih.gov/pubmed/26150817.

Pacheco, Alline R et al. 2012. "Fucose Sensing Regulates Bacterial Intestinal Colonization." *Nature* 492(7427): 113–17.

Paramsothy, Sudarshan et al. 2017. "Multidonor Intensive Faecal Microbiota Transplantation for Active Ulcerative Colitis: A Randomised Placebo-Controlled Trial." *The Lancet* 389(10075): 1218–28. https://doi.org/10.1016/S0140-6736(17)30182-4.

Park, Heon et al. 2005. "A Distinct Lineage of CD4 T Cells Regulates Tissue Inflammation by Producing Interleukin 17." *Nature I* 6(11): 1133–41.

Parkes, Gareth C, Kevin Whelan, and James O Lindsay. 2014. "Smoking in Inflammatory Bowel Disease: Impact on Disease Course and Insights into the Aetiology of Its Effect." *Journal of Crohn's & colitis* 8(8): 717–25. http://www.ncbi.nlm.nih.gov/pubmed/24636140.

Parragi, Levente et al. 2018. "Colectomy Rates in Ulcerative Colitis Are Low and Decreasing: 10-Year Follow-up Data From the Swiss IBD Cohort Study." *Journal of Crohn's and Colitis* 12(7): 811–18. https://doi.org/10.1093/ecco-jcc/jjy040.

Peterson, Lance W, and David Artis. 2014. "Intestinal Epithelial Cells: Regulators of Barrier Function and Immune Homeostasis." *Nature reviews. Immunology* 14(3): 141–53. http://www.nature.com/nri/journal/v14/n3/pdf/nri3608.pdf%5Cnhttp://www.nature.com/nri/journal/v14/n3/pdf/nri3608.pdf?WT.ec_id=NRI-201403%5Cnhttp://dx.doi.org/10.1038/nri3608%5Cnhttp://www.ncbi.nlm.nih.gov/pubmed/24566914.

Piccioli, Patrizia, and Anna Rubartelli. 2013. "The Secretion of IL-1β and Options for Release." *Seminars in Immunology* 25(6): 425–29. http://www.sciencedirect.com/science/article/pii/S1044532313000882.

Poland, a, E Glover, and a S Kende. 1976. “Stereospecific, High Affinity Binding of 2,3,7,8-Tetrachlorodibenzo-p-Dioxin by Hepatic Cytosol.” *Journal of Biological Chemistry* 251(16): 4936–46.

Pollenz, Richard S, and Edward J Dougherty. 2005. “Redefining the Role of the Endogenous XAP2 and C-Terminal Hsp70-Interacting Protein on the Endogenous Ah Receptors Expressed in Mouse and Rat Cell Lines.” *The Journal of Biological Chemistry* 280(39): 33346–56.

Qiu, Ju et al. 2012. “The Aryl Hydrocarbon Receptor Regulates Gut Immunity through Modulation of Innate Lymphoid Cells.” *Immunity* 36(1): 92–104. http://linkinghub.elsevier.com/retrieve/pii/S107476131100505X.

———. 2013. “Group 3 Innate Lymphoid Cells Inhibit T-Cell-Mediated Intestinal Inflammation through Aryl Hydrocarbon Receptor Signaling and Regulation of Microflora.” *Immunity* 39(2): 386–99. http://dx.doi.org/10.1016/j.immuni.2013.08.002%5Cnpapers2://publication/doi/10.1016/j.immuni.2013.08.002.

Quintana, Francisco J et al. 2008. “Control of T(Reg) and T(H)17 Cell Differentiation by the Aryl Hydrocarbon Receptor.” *Nature* 453(7191): 65–71.

Ramsay, George, and Doreen Cantrell. 2015. “Environmental and Metabolic Sensors That Control T Cell Biology.” *Frontiers in Immunology* 6(March): 1–8. http://www.frontiersin.org/T_Cell_Biology/10.3389/fimmu.2015.00099/abstract.

Rankin, Lucille et al. 2013. “Diversity, Function, and Transcriptional Regulation of Gut Innate Lymphocytes.” *Frontiers in Immunology* 4(MAR): 1–15.

Rescigno, M. et al. 1998. “Dendritic Cell Survival and Maturation Are Regulated by Different Signaling Pathways.” *Journal of Experimental Medicine* 188(11): 2175–80. http://jem.rupress.org/content/188/11/2175.abstract.

Reynolds, Lindsay M. et al. 2015. “DNA Methylation of the Aryl Hydrocarbon Receptor Repressor Associations with Cigarette Smoking and Subclinical Atherosclerosis.” *Circulation: Cardiovascular Genetics* 8(5): 707–16.

Ririe, Kirk M, Randy P Rasmussen, and Carl T Wittwer. 1997. “Product Differentiation by Analysis of DNA Melting Curves during the Polymerase Chain Reaction.” *Analytical Biochemistry* 245(2): 154–60. http://www.sciencedirect.com/science/article/pii/S0003269796999169.

Roediger, W E. 1980. “Role of Anaerobic Bacteria in the Metabolic Welfare of the Colonic Mucosa in Man.” *Gut* 21(9): 793–98. https://www.ncbi.nlm.nih.gov/pubmed/7429343.

Rothhammer, Veit et al. 2016. “Type I Interferons and Microbial Metabolites of Tryptophan Modulate Astrocyte Activity and Central Nervous System Inflammation via the Aryl Hydrocarbon Receptor.” *Nature Medicine* 22(6).

Rothhammer, Veit, and Francisco J Quintana. 2019. “The Aryl Hydrocarbon Receptor: An Environmental Sensor Integrating Immune Responses in Health and Disease.” *Nature Reviews Immunology* 19(3): 184–97. https://doi.org/10.1038/s41577-019-0125-8.

Rutgeerts, Paul et al. 1995. “Controlled Trial of Metronidazole Treatment for Prevention of Crohn ’ s Recurrence After Ileal Resection.” *Gastroenterology* 108: 1617–21.

Safe, Stephen et al. 2018. “Aryl Hydrocarbon Receptor (AhR) Ligands as Selective AhR Modulators: Genomic Studies.” *Current Opinion in Toxicology* 11–12: 10–20. http://www.sciencedirect.com/science/article/pii/S2468202018300561.

Sallusto, By Federica, and Antonio Lanzavecchia. 1994. “Efficient Presentation of Soluble Antigen by Cultured Human Dendritic Cells Is Maintained by Granulocyte/Macrophage Colony-Stimulating Factor Plus Iuterleukin 4 and Downregulated by Tumor Necrosis Factor Alpha.” *J Exp Med* 179(April): 1109–18.

Sanchez, Yuriko et al. 2010. “The Unexpected Role for the Aryl Hydrocarbon Receptor on

Susceptibility to Experimental Toxoplasmosis." *Journal of Biomedicine and Biotechnology* 2010.

Sands, Bruce E et al. 2017. "Efficacy and Safety of MEDI2070, an Antibody Against Interleukin 23, in Patients With Moderate to Severe Crohn's Disease: A Phase 2a Study." *Gastroenterology* 153(1): 77-86.e6. http://dx.doi.org/10.1053/j.gastro.2017.03.049.

———. 2019. "Mongersen (GED-0301) for Active Crohn's Disease: Results of a Phase 3 Study." *American Journal of Gastroenterology*. https://journals.lww.com/ajg/Fulltext/publishahead/Mongersen__GED_0301__for_Active_Crohn_s_Disease_.99464.aspx.

Sarić, Nemanja et al. 2020. "The AHR Pathway Represses TGFβ-SMAD3 Signalling and Has a Potent Tumour Suppressive Role in SHH Medulloblastoma." *Scientific Reports* 10(1): 148. https://doi.org/10.1038/s41598-019-56876-z.

Sartor, Maureen A. et al. 2009. "Genomewide Analysis of Aryl Hydrocarbon Receptor Binding Targets Reveals an Extensive Array of Gene Clusters That Control Morphogenetic and Develomental Programs." *Environmental Health Perspectives* 117(7): 1139–46.

Satoh-Takayama, Naoko et al. 2009. "The Natural Cytotoxicity Receptor NKp46 Is Dispensable for IL-22-Mediated Innate Intestinal Immune Defense against Citrobacter Rodentium." *The Journal of Immunology* 183(10): 6579 LP – 6587. http://www.jimmunol.org/content/183/10/6579.abstract.

Savas, U, and C R Jefcoate. 1994. "Dual Regulation of Cytochrome P450EF Expression via the Aryl Hydrocarbon Receptor and Protein Stabilization in C3H/10T1/2 Cells." *Molecular Pharmacology* 45(6): 1153 LP – 1159. http://molpharm.aspetjournals.org/content/45/6/1153.abstract.

Schiering, Chris et al. 2017. "Feedback Control of AHR Signalling Regulates Intestinal Immunity." *Nature* 542(7640): 242–45. http://www.nature.com/doifinder/10.1038/nature21080%5Cnhttp://www.ncbi.nlm.nih.gov/p

ubmed/28146477.

Schmidt, J V et al. 1996. “Characterization of a Murine Ahr Null Allele: Involvement of the Ah Receptor in Hepatic Growth and Development.” *Proceedings of the National Academy of Sciences of the United States of America* 93(13): 6731–36.

Schrader, C, A Schielke, L Ellerbroek, and R Johne. 2012. “PCR Inhibitors – Occurrence, Properties and Removal.” *Journal of Applied Microbiology* 113(5): 1014–26. https://doi.org/10.1111/j.1365-2672.2012.05384.x.

Schroeder, Jennifer C et al. 2010. “The Uremic Toxin 3-Indoxyl Sulfate Is a Potent Endogenous Agonist for the Human Aryl Hydrocarbon Receptor.” *Biochemistry* 49(2): 393–400.

Schurch, Nicholas J. et al. 2016. “How Many Biological Replicates Are Needed in an RNA-Seq Experiment and Which Differential Expression Tool Should You Use?” *Rna* 22(10): 1641–1641. http://rnajournal.cshlp.org/lookup/doi/10.1261/rna.058339.116.

de Silva, Punyanganie S A et al. 2010. “An Association Between Dietary Arachidonic Acid, Measured in Adipose Tissue, and Ulcerative Colitis.” *Gastroenterology* 139(6): 1912–17. https://doi.org/10.1053/j.gastro.2010.07.065.

Singh, Narendra P. et al. 2011. “Activation of Aryl Hydrocarbon Receptor (AhR) Leads to Reciprocal Epigenetic Regulation of Foxp3 and IL-17 Expression and Amelioration of Experimental Colitis.” *PLoS ONE* 6(8).

Smillie, Christopher S et al. 2019. “Intra- and Inter-Cellular Rewiring of the Human Colon during Ulcerative Colitis.” *Cell* 178(3): 714-730.e22. http://www.sciencedirect.com/science/article/pii/S0092867419307329.

Smith, Susan H et al. 2017. “Tapinarof Is a Natural AhR Agonist That Resolves Skin Inflammation in Mice and Humans.” *Journal of Investigative Dermatology* 137(10): 2110–19. https://doi.org/10.1016/j.jid.2017.05.004.

Sokol, Harry et al. 2006. “Specificities of the Fecal Microbiota in Inflammatory Bowel Disease.” *Inflammatory Bowel Diseases* 12(2): 106–11. https://doi.org/10.1097/01.MIB.0000200323.38139.c6.

———. 2008. “Faecalibacterium Prausnitzii Is an Anti-Inflammatory Commensal Bacterium Identified by Gut Microbiota Analysis of Crohn Disease Patients.” *Proceedings of the National Academy of Sciences* 105(43): 16731–36. http://www.pnas.org/cgi/doi/10.1073/pnas.0804812105.

Soulard, Alexandre, Adiel Cohen, and Michael N Hall. 2009. “TOR Signaling in Invertebrates.” *Curr Opin Cell Biol* 21(6): 825–36.

Spits, Hergen et al. 2013. “Innate Lymphoid Cells--a Proposal for Uniform Nomenclature.” *Nature reviews. Immunology* 13(2): 145–49. http://www.ncbi.nlm.nih.gov/pubmed/23348417.

Spor, Aymé, Omry Koren, and Ruth Ley. 2011. “Unravelling the Effects of the Environment and Host Genotype on the Gut Microbiome.” *Nature reviews. Microbiology* 9(4): 279–90. http://dx.doi.org/10.1038/nrmicro2540.

Stefanich, Eric G et al. 2018. “Pre-Clinical and Translational Pharmacology of a Human Interleukin-22 IgG Fusion Protein for Potential Treatment of Infectious or Inflammatory Diseases.” *Biochemical Pharmacology* 152: 224–35. http://www.sciencedirect.com/science/article/pii/S0006295218301369.

Stockinger, Brigitta, Paola Di Meglio, Manolis Gialitakis, and João H. Duarte. 2014. “The Aryl Hydrocarbon Receptor: Multitasking in the Immune System.” *Annual Review of Immunology* 32(1): 403–32. http://www.annualreviews.org/doi/abs/10.1146/annurev-immunol-032713-120245.

Strong, Scott A et al. 1998. “Proinflammatory Cytokines Differentially Modulate Their Own Expression in Human Intestinal Mucosal Mesenchymal Cells.” *Gastroenterology* 114(6): 1244–56. https://doi.org/10.1016/S0016-5085(98)70431-7.

Sugihara, Kohei, Tina L Morhardt, and Nobuhiko Kamada. 2019. “The Role of Dietary Nutrients in Inflammatory Bowel Disease.” *Frontiers in immunology* 9: 3183. https://www.ncbi.nlm.nih.gov/pubmed/30697218.

Sugimoto, Shinya, Makoto Naganuma, and Takanori Kanai. 2016. “Indole Compounds May Be Promising Medicines for Ulcerative Colitis.” *Journal of Gastroenterology* 51(9): 853–61. https://doi.org/10.1007/s00535-016-1220-2.

Sulem, Patrick et al. 2011. “Sequence Variants at CYP1A1-CYP1A2 and AHR Associate with Coffee Consumption.” *Human Molecular Genetics* 20(10): 2071–77.

Surawicz, Christina M, Rodger C Haggitt, Michael Husseman, and Lynne V McFarland. 1994. “Mucosal Biopsy Diagnosis of Colitis: Acute Self-Limited Colitis and Idiopathic Inflammatory Bowel Disease.” *Gastroenterology* 107(3): 755–63. https://doi.org/10.1016/0016-5085(94)90124-4.

Suzuki, Hideo et al. 2013. “Therapeutic Efficacy of the Qing Dai in Patients with Intractable Ulcerative Colitis.” *World journal of gastroenterology* 19(17): 2718–22. https://www.ncbi.nlm.nih.gov/pubmed/23674882.

Takahiro, Hiraide et al. 2019. “Abstract 640: Indigo Naturalis, a Promising Herbal Medicine for Ulcerative Colitis, Can Induce Experimental Pulmonary Arterial Hypertension via Aryl Hydrocarbon Pathway.” *Circulation Research* 125(Suppl_1): A640–A640. https://doi.org/10.1161/res.125.suppl_1.640.

Takamura, Takeyuki et al. 2010. “Activation of the Aryl Hydrocarbon Receptor Pathway May Ameliorate Dextran Sodium Sulfate-Induced Colitis in Mice.” *Immunology and Cell Biology* 88(6): 685–89. http://dx.doi.org/10.1038/icb.2010.35.

———. 2011. “Lactobacillus Bulgaricus OLL1181 Activates the Aryl Hydrocarbon Receptor Pathway and Inhibits Colitis.” *Immunology and Cell Biology* 89(7): 817–22.

http://www.ncbi.nlm.nih.gov/pmc/articles/PMC3257032/.

Takeuchi, Ken et al. 2006. “Prevalence and Mechanism of Nonsteroidal Anti-Inflammatory Drug Induced Clinical Relapse in Patients With Inflammatory Bowel Disease.” *Clinical Gastroenterology and Hepatology* 4(2): 196–202. https://doi.org/10.1016/S1542-3565(05)00980-8.

Talbot, Jhimmy et al. 2018. “Smoking-Induced Aggravation of Experimental Arthritis Is Dependent of Aryl Hydrocarbon Receptor Activation in Th17 Cells.” *Arthritis Research & Therapy* 20(1): 119. https://doi.org/10.1186/s13075-018-1609-9.

Tanner, A R, and A S Raghunath. 1988. “Colonic Inflammation and Nonsteroidal Anti-Inflammatory Drug Administration.” *Digestion* 41(2): 116–20. https://www.karger.com/DOI/10.1159/000199740.

Tardif, François, Geneviève Ross, and Mahmoud Rouabhia. 2004. “Gingival and Dermal Fibroblasts Produce Interleukin-1β Converting Enzyme and Interleukin-1β but Not Interleukin-18 Even after Stimulation with Lipopolysaccharide.” *Journal of Cellular Physiology* 198(1): 125–32. https://doi.org/10.1002/jcp.10400.

Terashima, Jun et al. 2013. “An Aryl Hydrocarbon Receptor Induces VEGF Expression through ATF4 under Glucose Deprivation in HepG2.” *BMC molecular biology* 14: 27. https://pubmed.ncbi.nlm.nih.gov/24330582.

Theochari, Nikoletta A, Anastasios Stefanopoulos, Konstantinos S Mylonas, and Konstantinos P Economopoulos. 2018. “Antibiotics Exposure and Risk of Inflammatory Bowel Disease: A Systematic Review.” *Scandinavian Journal of Gastroenterology* 53(1): 1–7. https://doi.org/10.1080/00365521.2017.1386711.

Torres, Joana et al. 2020. “Infants Born to Mothers with IBD Present with Altered Gut Microbiome That Transfers Abnormalities of the Adaptive Immune System to Germ-Free Mice.” *Gut* 69(1):

42 LP – 51. http://gut.bmj.com/content/69/1/42.abstract.

Trifari, Sara et al. 2009. “Identification of a Human Helper T Cell Population That Has Abundant Production of Interleukin 22 and Is Distinct from T H -17 , T H 1 and T H 2 Cells.” *Nature immunology* 10(8): 864–71. http://dx.doi.org/10.1038/ni.1770.

Trivedi, Palak J, and David H Adams. 2018. “Chemokines and Chemokine Receptors as Therapeutic Targets in Inflammatory Bowel Disease; Pitfalls and Promise.” *Journal of Crohn’s & colitis* 12(suppl_2): S641–52. https://pubmed.ncbi.nlm.nih.gov/30137309.

Tysk, C, E Lindberg, G Järnerot, and B Flodérus-Myrhed. 1988. “Ulcerative Colitis and Crohn’s Disease in an Unselected Population of Monozygotic and Dizygotic Twins. A Study of Heritability and the Influence of Smoking.” *Gut* 29(7): 990–96. https://www.ncbi.nlm.nih.gov/pubmed/3396969.

van Uden, Patrick et al. 2011. “Evolutionary Conserved Regulation of HIF-1β by NF-KB.” *PLOS Genetics* 7(1): e1001285. https://doi.org/10.1371/journal.pgen.1001285.

Ueno, Aito et al. 2015. “Th17 Plasticity and Its Changes Associated with Inflammatory Bowel Disease.” *WJG* 21(43): 12283–95.

de Vallière, Cheryl et al. 2016. “Hypoxia Positively Regulates the Expression of PH-Sensing G-Protein-Coupled Receptor OGR1 (GPR68).” *Cellular and molecular gastroenterology and hepatology* 2(6): 796–810. https://pubmed.ncbi.nlm.nih.gov/28174749.

Veldhoen, Marc et al. 2008. “The Aryl Hydrocarbon Receptor Links Th17-Cell-Mediated Autoimmunity to Environmental Toxins.” *Nature* 453(May): 2–6.

Vernia, P et al. 2000. “Combined Oral Sodium Butyrate and Mesalazine Treatment Compared to Oral Mesalazine Alone in Ulcerative Colitis.” *Digestive Diseases and Sciences* 45(5): 976–81. https://doi.org/10.1023/A:1005537411244.

Vivier, Eric et al. 2018. “Innate Lymphoid Cells: 10 Years On.” *Cell* 174(5): 1054–66. https://doi.org/10.1016/j.cell.2018.07.017.

Vogel, Christoph F A et al. 2007. “RelB , a New Partner of Aryl Hydrocarbon Receptor-Mediated Transcription.” *Molecular Endocrinology* 21(August): 2941–55.

———. 2008. “Aryl Hydrocarbon Receptor Signaling Mediates Expression of Indoleamine 2,3-Dioxygenase.” *Biochem Biophys Res Commun* 375(3): 331–35.

———. 2013. “Aryl Hydrocarbon Receptor Signaling Regulates NF-KB RelB Activation during Dendritic-Cell Differentiation.” *Immunology and Cell Biology* 91(9): 568–75. http://www.nature.com/doifinder/10.1038/icb.2013.43.

Vogel, Christoph F A, and Fumio Matsumura. 2009. “A New Cross-Talk between the Aryl Hydrocarbon Receptor and RelB, a Member of the NF-KB Family.” *Biochem Pharmacol* 77(4): 734–45.

Voyvodic, Peter L et al. 2014. “Loss of Syndecan-1 Induces a pro-Inflammatory Phenotype in Endothelial Cells with a Dysregulated Response to Atheroprotective Flow.” *The Journal of biological chemistry* 289(14): 9547–59. https://pubmed.ncbi.nlm.nih.gov/24554698.

de Vries, Hilbert S et al. 2012. “A Functional Polymorphism in UGT1A1 Related to Hyperbilirubinemia Is Associated with a Decreased Risk for Crohn’s Disease.” *Journal of Crohn’s and Colitis* 6(5): 597–602. https://doi.org/10.1016/j.crohns.2011.11.010.

Wagner, Anika E et al. 2013. “DSS-Induced Acute Colitis in C57BL/6 Mice Is Mitigated by Sulforaphane Pre-Treatment.” *The Journal of Nutritional Biochemistry* 24(12): 2085–91. http://dx.doi.org/10.1016/j.jnutbio.2013.07.009.

Wang, Bao-Long et al. 2019. “Lipidomics Reveal Aryl Hydrocarbon Receptor (Ahr)-Regulated Lipid Metabolic Pathway in Alpha-Naphthyl Isothiocyanate (ANIT)-Induced Intrahepatic Cholestasis.” *Xenobiotica; the fate of foreign compounds in biological systems* 49(5): 591–601.

https://www.ncbi.nlm.nih.gov/pubmed/29737914.

Wang, Gui-Zhen et al. 2019. “The Aryl Hydrocarbon Receptor Mediates Tobacco-Induced PD-L1 Expression and Is Associated with Response to Immunotherapy.” *Nature Communications* 10(1): 1125. https://doi.org/10.1038/s41467-019-08887-7.

Weaver, Casey T, Charles O Elson, Lynette A Fouser, and Jay K Kolls. 2013. “The Th17 Pathway and Inflammatory Diseases of the Intestines, Lungs, and Skin.” *Annual Review of Pathology: Mechanisms of Disease* 8(1): 477–512. https://doi.org/10.1146/annurev-pathol-011110-130318.

Wehkamp, J et al. 2004. “NOD2 (CARD15) Mutations in Crohn’s Disease Are Associated with Diminished Mucosal α-Defensin Expression.” *Gut* 53(11): 1658 LP – 1664. http://gut.bmj.com/content/53/11/1658.abstract.

Weichhart, Thomas, Markus Hengstschläger, and Monika Linke. 2015. “Regulation of Innate Immune Cell Function by MTOR.” *Nature reviews. Immunology* 15(10): 599–614. https://pubmed.ncbi.nlm.nih.gov/26403194.

Van Welden, Sophie, Andrew C Selfridge, and Pieter Hindryckx. 2017. “Intestinal Hypoxia and Hypoxia-Induced Signalling as Therapeutic Targets for IBD.” *Nature Reviews Gastroenterology & Hepatology* 14(10): 596–611. https://doi.org/10.1038/nrgastro.2017.101.

West, Nathaniel R et al. 2017. “Oncostatin M Drives Intestinal Inflammation in Mice and Its Abundance Predicts Response to Tumor Necrosis Factor- Neutralizing Therapy in Patients with Inflammatory Bowel Disease.” *Nature Medicine* 23(5): 579–89.

Wheeler, Jennifer L H, Kyle C Martin, Emily Resseguie, and B Paige Lawrence. 2014. “Differential Consequences of Two Distinct AhR Ligands on Innate and Adaptive Immune Responses to Influenza A Virus.” *Toxicological sciences : an official journal of the Society of Toxicology* 137(2): 324–34. https://pubmed.ncbi.nlm.nih.gov/24194396.

Wiest, Elani F et al. 2016. “Dietary Omega-3 Polyunsaturated Fatty Acids Prevent Vascular Dysfunction and Attenuate Cytochrome P4501A1 Expression by 2,3,7,8-Tetrachlorodibenzo-P-Dioxin.” *Toxicological sciences : an official journal of the Society of Toxicology* 154(1): 43–54. https://pubmed.ncbi.nlm.nih.gov/27492226.

Wild, Christopher Paul. 2005. “Complementing the Genome with an ‘Exposome’: The Outstanding Challenge of Environmental Exposure Measurement in Molecular Epidemiology.” *Cancer epidemiology, biomarkers & prevention : a publication of the American Association for Cancer Research, cosponsored by the American Society of Preventive Oncology* 14(8): 1847–50. http://apps.webofknowledge.com/full_record.do?product=UA&search_mode=GeneralSearch&qid=26&SID=T2yydBUiYXDKWLsSpvs&page=1&doc=4&cacheurlFromRightClick=no.

Williams, C N. 2008. “Does the Incidence of IBD Increase When Persons Move from a Low- to a High-Risk Area?” *Inflammatory Bowel Diseases* 14(suppl_2): S41–42. https://doi.org/10.1002/ibd.20562.

Willing, B et al. 2009. “Twin Studies Reveal Specific Imbalances in the Mucosa-Associated Microbiota of Patients with Ileal Crohn’s Disease.” *IBD* 15(5). https://www.osti.gov/biblio/970049.

Wincent, Emma et al. 2012. “Inhibition of Cytochrome P4501-Dependent Clearance of the Endogenous Agonist FICZ as a Mechanism for Activation of the Aryl Hydrocarbon Receptor.” *PNAS*: 1–6.

Wolff, S et al. 2001. “Cell-Specific Regulation of Human Aryl Hydrocarbon Receptor Expression by Transforming Growth Factor-Beta(1).” *Molecular Pharmacology* 59(4): 716–24.

Xiao, Wusheng et al. 2015. “Ligand-Independent Activation of Aryl Hydrocarbon Receptor Signaling in PCB3-Quinone Treated HaCaT Human Keratinocytes.” *Toxicology letters* 233(3): 258–66. https://pubmed.ncbi.nlm.nih.gov/25668756.

Xu, L et al. 2018. “Systematic Review with Meta-Analysis: Breastfeeding and the Risk of Crohn’s

Disease and Ulcerative Colitis." *APT* 46(9): 780–89.

Xue, Jing et al. 2016. "Aryl Hydrocarbon Receptor Ligands in Cigarette Smoke Induce Production of Interleukin-22 to Promote Pancreatic Fibrosis in Models of Chronic Pancreatitis." *Gastroenterology* 151(6): 1206–17. https://doi.org/10.1053/j.gastro.2016.09.064.

Yang, Sunny Y, Shaimaa Ahmed, Somisetty V Satheesh, and Jason Matthews. 2018. "Genome-Wide Mapping and Analysis of Aryl Hydrocarbon Receptor (AHR)- and Aryl Hydrocarbon Receptor Repressor (AHRR)-Binding Sites in Human Breast Cancer Cells." *Archives of toxicology* 92(1): 225–40. https://pubmed.ncbi.nlm.nih.gov/28681081.

Yao, K et al. 1996. "Increased Numbers of Macrophages in Noninflamed Gastroduodenal Mucosa of Patients with Crohn's Disease." *Digestive Diseases and Sciences* 41(11): 2260–67. https://doi.org/10.1007/BF02071410.

Yin, Jiuheng et al. 2019. "Aryl Hydrocarbon Receptor Activation Alleviates Dextran Sodium Sulfate-Induced Colitis through Enhancing the Differentiation of Goblet Cells." *Biochemical and Biophysical Research Communications* 514(1): 180–86. http://www.sciencedirect.com/science/article/pii/S0006291X19307867.

Yu, Lianbo, Soledad Fernandez, and Guy Brock. 2017. "Power Analysis for RNA-Seq Differential Expression Studies." *BMC Bioinformatics* 18(1): 234. https://doi.org/10.1186/s12859-017-1648-2.

Zaid, Ali et al. 2014. "Persistence of Skin-Resident Memory T Cells within an Epidermal Niche." *Proceedings of the National Academy of Sciences of the United States of America* 111(14): 5307–12. http://www.pnas.org/content/111/14/5307.abstract.

Zelante, Teresa et al. 2013. "Tryptophan Catabolites from Microbiota Engage Aryl Hydrocarbon Receptor and Balance Mucosal Reactivity via Interleukin-22." *Immunity* 39(2): 372–85. http://dx.doi.org/10.1016/j.immuni.2013.08.003.

Zenewicz, Lauren A. 2018. “IL-22: There Is a Gap in Our Knowledge.” *ImmunoHorizons* 2(6): 198 LP – 207. http://www.immunohorizons.org/content/2/6/198.abstract.

Zhang, Limin et al. 2015. “Persistent Organic Pollutants Modify Gut-Microbiota Host Metabolic Homeostasis in Mice through Aryl Hydrocarbon Receptor Activation.” *Environmental Health Perspectives* 123(7): 679–88.

Zhang, Linda S, and Sean S Davies. 2016. “Microbial Metabolism of Dietary Components to Bioactive Metabolites: Opportunities for New Therapeutic Interventions.” *Genome medicine* 8(1): 46. http://www.pubmedcentral.nih.gov/articlerender.fcgi?artid=4840492&tool=pmcentrez&rendertype=abstract.

Zhang, Luhua H, June Ho Shin, Mikel D Haggadone, and John B Sunwoo. 2016. “The Aryl Hydrocarbon Receptor Is Required for the Maintenance of Liver-Resident Natural Killer Cells.” *The Journal of experimental medicine* 213(11): 2249–57. https://www.ncbi.nlm.nih.gov/pubmed/27670593.

Zhao, Bin et al. 2010. “CH223191 Is a Ligand-Selective Antagonist of the Ah (Dioxin) Receptor.” *Toxicological Sciences* 117(2): 393–403.

Zhao, Xia, Wei Zhang, Li Wang, and Wei-li Zhao. 2013. “Genetic Methylation and Lymphoid Malignancies : Biomarkers of Tumor Progression and Targeted Therapy.” 1(1): 1.

Zuk, Or, Eliana Hechter, Shamil R Sunyaev, and Eric S Lander. 2012. “The Mystery of Missing Heritability: Genetic Interactions Create Phantom Heritability.” *Proceedings of the National Academy of Sciences* 109(4): 1193 LP – 1198. http://www.pnas.org/content/109/4/1193.abstract.

Appendix

1 - Determining MACS purity – CD14+ PBMC

A

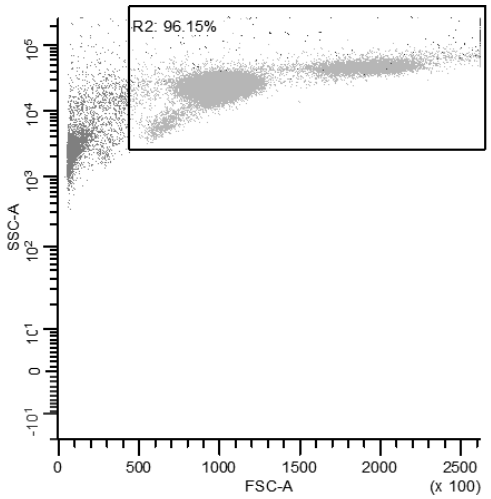

B

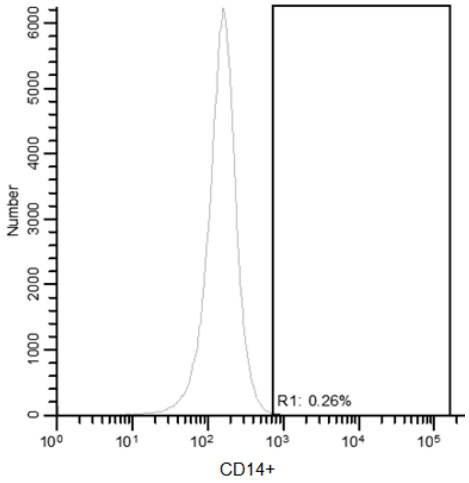

C

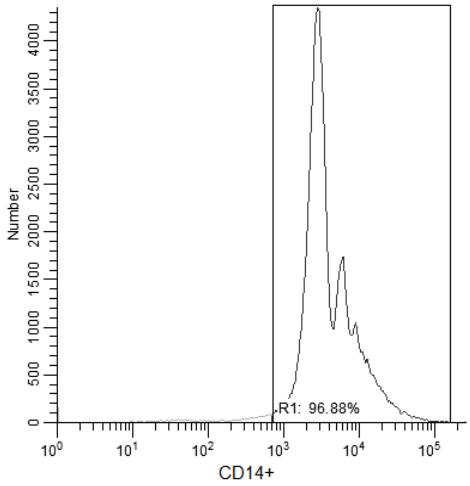

D

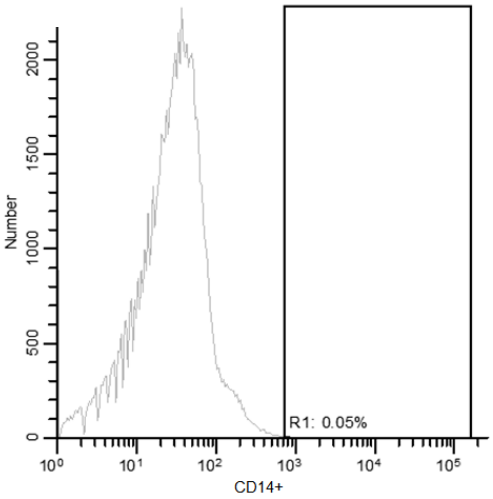

E

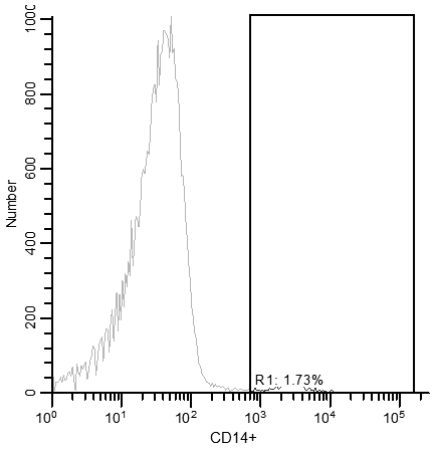

Appendix Figure 1 Using FACS to determine purity of MACS sorted CD14+ PBMC. PBMC were isolated using a Ficoll gradient. Cells were labelled using anti-CD14 microbeads and separated using MACS columns as described in Chapter 2. The positively and negatively selected fraction were collected and subsequently labelled with anti-CD14 conjugated to Pacific Blue or an isotype-matched control. PBMC were identified using SSC and FSC properties (1A). CD14 expression was seen in 96.9% MACS selected CD14 positive cells (1B) compared to 0.26% with isotype-matched control (1C). CD14 expression was detected in 1.7% MACS selected CD14 negative cells (1E) compared to 0.05% with isotype matched control (1D). There was higher high background signal in this channel in the CD14- fraction (both isotype and anti-CD14 labelled).

2 - R scripts for RNASeq analysis (with thanks to David Watson)

```
# Set working directory
setwd ('~/Documents/QMUL/Crohns')

# Load libraries, register cores
library (data.table)
library (tximport)
library (DESeq2)
library (IHW)
library (tidyverse)
library (bioplotr)
library (BiocParallel)
register (MulticoreParam (8))

# Import data
clin <- fread ('./Data/clinical.csv')
t2g <- readRDS ('./Data/Hs91.t2g.rds')
anno <- fread ('./Data/Hs.anno.csv')
rld <- readRDS ('./Data/rld.rds')

# Remove outliers
outliers <- c ('1911B-D', '2502A-F', '2502A-CH')
clin <- clin[!SampleID %in% outliers]

# Run tximport
files <- file.path ('./Data/Kallisto', clin$SampleID, 'abundance.tsv')
txi <- tximport (files, type = 'kallisto', tx2gene = t2g, importer = fread)

# Build DESeqDataSet
dds <- DESeqDataSetFromTximport (txi, colData = clin,
            design = ~ Patient + Condition)
# Run DESeq2
dds <- DESeq (dds, parallel = TRUE)

# Prepare gene index and gene name table
idx <- rownames (dds)
e2g <- t2g %>%
```

```
 select (gene_id, gene_name) %>%
 distinct (.)

# Output function
output <- function (trt) { lfc <- lfcShrink (dds, contrast = c ('Condition', trt, 'Control'),
        parallel = TRUE, quiet = TRUE) %>%
  as_tibble (.) %>%
  mutate (gene_id = idx) %>%
  rename (logFC = log2FoldChange) %>%
  select (gene_id, logFC)
 res <- results (dds, contrast = c ('Condition', trt, 'Control'), tidy = TRUE,
       filterFun = ihw, alpha = 0.05) %>%
  na.omit (.) %>%
  mutate (AvgExpr = log2 (baseMean)) %>%
  rename (gene_id = row,
     p.value = pvalue,
     q.value = padj) %>%
  inner_join (lfc, by = 'gene_id') %>%
  inner_join (e2g, by = 'gene_id') %>%
  rename (EnsemblID = gene_id, GeneName = gene_name) %>%
  arrange (p.value) %>%
  select (EnsemblID, GeneName, AvgExpr, logFC, p.value, q.value)
 return (res) }

# Agonist vs. Control
res_h1 <- output ('Agonist')
fwrite (res_h1, './Results/Agonist_vs_Control.csv')
plot_md (res_h1, probes = 'EnsemblID',
   title = 'Mean-Difference Plot:\nAgonist vs. Control')
plot_volcano (res_h1, probes = 'EnsemblID',
      title = 'Volcano Plot:\nAgonist vs. Control')
top_genes <- res_h1$EnsemblID[seq_len (1000)]
tmp <- clin[Condition != 'Antagonist']
mat <- rld[rownames (rld) %in% top_genes, tmp$SampleID]
plot_heatmap (mat, group = list (Condition = tmp$Condition),
      title = 'Top Genes:\nAgonist vs. Control')

# Antagonist vs. Control
res_h2 <- output ('Antagonist')
fwrite (res_h2, './Results/Antagonist_vs_Control.csv')
plot_md (res_h2, probes = 'EnsemblID',
   title = 'Mean-Difference Plot:\nAntagonist vs. Control')
plot_volcano (res_h2, probes = 'EnsemblID',
      title = 'Volcano Plot:\nAntagonist vs. Control')
top_genes <- res_h2$EnsemblID[seq_len (1000)]
tmp <- clin[Condition != 'Agonist']
mat <- rld[rownames (rld) %in% top_genes, tmp$SampleID]
plot_heatmap (mat, group = list (Condition = tmp$Condition),
      title = 'Top Genes:\nAntagonist vs. Control')
```

3 – tSNE plot of RNASeq samples

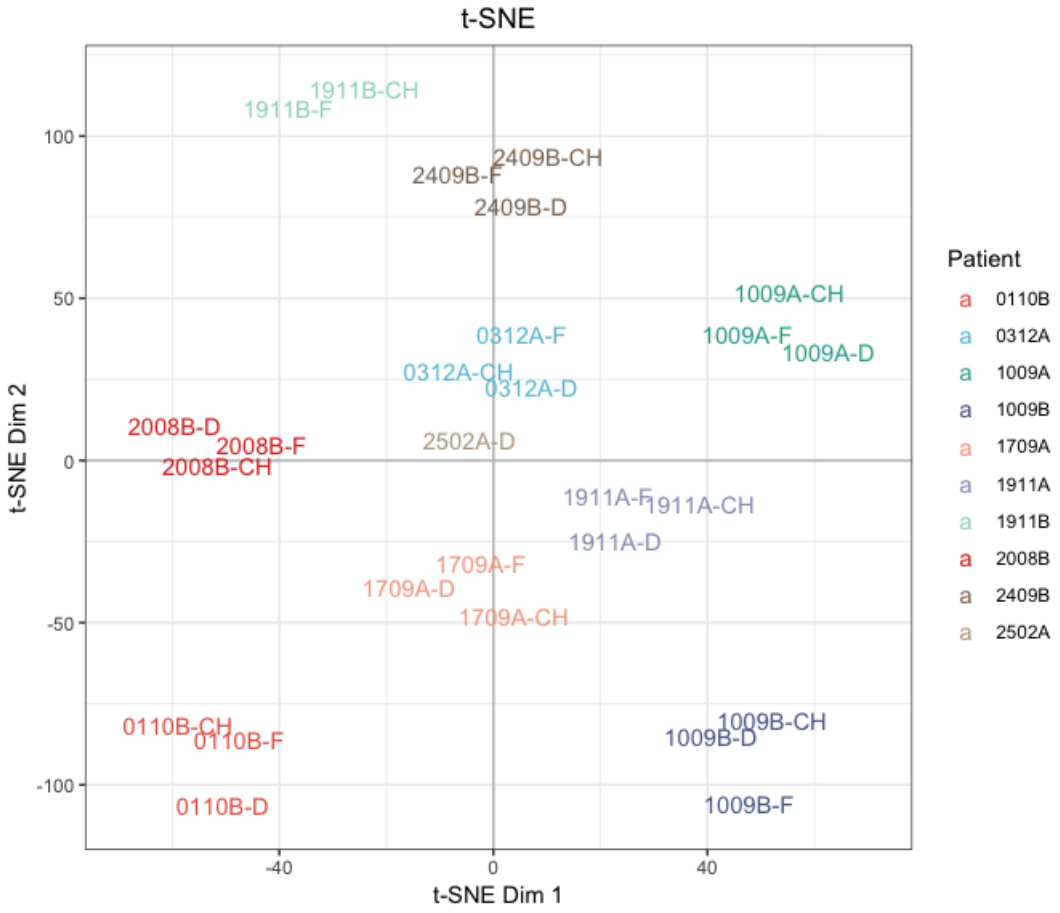

Appendix 3: tSNE plot of gene expression data from RNASeq was used to further identify outliers after three outliers already identified by PCA had been removed. Samples appear to cluster by patient without extreme outliers.

4 Characteristics & clinical features of included patients - Lysed whole biopsy cohort

Gene expression in lysed whole biopsies (used in Chapter 4, Figure 4.1). Patients aged 18-70.

Patient	Sex	Diagnosis	IBD Activity
Snap 1	Female	Healthy	
Snap 2	Male	Healthy	
Snap 3	Female	Healthy	
Snap 4	Male	Healthy	
Snap 5	Male	Healthy	
Snap 6	Male	Healthy	
Snap 7	Female	Healthy	
Snap 8	Female	Healthy	

Snap 9	Female	Crohn's	Not recorded
Snap 10	Male	Crohn's	Inactive
Snap 11	Female	Crohn's	Not recorded
Snap 12	Male	Crohn's	Inactive
Snap 13	Male	Crohns' disease (ileal)	Active
Snap 14	Male	Crohn's disease (ileal)	Active
Snap 15	Female	Ulcerative colitis	Inactive
Snap 16	Female	Ulcerative colitis	Active

5 - MACS sorted and stimulated mucosal cells

The demographics of each donor was recorded prospectively. Study participants between the age of 18-70 were recruited. Healthy donors were recruited if the colonoscopy was macroscopically normal, with the exception that <4 adenomatous polyps <1cm were permitted. Patients with major comorbidities including cancer, any immunological disease or drugs or chronic infections (TB, HIV, hepatitis) were excluded.

Detailed Characteristics & clinical features of included patients

Patient	**Age**	**Sex**	**Comorbidity**	**Diagnosis**	**IBD activity**	**IBD Treatment**
HC1	M	39.0	Nil	Normal		
HC2	F	65.0	Anaemia	Normal		
HC3	M	46.6	Nil	Normal		
HC4	M	41.0	Nil	Normal		
HC5	M	58.8	Type 2 Diabetes	Normal		
HC6	M	67.3	Hypertension	Normal		
HC7	F	40.8	Nil	Normal		
HC8	M	61.4	COPD	Normal - 2 small adenomas		
HC11	M	35.1	Nil	normal		
HC12	F	44.9	Nil	Normal – 1 small adenoma		

CD1	M	28.7	Nil	Crohn's disease	Yes	Azathioprine Vedolizumab
CD2	F	40.8	Nil	Crohn's disease	No	Azathioprine Adalimumab
CD3	F	22.6	Nil	Crohn's disease	Yes	Azathioprine Adalimumab
CD4	F	36.9	Nil	Crohn's disease	Yes	Adalimumab
CD5	F	43.2	Nil	Crohn's disease	Yes	Adalimumab
CD6	F	22.2	Nil	Crohn's disease	Yes	Azathioprine Adalimumab
CD7	M	41.9	Nil	Crohn's disease	No	Azathioprine
CD8	M	41.3	Nil	Crohn's disease	No	Adalimumab
CD9	F	26.5	Nil	Crohn's disease	No	Nil
CD10	F	61.6	Hypertension	Crohn's disease	No	Methotrexate
CD11	F	23.8	Nil	Crohn's disease	Yes	Nil

The median age of healthy controls was significantly older than Crohn's patients. More healthy donors were male. Smoking status was not recorded.

	Healthy (n = 10)	**Crohn's Disease (n = 11)**	**Significance**
Median Age	45.8	36.9	p = 0.025 (M-W-test)
% Male	70%	27%	p = 0.09 (M-W test)

Anatomical location of biopsy

Location of biopsy	**Healthy (n = 10)**	**Crohn's Disease (n = 11)**
Terminal / neo-terminal ileum	0/10	3/11
Ascending colon / caecum	8/10	4/11
Splenic flexure	2/10	4/11

6 - Comparing *AHR* expression in male and female donors

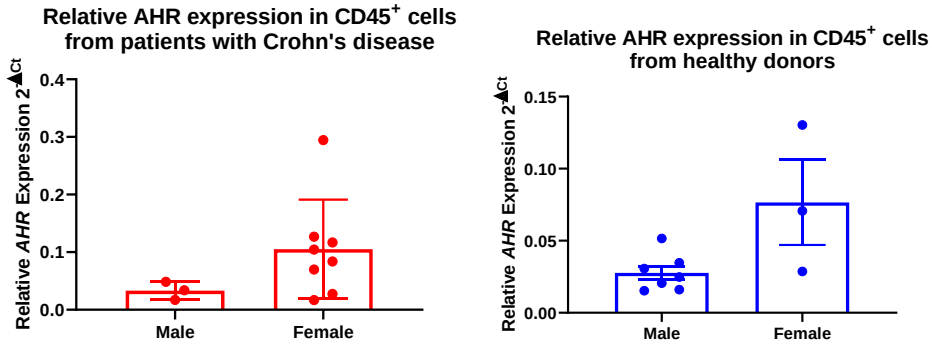

Relative AHR expression in intestinal CD45+ cells from female and male patients subdivided into Crohns disease (red) or healthy donors (blue). Apparent differences are not statistically significant

7 - Comparing cell counts and reference gene expression

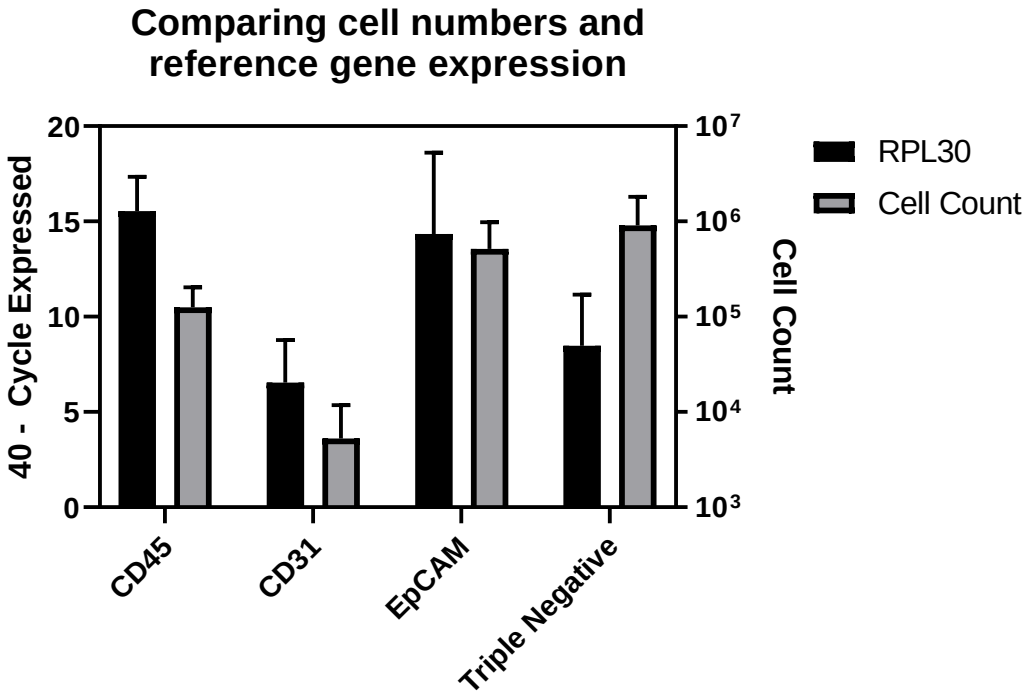

Appendix 7 The number of cells recovered in each population compared to (40 - reference gene expression). The number of cells recovered from each patient is shown in comparison to normalised RPL30 expression (40-Ct), a measure of RNA quantity. There was a mismatch between cell numbers and RPL30 gene expression in triple negative cells. n = 6.

8 – Differentially expressed genes in AHR+ cells compared to AHR- cells in 10X

Gene	AHRpos Average	AHRpos Log2 Fold Change	AHRpos P-Value	negative Average	negative Log2 Fold Change	negative P-Value
AHR	1.231968023	11.04670743	8.55E-54	0	-11.04670743	8.55E-54
IL22	1.316931335	10.14212699	0.002499	0.000582	-10.14212699	0.002499
CXCL8	8.570674093	5.874552258	0.000407	0.144229	-5.874552258	0.000407
MMP9	1.274449679	4.791425196	0.048911	0.045362	-4.791425196	0.048911
C15orf48	1.200106781	4.485670765	0.005915	0.052923	-4.485670765	0.005915
CCL3L1	1.391274233	3.982332087	4.83E-05	0.087235	-3.982332087	4.83E-05
BATF	1.242588437	3.960953673	5.21E-10	0.079093	-3.960953673	5.21E-10
SOD2	2.336491079	3.702150421	3.19E-05	0.17796	-3.702150421	3.19E-05
SLC7A11	1.189486367	2.985294414	0.013789	0.149463	-2.985294414	0.013789
KLF6	2.517038117	2.651200293	2.38E-05	0.397793	-2.651200293	2.38E-05
ANXA1	5.384549895	2.52207317	6.17E-05	0.929348	-2.52207317	6.17E-05
TNFAIP3	1.072661813	2.513377694	0.001651	0.187265	-2.513377694	0.001651
HLA-DQA1	1.380653819	2.405634687	0.005915	0.25938	-2.405634687	0.005915
RBPJ	1.720507067	2.230450112	0.000381	0.364644	-2.230450112	0.000381
HLA-DRA	7.147538618	2.200626533	0.004103	1.541159	-2.200626533	0.004103
HLA-DRB1	3.00557716	2.182706613	0.006309	0.657173	-2.182706613	0.006309
ZFP36L1	1.678025411	2.109847295	0.001244	0.386744	-2.109847295	0.001244
ZNF267	1.019559743	2.093260966	0.003548	0.238443	-2.093260966	0.003548
GPR183	1.954156175	2.065672475	0.001685	0.464092	-2.065672475	0.001685
TRBC1	2.251527767	2.049965421	0.003221	0.540278	-2.049965421	0.003221
IL32	2.400213563	2.018472736	0.002801	0.588548	-2.018472736	0.002801
HLA-DQB1	1.168245539	1.931839584	0.036459	0.305324	-1.931839584	0.036459
ARL6IP5	3.260467096	1.906882032	0.002704	0.863049	-1.906882032	0.002704
KLRB1	1.901054105	1.862451931	0.016782	0.519923	-1.862451931	0.016782
TSC22D3	1.465617131	1.82767823	0.012297	0.411169	-1.82767823	0.012297
CD52	2.538278945	1.814106624	0.006621	0.717075	-1.814106624	0.006621
LGALS3	3.685283656	1.803102521	0.045452	1.047988	-1.803102521	0.045452
ARL4C	1.401894647	1.782476497	0.01519	0.405935	-1.782476497	0.01519
LDHA	2.623242257	1.777392192	0.007709	0.760111	-1.777392192	0.007709
IL7R	5.671301073	1.739393819	0.01567	1.684225	-1.739393819	0.01567
CD2	2.729446396	1.732242742	0.015306	0.815942	-1.732242742	0.015306
RORA	1.550580443	1.724963361	0.021213	0.467	-1.724963361	0.021213
DEK	1.635543755	1.69091588	0.018237	0.504221	-1.69091588	0.018237
LAPTM5	2.060360315	1.582774416	0.035279	0.683925	-1.582774416	0.035279
LPXN	1.072661813	1.577305021	0.042586	0.358828	-1.577305021	0.042586
PKM	2.272768595	1.537595311	0.040796	0.77814	-1.537595311	0.040796

A list of all genes showing increased expression in CD45+ cells expressing AHR compared to CD45+ cells not expressing AHR, using expression data generated by 10X single cell sequencing

9 – *CYP1A1* expression in unstimualted CD45+ cells from different anatomical

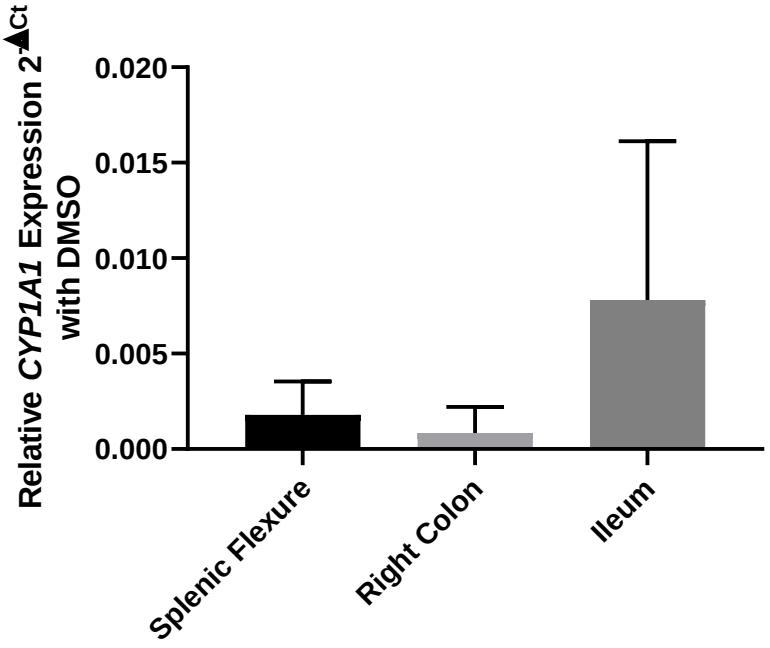

Relative CYP1A1 expression with DMSO (Control) in CD45+ cells from different anatomical locations. CD45+ cells from the ileum showed the highest *CYP1A1* expression ex-vivo. This difference was not significant (n = 21; analysis using Kruskal–Wallis test).

10 – *Ex-vivo CYP1A1* expression in different intestinal samples

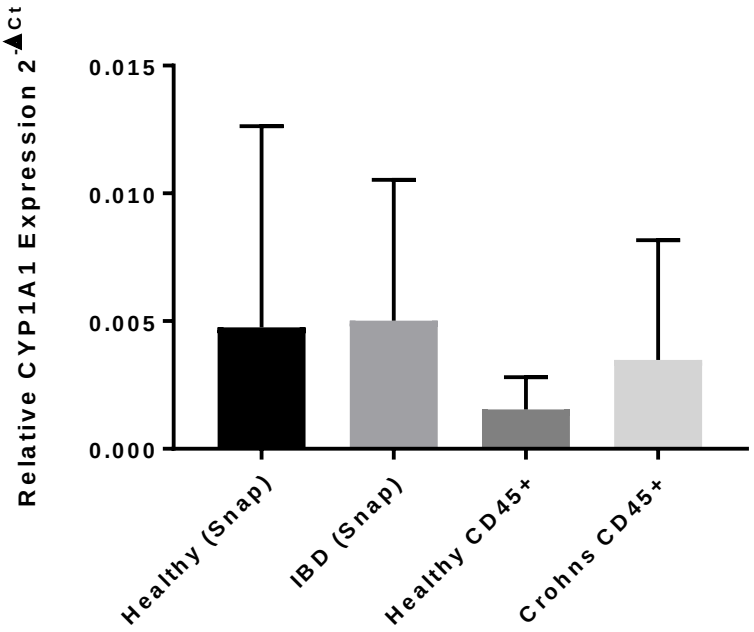

Relative *CYP1A1* expression in freshly processed whole biopsies (snap lysed) is not significantly different to *CYP1A1* expression in MACS sorted CD45+ cells derived from digested intestinal biopsies

11 - Characteristics and clinical fetures of included patients – RNASeq cohort

Patient	Age	Ethnicity	Sex	Comorbidity	Endoscopic Findings
RNASeq 1	57.3	White British	Male	None	Polyps
RNASeq 2	27.4	White Other	Male	None	Normal
RNASeq 3	56.7	Bangladeshi	Male	None	Normal
RNASeq 4	45.3	Bangladeshi	Male	None	Normal
RNASeq 5	66.5	White British	Male	None	Diverticulosis
RNASeq 6	55.5	Black African	Male	None	Normal
RNASeq 7	30.6	White British	Female	Ehlers-Danlos	Normal
RNASeq 8	31.2	Vietnamese	Female	None	Normal
RNASeq 9	52.1	White British	Female	Type 2 Diabetes, psoriasis	Polyps
RNASeq 10	63.7	Bangladeshi	Male	Spinal injury	Polyps

Demographic and sample characteristic of patients included in RNASeq analysis

12 - Differentially expressed genes with FICZ (q<0.05)

EnsemblID	GeneName	AvgExpr	logFC	p.value	q.value
ENSG00000005436	GCFC2	8.050853	0.793264	5.67E-06	**0.004913**
ENSG00000117090	SLAMF1	10.4048	0.546666	9.52E-05	**0.039592**
ENSG00000110031	LPXN	12.33706	0.325595	1.09E-05	**0.004277**
ENSG00000227038	GTF2IP7	4.505389	0.273669	3.13E-05	**0.011778**
ENSG00000167554	ZNF610	4.81171	0.241663	3.62E-05	**0.01818**
ENSG00000115884	SDC1	13.38226	0.213414	0.000155	**0.032019**
ENSG00000228144	AC078927.1	3.786108	0.042909	4.55E-15	**3.09E-11**
ENSG00000232237	ASCL5	-0.98874	0.04289	3.31E-07	**0.001108**
ENSG00000254673	AC110275.1	2.45389	0.034394	4.94E-11	**1.42E-07**
ENSG00000248126	AC091849.1	1.009663	0.03382	3.57E-15	**1.60E-10**
ENSG00000228491	MICE	0.57397	0.03309	1.44E-14	**2.17E-10**
ENSG00000234367	PFN1P3	1.931552	0.031577	3.04E-15	**1.22E-10**
ENSG00000275520	FAM236A	1.82516	0.029514	4.36E-17	**1.32E-11**
ENSG00000148377	IDI2	1.027548	0.026456	1.41E-14	**2.17E-10**
ENSG00000284057	AP001273.2	3.367027	0.022821	2.39E-14	**1.42E-10**
ENSG00000265366	GLUD1P2	1.425412	0.022062	6.66E-15	**2.17E-10**
ENSG00000215221	UBA52P6	0.535325	0.021747	1.64E-14	**2.18E-10**
ENSG00000230230	TRIM26	6.31909	0.020362	2.12E-08	**0.000116**
ENSG00000170236	USP50	1.734961	0.018041	6.47E-10	**3.25E-06**
ENSG00000269711	AC008763.3	4.458362	0.017592	1.20E-14	**8.64E-11**
ENSG00000248485	PCP4L1	2.388514	0.016566	2.33E-13	**2.96E-10**
ENSG00000258794	DUX4L27	1.710658	0.015938	3.49E-06	**0.02722**
ENSG00000273340	MICE	1.400734	0.014796	3.36E-14	**8.61E-10**
ENSG00000270339	AC243756.1	-0.0174	0.013799	6.83E-09	**0.000123**
ENSG00000268975	MIA-RAB4B	2.666671	0.012659	8.28E-05	**0.035823**
ENSG00000284099	AC008393.2	5.65081	0.011964	4.50E-14	**1.42E-10**
ENSG00000224831	AC117395.1	4.992378	0.006169	0.000129	**0.024009**
ENSG00000277858	H2AFB2	2.623965	0.005956	4.77E-09	**4.63E-06**
ENSG00000154415	PPP1R3A	2.43977	0.003578	1.49E-06	**0.001194**
ENSG00000265746	KYNUP2	0.961213	0.003512	7.62E-15	**1.23E-10**
ENSG00000257921	AC025165.3	-0.51453	-0.01266	2.24E-05	**0.035823**
ENSG00000223654	FLOT1	3.869863	-0.0214	1.41E-06	**0.001186**
ENSG00000229107	ABHD17AP4	0.517222	-0.02784	2.28E-07	**0.000792**
ENSG00000262299	AL513523.6	-0.05228	-0.02795	9.62E-06	**0.032019**
ENSG00000184659	FOXD4L4	1.213497	-0.03208	9.12E-08	**0.000662**
ENSG00000086205	FOLH1	1.034509	-0.03213	1.95E-09	**8.69E-06**
ENSG00000226491	FTOP1	0.059027	-0.03606	3.16E-06	**0.006528**
ENSG00000274788	LILRP2	1.193606	-0.03639	2.00E-06	**0.004463**
ENSG00000284663	AC068587.8	-0.6972	-0.0371	1.25E-06	**0.005514**
ENSG00000130950	NUTM2F	1.019131	-0.03895	2.01E-08	**0.000289**
ENSG00000250424	AC004691.2	-0.61593	-0.03906	8.95E-07	**0.004277**
ENSG00000241890	RPL13P4	-0.58278	-0.03908	1.10E-06	**0.002768**
ENSG00000146151	HMGCLL1	-0.35719	-0.04047	8.39E-07	**0.00406**
ENSG00000277745	H2AFB3	-0.03643	-0.04315	6.38E-07	**0.001754**

ENSG00000268133	AC003002.1	0.363884	-0.04318	2.93E-07	**0.002768**
ENSG00000232134	RPS15AP12	0.690952	-0.04415	3.87E-07	**0.001186**
ENSG00000237289	CKMT1B	1.042875	-0.04665	2.93E-07	**0.001672**
ENSG00000163661	PTX3	4.959149	-0.16254	0.000124	**0.036548**
ENSG00000171570	RAB4B-EGLN2	5.57878	-0.17747	1.80E-05	**0.013316**
ENSG00000135436	FAM186B	4.588354	-0.20178	0.000107	**0.020289**
ENSG00000271303	SRXN1	12.64309	-0.28421	2.55E-05	**0.013316**
ENSG00000125755	SYMPK	11.02401	-0.3898	0.000253	**0.047218**
ENSG00000118564	FBXL5	10.91615	-0.39771	6.25E-06	**0.002768**

All differentially expressed genes (q<0.05) in intestinal CD45+ cells exposed to FICZ compared to DMSO control

13 - Differentially expressed genes with CH223191 (q<0.05)

EnsemblID	GeneName	AvgExpr	logFC	p.value	q.value
ENSG00000163659	TIPARP	11.74048	-1.19297	2.78E-22	1.93E-18
ENSG00000138061	CYP1B1	12.85924	-1.12655	4.81E-19	1.23E-15
ENSG00000167680	SEMA6B	12.61217	-0.99996	7.99E-24	8.19E-20
ENSG00000119714	GPR68	9.414909	-0.9587	4.06E-08	1.41E-05
ENSG00000182162	P2RY8	11.78208	-0.83445	1.58E-16	2.69E-13
ENSG00000100628	ASB2	9.274272	-0.76087	2.71E-07	7.72E-05
ENSG00000278693	ASB2	9.274272	-0.76087	2.71E-07	7.73E-05
ENSG00000108932	SLC16A6	9.477409	-0.75915	1.44E-05	0.003024
ENSG00000127533	F2RL3	8.352354	-0.75814	8.84E-06	0.00193
ENSG00000229685	HLA-DPA1	7.190499	-0.75038	1.42E-05	0.003024
ENSG00000231389	HLA-DPA1	7.187628	-0.74053	1.82E-05	0.003856
ENSG00000171236	LRG1	8.284665	-0.7005	4.11E-05	0.007952
ENSG00000178623	GPR35	8.604015	-0.69524	6.68E-06	0.001487
ENSG00000236177	HLA-DPA1	7.178187	-0.69428	7.86E-05	0.013641
ENSG00000111344	RASAL1	9.460287	-0.67977	0.000151	0.023882
ENSG00000188042	ARL4C	11.58499	-0.65725	3.53E-09	1.57E-06
ENSG00000186480	INSIG1	11.41354	-0.65352	2.45E-06	0.00061
ENSG00000128268	MGAT3	12.03656	-0.62463	3.90E-06	0.000899
ENSG00000138641	HERC3	10.7532	-0.62398	0.000268	0.037588
ENSG00000137801	THBS1	11.45375	-0.62155	0.000293	0.040418
ENSG00000133317	LGALS12	7.553612	-0.61526	0.000196	0.02907
ENSG00000008516	MMP25	11.46663	-0.60532	2.52E-07	7.40E-05
ENSG00000235844	HLA-DPA1	7.089412	-0.60228	0.000403	0.049807
ENSG00000188822	CNR2	9.209274	-0.59041	3.68E-05	0.007447
ENSG00000141384	TAF4B	10.41832	-0.54907	4.22E-06	0.000964

ENSG00000171051	FPR1	9.213827	-0.53903	0.000355	0.044653
ENSG00000282608	ADORA3	9.895928	-0.52537	0.000318	0.042035
ENSG00000141506	PIK3R5	10.81891	-0.52113	8.09E-05	0.013916
ENSG00000196214	ZNF766	9.389631	-0.52065	0.00032	0.042035
ENSG00000082781	ITGB5	11.01168	-0.51612	0.000184	0.02753
ENSG00000154165	GPR15	12.14021	-0.50928	5.85E-06	0.001341
ENSG00000104081	BMF	12.78426	-0.50871	1.24E-05	0.002748
ENSG00000157404	KIT	12.58246	-0.50799	1.01E-07	3.35E-05
ENSG00000141179	PCTP	8.916952	-0.50139	0.000158	0.024788
ENSG00000139289	PHLDA1	10.00989	-0.50009	5.10E-05	0.009659
ENSG00000004799	PDK4	9.198975	-0.49851	0.000134	0.021363
ENSG00000160588	MPZL3	10.03744	-0.49155	0.000151	0.023882
ENSG00000005844	ITGAL	12.37181	-0.48716	0.000339	0.042524
ENSG00000165178	NCF1C	10.84503	-0.48416	1.90E-07	5.92E-05
ENSG00000265972	TXNIP	13.42102	-0.45139	3.52E-06	0.000851
ENSG00000169224	GCSAML	9.761747	-0.44205	0.000319	0.042035
ENSG00000138496	PARP9	9.648934	-0.43996	3.18E-05	0.006555
ENSG00000154217	PITPNC1	10.03904	-0.43695	3.55E-05	0.007246
ENSG00000179163	FUCA1	13.42837	-0.394	4.35E-11	3.10E-08
ENSG00000182487	NCF1B	10.22591	-0.38443	0.000179	0.026587
ENSG00000020633	RUNX3	11.94353	-0.38243	0.000254	0.036827
ENSG00000069188	SDK2	7.779878	-0.36567	2.04E-05	0.004185
ENSG00000158517	NCF1	11.82915	-0.36456	9.60E-05	0.016366
ENSG00000008083	JARID2	10.35892	-0.34993	0.000318	0.042186
ENSG00000259414	HERC2P7	5.017853	-0.33311	2.01E-06	0.000509
ENSG00000204653	ASPDH	4.629367	-0.30514	0.000128	0.020914
ENSG00000160593	JAML	12.42489	-0.30369	0.000139	0.022075
ENSG00000093134	VNN3	4.495693	-0.24946	6.74E-05	0.012108
ENSG00000166828	SCNN1G	4.525774	-0.18535	0.000271	0.037665
ENSG00000184163	C1QTNF12	3.953236	-0.1817	0.000107	0.017948
ENSG00000163661	PTX3	4.959149	-0.17158	0.00027	0.037665
ENSG00000225932	CTAGE4	5.34041	-0.16841	0.000326	0.042348
ENSG00000154175	ABI3BP	5.380408	-0.11904	0.000376	0.046599
ENSG00000187510	PLEKHG7	4.573221	-0.11319	0.000239	0.035138
ENSG00000171570	RAB4B-EGLN2	5.57878	-0.10926	6.45E-05	0.011802
ENSG00000265590	AP000275.2	6.557632	-0.10689	0.000147	0.023099
ENSG00000172995	ARPP21	2.866826	-0.04909	1.57E-09	2.07E-06
ENSG00000277741	GOLGA6L17P	2.896509	-0.04886	2.69E-11	5.46E-08
ENSG00000108602	ALDH3A1	-0.21566	-0.04289	2.33E-09	3.05E-06
ENSG00000227394	AC007386.1	1.291101	-0.04142	1.45E-08	1.55E-05
ENSG00000260170	AC090527.2	3.034084	-0.04114	1.75E-14	6.51E-11
ENSG00000188985	DHFRP1	2.612249	-0.04027	5.92E-15	2.25E-11
ENSG00000105549	THEG	-0.12389	-0.03893	7.62E-11	1.45E-07
ENSG00000189325	C6orf222	2.250881	-0.03835	2.45E-10	4.68E-07
ENSG00000165181	C9orf84	1.156854	-0.03639	2.91E-09	3.60E-06

ENSG00000089101	CFAP61	2.23651	-0.036	1.68E-09	2.36E-06
ENSG00000237829	PPP1R11	4.382042	-0.03588	9.61E-05	0.016125
ENSG00000233765	AL591479.1	0.799994	-0.0356	9.25E-17	4.64E-13
ENSG00000213304	AC008481.2	0.890137	-0.0354	4.11E-10	7.39E-07
ENSG00000275374	AC113385.3	-1.14608	-0.03427	5.28E-09	6.19E-06
ENSG00000254899	BX248516.1	4.107806	-0.03326	9.65E-12	1.32E-08
ENSG00000250050	MTND4P9	0.569308	-0.03123	5.42E-13	1.46E-09
ENSG00000248710	AC079594.2	2.807281	-0.03106	2.77E-09	3.49E-06
ENSG00000197360	ZNF98	0.89639	-0.03095	1.32E-09	1.93E-06
ENSG00000273907	CA15P2	1.010396	-0.03022	9.77E-19	7.25E-15
ENSG00000284484	AC025287.4	0.390314	-0.03017	1.57E-11	3.49E-08
ENSG00000271321	CTAGE6	2.228985	-0.02897	1.06E-11	2.45E-08
ENSG00000266145	RHOT1P1	1.291552	-0.0285	1.97E-10	3.84E-07
ENSG00000176020	AMIGO3	6.35817	-0.02843	3.67E-06	0.000878
ENSG00000092054	MYH7	2.246522	-0.02717	4.53E-16	1.87E-12
ENSG00000282466	TRBV5-4	1.183397	-0.02664	3.76E-21	6.64E-17
ENSG00000238086	PPP1R26P1	1.324894	-0.02476	4.70E-08	4.87E-05
ENSG00000283321	AC019117.3	1.795003	-0.02333	2.55E-11	5.46E-08
ENSG00000251155	SEPT14P4	-0.32146	-0.02111	6.99E-08	6.83E-05
ENSG00000163673	DCLK3	3.005128	-0.02022	1.12E-16	5.13E-13
ENSG00000155087	ODF1	0.178407	-0.02012	3.65E-08	3.94E-05
ENSG00000117834	SLC5A9	1.328818	-0.01857	5.59E-12	1.45E-08
ENSG00000182950	ODF3L1	-0.05859	-0.01753	6.69E-09	7.49E-06
ENSG00000233217	MROH3P	1.753031	-0.01341	1.17E-09	1.76E-06
ENSG00000106536	POU6F2	0.939203	-0.01305	4.76E-10	8.62E-07
ENSG00000212710	CTAGE1	1.671749	-0.01092	7.96E-10	1.21E-06
ENSG00000282841	CTAGE1	1.671749	-0.01092	7.96E-10	1.17E-06
ENSG00000157343	ARMC12	1.909756	-0.01078	5.04E-11	1.07E-07
ENSG00000213538	KRT8P41	1.157614	-0.01006	7.08E-08	6.68E-05
ENSG00000170236	USP50	1.734961	-0.00881	2.06E-05	0.012375
ENSG00000197992	CLEC9A	1.815882	-0.00858	3.07E-08	3.42E-05
ENSG00000055813	CCDC85A	1.024346	-0.00768	5.92E-10	9.65E-07
ENSG00000142606	MMEL1	1.859076	-0.00657	4.64E-13	1.35E-09
ENSG00000277131	MMEL1	1.859076	-0.00657	4.64E-13	1.35E-09
ENSG00000284651	AP000553.5	-0.71893	-0.00553	1.33E-05	0.008884
ENSG00000274945	KIR2DL4	0.971343	-0.00515	4.88E-07	0.000422
ENSG00000182393	IFNL1	2.070334	-0.0036	4.48E-07	0.00041
ENSG00000095777	MYO3A	4.24961	-0.00285	1.87E-09	9.65E-07
ENSG00000152214	RIT2	2.553957	-0.0017	2.56E-09	3.29E-06
ENSG00000123561	SERPINA7	3.87617	-0.00052	1.26E-06	0.000509
ENSG00000268975	MIA-RAB4B	2.666671	0.003148	3.20E-05	0.017399
ENSG00000228144	AC078927.1	3.786108	0.006581	1.30E-07	6.68E-05
ENSG00000235655	H3F3AP4	6.28985	0.00884	6.50E-05	0.0121
ENSG00000248126	AC091849.1	1.009663	0.014776	2.44E-14	8.34E-11
ENSG00000254673	AC110275.1	2.45389	0.014839	4.68E-18	3.13E-14
ENSG00000228491	MICE	0.57397	0.015218	9.21E-08	8.79E-05

ENSG00000234367	PFN1P3	1.931552	0.017536	1.26E-08	1.39E-05
ENSG00000148377	IDI2	1.027548	0.022221	2.27E-20	2.67E-16
ENSG00000215221	UBA52P6	0.535325	0.026543	5.93E-10	9.97E-07
ENSG00000275520	FAM236A	1.82516	0.026574	4.95E-17	2.69E-13
ENSG00000284057	AP001273.2	3.367027	0.026614	6.09E-10	1.00E-06
ENSG00000265366	GLUD1P2	1.425412	0.026844	3.09E-12	8.45E-09
ENSG00000230230	TRIM26	6.31909	0.029245	4.76E-05	0.009106
ENSG00000269711	AC008763.3	4.458362	0.031944	1.92E-06	0.0005
ENSG00000258794	DUX4L27	1.710658	0.03308	7.87E-11	1.58E-07
ENSG00000270339	AC243756.1	-0.0174	0.033834	2.83E-09	3.63E-06
ENSG00000273340	MICE	1.400734	0.034088	6.00E-18	3.85E-14
ENSG00000248485	PCP4L1	2.388514	0.037011	1.08E-19	1.08E-15
ENSG00000284099	AC008393.2	5.65081	0.037632	2.51E-20	1.04E-16
ENSG00000277858	H2AFB2	2.623965	0.043348	4.45E-16	1.87E-12
ENSG00000265746	KYNUP2	0.961213	0.045051	1.81E-24	8.19E-20
ENSG00000154415	PPP1R3A	2.43977	0.045603	3.66E-08	3.82E-05
ENSG00000258529	AP001781.3	4.862002	0.047141	0.000333	0.042372
ENSG00000242887	IGHJ3	4.214052	0.049492	8.41E-13	1.32E-09
ENSG00000058262	SEC61A1	13.86751	0.136865	5.28E-05	0.009907
ENSG00000100314	CABP7	3.749735	0.143233	0.000269	0.037665
ENSG00000181418	DDN	4.101047	0.213142	0.000265	0.037588
ENSG00000169885	CALML6	4.059298	0.229486	1.95E-05	0.006444
ENSG00000266074	BAHCC1	5.735268	0.260116	0.000173	0.026144
ENSG00000227315	NEU1	4.685142	0.266984	2.95E-06	0.000713
ENSG00000183439	TRIM61	4.689687	0.283329	0.000172	0.026144
ENSG00000051108	HERPUD1	14.63428	0.289028	1.57E-06	0.000419
ENSG00000152527	PLEKHH2	5.794392	0.292251	0.000268	0.037497
ENSG00000219607	PPP1R3G	3.887249	0.294597	4.69E-05	0.009056
ENSG00000163930	BAP1	11.30974	0.333486	1.35E-05	0.002957
ENSG00000161011	SQSTM1	15.73572	0.353914	0.000166	0.025194
ENSG00000173442	EHBP1L1	12.08874	0.371509	0.000247	0.035699
ENSG00000105205	CLC	12.63489	0.374008	6.12E-06	0.001399
ENSG00000100292	HMOX1	13.78696	0.390072	1.44E-08	5.36E-06
ENSG00000122224	LY9	10.79914	0.396337	9.00E-05	0.015503
ENSG00000107959	PITRM1	10.74513	0.421586	0.000328	0.042372
ENSG00000142687	KIAA0319L	10.65176	0.448617	0.000304	0.040625
ENSG00000175197	DDIT3	10.05388	0.466979	0.000308	0.041895
ENSG00000197355	UAP1L1	10.70966	0.480262	9.20E-05	0.015948
ENSG00000116679	IVNS1ABP	11.53704	0.494215	3.85E-05	0.007522
ENSG00000109065	NAT9	9.646058	0.496395	0.000373	0.047089
ENSG00000171492	LRRC8D	9.78971	0.51081	7.59E-05	0.013516
ENSG00000031823	RANBP3	10.51675	0.51758	0.000164	0.025194
ENSG00000118515	SGK1	11.54264	0.522533	7.32E-05	0.013242
ENSG00000173846	PLK3	9.641329	0.532224	3.25E-06	0.000795
ENSG00000147872	PLIN2	11.58193	0.543968	0.000131	0.021363
ENSG00000100888	CHD8	11.12855	0.553059	0.000326	0.042372

ENSG00000007944	MYLIP	9.357717	0.566365	0.000235	0.033851
ENSG00000064225	ST3GAL6	9.683648	0.580094	5.55E-07	0.000152
ENSG00000140463	BBS4	8.294614	0.624237	0.000117	0.01895
ENSG00000160179	ABCG1	9.096325	0.771	1.08E-06	0.000295

All differentially expressed genes (q<0.05) in intestinal CD45+ cells exposed to CH223191 compared to DMSO control